2012

PHDS, Stress, And Starvation: The Identification Of A New RPD3 Deacetylase Complex Involved In The Yeast Oxidative Stress And Metabolism Pathways

Lindsey A. Baker

PHDS, STRESS, AND STARVATION: THE IDENTIFICATION OF A NEW RPD3 DEACETYLASE COMPLEX INVOLVED IN THE YEAST OXIDATIVE STRESS AND METABOLISM PATHWAYS

A Thesis Presented to the Faculty of

The Rockefeller University

in Partial Fulfillment of the Requirements for

the degree of Doctor of Philosophy

by

Lindsey A. Baker

June 2012

PHDS, STRESS, AND STARVATION:

THE IDENTIFICATION OF A NEW RPD3 DEACETYLASE COMPLEX INVOLVED IN THE YEAST OXIDATIVE STRESS AND METABOLISM PATHWAYS

Lindsey A. Baker, Ph.D.

The Rockefeller University 2012

The cellular pathways that govern survival in the face of diverse stresses rely on gene expression changes as one mechanism to respond to or protect against internal and external threats. Because eukaryotic DNA is packaged into chromatin, these gene expression changes depend on the targeting of regulatory proteins to specific regions of the genome to alter chromatin structure, promoting or repressing transcription. One protein domain involved in targeting chromatin regulators is the plant homeodomain, or PHD finger, a module that preferentially interacts with either methylated or unmethylated lysines on histones, and has important functions in human health. Despite recent advances in identifying the histone ligands for some PHD fingers as well as the functions of the proteins that contain them, for many other PHD fingers, including some of the 17 PHD fingers of the budding yeast *Saccharomyces cerevisiae*, these questions remain unanswered.

In the research presented in this thesis, I sought to gain insight into the ligands and functions for three yeast PHD finger proteins, the Yng1 subunit of the NuA3 acetyltransferase complex, Jhd2, and Ecm5, the latter two both being homologous to the mammalian JARID family of histone demethylases. In Chapter 2, I demonstrate that the PHD fingers of these proteins interact with histone H3 enriched for different sites of methylation depending on the

PHD and present results of an *in vitro* assay used to test whether any yeast PHD fingers possess ubiquitin E3 ligase activity, a function ascribed to the PHD-related RING domain. In Chapter 3, I discuss experiments performed to identify the protein interaction partners of Jhd2 and Ecm5, culminating in the discovery that Ecm5 interacts with the PHD finger protein Snt2 as well as the Rpd3 deacetylase, forming a complex I have named Rpd3(T). I also discuss experiments showing that the *ecm5* knockout strain does not have obvious defects in many yeast pathways.

In Chapter 4, I present evidence that Rpd3(T) complex members are involved in the cellular oxidative stress and metabolism pathways, and discuss chromatin immunoprecipitation experiments followed by high-throughput sequencing which were performed to map Ecm5 and Snt2 localization before and after hydrogen peroxide-mediated oxidative stress. I then discuss how the Ecm5 and Snt2 localization patterns relate to gene expression changes in wild-type cells after oxidative stress and in *snt2* knockout cells. I compare Ecm5 and Snt2 localization patterns in rich media before and after oxidative stress to patterns in less rich media before and after nutrient stress induced by the TOR pathway inhibitor rapamycin. Finally, I discuss potential mechanisms through which Ecm5 and Snt2, either as a pair or as a part of the Rpd3(T) complex, may help to coordinate the cellular responses to oxidative and nutrient stresses, and the greater implications of this work.

ACKNOWLEDGEMENTS

First, I would like to thank my advisor, Dr. David Allis, for providing scientific guidance over the course of my graduate career and more importantly, providing moral support through the difficult parts of this project. Dave's unquestioning faith in my abilities to become a successful scientist have inspired me to surpass what I intially thought I was capable of. I have particularly enjoyed his enthusiasm for all things chromatin and his love of puns (which I share).

I also owe an immense debt of gratitude to my Faculty Committee members, Dr.'s Tom Muir and Michael Rout, who were always willing to listen to my ideas and offer helpful feedback. No matter how nervous I felt going into a Committee Meeting, their enthusiasm for my project always left me feeling elated afterwards.

I am extremely thankful to Dr. Beatrix (Trixi) Ueberheide, who has been not only an amazing collaborator, but also a good friend. All of that cryo-grinding wouldn't have been nearly as enjoyable without a fellow show tune lover to belt out songs with.

Over the years, I have received scientific support from numerous sources without whom many of the experiments described in this thesis would not have been possible. I thank Dr. Sean Taverna for introducing me to the Allis lab, coaching me through my rotation, teaching me the art of *Tetrahymena* nuclear preparations, and writing me an awesome karaoke song. I thank Dr. Beth Duncan for being an excellent bay-mate, and for teaching me the ins and outs of qPCR. I thank Dr. Peter Lewis for showing me that radioactivity is not scary, guiding me through my first northern blots, and always having useful suggestions for ways to improve my biochemical techniques. I also owe thanks to Dr. Ronen Sadeh for teaming up with me for *in vitro* ubiquitylation assays, for providing useful feedback throughout this project, for providing critical comments on this thesis, and for keeping the yeast alliance alive. I also would like to thank the other members of "yeast club," Dr. Jung Ae Kim, who has become my go-to person in the lab for all questions relating to yeast, FACS, and DNA damage, and Dr. Christina Hughes, who provided useful feedback on this thesis, as well as many hours of stimulating coversation. I thank Dr. Laura Banaszynski for advice on high-throughput sequencing procedures and for her helpful suggestions regarding the fourth chapter of this work. I also thank Bryce Carey for being willing to become my metabolism buddy; it has been immensely satisfying to finally have someone to discuss the Krebs Cycle with. In addition, I have appreciated the interactions I have had with all

the other Allis lab members, past and present, who have shaped the way I think about science.

The Allis Lab Manager, Jamie Winshell, deserves special thanks. Without her untiring efforts to keep things in the lab running smoothly, the lab would have been a much different place in which to work. In addition, I have been happy to call Jamie a friend for many years now, and I am thankful for our many good conversations in our bay.

I am hugely indebted to my two collaborators on my high-throughput sequencing projects: Dr. Deyou Zhang has always been willing to answer my queries with insightful and throrough comments, and Dr. Scott Dewell has been very helpful in teaching me to do my own data analysis, coming up with new ways to look at my data, and providing technical support. Without the contributions and support of these two collaborators, many of the insights presented in this work would never have been made.

I must also thank Dr. Oliver Rando, who was willing to hire an undergraduate student with no lab experience, and his amazingly talented technician, Mike Dion, who taught me yeast genetics. The miccrococcal nuclease experiments I performed in Ollie's lab first sparked my interest in chromatin, and led me here.

I am thankful for the financial and administrative support I have received through the David Rockefeller Graduate Program. Throughout the years, the Dean's Office staff have been incredibly kind and helpful. I am also thankful to have received financial support for this research through an NIH Cancer Training Grant.

I want to conclude by thanking my friends and family for their untiring support during this journey. My father and my sister Jennifer (Little Sue) have been my life-lines through this process. Lastly, I must thank Chris for being so patient and caring with me throughout the last few years. I have been incredibly fortunate to have had a partner who is a joy to come home to, who wants to talk with me about my research, and who is so supportive.

TABLE OF CONTENTS

LIST OF FIGURES

LIST OF TABLES

CHAPTER 1: GENERAL INTRODUCTION

Eukaryotic genomes are packaged into chromatin

Eukaryotic cells face the challenge of fitting extensive genomes into relatively modest-sized nuclei. They must do this in a manner that is space-efficient but still flexible enough to allow DNA-templated processes, such as transcription and replication, to occur. This feat is accomplished by the packaging of the genome into a structure known as chromatin. The cell biologist Walter Flemming first used the term "chromatin" in late 1800's, to describe a string-like material within cells that readily absorbed basophilic aniline stain (Flemming, 1882). Approximately 45 years later, another biologist named Emil Heitz noticed that certain regions of chromatin remained darkly stained and condensed throughout the cell cycle, while other regions decondensed when not undergoing mitosis. He named the former "heterochromatin" and the latter "euchromatin" (Figure 1.1A) (Heitz, 1928). These two early studies helped launch the field of chromatin biology, which in recent decades, has become immensely important to understanding genome regulation.

Working around the same time as Flemming, biochemist Albrecht Kossel discovered an acid-soluble substance associated with the nulcei of goose erythrocytes, and named it "histon" (Kossel, 1884). Until the 1940's, many scientists believed the histone proteins, which showed some degree of diversity depending on the source organism, were the source of hereditary information, rather than the DNA, which was thought to be too uniform between species to encode information (Schultz, 1941). One partial proponent of this view was Alfred Mirsky, a protein biochemist working at The Rockefeller University (then The Rockefeller Institute), who

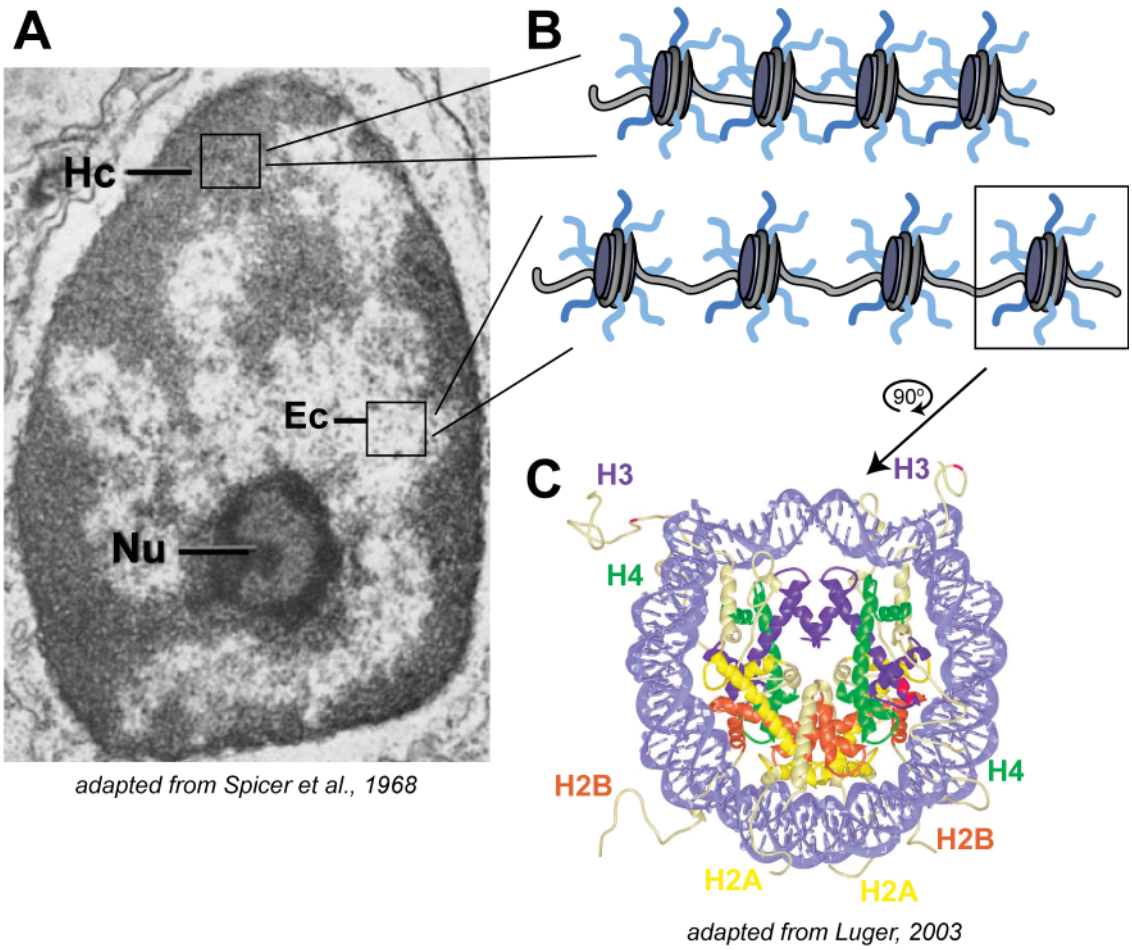

Figure 1.1 Chromatin structure

A. Electron micrograph of a lymphocyte nucleus, with heterochromatin (Hc) and euchromatin (Ec) labeled. The nucleolus (Nu) is also labeled. **B.** Schematic of chromatin as "beads on a string," showing that heterochromatin has a more compact structure than euchromatin. **C.** Front view structure of the nucleosome core particle. DNA is labeled in light blue, while histones H3, H4, H2A, and H2B are colored blue, green, yellow, and red, respectively.

pioneered many of the early biochemical studies of histone proteins (Daly and Mirsky, 1955; Mirsky and Pollister, 1946). However, in 1944, Oswald Avery, Colin MacLeod, and Maclyn McCarty, also working at The Rockefeller Institute, reported that the "transforming principle" responsible for converting a non-virulent strain of bacteria into a virulent strain was DNA, initiating many future studies that proved that DNA is the basis for heredity in bacteria and eukaryotes (Avery et al., 1944). As DNA became increasingly accepted as the carrier of genetic information, the proposed function of the histone proteins switched from information carrier to DNA "packager," although there was also early speculation that histones might inhibit gene transcription (Stedman and Stedman, 1951). However, the details of DNA-histone interactions remained unclear.

In the 1970's several studies helped to uncover the overall primary structure of chromatin. First, multiple studies found that digesting chromatin with endonucleases resulted in a series of fragments, differing in size by approximately 200 bp, that produced a regular ladder when separated on a gel, suggesting that chromatin consisted of a repeating unit and that DNA and protein were associated within this unit (Billing and Bonner, 1972; Hewish and Burgoyne, 1973; Mirsky, 1971). Electron microscopy studies from C.L.F. Woodcock as well as Ada and Donald Olins showed that chromatin from multiple organisms formed a thin fiber broken up by thicker particles, a structure that Roger Kornberg described as "beads on a string" (Figure 1.1B) (Kornberg, 1974; Olins and Olins, 1974; Woodcock et al., 1976). Around the same time, Roger Kornberg published a model of chromatin structure based largely on biochemical and biophysical studies, describing a repeating unit of chromatin, consisting of an octamer of two copies each of the four core histone proteins, H2A, H2B, H3, and H4 (Kornberg, 1974; Kornberg and Thomas,

1974). A subsequent study named this repeating unit of chromatin the "nucleosome" which both referenced the nuclear origin of these particles and the original term for these structures used by the Olinses, "nu bodies" (Oudet et al., 1975). Whether physiologically relevant variation occurred within nucleosomes, and if so, how this variation was achieved, remained unclear at the time.

In 1997, Karolin Luger and Timothy Richmond published the crystal structure of the nucleosome at 2.8Å resolution, showing that the nucleosome core particle consists of an octamer of histone proteins which are wrapped with 146 basepairs of DNA in 1.65 left-handed superhelical turns (Figure 1.1C) (Luger et al., 1997). A linker histone, called H1, associates with the DNA between two nucleosomes and assists in compaction of the chromatin into a tight fiber (Happel and Doenecke, 2009). The core histone proteins that make up the nucleosome octamer are extremely conserved throughout eukaryotes, indicating the importance of the chromatin structure in nuclear function. Importantly, this high level of conservation allows studies of chromatin function in model organisms to be highly informative.

Mechanisms of chromatin regulation

Initially thought of as just a method to package DNA, chromatin is now understood to actively regulate most, if not all, DNA processes. This is achieved through mechanisms that alter nucleosome structure, resulting in either increased accessibility of nucleosome-bound DNA or increased association between regulatory factors and the histones proteins themselves. At least four different mechanisms are known to regulate chromatin structure. First, ATP-dependent chromatin remodelers can alter the histone-DNA contacts of a nucleosome, rendering

it more accessible. Numerous outcomes have been reported for remodeling, including the complete eviction of the histones from the nucleosome, the repositioning or sliding of the nucleosome along the DNA fiber, replacement of certain histones within the nucleosome, or a reconfiguration of the nucleosome to a more accessible structure (Flaus and Owen-Hughes, 2011). The downstream consequence of these activities is to render DNA more or less accessible to regulatory factors such as the transcription machinery.

A second means of chromatin regulation involves the replacement of individual histones with "histone variants," which can substitute for the canonical H2A, H2B, H3, and H4 (Talbert and Henikoff, 2010). While some variants only contain slight differences in amino acid composition compared to their canonical counterparts, others are quite distinct. In higher eukaryotes, where many cells are post-mitotic, variants provide an important way to alter chromatin structure without having to go through S phase, the point in the cell cycle when the canonical histones are synthesized and packaged with DNA (Frank et al., 2003). However, even rapidly dividing eukaryotes such as the budding yeast, *Saccharomyces cerevisiae*, the model used in this thesis research, utilize variant histones to help regulate certain key processes. For example, the yeast histone variant H2A.Z, which can substitute for histone H2A, is incorporated into the two nucleosomes flanking transcription start sites, and is involved in initiation of transcription (Raisner and Madhani, 2006). In addition, the yeast H3 variant, CenH3, marks centromeres and is important for genome integrity (Choy et al., 2012).

Another way that chromatin can be regulated is through the proteolytic cleavage of the histone tail from the core of the protein. Site-specific histone cleavage was first reported by Thomas Eickbush, Dennis Watson, and Evangelos Moudrianakis in the late 1970's, who had

found a shorter isoform of histone H2A in histones extracted from calf thymus (Eickbush et al., 1976). Shortly after, David Allis and colleagues reported a clipped isoform of histone H3 in the transcriptionally inactive micronuclei of the ciliated protozoan *Tetrahymena thermophila* (Allis et al., 1980). While studies into histone proteolysis continued into the early 1990's, as more discoveries emerged about the fourth mechanism of chromatin regulation, post-translational modification of the histone proteins, attention shifted away from histone "clipping." Recently, the histone H3 tail was found to be cleaved during mouse ES cell differentiation (Duncan et al., 2008), suggesting that histone proteolysis might play important roles in development. Furthermore, in budding yeast, H3 cleavage during sporulation and stationary phase growth was also recently reported (Santos-Rosa et al., 2009). These new findings may prompt a resurgence of interest in this mechanism.

Histones are the substrates for a wide range of post-translational modifications

One of the more widely studied mechanisms of chromatin regulation is histone post-translational modification, the covalent attachment of chemical moieties to the N termini and amino acid side chains of the histone polypeptides. The first scientist to describe the post-translational modification of histones was Kenneth Murray, who showed that histones from cells treated with radioactive methionine contained radioactive ε-*N*-methyl-lysine (Murray, 1964). Shortly thereafter, Vincent Allfrey, a histone biochemist and protégé of Alfred Mirsky (and another Rockefeller chromatin biologist), reported that histones could be acetylated as well as methylated (Allfrey et al., 1964). Seeking to explain the observation that histones sometimes inhibited RNA synthesis and sometimes did not, Vincent Allfrey hypothesized that "relatively

minor modifications of histone structure, taking place on the intact protein molecule, offer a means of switching-on or –off RNA synthesis at different loci along the chromosome." As proof of the existence of these "relatively minor modifications," he showed that when isolated nuclei were incubated with radioactive sodium acetate or methionine, histones became radioactively acetylated or methylated, respectively.

Since these initial discoveries, a wide variety of other histone post-translational modifications have been described, including phosphorylation, ubiquitylation, sumoylation, crotonylation, propionylation, butyrylation, formylation, citrullination, O-GlcNAcylation, and ADP ribosylation (Banerjee and Chakravarti, 2011; Bannister and Kouzarides, 2011; Jiang et al., 2007; Messner and Hottiger, 2011; Sakabe et al., 2010; Tan et al., 2011; Zhang et al., 2009). The diverse array of modification types combined with the many histone residues that can act as substrates for these marks, results in a mind-boggling number of diverse combinations. Noting this combinatorial complexity, Brian Strahl and David Allis hypothesized that "multiple histone modifications, acting in a combinatorial or sequential fashion on one or multiple histone tails, specify unique downstream functions," an idea they named the "histone code hypothesis" (Strahl and Allis, 2000). Indeed, there are many well documented associations between particular modifications and cellular outcomes, such as those between phosphorylation of histone H3 at serine 10 (H3S10) and mitosis, and between H3K4 methylation and transcription (Ng et al., 2003; Santos-Rosa et al., 2002; Sims et al., 2003).

While these examples provide striking proof of the coding potential for histone modifications, a key challenge in the chromatin field remains to be the identification of functions for each individual histone modification and for combinations of co-occurring marks. In that

regard, the budding yeast system has proved particularly useful. Because haploid yeast contain only two copies of each core histone and are amenable to gene deletion and mutation, studies in this organism have led to many key insights in chromatin biology (Hereford et al., 1979; Smith and Andresson, 1983). Furthermore, the ease with which non-histone genes can be deleted from yeast, allowing the search for synthetic phenotypes using combinations of mutations, has made the yeast system a powerful tool for unraveling chromatin pathways. One early pioneer of the use of yeast for chromatin studies is Michael Grunstein. Early histone mutant studies from the Grunstein laboratory helped established a much stronger causal link between histone deacetylation and yeast heterochromatin formation (Johnson et al., 1990; Kayne et al., 1988). For my own graduate studies, I was attracted to the genetic power of the yeast system, and all of the *in vivo* experiments that I will describe in this thesis were performed using budding yeast. However, where possible, I will note connections between this work and mammalian biology.

Histone post-translational modifications regulate chromatin structure in *cis* and *trans*

Histone modifications regulate chromatin structure in two ways. First, post-translational modifications can directly alter the strength of histone-DNA or histone-histone contacts, loosening the chromatin fiber and promoting access to the underlying DNA. This mechanism of nucleosome regulation in *cis*, is generally associated with histone modifications that alter the charge of the histone proteins, such as histone acetylation (Robinson et al., 2008; Shogren-Knaak et al., 2006). Another histone modification that regulates chromatin through a *cis* mechanism is histone ubiquitylation. This mark has recently been shown by Tom Muir's laboratory to impair compaction of the chromatin fiber, in a mechanism distinct from that of histone acetylation (Fierz et al., 2011).

In addition to affecting nucleosomal structure directly, histone post-translational modifications can also regulate chromatin in *trans*, by creating docking sites for other regulatory proteins. *Trans*-acting proteins recruited to chromatin through interactions with histone modifications can then promote changes in local chromatin structure, enhancing or repressing the expression of nearby genes. For instance, in metazoans and the fission yeast *Schizosaccharomyces pombe*, H3K9 methylation creates a binding site for the HP1 protein, which promotes chromatin compaction, resulting in the silencing of genes associated with this mark. (Bannister et al., 2001; Lachner et al., 2001; Nakayama et al., 2001). In addition to regulating chromatin in *cis*, histone acetylation can also promote recruitment of regulatory factors in *trans*: in yeast, this mark creates binding sites for the Gcn5 protein, which is known to catalyze histone acetylation, thus creating a positive feedback loop (Owen et al., 2000).

Readers, writers, and erasers regulate histone post-translational modifications

When discussing chromatin regulation, it is useful to categorize the protein players into writers, erasers and readers (Figure 1.2). Writers are the enzymes that catalyze particular histone modifications. Similarly, erasers are the enzymes that remove those marks. The last category of histone regulator, readers, are proteins that are recruited to or stabilized on chromatin by interactions with specific histone modifications. Generally, specific modules within reader proteins mediate histone interactions. Many families of reader modules have now been described. For instance, bromodomains are known to interact with acetylated histones, while chromodomains show specificity towards histone methylation (Jacobs et al., 2001; Min et al., 2003; Owen et al., 2000). To further add to the complexity of chromatin regulation, often a

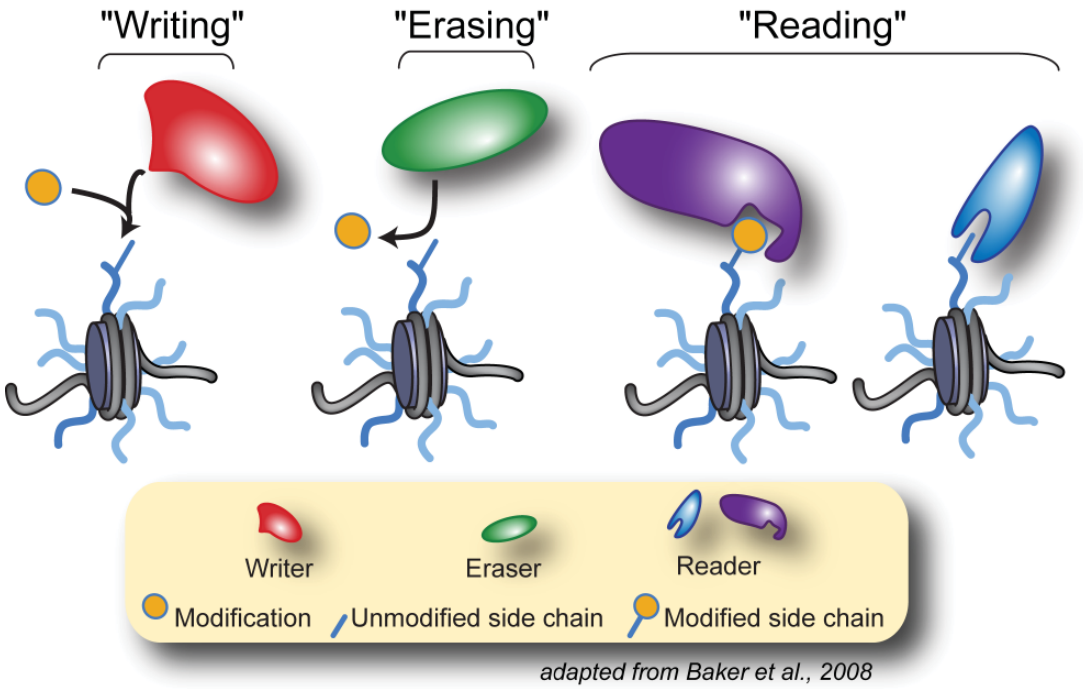

Figure 1.2 Writers, erasers, and readers

Histone regulation is achieved by proteins that catalyze histone modifications (writers), proteins that enzymatically remove histone modifications (erasers), and proteins that specifically recognize either unmodified or modified histone amino acids (readers).

single protein or protein complex can fall into more than one of these roles (Ruthenburg et al., 2007). For instance, the yeast Rpd3(S) histone deacetylase complex, which I will discuss more below, functions primarily as an eraser, removing acetyl groups from histones, but the Rco1 and Eaf3 subunits of this complex contain a PHD finger and chromodomain, respectively, two reader modules that promote association with H3K36 methylation (Joshi and Struhl, 2005; Li et al., 2007). It should be noted that while these concepts have generally been applied to histone modifications, many examples of post-translational modification of non-histone proteins have been documented. One of the better-studied examples of a non-histone substrate for post-translation modification is p53, which was demonstrated to be acetylated by Wei Gu and Robert Roeder, working at The Rockefeller University (Dai and Gu, 2010; Gu and Roeder, 1997; Huang and Berger, 2008; Spange et al., 2009). Therefore, many of the readers, writers, and erasers known to regulate histones are likely to have non-histone substrates as well.

Histone acetylation is a modification associated with transcriptional activity in yeast

Because histone acetylation and lysine methylation are two modifications most relevant to this work, I will introduce more about these marks. Histone acetylation has been found at many, though not all, of the lysines in histones, and more recently, in non-histone proteins as well (Basu et al., 2009; Choudhary et al., 2009). The writers for this mark are proteins known as histone acetyltransferases (HATs), or more recently, as lysine acetyltransferases (KATs), in recognition of these enzymes' abilities to acetylate nonhistone substrates as well as histones. The first transcription-associated HAT was discovered by James Brownell and David Allis in 1995, who fractionated an acetylating activity from the transcriptionally active macronuclei of

Tetrahymena, and used an in-gel acetylation assay to show that this activity came from a 55 kDa polypeptide which was later identified as the homolog of the yeast Gcn5 protein (Brownell and Allis, 1995; Brownell et al., 1996). Around the same time, Susanne Kleff and Rolf Sternglanz identified another yeast HAT activity and linked this activity to a gene which they named *HAT1* (Kleff et al., 1995), and work from Daniel Gottschling's laboratory also identified the yeast histone acetyltransferase Hat1 (Parthun et al., 1996). Following on these initial discoveries, the human Gcn5 homolog; the mammalian transcriptional coactivators p300, CBP, PCAF, ACTR, and SRC-1; as well as the TAF(II)250 subunit of the TFIID transcription initiation factor were all shown to have HAT activity, suggesting histone acetylation and active transcription might be linked (Bannister and Kouzarides, 1996; Candau et al., 1996; Chen et al., 1997; Mizzen et al., 1996; Ogryzko et al., 1996; Spencer et al., 1997; Yang et al., 1996).

Budding yeast contain at least 10 HATs, Gcn5, Hat1, Elp3, Hpa2, Esa1, Sas3, Sas2, Taf1, Nut1, and Rtt109 (Han et al., 2007; Kimura et al., 2005). *In vivo*, many of these HATs function in multi-protein complexes, and at least 12 different yeast HAT complexes have been described (Han et al., 2007; Lee and Workman, 2007). For instance, the NuA3 complex, which will be discussed more in Chapter Two of this thesis, consists of the Sas3 catalytic subunit as well as Taf30 (Taf14/Anc1/Tfg3), Yng1, Nto1, and Eaf6, and is capable of acetylating multiple lysines on histone H3 (John et al., 2000; Taverna et al., 2006). In some cases, the noncatalytic subunits of these complexes stimulate HAT activity (Han et al., 2007), while in others they help target these complexes to specific regions of the genome (Bian et al., 2011; Joshi and Struhl, 2005).

Functions of histone acetylation

Since its discovery, histone acetylation has been largely linked with active transcription. Vincent Allfrey, himself, showed that chemically acetylated histones stimulate transcription in an *in vitro* assay (Allfrey et al., 1964). Consistent with this result, numerous studies have shown that *in vivo*, chromatin with abundant H4 acetylation is transcriptionally active, and transcriptionally active chromatin preparations are enriched for H4 acetylation (Allegra et al., 1987; Hebbes et al., 1988; Johnson et al., 1987; Lin et al., 1989; Ridsdale and Davie, 1987). While these studies convincingly showed correlations between histone acetylation and transcriptional activity, whether increased acetylation is a cause or a consequence of transcription remained a question for the field (Turner, 1991).

However, later studies have established causal links between increased histone acetylation and increased transcription. For instance, while deleting the H4 N-terminal tail or mutating the acetylatable H4 lysines were generally found to impair gene activation, these mutations have been shown to activate the normally repressed yeast *GAL1* promoter (Durrin et al., 1991; Fisher-Adams and Grunstein, 1995). In addition, yeast strains with catalytic point mutations in the Gcn5 HAT fail to acetylate gene promoters and to activate genes in response to de-repressing stimuli (Kuo et al., 1998; Lee et al., 2000). Furthermore, more recent experiments have found that the presence of HAT complexes and histone acetylation both stimulate transcription *in vitro* (Guermah et al., 2006; Ikeda et al., 1999; Kundu et al., 2000; Tse et al., 1998).

Acetylation has functions beyond just stimulating transcription. For instance, this mark helps prevent the spread of silent heterochromatin. In yeast, the telomeres, rDNA, and silent

mating type loci are actively deacetylated and silenced by the SIR (silent information regulator) proteins, most notably, the Sir2 histone deacetylase (Bryk et al., 1997; Gottschling et al., 1990; Imai et al., 2000; Rine and Herskowitz, 1987; Smith and Boeke, 1997). The confinement of silencing factors to these regions is enacted, in part, by acetylation of H4 on lysine 16 (H4K16) by the Sas2 (something about silencing) and Esa1 HATs (Kimura et al., 2002; Suka et al., 2002). Because the Sir3 silencing protein requires deacetylated H4K16 to spread Sir2 mediated-silencing along the chromatin fiber, Sas2-catalyzed H4K16 acetylation presents a barrier to Sir spreading (Liou et al., 2005).

Histone deposition and chromatin assembly have also been linked to histone acetylation. During S phase, histone H4 is rapidly acetylated on K5 and K12 in many eukaryotes (Chicoine et al., 1986; Sobel et al., 1995). This modification promotes associations between newly synthesized histones and chaperone proteins, which help to deposit the new histones into chromatin (Smith and Stillman, 1991). In yeast, acetylation of H4K5/12 is carried out by the HAT1 complex (Ai and Parthun, 2004; Poveda et al., 2004). However, unlike in other eukaryotes, in yeast, H4 K5, K8, and K12 acetylation all function redundantly to promote histone deposition (Ma et al., 1998). Once deposited into chromatin, these acetyl marks are rapidly removed, allowing other patterns of histone modifications, specific to the genomic region, to be set up (Annunziato and Seale, 1983; Jackson et al., 1976; Ruiz-Carrillo et al., 1975).

Rpd3 is a histone deacetylase with broad functions

Acetylation is not a permanent mark, but rather is actively removed from histones by eraser proteins called histone deacetylases or HDACs (also known as KDACs). Jack Taunton,

Christian Hassig, and Stuart Schreiber are credited with identifying the first HDAC. Taunton and colleagues used the irreversible HDAC inhibitor trapoxin to purify a protein from human thymus cells which turned out to be homologous to the known yeast repressor Rpd3 (Taunton et al., 1996). Shortly after, the Grunstein laboratory purified two complexes with HDAC activity from yeast, and identified the proteins Hda1 and Rpd3 as the subunits responsible for activity (Rundlett et al., 1996). These initial studies paved the way for the identification of many more HDAC proteins and complexes, including the discovery of at least seven more yeast HDACs, Hos1, Hos2, Hos3, Sir2, Hst1, Hst3, and Hst4 (Kurdistani and Grunstein, 2003).

Long before its HDAC function was known, the *RPD3* gene was identified by Marc Vidal and Richard Gaber in a screen for mutants that derepress the Trk2 potassium transporter in the absence of its activating protein, Trk1, and therefore had a reduced potassium dependency, compared with *trk1*Δ single mutants (Vidal and Gaber, 1991). This study also found that Rpd3 was required for both full repression and full activation of certain genes, suggesting that Rpd3 might be a transcriptional regulator. Consistent with this idea, Rpd3 has been linked with gene repression (Kadosh and Struhl, 1997, 1998; McKenzie et al., 1993; Stillman et al., 1994), a function which makes sense in light of the links between histone acetylation and transcription described above. In addition to a repressive function, some studies have found a requirement for Rpd3 activity in gene activation (Bowdish and Mitchell, 1993; Sharma et al., 2007; Xin et al., 2007). Because these studies did not demonstrate Rpd3 localization to the genes that require it for activation, some scientists have dismissed these findings as indirect effects of *RPD3* deletion (Humphrey et al., 2004). However, more recent studies have demonstrated that Rpd3 directly binds to the promoters of some of the genes that require it for activation (De Nadal et

al., 2004; Ruiz-Roig et al., 2010; Sertil et al., 2007; Sharma et al., 2007). Intriguingly, Rpd3 has also been shown to be required for activation of the *FLO11* gene locus, through a mechanism involving repression of *FLO11*-repressive noncoding RNAs originating in the *FLO11* promoter (Bumgarner et al., 2009). It remains unclear whether other examples of Rpd3-mediated gene activation are also cases where Rpd3 functions to repress noncoding RNAs that repress gene activity. Taken together, these studies suggest that while Rpd3 primarily functions to repress target genes, in certain contexts, this protein can function as a transcriptional activator.

In addition to gene regulation, Rpd3 also functions to antagonize silencing. In this regard, Rpd3 functions in an opposite fashion to the Sir2 HDAC mentioned above, which is required for silencing in yeast. Cells lacking Rpd3 have greater levels of silencing at telomeres, silent mating type loci, and rDNA (De Rubertis et al., 1996; Rundlett et al., 1996; Smith et al., 1999; Vannier et al., 1996). In addition, *rpd3*Δ cells have increased levels of Sir2 in heterochromatic regions and neighboring euchromatic regions (Zhou et al., 2009). Given that histone deacetylation is generally associated with gene repression, the increased silencing seen in *rpd3*Δ mutants may seem a bit puzzling. To reconcile these findings, some have suggested a model in which Rpd3 and Sir2 compete for binding sites at boundary regions (Smith et al., 1999; Sun and Hampsey, 1999; Zhou et al., 2009). According to this model, deletion of *RPD3* frees up more binding sites for Sir2, which then enhances silencing. Intriguingly, a recent study has found low levels of H4K12 acetylation, one of the preferred targets of Rpd3 deacetylation, at telomeric regions (Zhou et al., 2011). It is possible that the presence of this mark promotes heterochromatin formation, and that the higher levels of H4K12 acetylation found in *rpd3* knockout cells result in increased levels of silencing. While the exact mechanism by which Rpd3

antagonizes silencing is still unclear, this function for Rpd3 may explain the observation that *rpd3*Δ cells have increased lifespans, since loss of rDNA silencing is known to promote aging in yeast (Kim et al., 1999).

Rpd3 is a member of two known yeast complexes: Rpd3(S) and Rpd3(L). Rpd3(L) is the larger of the two known Rpd3 complexes, with 12 reported subunits (Carrozza et al., 2005b; Keogh et al., 2005). This complex localizes to the promoters of numerous genes and regulates transcription (Carrozza et al., 2005a). Rpd3(L)-mediated gene regulation has been shown to be important in diverse cellular processes. For instance, Rpd3 represses genes involved in meiosis, and *rpd3* mutants have sporulation defects (Dora et al., 1999; Hepworth et al., 1998; Lamb and Mitchell, 2001). Rpd3 also represses cell cycle genes (Bernstein et al., 2000; Takahata et al., 2009) and the *HO* endonuclease gene, which is important for yeast mating type switching (Vannier et al., 2001). In addition, and of particular interest to the research discussed in this thesis, Rpd3 has been shown to regulate both cellular stress and nutrient metabolism genes, a function that will be discussed in greater depth later in this introduction.

The Rpd3(S) complex consists of the subunits Sin3, Ume1, and Rpd3, which are shared with Rpd3(L), as well as the unique subunits Eaf3 and Rco1 (Carrozza et al., 2005b; Keogh et al., 2005). As mentioned earlier, the chromodomain and PHD finger of Eaf3 and Rco1, respectively, both interact with H3K36me2/3. Together, these interactions recruit Rpd3(S) to gene bodies to deacetylate histones within coding sequences and help reset chromatin that has been activated by transcribing RNA polymerase II (Krogan et al., 2003; Li et al., 2007; Li et al., 2003; Xiao et al., 2003). This genic deacetylation is most important at genes whose coding sequences serendipitously harbor regions that look like gene promoters. At these genes,

Rpd3(S)-mediated deacetylation helps suppress transcriptional initiation from these "cryptic" internal promoters, promoting transcriptional fidelity (Carrozza et al., 2005b; Joshi and Struhl, 2005; Keogh et al., 2005). In addition, a recent study has found Rpd3(S) at gene promoter regions, where it suppresses noncoding antisense transcription (Churchman and Weissman, 2011). The research described in this thesis pertains to the discovery of a third Rpd3 complex and my attempts to compare the function of that complex with known Rpd3(L) and Rpd3(S) functions.

Histone methylation also marks transcriptionally active chromatin in yeast

In contrast to acetylation, methylation does not alter the charge of the lysine side chain. Therefore, this modification is not thought to regulate chromatin structure in *cis*. Rather, the effects of lysine methylation are mediated primarily through the reader proteins that interact with this mark. There are three distinct states of lysine methylation. One, two, or even three methyl groups can be attached to the epsilon amino group of the lysine side chain, resulting in monomethylation (me1), dimethylation (me2), or trimethylation (me3), respectively. While the distinct roles of these three types of methylations at different lysines have not all been elucidated, there is evidence that different states of methylation are associated with different functions. For instance, in mammalian cells, H3K4me1 and H3K4me3 have different patterns of localization, with the former enriched in enhancer regions, and the latter enriched in gene promoters (Heintzman et al., 2007). In yeast, Oliver Rando and colleagues have shown that H3K4 methylation exists in a gradient throughout genes, with H3K4me3 levels peaking at the 5' ends, H3K4me2 levels high in the middle, and H3K4me1 levels high at the 3' ends (Liu et al., 2005).

Methylation of different histone residues is associated with different outcomes. At least 5 different sites of lysine methylation exist in mammalian H3 (K4, K9, K27, K36, and K79), along with one well characterized site of methylation on histone H4 (K20) (reviewed in Goll and Bestor, 2002; Lachner et al., 2003). H3K9, H3K27, and H4K20 methylation are all correlated with heterochromatin formation (Cao et al., 2002; Lachner et al., 2001; Muller et al., 2002; Nakayama et al., 2001; Schotta et al., 2004). In contrast, methylation of H3K4, K36, and K79, are all associated with transcriptionally active regions (reviewed in Martin and Zhang, 2005).

Of those six well-studied methylation sites, only H3K4, K36, and K79 are known to be methylated in budding yeast. Levels of H3K4 methylation peak in the promoters and 5' ends of genes (Pokholok et al., 2005). In contrast, H3K36 methylation is enriched in the middle and 3' ends of active genes, largely as a consequence of the association between the enzyme that writes this mark, Set2, and elongating RNA polymerase II (Krogan et al., 2003; Pokholok et al., 2005; Xiao et al., 2003). H3K79 methylation is also enriched in coding regions and is important for silencing (Ng et al., 2002; Pokholok et al., 2005; van Leeuwen et al., 2002). In addition to these sites, recent studies have identified H2BK37, H4K5, H4K8, H4K12, and H4K31 as sites of methylation in yeast, as well as H2AK99, H2BK43, H3K23, and H4K59 in mammals (Garcia et al., 2007; Gardner et al., 2011; Green et al., 2012; Hyland et al., 2011; Zhang et al., 2003). Future research will be key to discovering what roles these additional modifications play.

Histone methylation is catalyzed by a group of enzymes called histone methyltransferases (HMTs, also called lysine methyltransferases, or KMTs). These enzymes use the metabolite S-adenosyl-L-methionine (SAM) as a methyl donor. The first HMT was characterized by Steven Rea, Thomas Jenuwein, and colleagues who were studying Suv39h1, the mammalian homolog

of the *Drosophila* Su(var)3-9 suppressor of position effect variegation (Rea et al., 2000). The region of this protein responsible for methyltransferase activity was shared between SU(VAR)3-9 proteins, the *Polycomb*-group E(Z) protein, and the *trithorax*-group TRX protein, so this motif was named the "SET" domain. Shortly after this discovery, Scott Briggs and colleagues reported that in yeast, the Set1 protein functions as an H3K4 methyltransferase (Briggs et al., 2001), and the yeast Set2 and Dot1 proteins were found to methylate H3K36 and K79, respectively (Ng et al., 2002; Strahl et al., 2002; van Leeuwen et al., 2002).

While for many years, histone methylation was thought to be an irreversible modification, the discovery of a class of enzymes that erase this mark, called histone demethylases (HDMs, also called lysine demethylases, or KDMs) challenged this idea. Yang Shi and colleagues identified the first HDM, the mammalian LSD1 protein, based on its similarity to a class of enzymes called amino oxidases, which were known to be capable of oxidizing methylated proteins (Shi et al., 2004). LSD1 was shown to demethylate H3K4me1 and me2. However, this enzyme could not utilize H3K4me3 as a substrate, leaving open the question of whether histone trimethylation could be enzymatically erased. Subsequent work from Yi Zhang's laboratory identified a second class of HDMs, the Jumonji C, or JmjC, proteins, which were capable of erasing histone trimethylation (Tsukada et al., 2006). Further studies led to the identification of five JmjC proteins in budding yeast, Rph1, Gis1, Jhd1, Jhd2, and Ecm5, of which all but Ecm5 have been found to have activity (Kim and Buratowski, 2007; Klose et al., 2007a; Liang et al., 2007; Seward et al., 2007; Tu et al., 2007).

The PHD finger acts as a methyl-reader module

Numerous protein domains act as readers for histone lysine methylation, including chromodomains, Tudor domains, and MBT domains (Taverna et al., 2007). However, at the start of my graduate research, I took an interest in one type of reader module in particular, called the PHD, or plant homeodomain, finger. Initially identified in two plant homeodomain proteins that gave this module its name, the PHD finger is a protein domain that, depending on the specific example, differentially recognizes either methylated or unmodified lysine residues on histone tails. The PHD domain typically consists of a Cys4-His-Cys3 structure that coordinates two Zn^{2+} ions and contains two anti-parallel β sheets (Figure 1.3). There are 14 PHD finger-containing proteins, and a total of 18 PHD domains in yeast (Table 1.1), while humans have approximately 150 PHD finger proteins (Bienz, 2006).

Because of structural similarities between the PHD domain and the RING finger, a domain associated with ubiquitin E3 ligase activity, the PHD finger was initially thought to also be capable of ubiquitylation. However, all early examples of PHD fingers with E3 ligase activity were later shown to be misclassified RING domains, leading most researchers to abandon the hypothesis that PHD fingers could function as ubiquitin ligases (Aravind et al., 2003), an idea that I will revisit in the second chapter of this thesis. As the popularity of this hypothesis flagged, focus switched to the idea that PHD fingers might mediate chromatin interactions. Consistent with a chromatin function for these domains, many PHD finger-containing proteins are known to be nuclear and to contain other domains associated with chromatin regulation (Bienz, 2006). In addition, early studies showed that PHD fingers can interact with nucleosomes (Eberharter et al., 2001; Ragvin et al., 2004; Xiao et al., 2001). Soon after, the PHD fingers

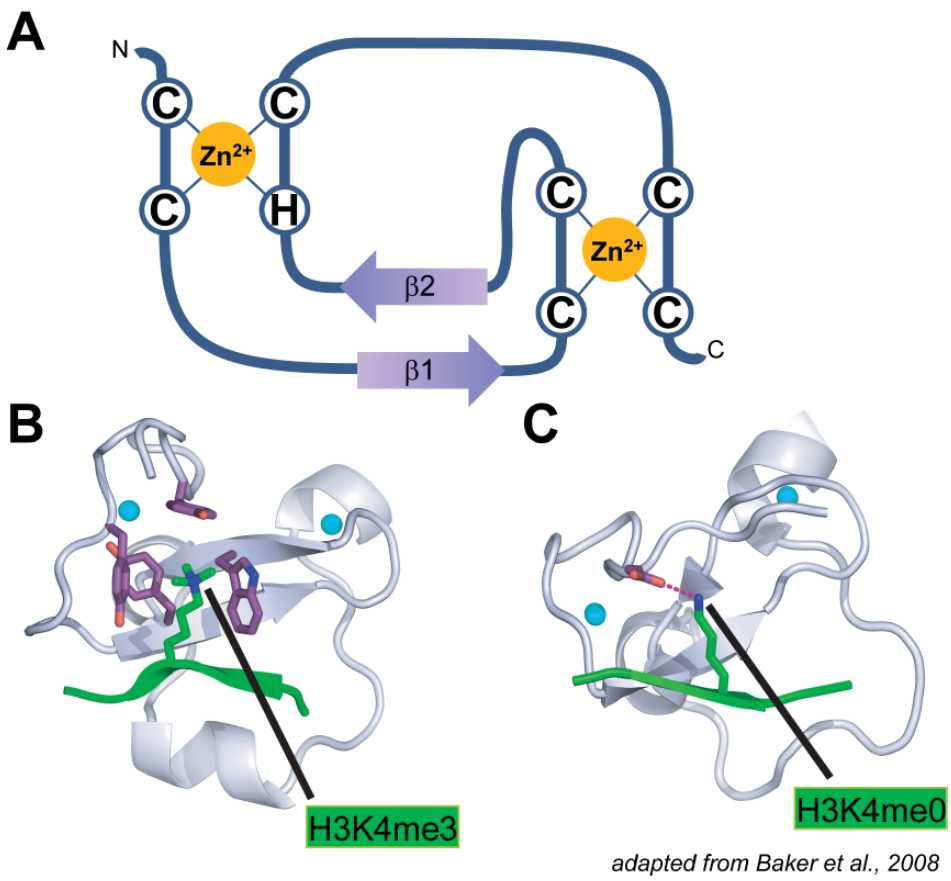

Figure 1.3 The PHD finger is a reader module that recognizes lysine methylation states **A.** The PHD finger fold is characterized by 4 cysteines, 1 histidine, and 3 more cysteines that coordinate 2 Zn^{2+} ions in a structure containing two anti-parallel β-sheets. **B and C.** The structures of the H3K4me3-binding PHD finger from the human BPTF protein (**B**) and the H3K4me0-binding PHD from human BHC80 (**C**) are shown with the PHD domain in silver, the H3K4 peptide in green, and the Zn^{2+} ions in cyan. Side chains of the residues critical for K4me0 or me3 interaction are in purple.

Table 1.1 The 14 PHD finger-containing proteins in *S. cerevisiae*[a]

Protein	# PHDs	Additional domains[c]	Nuclear	Related mammamlian proteins	Function
Set3	1	SET	Yes	MLL	Set3C HDAC complex
Yng2	1	n.d.	Yes	ING	NuA4 HAT complex
Jhd1	1	JmjC	Unknown	FBX10/11	H3K36 demethylase[d]
Set4	1	SET	Unknown	MLL	Predicted methyltransferase
Jhd2[b]	1	JmjN, JmjC	Yes	JARID	H3K4 demethylase[d]
Pho23	1	n.d.	Yes	ING	Rpd3(L) HDAC complex
Snt2[b]	3	SANT, BAH	Yes	Phf14	Unknown
Spp1	1	n.d.	Yes	CXXC1	Set1C HMT complex
Ecm5[b]	1	ARID, JmjC	Yes	JARID	Unknown
Rco1	2	n.d.	Yes	Phf12	Rpd3(S) HDAC complex
Yng1[b]	1	n.d.	Yes	ING	NuA3 HAT complex
Nto1	2	n.d.	Yes	BRD, BRPF	NuA3 HAT complex
Cti6	1	n.d.	Yes	BPTF	Rpd3(L) HDAC complex
Bye1	1	TFS2M	Unknown	ASH1L, TFIIS	Transcription elongation

[a] Adapted from Bienz, 2006

[b] These proteins are a particular focus of this thesis research

[c] n.d.: no additional domains found

[d] Discovered since I started this project (Liang et al., 2007; Seward et al., 2007, Tu et al., 2007)

of human BPTF (bromodomain and PHD finger transcription factor) and ING2 (inhibitor of growth-2) were shown to interact preferentially with histone H3K4me2/3, functionally linking PHD fingers to readout of histone methylation (Li et al., 2006; Pena et al., 2006; Shi et al., 2006; Wysocka et al., 2006).

Spurred by the excitement of those early discoveries, the chromatin field has seen a dramatic expansion of research into PHD fingers in recent years, leading to discoveries of histone ligands for a number of additional PHDs. These newer studies have reported many more examples of H3K4me-interacting PHD fingers. In addition, PHD fingers that preferentially associate with other methylated lysines, unmethylated lysines, acetylated lysines, and even methylated arginines on histones have also been found (reviewed in Li and Li, 2012). Furthermore, while PHD fingers have traditionally been thought of as mediators of histone interactions, the PHDs of the mammalian MLL1 and PYGO1 proteins have been shown to interact with non-histone proteins, expanding the potential roles of these domains (Fiedler et al., 2008; Miller et al., 2010; Wang et al., 2010).

The importance of PHD fingers in chromatin regulation is underscored by the number of human diseases that result from either direct mutation or altered regulation of this domain (Baker et al., 2008). For instance, mutations in the human RAG2 PHD finger, which normally interacts with H3K4me3 to recruit RAG2 to segments of the genome poised to undergo V(D) J recombination, are associated with the immunodeficiency disorders T-B-SCID and Omenn Syndrome (Matthews et al., 2007; Ramon-Maiques et al., 2007; Schwarz et al., 1996; Sobacchi et al., 2006). In addition, mutations in the first PHD of the AIRE (autoimmune regulator) protein, which is known to interact with unmethylated H3K4, are associated with another

immune disorder called autoimmune polyendocrinopathy-candidiasis-ectodermal dystrophy (APECED) (Bjorses et al., 2000; Org et al., 2008; Saugier-Veber et al., 2001). PHD mutations have also been associated with the neurological disorders Sotos Syndrome, Weaver Syndrome, ATR-X Syndrome, Rubenstein–Taybi Syndrome, and Borjeson–Forssman–Lehmann Syndrome (Argentaro et al., 2007; Douglas et al., 2003; Kalkhoven et al., 2003; Lower et al., 2002). Lastly, PHD translocations and point mutations are associated various types of cancer (Ayton and Cleary, 2001; Campos et al., 2004; Chen et al., 2003; Chen et al., 2001; Lochner et al., 1996; Reader et al., 2007; van Zutven et al., 2006; Wang et al., 2009). The links between mutations in the PHD module and so many different types of human disease give added importance to the goal of understanding the biology of these domains.

While many published studies have provided detailed examples of the mechanisms by which PHD fingers interact with chromatin and effect changes in chromatin regulation, there are still a large number of PHD finger proteins for which this understanding is lacking. Even in budding yeast, which has had the advantage of many years of genetic dissection, the exact ligands for many PHDs and the functions of the proteins that contain them are still not fully understood. In the research described in this thesis, I set out to better characterize the *in vivo* functions of two yeast PHD finger proteins, Jhd2 and Ecm5, and the contributions of their PHD fingers to those functions. When I started this work, very little had been published about these proteins, except that they contained other potential chromatin interacting domains (such as JmjC and ARID domains), and were known to be nuclear (Figure 1.4) (Bienz, 2006). In addition, Ecm5, or extracellular mutant 5, had been discovered in a screen from Howard Bussey's laboratory for mutants with impaired cell walls (Lussier et al., 1997). Based on this

knowledge, I hypothesized that both proteins were likely to have interesting and novel chromatin functions, and in the case of Ecm5, this might involve regulating genes involved in the cell wall. Shortly after starting this project, Jhd2 was shown to have H3K4 demethylase activity and was given its name, JmjC domain-containing histone demethylase 2, leading me to become all the more interested in what the function of Jhd2-catalyzed demethylation might be. (Liang et al., 2007; Seward et al., 2007; Tu et al., 2007) . At the same time, Ecm5, which also contains a JmjC domain, was shown not to have demethylase activity, leaving the function of this protein unknown.

Ecm5 and Jhd2 are homologous to the *Drosophila melanogaster* Lid protein, as well as to a mammalian family of proteins called the JARID proteins (Figure 1.4). This family consists of the RBP2, PLU-1, SMCX, and SMCY proteins (also called JARID1A/KDM5A, JARID1B/KDM5B, JARID1C/KDM5C, and JARID1D/KDM5D, respectively), and proper functioning of these proteins is important to human health. Mutations in SMCX are correlated with X-linked mental retardation and autism spectrum disorder (Adegbola et al., 2008; Ounap et al., 2012; Santos-Reboucas et al., 2011; Tzschach et al., 2006). PLU-1 is upregulated in breast cancer (Barrett et al., 2002; Lu et al., 1999). Furthermore, RBP2, a protein that interacts with retinoblastoma tumor suppressor protein is upregulated in gastric cancer, and translocations involving this protein, are found in some cases of acute myeloid leukemia (Fattaey et al., 1993; Reader et al., 2007; van Zutven et al., 2006; Wang et al., 2009; Zeng et al., 2010).

Like Jhd2, the mammalian JARID proteins are H3K4 demethylases (Christensen et al., 2007; Iwase et al., 2007; Klose et al., 2007b; Lee et al., 2007; Seward et al., 2007; Yamane et al., 2007). Intriguingly, Jhd2 and Ecm5 are each homologous to different sets of domains

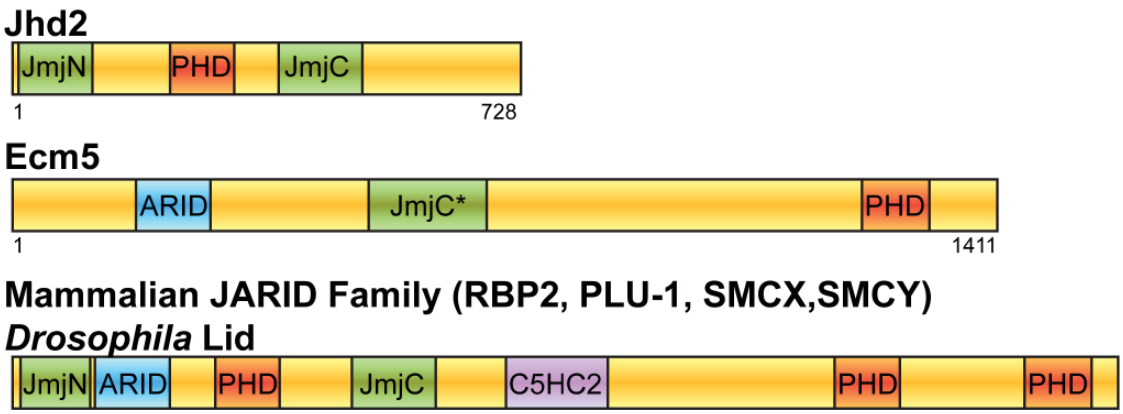

Figure 1.4 Jhd2 and Ecm5 are homologous to the *Drososphila* Lid and mammalian JARID proteins

Domain structures of Jhd2, Ecm5, and a typical JARID/Lid protein are shown. Domains are abbreviated as follows - JmjN: Jumonji N, JmjC: Jumonji C, PHD: Plant Homeodomain, ARID: AT-Rich Interaction Domain, C5HC2: Zinc Finger Domain with $Cys_5HisCys_2$-type structure. The asterisk in the Ecm5 JmjC domain denotes that this domain lacks demethylase activity.

within the JARID proteins, suggesting that yeast might have evolved two separate proteins that perform the JARID function together, while in mammals, this functionality is contained within one polypeptide. A detailed analysis of the functions of Jhd2 and Ecm5 will both aid in our understanding of general chromatin regulatory mechanisms and provide specific insights into how the mammalian JARID proteins function and contribute to human disease.

Chromatin regulation as a part of the yeast stress response and metabolism pathways

Many cellular pathways ultimately culminate in gene expression changes, and therefore rely on chromatin factors to enable transcription. This is certainly true of many of the yeast stress and metabolism pathways, which are related to this research (Figure 1.5). Regulation of yeast metabolism is governed by multiple major cellular pathways. (See Zaman et al., 2008, for an extensive review of yeast nutrient response regulation.) These pathways can be broadly divided into those that respond to carbon sources and those that respond to nitrogen sources. For instance, high glucose levels activate the yeast protein kinase A pathway through the Ras1 and Ras2 GTPases, which stimulate the production of cyclic AMP (cAMP) (Dechant and Peter, 2008). High levels of cAMP relieve repression of PKA, resulting in the phosphorylation of targets that promote glucose utilization and cellular growth. PKA signaling also activates genes involved in ribosome biogenesis and glycolysis and represses stress response genes. In a parallel pathway, the yeast Sch9 kinase, which is a homolog of the mammalian Akt/Protein Kinase B and S6 kinases, also promotes growth in response to glucose. Sch9 is also involved in nitrogen sensing, through the TOR pathway that will be discussed below (Jorgensen et al., 2004; Urban et al., 2007).

Figure 1.5 The complicated world of cell metabolism and oxidative stress regulation converges on the nucleus

Many of the yeast pathways involved in cellular metabolism and oxidative stress response are shown, with key pathway names are in blue boxes. Oxidative stressors (hydrogen peroxide: H_2O_2; superoxide: $O_2^{\cdot-}$; oxidized proteins: SOH) are in yellow. Nutrient stimuli (glucose: GLU; amino acids: AAs) are in dark green. Membrane receptors for some pathways are in pink. A cysteine-containing protein is shown in red. The main kinases or effectors of the pathways are in orange, except for Yap1, which is in purple. Transcription factors downstream of the various pathways are in light green.

Figure 1.5 The complicated world of cell metabolism and oxidative stress regulation converges on the nucleus

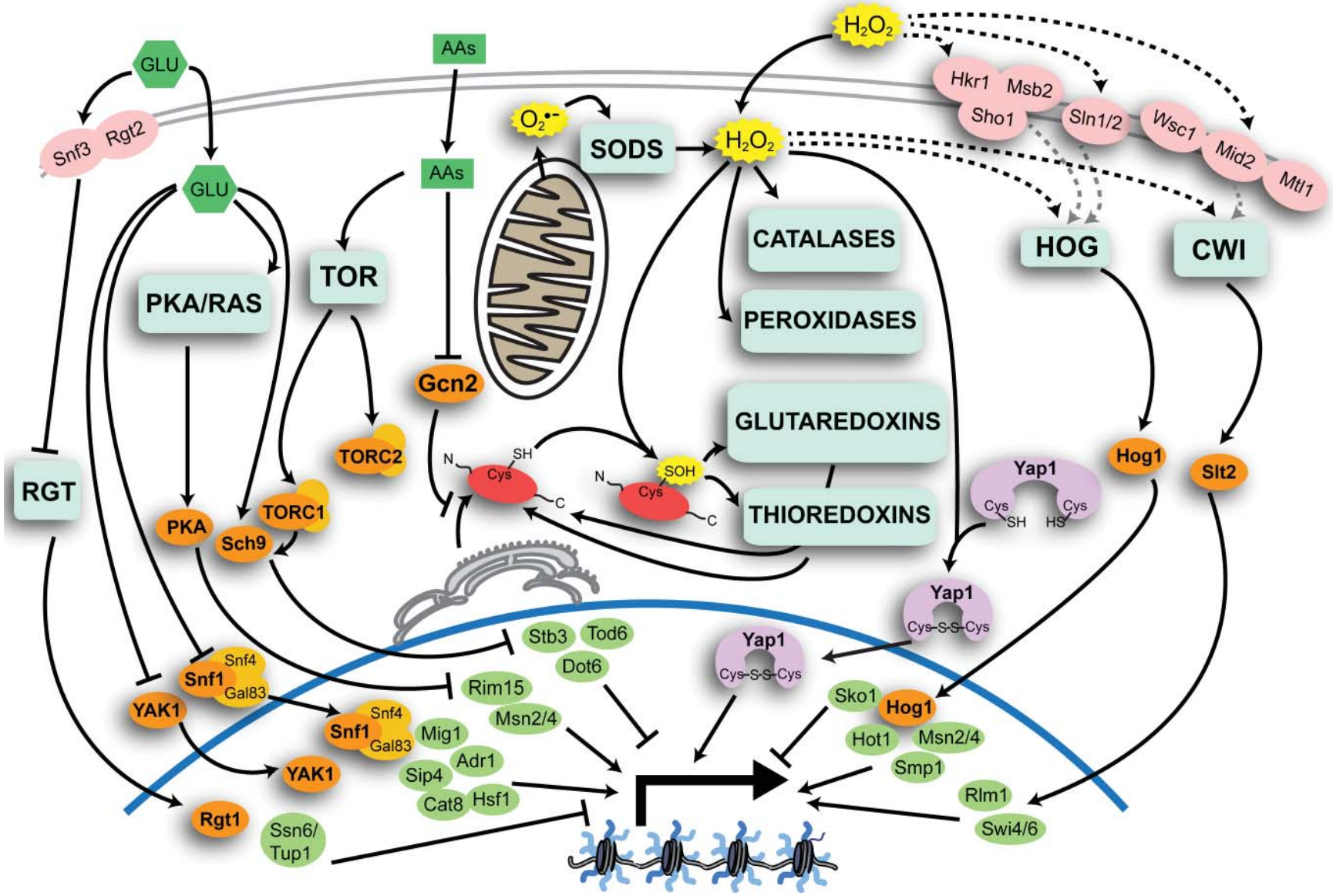

When glucose is limiting, the Yak1, Snf1(AMPK), and RGT pathways work to inhibit biomass production and promote utilization of alternate carbon sources. The absence of glucose promotes the nuclear localization of both the Yak1 and Snf1 kinases. Nuclear Yak1 phosphorylates downstream targets, including the Pop2 subunit of the Ccr4-Not complex which functions in both RNA degradation and transcriptional regulation (Moriya et al., 2001). Nuclear Snf1, the yeast homolog of the mammalian AMP-activated protein kinase (AMPK), promotes the repression of glucose catabolism genes through the Mig1 protein (Hedbacker and Carlson, 2008). Snf1 also promotes the activation of genes involved in nonfermentable carbon source metabolism, fatty acid oxidation, and stress response through a variety of transcription factors, including Adr1, Cat8, Sip4, and Hsf1. In the absence of glucose, the RGT network promotes repression of different hexose transporter genes by the Rgt1 and Ssn6-Tup1 repressors (Johnston and Kim, 2005). In low to moderate levels of glucose, this network also ensures selective expression of the hexose transporters with the appropriate affinities for the amount of glucose present.

Two key pathways are associated with nitrogen sensing in yeast. First, low amino acid levels activate the GCN (general control non-derepressable) pathway. The effector of this pathway is the Gcn2 kinase, which is activated by interaction with the uncharged tRNAs that accumulate when amino acid concentrations are low. Activated Gcn2 phosphorylates the translation initiation factor eIF2α, inhibiting translation of most genes, while at the same time, promoting translation of the transcription factor Gcn4. Once translated, Gcn4 activates genes involved in amino acid biosynthesis. The TOR pathway responds to nitrogen levels through two protein kinase complexes: TORC1 and TORC2. In contrast to the GCN pathway, TOR

complexes are active when amino acids are abundant. While both TOR complexes regulate growth, TORC1 does so by promoting protein synthesis, production of translation machinery, and cellular uptake of nitrogen and carbon sources, while TORC2 is regulates cell polarity and endocytosis (De Virgilio and Loewith, 2006). In addition, TORC1, but not TORC2, is sensitive to inhibition by the antifungal and chemotherapeutic agent rapamycin. Treatment of yeast cells with rapamycin, promotes many of the same cellular changes as starvation, making this drug a useful tool in studying nutrient stress (Loewith et al., 2002). The exact mechanisms by which amino acid levels stimulate TORC activation are still unclear, although many of the downstream targets of TORC1, including the Sch9 kinase, are known. In response to TOR signaling, Sch9 inhibits repressors like Stb3, Dot6, and Tod6, promoting expression of ribosome biosynthesis and ribosomal protein genes .

In addition to pathways that sense nutrient levels, yeast have multiple pathways that sense and respond to cellular stressors like oxidative stress, which is another focus of this work. Oxidative stress is primarily caused by reactive oxygen species (ROS), highly reactive oxygen-containing molecules including oxygen ions and peroxides (Freinbichler et al., 2011). At low levels, ROS do not necessarily present a challenge to yeast cells because dedicated families of enzymes can detoxify them. In fact, yeast actively generate small amounts of ROS as a biproduct of oxidative phosphorylation through the mitochondrial electron transport chain (ETC), which couples NADH production in the TCA cycle to ATP generation (Kowaltowski et al., 2009; Lambert and Brand, 2009). Usually, electrons flowing through the ETC eventually interact with molecular oxygen, to generate water. On occasion, this transfer can be incomplete, resulting in the ROS superoxide ($O_2^{\bullet -}$). Superoxide, itself, is quite toxic, but superoxide dismutase (SOD)

enzymes in the mitochondria and cytoplasm can convert superoxide to hydrogen peroxide (H_2O_2) (Fridovich, 1995). H_2O_2 is also a byproduct of fatty acid oxidation in peroxisomes. While this ROS is less toxic than superoxide, it can still cause damage by oxidizing macromolecules in the cell directly, or by being partially reduced to the hydroxyl radical ($^{\bullet}OH$), an extremely powerful oxidant. Proteins are particularly sensitive to oxidation, which can convert the sulfhydryl group of cysteine and methionine side chains into sulfenic, sulfinic, or sulfonic acid (D'Autreaux and Toledano, 2007). Cellular catalase and peroxidase enzymes perform an important function by converting H_2O_2 to water (Herrero et al., 2008). In addition, some small molecules in the cell, such as reduced glutathione (GSH), ascorbate or vitamin E can act as antioxidants, further protecting cells from ROS-induced damage (Evans and Halliwell, 2001).

While these enzymes and antioxidants work well at detoxifying small amounts of ROS, larger doses of oxidants require the use of cellular stress response pathways for detoxification. Damaged proteins can be repaired by thioredoxin, glutaredoxin, and the methionine sulphoxide reductase proteins (Herrero et al., 2008). The Yap1 transcription factor also helps cells cope with ROS (Rodrigues-Pousada et al., 2010). Yap1 is known to be localized to the cytoplasm in unstressed cells. Upon exposure to ROS, the peroxidase protein Gpx3 acts as redox sensor and ultimately causes a intramolecular double bond to form between two cysteines in Yap1, resulting in a conformational change that causes Yap1 to accumulate in the nucleus and activate stress genes.

In addition to these pathways, yeast respond to oxidative stress through two mitogen activated protein kinase (MAPK) pathways. The high-osmolarity glycerol (HOG) pathway is primarily associated with osmotic stress response. In response to this stress, the HOG pathway

becomes activated, leading to phosphorylation of the Hog1 MAPK (de Nadal and Posas, 2010). Active Hog1 relocalizes to the nucleus and both associates with genes directly and promotes a transcriptional response through the Smp1, Hot1, and Msn2/4 transcriptional activators and the Sko1 repressor (Alepuz et al., 2001). Oxidative stress also activates the HOG pathway (Bilsland et al., 2004; Haghnazari and Heyer, 2004; Singh, 2000). Furthermore, a recent study found that hypoxia activates this pathway as well (Hickman et al., 2011). While osmotic stress results in rapid phosphorylation of Hog1 within minutes (Maeda et al., 1995), both oxidative stress and hypoxia promote a more gradual phosphorylation of Hog1, with the former peaking 1 hour after the onset of stress and the latter peaking 4-5 hours afterward (Bilsland et al., 2004; Hickman et al., 2011). These results suggest that timing of the HOG response may help dictate which genes are regulated. Acute hypoxia is known to transiently induce oxidative stress in yeast, most likely through increased ROS production caused by impaired flux through the mitochondrial ETC (Dirmeier et al., 2002). Thus, these two Hog1 responses might be linked.

The Cell Wall Integrity (CWI) MAPK pathway, has also been reported to respond to oxidative stress (Alic et al., 2003; Vilella et al., 2005). This pathway is activated by numerous inducers of cell wall stress, including acid exposure, heat shock, and hypo-osmolarity, chemicals that bind to or degrade the cell wall, and caffeine treatment (Levin, 2005). Once activated, the CWI pathway activates the Slt2 MAPK, which regulates cell wall remodeling, vesicular trafficking to the cell wall, and the expression of cell wall biosynthesis genes through the Swi4/6 transcription factors. Oxidative stress is thought to activate this pathway either through direct oxidation of lipids in the plasma membrane, where sensors of cell wall stress are located, or through the activation of Ask10, which may activate Slt2 via activation of an upstream kinase (Levin, 2005).

There are numerous lines of evidence that the yeast nutrient sensing and oxidative stress response pathways are linked. As mentioned above, respirative ATP metabolism is known to produce ROS. Both caloric restriction and the presence of yeast antioxidant genes have been shown to extend replicative lifespan (Barker et al., 1999; Lin et al., 2002). Furthermore, both starvation and oxidative stress trigger yeast to produce trehalose (Benaroudj et al., 2001; Lillie and Pringle, 1980). This disaccharide is thought to help yeast cope with these stresses, both by preserving the integrity of the plasma membrane and by acting as a protein chaperone (Crowe et al., 1984; Singer and Lindquist, 1998). Furthermore, inhibition of the TOR pathway, which mimics starvation, leads to the activation of the known stress transcription factors Msn2/4 as well as activation of genes involved in the oxidative stress response (Bandhakavi et al., 2008; Beck and Hall, 1999). Conversely, oxidative stress leads to the inhibition of protein synthesis and is known to activate the Snf1 kinase (Hong and Carlson, 2007; Shenton and Grant, 2003). In addition, diverse forms of stress as well as starvation activate the same set of genes, called "the environmental stress response" (Gasch et al., 2000).

Many chromatin regulators are known to be involved in the yeast metabolic and stress pathways. For instance, numerous studies have linked diverse chromatin regulators, including the NuA4, Gcn5, and Rtt109 HATs; the Swi/Snf and Ino80 remodelers; and the Asf1 and Spt6 chaperones, to regulation of the *PHO5* gene, which is known to be induced by low phosphate levels, resulting in the loss of positioned nucleosomes at the *PHO5* promoter (Rando and Winston, 2012). Gcn5 is also needed for the activation of the Snf1 target gene, *ADY2* (Abate et al., 2012). Yeast growth and stress genes are known to be differentially regulated by the TFIID and SAGA complexes, respectively, both of which have HAT activity (Huisinga and Pugh,

2004). SAGA, SWI/SNF, and RSC (another chromatin remodeler), are all needed to activate genes in response to osmotic stress (Mas et al., 2009; Pokholok et al., 2006), while Rtt109, Asf1, and Ino80 are needed to repress genes that have become activated in response to this stress (Klopf et al., 2009). Moreover, a genome-wide ChIP study reported that the associations of a myriad of chromatin regulators with the stress gene promoters change after heat shock, consistent with roles for many of these proteins in regulating transcription in response to stress (Venters et al., 2011).

Notably for the research presented in this thesis, multiple studies have linked the Rpd3 HDAC with regulation of stress and metabolic genes. Rpd3 and Sin3 are needed for the repression of rRNA and ribosomal protein genes after rapamycin treatment (Rohde and Cardenas, 2003; Tsang et al., 2003). A separate study found that Rpd3(L) is recruited to promoters of ribosomal biogenesis and ribosomal protein genes, which it represses in response to inactivation of the Sch9 TOR pathway effector (Huber et al., 2011). Rpd3 is also required for gene activation after rapamycin treatment, although it is unclear whether this is due to a direct activating role of Rpd3 or due to indirect effects (Humphrey et al., 2004). Rpd3 is also needed for gene activation and repression following heat shock (Kremer and Gross, 2009; Ruiz-Roig et al., 2010), and for gene activation after osmotic shock (De Nadal et al., 2004).

While these studies link chromatin function to gene expression following nitrogen stress, heat shock, and osmotic stress, less is known about the chromatin proteins needed to regulate gene expression following oxidative stress. Furthermore, the field still does not know all of the proteins involved in gene regulation upon these stresses. A recent study mapped the localization of 200 transcription-related proteins and found that 93% of yeast genes were occupied by at least 10 regulators, suggesting that diverse combinations of regulators at different sets of genes

may underlie the complex regulation downstream of many of these pathways (Venters et al., 2011). Even in yeast, in which most of these pathways have been studied extensively, there are still many proteins, like the PHD finger proteins I described above, that are suspected or known to interact with chromatin, but whose functions remain unclear. Sorting out these how these stress and metabolism pathways are regulated has relevance to numerous human disease states, including cancer, diabetes, and aging (Alic and Partridge, 2011; Dazert and Hall, 2011; Lin and Beal, 2006; Roberts and Sindhu, 2009).

Chromatin as a sensor of metabolic state

In addition to regulating metabolism genes, chromatin and metabolism are intimately linked by the use of cellular metabolites as precursors for histone modifications (Table 1.2) (Teperino et al., 2010; Wallace and Fan, 2010; Wellen and Thompson, 2010). The best-studied example of a metabolite that connects chromatin and cellular energy state is acetyl-CoA, a key molecule in the tricarboxylic acid (TCA) cycle which also serves as the acetyl source for histone acetylation. Recent studies have shown that yeast go through metabolic cycles, oscillating between using glycolysis and oxidative respiration as the main source of energy (Slavov et al., 2011; Tu et al., 2005). Just as levels of oxygen consumed fluctuate through these cycles, acetyl CoA levels also show periodicity (Cai et al., 2011). The levels of histone acetylation also fluctuate in these cycles, suggesting that histone proteins may also be a cellular metabolic sink. The link between acetylation levels and energy status makes some sense: since acetylation levels and transcriptional activity are correlated, the enrichment of histone acetyl levels when acetyl-CoA is abundant ensures that cells will be transcribing at maximal rates when they have enough energy stored to make biomass.

Table 1.2 Cellular metabolites used by histone writer and eraser enzymes

Metabolite	Histone writer or reader that uses metabolite	Metabolic function
Acetyl coenzyme A (acetyl-CoA)	Histone acetyltransferases	Produced during aerobic respiration
Nicotinamide adenine dinucleotide (NAD^+)	Sirtuin-family histone deacetylases	Facilitates metabolic redox reactions
S-Adenosyl methionine (SAM)	Histone methyltransferases	Used in metabolic methylation pathways
Uridine diphosphate N-acetylglucosamine (UDP-GlcNAc)	Histone glycosyltransferase	Used to make nitrogen-containing sugars
α-ketoglutarate (α-KG)	Histone demethylases	Intermediate in the TCA cycle

Acetyl-CoA is not the only chromatin enzyme cofactor that is also involved in metabolism. The Sirtuin family of HDACs require NAD^+ for activity, linking histone deacetylation to the cellular NAD^+/NADH ratio, a readout of the redox state of the cell (Imai et al., 2000). The precursor for histone methylation, S-adenosyl methionine (SAM), is a key metabolite involved in the generation of the amino acids cysteine and methionine (Teperino et al., 2010). In addition, histone demethylation depends on α-ketoglutarate, an intermediate in the TCA cycle. Lastly, histone O-GlcNAcylation requires the molecule UDP-GlcNAc as a donor (Hanover, 2010). This sugar is created by the hexosamine biosynthesis pathway and is used to make cellular glycosaminoglycans, proteoglycans, and glycolipids.

Intriguingly, some metabolic enzymes have been detected in the nucleus, suggesting that metabolic regulation of chromatin is occurring locally. For instance, the metabolic enzyme S-adenosylhomocysteine hydrolase (SAHH), which cleaves S-adenosylhomocysteine, a byproduct of cellular methylation reactions, can be found in the nuclei of frog embryos (Radomski et al., 1999). Furthermore, the enzyme S-adenosyl methionine transferase, which is known to generate SAM from methionine, is partially localized to the nuclei of rat cells (Reytor et al., 2009). In yeast, the enzymes Arg5/6, which are involved in arginine biosynthesis, also can be found in the nucleus and regulate gene expression (Hall et al., 2004). In addition, the enzymes that generate acetyl-CoA in yeast, Acs1 and Acs2, have been found in the nucleus as well (Huh et al., 2003; Takahashi et al., 2006). The reason for the nuclear localization of these metabolism enzymes is not clear. In some cases, they might be creating locally high concentrations of cofactors needed for histone modification. Alternatively, they might have entirely novel nuclear functions, potentially acting as transcription factors.

PHD finger proteins, stress, and metabolism

The research described in this thesis initiated with my wanting to understand how PHD finger-containing proteins contribute to chromatin regulation. Specifically, this thesis describes my work to explore the functions and associations of the yeast PHD finger proteins Jhd2 and Ecm5. In the next chapter, I will describe experiments I performed to characterize the chromatin associations of the Jhd2 and Ecm5 PHD domains. I will also summarize experiments to test the hypothesis that a yeast PHD domain might function as a ubiquitin ligase. In the third chapter of this work, I will describe experiments aimed at determining the functions of Jhd2 and Ecm5, and the exciting discovery that Ecm5 forms a complex with Snt2 and the Rpd3 HDAC. In the fourth chapter I will present evidence that this new Rpd3 complex functions in the yeast oxidative stress and metabolic response pathways. Finally, in the fifth chapter, I will some discuss potential mechanisms by which this new Rpd3 complex regulates these pathways, future experiments to test these mechanisms, and the greater implications of this work.

CHAPTER 2: BIOCHEMICAL EXPERIMENTS TO CHARACTERIZE THE YNG1, JHD2, AND ECM5 PHD FINGERS

Chapter Introduction

The PHD finger is one member of a diverse set of domains that interact with specific histone modification states. Originally named for the plant homeodomain proteins first shown to contain this domain, the PHD finger has a characteristic Cys4-His-Cys3 signature which coordinates two Zn^{2+} ions (Bienz, 2006). As discussed in the previous chapter, this domain is capable of recognizing specific lysine methylation states on histone proteins. In recent years, a number of elegant studies have characterized the structures and histone associations of a diverse array of PHD domains. A recent review from Li and Li (2012) elegantly summarizes these studies. However, in spite of these advances, there is still much to be discovered. Although many PHD domains have been characterized structurally and biochemically, there are abundant examples of PHDs for which a ligand has not been found, making it difficult to ascertain how these domains contribute to the functions of the proteins that contain them. Having studied yeast genetics and chromatin biology as an undergraduate, I immediately sought to take advantage of the potential of the budding yeast, *S. cerevisiae*, to address some of these questions. There are 14 PHD-finger-containing proteins in yeast. (See Table 1.1, in the introductory chapter, for more information about these proteins.) Many of these yeast PHD-containing proteins are known subunits of chromatin regulatory complexes, and all but three are known to localize to the nucleus (Bienz, 2006). Thus, it is likely that most, if not all, yeast PHD finger proteins play important roles in chromatin regulation.

Because of my interest in these domains, I began to work with Sean Taverna, a former postdoctoral fellow in the Allis laboratory, to assist him in the characterization of the interactions of the NuA3 Yng1 PHD finger with chromatin. The first part of this chapter will focus on pull-downs I performed with Sean's help, to confirm an association between the Yng1 PHD finger and H3K4me3. Upon completion of the Yng1 project with Sean, I became interested in two additional PHD-containing proteins, Ecm5 and Jhd2. Unlike Yng1, whose interaction with the NuA3 histone acetyltransferase complex had been known before Sean and I started our experiments, the functions of Jhd2 and Ecm5 were largely unknown. I therefore set out to determine whether the PHD fingers of Jhd2 and Ecm5 could interact with histones. This work is the focus of the second part of this chapter.

The third section of this chapter describes *in vitro* experiments I performed to explore whether yeast PHD fingers might function as ubiquitin E3 ligases. PHD fingers are structurally similar to RING domains, which are known to have ubiquitin ligase activity (Jackson et al., 2000). As part of my work studying PHD fingers, I noticed that the Ecm5 PHD was extremely similar to that of the *S. pombe* protein Msc1, a protein whose three PHD fingers were all reported to have ubiquitin ligase activity (Dul and Walworth, 2007). I therefore wondered whether the Ecm5 PHD finger, or for that matter any other yeast PHD finger, might function as a ubiquitin E3 ligase. With the help of Ronen Sadeh, a postdoctoral fellow in the Allis laboratory, I set out to test whether yeast PHD domains translated *in vitro* possessed ubiquitin E3 ligase activity.

The Yng1 PHD Finger Preferentially Interacts with H3K4me3

The NuA3 histone acetyltransferase (HAT) complex is one of at least eight complexes in yeast responsible for setting and maintaining the high levels of histone acetylation characteristic of yeast chromatin (Carrozza et al., 2003). The isolated NuA3 complex is about 500 kDa, and has been shown to contain the proteins Taf30 (Taf14/Anc1/Tfg3), Yng1, and the HAT/MOZ domain-containing Sas3 protein, responsible for HAT activity (Eberharter et al., 1998; Howe et al., 2002; John et al., 2000). Because of his own interest in this complex, Sean Taverna purified the NuA3 complex, and identified the proteins Nto1 and Eaf6 as additional subunits of this complex (data not shown). Both Yng1 and Nto1 contain PHD fingers, suggesting the possibility that these domains might be involved in NuA3-chromatin interactions. In addition, the entire Yng1 protein had previously been shown to interact with H3K4me3, suggesting that this subunit in particular might play a role in mediating the interaction between NuA3 and chromatin (Martin et al., 2006). However, whether this interaction was mediated through the Yng1 PHD finger was unclear.

Thus, during my rotation in the Allis laboratory, Sean and I set out to determine whether the Yng1 PHD domain interacts with H3K4me3. To that end, Sean purified recombinant, N-terminally GST-tagged Yng1 PHD domain (residues 141-219 of full-length Yng1). I then purified endogenous yeast histones by acid extraction from cryogenically-prepared yeast lysates, to use in combination with the tagged Yng1 PHD for *in vitro* binding assays. We chose to use endogenous yeast histones rather than purified recombinant histones because we expected the former to have the full complement of histone modifications occurring in yeast, and thus, to potentially contain the "right" combination of modifications (if there is any) to interact with

the Yng1 PHD. As a negative control, we used a recombinant GST-Yng1 PHD point mutant, in which the tryptophan corresponding to position 180 in full-length Yng1 had been mutated to glutamate (GST-Yng1-W180E); based on comparisons to other PHD fingers, this mutation was predicted to abolish binding to methylated lysines (Martin et al., 2006).

When combined with the yeast histones, the GST-Yng1 PHD fusion preferentially pulled-down histone H3, and not appreciable amounts of the other core histones (Figure 2.1). In contrast, no enrichment of H3 was seen in pull-downs with the tagged Yng1-W180E PHD. Furthermore, the H3 pulled-down by the tagged Yng1 PHD was enriched for H3K4me3, and to a lesser extent, H3K4me2, suggesting that the Yng1 PHD domain might interact preferentially with this mark. Further fluorescence anisotropy experiments by Sean Taverna confirmed an association of the Yng1 PHD domain with H3K4me2/3, and found that the Yng1 PHD domain interacts preferentially with an N-terminal H3 peptide containing trimethylated lysine 4. The dissociation constant (K_d) for this interaction was 9.1 μM, compared to K_ds of 21.4, 50.7, and >400 μM for interactions with H3K4me2, H3K4me1, and unmodified H3K4 peptides, respectively (Taverna et al., 2006). Furthermore, using chromatin immunoprecipitation (ChIP), Sean was able to show that Yng1 localizes to genomic locations containing high levels of H3K4me3, and that when the Yng1 PHD finger was mutated, there was decreased H3K14 acetylation and transcription at target genes. All together, the *in vitro* binding assay performed by me, and the anisotropy and ChIP experiments performed by Sean all show that the Yng1 PHD finger can interact with H3K4me3, an interaction that helps target or stabilize an association of the NuA3 HAT complex with active chromatin regions of the yeast genome, where it can then acetylate H3 in these regions.

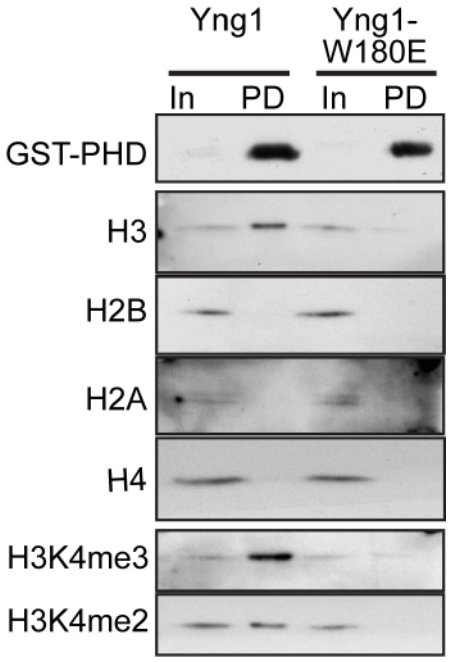

Figure 2.1 Recombinant, GST-tagged Yng1-PHD finger interacts with histone H3 enriched for K4me3

GST-tagged Yng1-PHD or Yng1-PHD-W180E fusions were incubated with acid-extracted yeast histones and pulled-down using glutathione sepharose. Western blotting with histone-specific antibodies was used to look for histones and modifications that preferentially associate with the Yng1 PHD finger. Inputs (In) are 8% of pull-downs (PD).

The Jhd2 and Ecm5 PHD Fingers Interact with Histone H3

Having helped to uncover an association between the Yng1 PHD domain and H3K4me3, I turned my attention to two other PHD finger-containing proteins, Ecm5 and Jhd2, the functions of which were completely unknown at the time. Because both proteins contained multiple domains (ARID, JmjN, JmjC) linked to chromatin function, in addition to their PHD fingers, I reasoned that they might have interesting and novel chromatin regulatory functions. I was intrigued that both proteins contained Jumonji C (JmjC) domains, which had just been shown to have histone lysine demethylase activity in other proteins, leading me to wonder whether Jhd2 and Ecm5 might be yeast histone demethylases. In fact, shortly after I started this project, Jhd2, which until that point was being referred to by its open reading frame name (*YJR119C*), was shown to have H3K4 demethylase activity through its JmjN and JmjC domains, and was therefore named JmjC domain-containing histone demethylase 2, or Jhd2 (Liang et al., 2007; Seward et al., 2007; Tu et al., 2007). However, it remained unclear whether the PHD domain of Jhd2 interacted with histones, and whether this interaction was dependent on specific histone modifications. Furthermore, the contribution of the Jhd2 PHD to the protein's histone demethylase function was also unknown.

In contrast to the JmjN and C domains of Jhd2, the Ecm5 JmjC domain was found not to have histone demethylase activity (Tu et al., 2007), and closer examination of this domain revealed that it lacks residues thought to be necessary for enzymatic activity, making it unlikely that Ecm5 functions as a demethylase. Therefore, I chose to focus on what functions this protein might possess besides histone demethylation. Ecm5 (or extra cellular mutant 5) was originally discovered in a screen for mutants with cell wall defects (Lussier et al., 1997). Because Ecm5

contains multiple chromatin-related domains and because Ecm5 is known to be nuclear, I originally hypothesized that Ecm5 might have some role in regulating genes involved in cell wall maintenance. In addition, Ecm5 and Jhd2 are roughly homologous to the mammalian JARID family of demethylases, RBBP2, PLU-1, SMCX, and SMCY (also called JARID1A/KDM5A, JARID1B/KDM5B, JARID1C/KDM5C, and JARID1D/KDM5D, respectively. As discussed in the previous chapter, improper regulation of these proteins is linked with various human diseases. Therefore, insights into the functions of Ecm5 and Jhd2 might have implications for the functions of the human JARID proteins, as well as for their roles in human disease.

In order to better understand Jhd2 and Ecm5, I first wanted to determine whether the PHD fingers of these proteins can interact with histones. I compared the Jhd2 and Ecm5 PHD finger sequences to those of the yeast Yng1 and human ING2 and BPTF PHD fingers, all of which are known H3K4me3-binders whose structures have been solved. Alignments of these PHDs show that while the Ecm5 PHD has a slightly longer second loop region than most other PHDs, it is similar to the H3K4me3-binding PHD domains (Figure 2.2). Three of the four key residues found to interact with H3K4me3, are conserved in the Ecm5 PHD (residues colored blue and red in Figure 2.2), as are two of the three residues known to be important for binding unmodified H3R2 (residues colored green and red). Thus, it seemed possible that the Ecm5 PHD finger might also recognize H3K4me3 or another methylation site (Figure 2.2). In contrast, the Jhd2 PHD was more divergent at these residues, suggesting this PHD either does not interact with histone methylation, or that it does so in an entirely different manner from other known H3K4me3-binding PHD fingers.

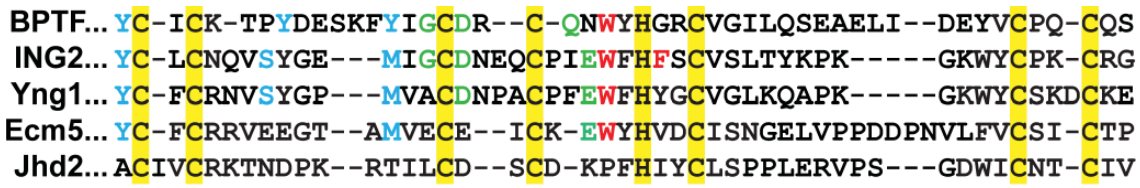

Figure 2.2 Alignments of the BPTF, ING2, Yng1, Ecm5, and Jhd2 PHD fingers
Shown are alignments of amino acids Y2743-S2791, Y214-G260, Y157-E204, Y1240-P1289, and A237-V284 of the full-length BPTF (*Homo sapiens*, NCBI accession # NP_872579.2), ING2 (*Homo sapiens*, # NP_001555.1), Yng1 (*S. cerevisiae*, # NP_014707.1), Ecm5 (*S. cerevisiae*, # NP_013901.1), and Jhd2 (*S. cerevisiae*, # NP_012653.1) proteins, respectively. The amino acids that make up the characteristic $Cys_4His_1Cys_3$ structure that defines the PHD finger are highlighted in yellow. For the BPTF, ING2, and Yng1 PHD fingers, whose structures have been solved, the residues known to interact with H3K4me3 are colored in blue, the residues that interact with H3R2 are in green, and the residues that form the separation between the H3R2 and H3K4me3 binding pockets are in red. Corresponding conserved residues in the Ecm5 PHD finger sequence are also colored in this manner.

I then set out to characterize the interactions of the Jhd2 and Ecm5 PHD fingers with histones, using the same *in vitro* binding assay described earlier in this chapter. I first purified recombinant, GST-tagged Jhd2 and Ecm5 PHD fingers (residues G221-L300 and S1232-D1295, respectively, of the full-length proteins), as well as GST alone, from *E. coli* (Figure 2.3). As a positive control for this assay, I used the GST-Yng1-PHD fusion, which again pulled down histone H3. The tagged Jhd2 PHD also pulled-down H3 in this assay (Figure 2.4). GST alone and the GST-Yng1-W180E-PHD fusion, which served as negative controls for this assay, did not pull down appreciable levels of any histone. These results suggest that the Jhd2 PHD finger interacts with histone H3.

To try to determine whether a specific histone modification on H3 mediates the Jhd2-PHD interaction, I then blotted the eluates from my tagged Jhd2 PHD pull-downs with antibodies recognizing specific histone modifications. In contrast to the H3 pulled-down by the tagged Yng1 PHD, which again was enriched for H3K4me3, the H3 pulled-down by the tagged Jhd2-PHD was enriched for H3K36me3 (Figure 2.4, bottom two panels). To confirm a direct interaction between the Jhd2 PHD and H3K36me3, I next conducted peptide pull-down experiments with tagged Jhd2 PHD finger and biotinylated peptides containing either trimethylated or unmodified H3K36. However, I failed to observe enrichment of the tagged Jhd2 PHD in pull-downs with H3K36me3 peptides (data not shown). Taken together, these data suggest an interaction between the Jhd2 PHD finger and histone H3 is unlikely to be mediated solely by a direct interaction with H3K36me3. Jhd2 may instead interact with a yet unknown histone modification state correlated with high levels of H3K36me3. Alternatively, Jhd2 may require a combination of more than one modification (e.g, H3K4me3 and H3K36me3) to interact with H3.

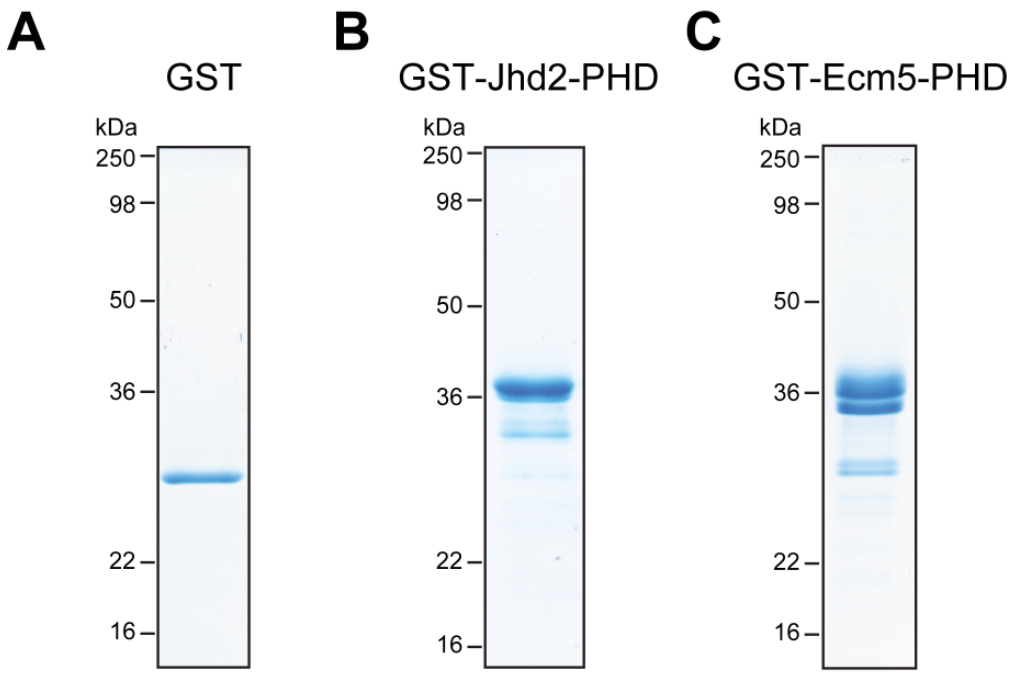

Figure 2.3 Recombinant free GST and GST-tagged Jhd2- and Ecm5-PHD fingers used for pull-downs

Coomassie-stained gels of GST (**A**), as well as N-terminally GST-tagged Jhd2 (**B**) and Ecm5 (**C**) PHD fingers (amino acids G221-L300 and S1232-D1295 of the full-length proteins, respectively), which were expressed in *E. coli* and purified using glutathione sepharose.

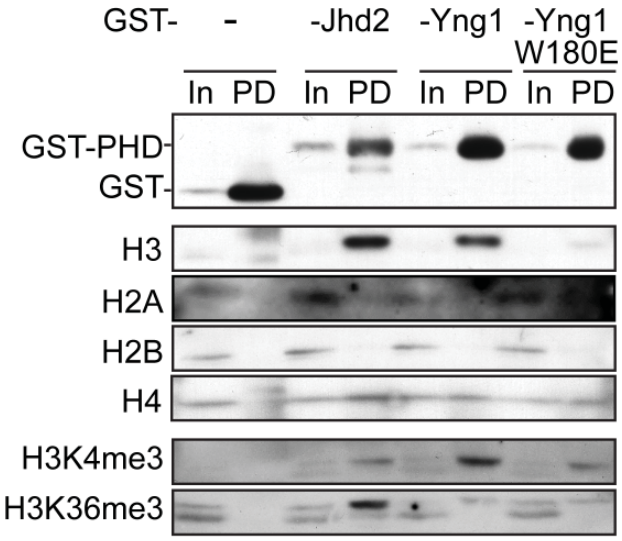

Figure 2.4 Recombinant, GST-tagged Jhd2-PHD finger interacts with histone H3 enriched for K36me3

GST alone or GST-tagged Jhd2-PHD, Yng1-PHD or Yng1-W180E-PHD fusions were incubated with acid-extracted yeast histones and pulled-down using glutathione sepharose. Western blotting with histone-specific antibodies was used to look for histones and modifications that preferentially associate with the PHD fingers. Inputs (In) are 8% of pull-downs (PD).

Next, I performed *in vitro* binding assays with the GST-Ecm5-PHD fusion. As was the case with the Yng1 and Jhd2 PHD fingers, the GST-Ecm5-PHD selectively pulled-down histone H3 (Figure 2.5). Intriguingly, and in contrast to my finding with the other PHD fingers, I also saw enrichment for histone H2A in tagged Ecm5 PHD pull-downs. Using H3 modification-specific antibodies, I checked whether H3K4 or K36 methylation was enriched in tagged Ecm5 PHD pull-downs. The H3 pulled-down by the Yng1 PHD, the Ecm5 PHD-precipitated H3 did show some enrichment for H3K4me3 compared to the GST control pull-down, although the levels of this modification in the GST-Ecm5-PHD pull-down were not higher than in the negative control Yng1-W180E-PHD pull-down. In addition, I found modest levels H3K36me3 enrichment in the Ecm5 PHD pull-down, though this enrichment was lower than the amount of H3K4me3 enriched on H3 pulled-down by the Yng1 PHD finger.

I was surprised to not see more H3K36me3 enriched on the H3 pulled-down by the Ecm5 PHD finger because Or Gozani's laboratory had reported that the Ecm5-PHD domain interacts with this mark (Shi et al., 2007). Therefore, I decided to look for evidence for this interaction using a peptide pull-down assay, despite not seeing strong enrichment of H3K36me3 in Ecm5 PHD-precipitated H3. However, using conditions under which a GST-Yng1-PHD fusion is selectively pulled-down with H3K4me3 peptides, I failed to observe enrichment of tagged Ecm5 PHD in pull-downs using methylated or unmethylated H3K4 or K36 peptides (Figure 2.6). In summary, while the Ecm5 PHD domain can interact with the H3 and H2A proteins under some assay conditions, I could not find any strong evidence for a direct interaction between the Ecm5 PHD finger and H3K36me3.

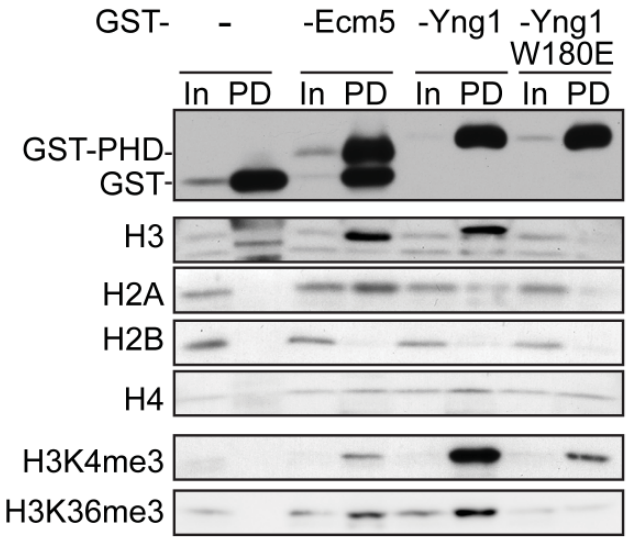

Figure 2.5 Recombinant, GST-tagged Ecm5-PHD finger interacts with histone H3
GST alone or GST-tagged Ecm5-PHD, Yng1-PHD or Yng1-W180E-PHD fusions were incubated with acid-extracted yeast histones and pulled-down using glutathione sepharose. Western blotting with histone-specific antibodies was used to look for histones and modifications that preferentially associate with the PHD fingers. Inputs (In) are 8% of pull-downs (PD).

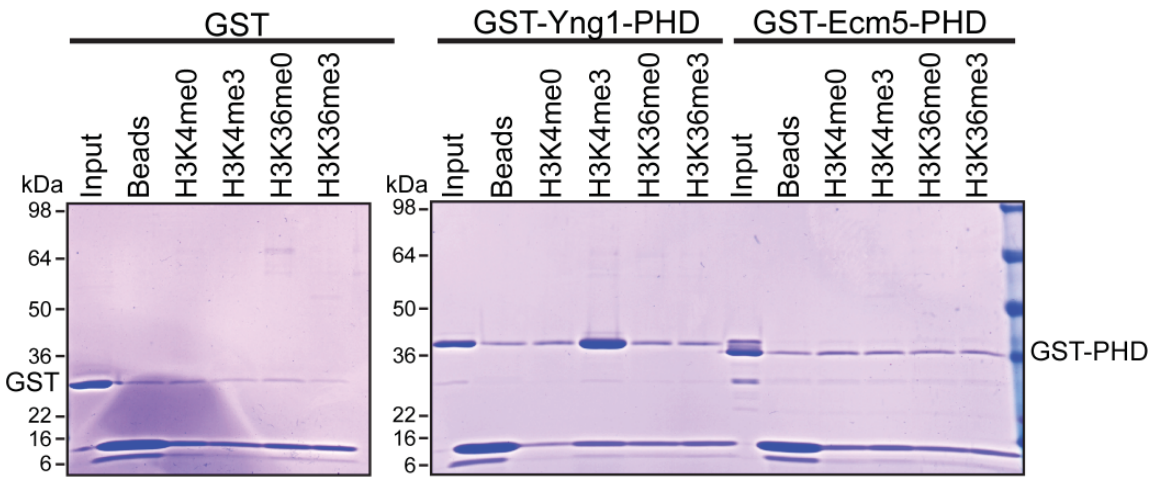

Figure 2.6 Tagged Ecm5 PHD finger is not enriched in pull-downs with an H3K36me3 peptide

Biotinylated peptides corresponding to the extreme N terminus of H3 or the region of H3 surrounding K36 and bearing the indicated modifications were pre-bound to high capacity streptavidin agarose. Peptide-bound beads (or beads alone) were then used in pull-downs with GST alone or GST-tagged Yng1 or Ecm5 PHD fingers. Input GST fusions and peptide pull-downs were separated by SDS-PAGE and analyzed by Coommassie staining. Locations of GST and GST-PHD fusions as well as molecular weight markers are indicated to the sides of gels.

Yeast PHD Fingers as Potential Ubiquitin E3 Ligases

PHD fingers are structurally similar to another class of zinc-coordinating domains, called RING (really interesting new gene) domains (Figure 2.7A) (Capili et al., 2001; Pascual et al., 2000). Just as a Cys4-His-Cys3 signature is characteristic of PHD fingers, a Cys3-His-Cys4 signature defines most RING domains. Many RING domains act as ubiquitin E3 ligases, catalyzing the final step in the cascade that covalently attaches the protein ubiquitin to lysine residues within protein substrates (Figure 2.7B) (Jackson et al., 2000; Weissman, 2001). The first step of the ubiquitylation cascade is ubiquitin activation. In this step ubiquitin forms an ATP-dependent attachment to a ubiquitin-activating enzyme, or E1, by means of a high energy thiol-ester bond between a cysteine in the E1 and the C-terminal glycine of ubiquitin. The ubiquitin is then transferred from the E1 to a conserved cysteine in a member of the ubiquitin-conjugating E2 enzyme family. The ubiquitin-charged E2 then associates with a RING-type ubiquitin E3 ligase. The E3 ligase acts in part as a scaffold, bringing together the ubiquitin-charged-E2 and the substrate protein, thus facilitating the transfer of ubiquitin from the E2 to the ε-amino group of a lysine side chain in the substrate.

In addition to forming attachments to substrate proteins, one ubiquitin moiety can be linked to a lysine in a second ubiquitin. In this way, a single, monoubiquitylated lysine in a protein substrate can become the site of a long polyubiquitin chain. Linkages via ubiquitin lysines 48 and 63 (K48 or K63) are the most common types of polyubiquitylation, although linkages at the other ubiquitin lysines have been found to exist *in vivo* (Xu et al., 2009). Different types of ubiquitin linkages promote different cellular outcomes. For instance, K48-linked polyubiquitin chains often target proteins for degradation by the 26S proteasome (Chau et

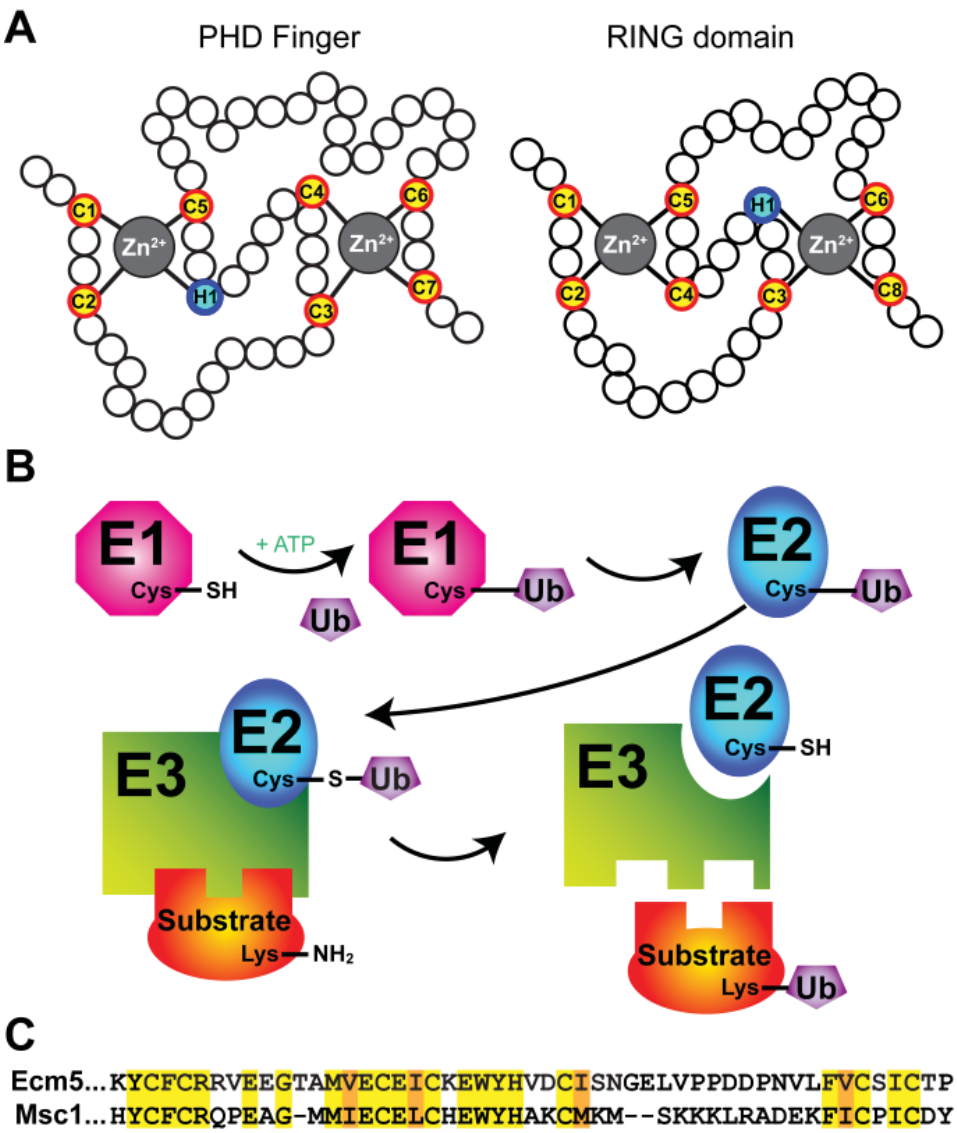

Figure 2.7 Overview of RING-type ubiquitin ligase function, and comparison with PHD fingers

A. Connectivity diagrams show the similarity between PHD fingers and RING domains. Diagrams were adapted from or modeled after Bienz (2006). **B.** Diagram showing how RING-type ubiquitin E3 ligases function. A ubiquitin moiety (Ub) first attaches to a cysteine (Cys) in an E1 ubiquitin-activating enzyme. The ubiquitin is then transfered to a cysteine in an E2 ubiquitin-conjugating enzyme. The RING domain-containing E3 ligase then brings together the ubiquitin-charged E2 and the final substrate, and catalyzes transfer of the ubiquitin to the substrate. **C.** Alignment of the *S. cerevisiae* Ecm5 PHD and second *S. pombe* Msc1 PHD fingers (amino acids K1239-P1289 and H1172-Y1219 of the full-length proteins, respectively), with identical residues highlighted in yellow and similar residues in orange.

al., 1989; Finley et al., 1994). On the other hand, K63-linked polyubiquitin chains are generally associated with cellular signaling functions, including protein trafficking and DNA repair (Clague and Urbe, 2010; Sun and Chen, 2004). Protein monoubiquitylation also seems to be involved in cell signaling rather than targeting proteins for degradation (Hicke, 2001).

Because of the similarity between PHD fingers and RING domains, it was originally thought that some PHD fingers might function as E3 ligases (Capili et al., 2001). In support of this hypothesis, the PHD fingers of the viral MIR1 and 2 (modulator of immune recognition) and the mammalian MEKK1 (MAP/ERK kinase kinase 1) proteins were all shown to have E3 ligase activity (Coscoy et al., 2001; Hewitt et al., 2002; Lu et al., 2002). However, these PHD fingers were later shown to be misclassified RING domains, casting doubt as to whether any true PHD fingers had ubiquitin ligase activity (Aravind et al., 2003; Scheel and Hofmann, 2003). Nevertheless, more recently, the three PHD fingers of the *S. pombe* Msc1 (multi-copy suppressor of Chk1) protein have been shown to have E3 ligase activity, suggesting that some PHD domains may indeed act as ubiquitin ligases (Dul and Walworth, 2007). Furthermore, the PHD finger of the KAP-1 corepressor was shown to act as an E3 ligase for the ubiquitin-related SUMO protein, facilitating the sumoylation of an adjacent domain on KAP-1, and expanding the potential roles for PHD fingers to encompass ubiquitylation and sumoylation, as well as histone interaction (Ivanov et al., 2007).

While BLAST searching with the Ecm5 PHD sequence I noticed it was strikingly similar to the sequence of the second PHD finger of the *S. pombe* Msc1 protein (Figure 2.7C), one of the PHD domains mentioned above that was found to have ubiquitin ligase activity. I therefore wondered whether the Ecm5 PHD finger might also have this function. Luckily, when I became

interested in this question, Ronen Sadeh, a new postdoctoral fellow with experience in the ubiquitin field, had just joined the Allis laboratory, and was also interested in seeing whether the Ecm5 PHD finger, or for that matter, any yeast PHD finger, possessed ubiquitin ligase activity.

Ronen and I were both intrigued with the possibility of a single PHD domain that might have the dual ability to bind to methylated histones and act as a ubiquitin ligase. We hypothesized that if this were the case, the presence of histone methylation might compete for the same regions of the PHD fold required for E3 ligase activity, and thereby inhibit ubiquitylation. Alternatively, histone methylation could stimulate ligase activity if the methyl-binding and catalytic regions of the PHD were separate. We thought this would be a novel and interesting way for chromatin modifications to regulate protein ubiquitylation.

Histones themselves are targets of ubiquitylation: H2B is known to be monoubiquitylated at lysine 123 (H2BK123ub) in yeast, and both H2A and H2B are ubiquitylated in higher eukaryotes (Goldknopf et al., 1975; Hunt and Dayhoff, 1977; Robzyk et al., 2000; West and Bonner, 1980). Moreover, in yeast and other eukaryotes, H2BK123ub is required for H3K4 and K79 methylation, providing precedent for the co-regulation of histone ubiquitylation and methylation (Chandrasekharan et al., 2010). In addition to the two well-studied ubiquitylation sites on H2A and H2B, H3 and H4 have been reported to be ubiquitylated in mammals, suggesting that there may be additional sites of histone ubiquitylation in yeast and mammals waiting to be discovered (Chen et al., 1998; Wang et al., 2006). Since PHD-finger containing proteins are generally localized in the nucleus, Ronen and I were interested in the possibilities that (1) any yeast PHD finger might act as a ubiquitin ligase, (2) histone methylation might regulate this activity, and (3) the substrate of this activity might be a histone.

We set out to test whether the first of these hypotheses, using an *in vitro* auto-ubiquitylation assay (Figure 2.8) (Ben-Saadon et al., 2006). In the first part of this assay, a wheat germ extract cell-free expression system is used to transcribe and translate a plasmid-encoded, HIS-tagged candidate PHD finger in the presence of ^{35}S-methionine. The translation mixture, containing the radiolabeled candidate protein to be tested for activity, is then combined with all of the components needed for ubiquitylation (E1 and E2 enzymes, ATP, ubiquitin, DTT, and ubiquitin-aldehyde to inhibit deubiquitylating enzymes). After the reaction is allowed to proceed, the components are separated on an SDS-PAGE gel which is dried and imaged using a phosphorimager.

In the absence of ubiquitin ligase activity, radiolabeled proteins are expected to appear as single bands on the audoradiogram. However, if the candidate protein has autoubiquitylated during the reaction, this protein should appear as a ladder of higher molecular weight bands or as a very high molecular weight smear, depending on the extent of ubiquitylation. Since many RING-type E3 ligases will auto-ubiquitylate *in vitro*, we were reasonably confident that if our PHD fingers possessed E3 ligase activity, we would be able to detect it using this assay, without the addition of a separate substrate (Fang and Weissman, 2004). Because we did not know the nature of the E2 that might act together with our PHD domains, we used recombinant human UbcH5c, Rad6a, and UbcH13-Uev1a as E2 enzymes for this assay, along with human Ube1 E1 enzyme. These human enzymes are extremely similar to their yeast homologs, represent most of the known nuclear E2s, and were either commercially available or available as gifts from Jaehoon Kim, a former postdoctoral fellow in Robert Roeder's laboratory. Throughout these assays, we used the full-length human Ring1B protein, a known H2A E3 ligase with self-ubiquitylation activity, as a positive control.

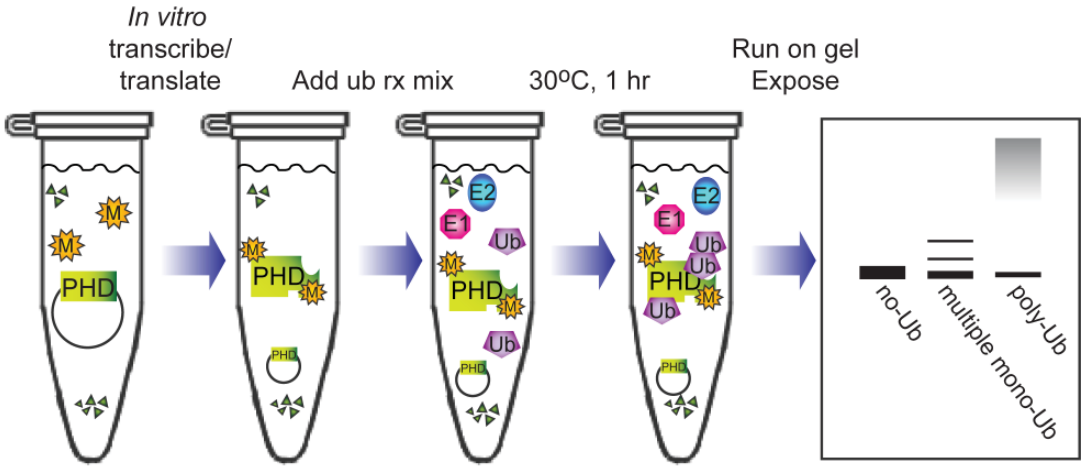

Figure 2.8 Diagram of *in vitro* auto-ubiquitylation assay

The protein or PHD domain (PHD) to be tested for E3 ligase activity is first transcribed and translated in the presence of ^{35}S-methionine, using a cell free expression system, generating a radiolabeled polypeptide. Ubiquitin reaction components (E1 and E2 enzymes, ubiquitin, ubiquitin aldehyde, DTT, ATP) are then added to the tube, which is incubated 1 hour at 30ºC to allow ubiquitylation to occur. The reaction contents are then separated by SDS-PAGE and imaged using a phosphorimager. If the candidate protein has self-directed E3 ligase activity, auto-ubiquitylated forms of the protein will be seen as either a few higher molecular weight bands or as a very high molecular weight smear.

When the 18 yeast PHD fingers were subjected to this assay, many of the yeast PHD fingers showed no activity, but the Nto1, Snt2, and Yng1 PHD fingers as well as the second Msc1 PHD, had a single higher molecular weight band, consistent with a monoubiquitylation event (Figure 2.9). Remarkably, three additional PHD fingers, the Ecm5, Spp1, and second Rco1 PHDs, had multiple higher molecular weight bands, suggesting they were the targets of multiple monoubiquitylations, or less likely, polyubiquitylation, in this assay. As expected, Ring1B ran as a high molecular smear, consistent with it having the ability to polyubiquitylate itself. This activity required the presence of ubiquitin (Figure 2.10A) and was proportional to the amount of E2 in the assay (Figure 2.10B). Exogenous E1 was not required for and did not stimulate activity, suggesting that a protein within the wheat germ extract could provide this function (Figure 2.10B). Furthermore, the activity was specific to the UbcH5c E2, since we did not see activity using the Rad6a or UbcH13-Uev1a E2 proteins (Figure 2.10C). Taken together, these data strongly suggested that our radiolabeled PHD fingers are the substrates for a ubiquitin ligase activity present in this assay.

While the Ecm5, Spp1, and second Rco1 PHD fingers were the targets of a specific E3 ubiquitin ligase activity, it was possible that the activity was coming from another protein in the assay, separate from the PHD domains. Given that the wheat germ extract introduces many proteins to this assay, and we had already seen that a protein in the assay could function as an E1 enzyme, we felt it imperative to determine whether the activity was coming from the PHD domains or another protein. We therefore attempted to recapitulate our results using a bacterial S30 expression system instead of the wheat germ system since the ubiquitylation machinery is absent in prokaryotes. Therefore, if we continued to see activity with PHDs translated in this

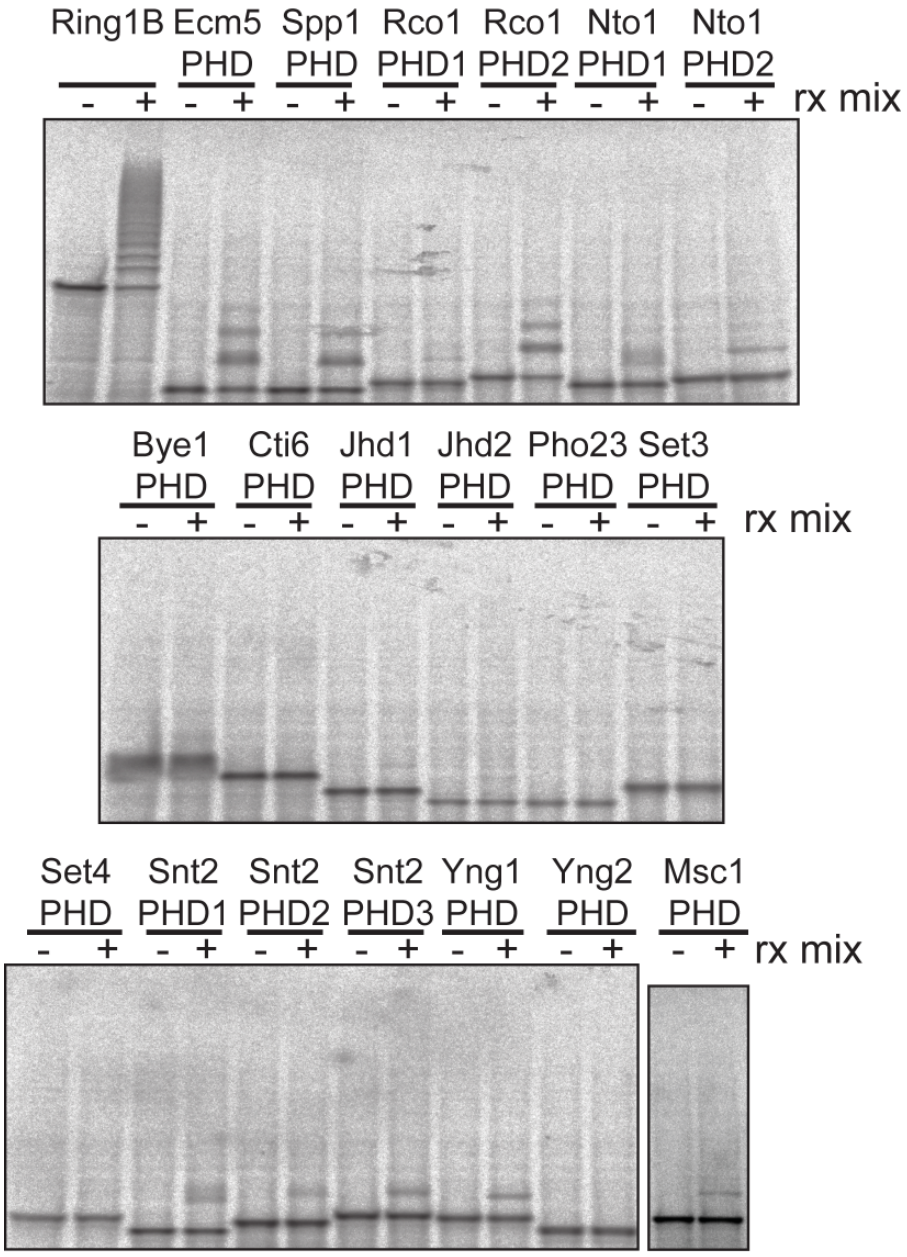

Figure 2.9 The Ecm5, Spp1, and second Rco1 PHD fingers are ubiquitylated *in vitro*
Each PHD finger was transcribed and translated using a wheat germ extract expression system, and then incubated with (+) or without (-) the ubiquitin reaction mixture (rx mix), as described in Figure 2.7. The full-length Ring1B protein, which is a known ubiquitin ligase, was used as a positive control.

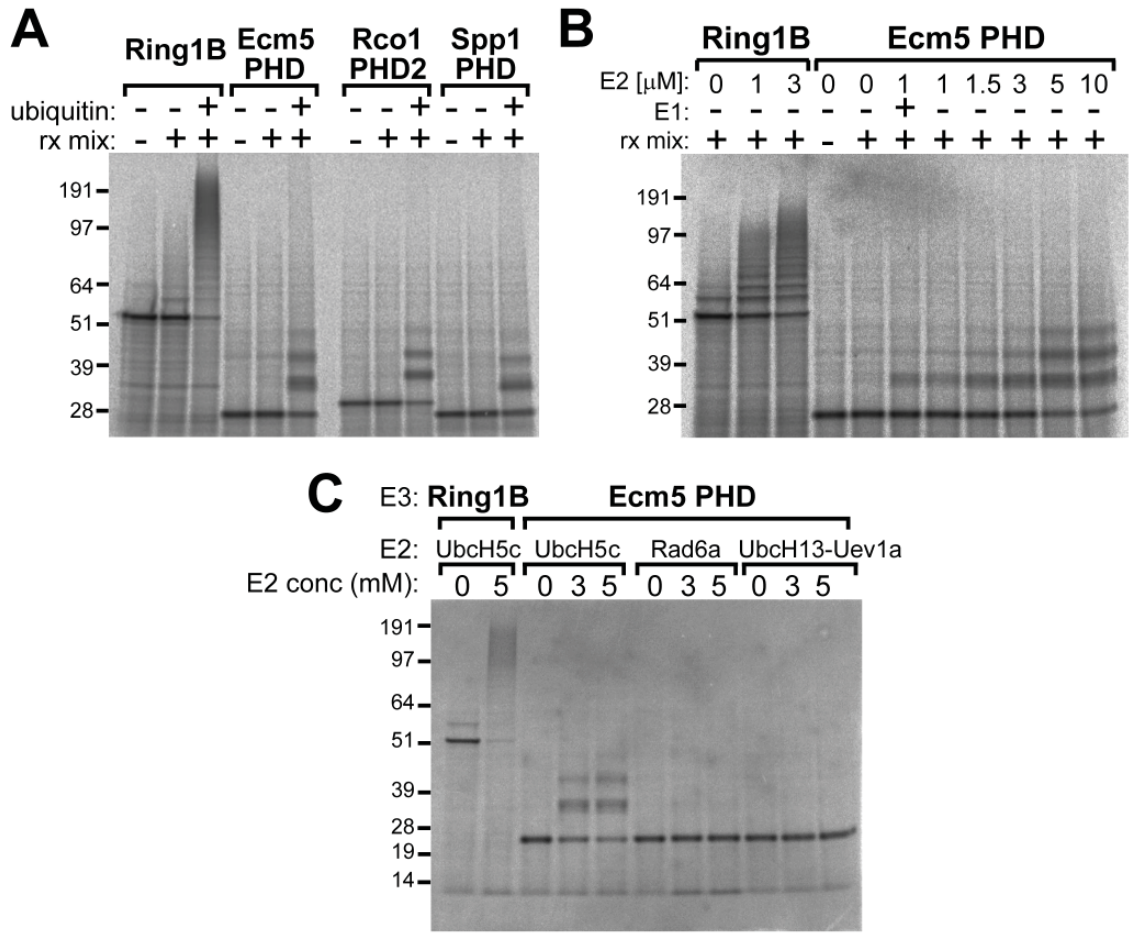

Figure 2.10 Ubiquitylation activity is ubiquitin- and UbcH5c-dependent

Autoradiograph of *in vitro* ubiquitylation assays carried out as in Figure 2.9, with (+) or without (-) ubiquitin or reaction mixture (rx mix) (**A**), using different concentrations of the UbcH5c E2 (**B**), or using different E2 enzymes (**C**).

extract, we could feel more confident that the source of the activity was the PHDs, themselves, and not an external, wheat germ extract-born E3. In *in vitro* assays using the S30 system, Ring1B continued to have activity. However, the Ecm5, Spp1, and second Rco1 PHD fingers did not, raising doubts as to whether these domains possessed intrinsic E3 ligase activity (Figure 2.11A and data not shown). Furthermore, when we added some of the wheat germ extract to the S30-translated PHD fingers, the activity returned, suggesting this activity was present in the wheat germ expression system and not intrinsic to the PHD fingers, and that the lack of activity in the S30 extract system is not due to improper folding of the PHD fingers (Figure 2.11A and data not shown).

We then mutated six of the eight PHD finger cysteines in each of the Ecm5, Spp1, and second Rco1 PHD fingers, to completely abolish proper folding of these domains. A mutant Ring1B with the RING domain deleted was used as a control. As expected, mutation of Ring1B completely abolished its E3 ligase activity (Figure 2.11B). Disappointingly, however, the mutated Ecm5, Spp1, and second Rco1 PHD fingers were still ubiquitylated in this assay, and to the same extent as the wild-type PHDs. Based on these results, we concluded that the ubiquitylation of the Ecm5, Spp1, and second Rco1 PHD fingers was the result of an activity in the wheat germ expression system, for which these particular PHD fingers made good substrates. Lacking solid evidence that the yeast PHD fingers could act as E3 ligases, Ronen and I chose to pursue other avenues of experimental investigation that seemed more promising, rather than continuing to seek support for this hypothesis.

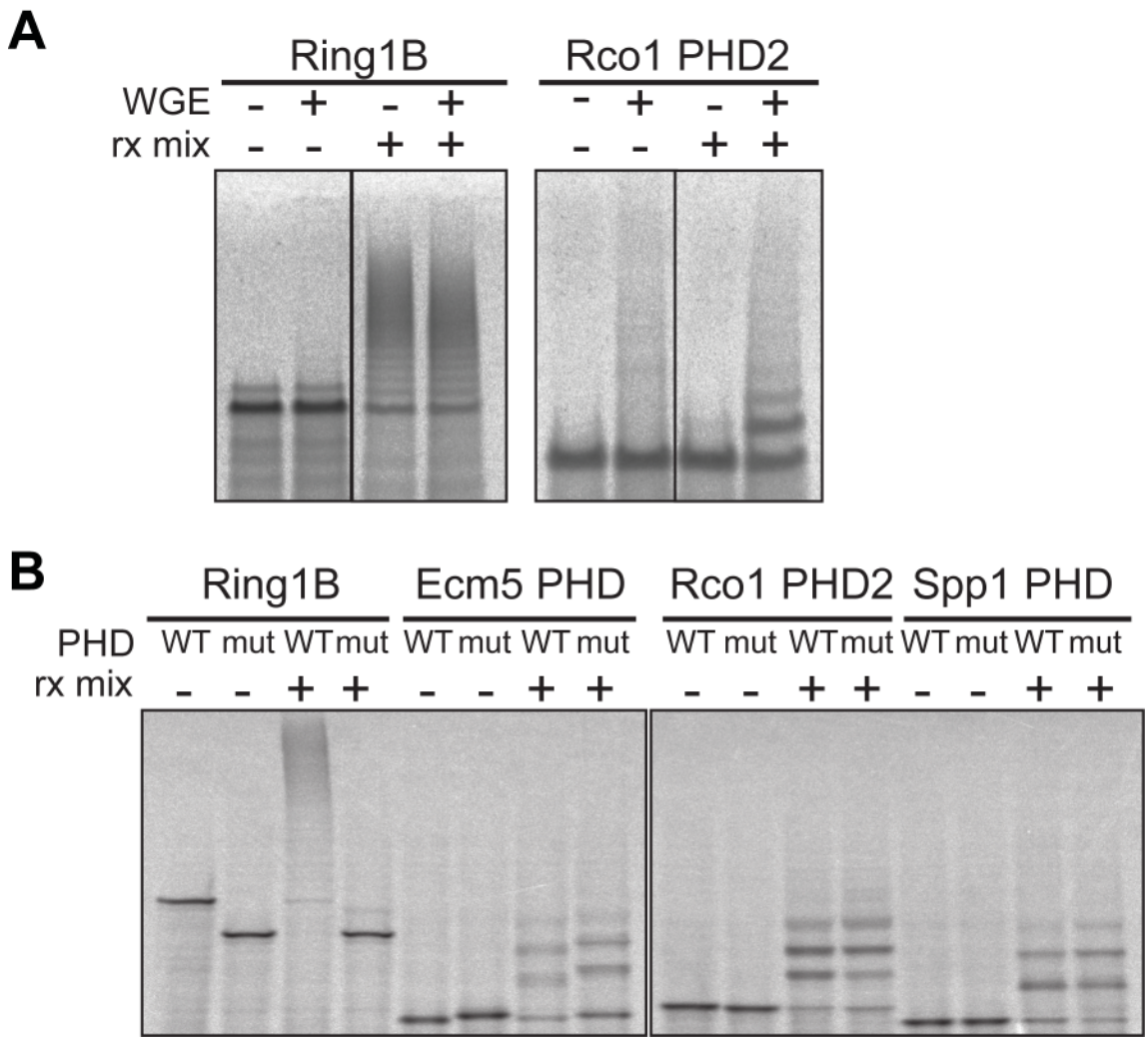

Figure 2.11 PHD-directed ubiquitylation is the result of a factor in the wheat germ expression system

A. Ring1B and the second Rco1 PHD were translated using the S30 expression system, and then *in vitro* ubiquitylation assays were performed in the presence (+) or absence (-) of reaction components (rx mix) and wheat germ extract (WGE). **B.** *In vitro* ubiquitylation assays were performed as in Figure 2.9 on Ring1B and either wild-type (WT) or 6-cysteine mutant (mut) PHD fingers. A Ring1B mutant, in which the RING domain has been deleted, was also used as a control.

Chapter 2 Discussion

The experiments described in this chapter were all performed with isolated purified PHD fingers, either to look for interactions with histones or to look for ubiquitin ligase activity. I have shown that a tagged Yng1 PHD finger preferentially pulls-down histone H3, and that H3K4me3 is enriched on the co-precipitated H3. These results, combined with other data collected by Sean Taverna, strongly support a direct interaction between the Yng1 PHD finger and H3K4me3, and further support a model in which the NuA3 HAT complex is recruited to or stabilized at sites of transcriptionally active chromatin, via interactions between the Yng1 PHD finger and H3K4me3, a mark known to be enriched in these regions (Pokholok et al., 2005). This allows NuA3 to catalyze histone acetylation at these loci, further promoting transcription.

Because many chromatin effector modules interact with histone modifications relatively weakly, a combination of many such interactions has been proposed to modulate chromatin complex targeting *in vivo* (Ruthenburg et al., 2007). While Sean's fluorescence anisotropy experiments found that the Yng1 PHD domain interacts with H3K4me3 with a K_d more than 40-fold lower than the K_d for the interaction with unmodified H3K4, showing a clear preference for the trimethylated state, this K_d is still relatively high, suggesting that additional histone and DNA interactions mediated by other domains within Yng1 or other subunits of NuA3, may also contribute to NuA3 localization. Consistent with this idea, the first 28 amino acids of Yng1 were recently shown to interact with the unmodified H3 tail (Chruscicki et al., 2010). The Nto1 subunit contains two PHD fingers of its own, which also might be involved in chromatin interactions. A recent study of yeast PHD fingers found a weak association between the first Nto1 PHD finger and H3K36me3 (Shi et al., 2007). Since this modification is enriched within

the coding regions of genes (Pokholok et al., 2005), and Sean's ChIP-chip studies found significant NuA3 localization in both the 5' ends and the middle of genes, an interaction between the Nto1 PHD and H3K36me3 might help direct NuA3 to gene coding regions, where levels of H3K36me3 predominate over H3K4me3. In addition, the Taf30 subunit of the NuA3 complex contains a YEATS (Yaf9, ENL, AF9, and TFIIF small subunit) domain, another domain known to mediate histone interactions, and it is possible that this domain also contributes to NuA3 complex localization or function (Schulze et al., 2010).

Having successfully used an *in vitro* binding assay to show interaction between H3 and the Yng1 PHD finger, I went on to use this assay to show that two additional PHD fingers, from the yeast Jhd2 and Ecm5 proteins, also interact with histone proteins. I found that a GST-Jhd2-PHD fusion was able to preferentially pull-down histone H3. In agreement with my results, a recent report found that the Jhd2 PHD finger can interact with nucleosomes, and that mutation of the Jhd2 PHD reduced Jhd2 binding to a target gene *in vivo* (Huang et al., 2010), underscoring the importance of this histone-PHD interaction in maintaining proper Jhd2 genomic localization. This report also showed that H3K4me3 was not necessary for the interaction between the Jhd2 PHD finger and immobilized nucleosomes, consistent with my own finding that H3K4me3 was not enriched in the H3 pulled-down by the GST-Jhd2-PHD fusion.

I did find H3K36me3 enriched in the H3 co-precipitating with the Jhd2 PHD finger. While it is possible that the Jhd2 PHD finger interacts directly with this modification, I was never able to confirm such an interaction using peptide pull-down assays. Experiments from the Gozani lab also did not find an interaction between the Jhd2 PHD finger and H3K36me3. It is possible that the Jhd2 PHD interacts with H3 indirectly, by means of an unknown acid soluble

protein contaminant (or contaminants) in my histone preparations. Alternatively, the Jhd2 PHD may interact with another region of H3 whose modification status is correlated with high levels of H3K36me3, require a longer region of the H3 tail than was covered by the H3K36me3 peptide for interaction, or require more than one histone modification, such as the combination of H3K4me3 and H3K36me3, for binding.

Given that Jhd2 demethylates H3K4, an activity associated with chromatin repression, the idea that Jhd2 might be recruited to transcriptionally active loci seems paradoxical. However, this paradox makes sense if Jhd2 is recruited to active genes that need to be turned off. Consistent with this idea, a recent study from Oliver Rando's laboratory found that patterns of H3K4me3 generated at genes activated by alpha factor or heat shock are actively removed by Jhd2 as these genes are returned to a repressed state (Radman-Livaja et al., 2010). Another study reported that Jhd2 was needed at the *GAL1* gene to both prevent over-activation in the presence of nonfermentable carbon sources and promote repression in the presence of glucose (Ingvarsdottir et al., 2007). Furthermore, a small-scale ChIP study found Jhd2 enriched in the 5' end of the *INO1* gene, consistent with the hypothesis that Jhd2 localizes to gene bodies to help maintain the localization differences between H3K4 and K36 methylation (Huang et al., 2010).

I also showed that a tagged Ecm5 PHD finger interacts with histone H3. As I noted earlier in this chapter, there was a report that the Ecm5 PHD finger weakly interacted with H3K36me3 (Shi et al., 2007). However, I did not find a specific enrichment for H3K36me3 in Ecm5 PHD-precipitated H3. Furthermore, peptide pull-downs with H3K4me3 and H3K36me3 peptides failed to confirm an association between the Ecm5 PHD and H3K36me3. The K_d the Gozani lab reported for this interaction was 155 μM, an order of magnitude weaker than that

of the Yng1-PHD H3K4me3 interaction. It is possible that my pull-down conditions, while not very stringent as evidenced by the background level of GST PHD pulled-down by each peptide, were still too stringent to detect such a weak interaction. However, as I will discuss in a later chapter of this thesis, my own ChIP experiments have found that Ecm5 localizes mainly to the promoter regions of genes, where H3K36me3 levels are low, and only to a small number of gene bodies. As with the Jhd2 PHD pull-down experiment, it is possible that the Ecm5 PHD interacts with H3 indirectly. Alternatively, the Ecm5 PHD finger may interact with H3 directly, although H3K36me3 is unlikely to be the sole target of this interaction *in vivo*.

What might other targets of the Ecm5 and Jhd2 PHDs be? In their interaction studies, the Gozani lab only tested for interactions with methylated and unmethylated H3K4, H3K36, and H3K79 peptides. However, there are a number of other known H3 modifications, such as H3R2 methylation, and it is possible that the Ecm5 and Jhd2 PHD fingers interact directly with one or more of these other marks. It is also possible that a combination of histone modifications, such as the presence of both H3R2me and H3K4me might be required for Ecm5 or Jhd2 PHD interaction, something that would have been missed in both the Gozani Lab's singly-modified peptide arrays, and my own peptide pull-down experiments. As newer technologies, such as large-scale arrays containing tens or hundreds of peptides with many combinations of modifications become less costly and easier to generate, it will become easier to determine if this is the case.

Surprisingly, the Ecm5 PHD finger also precipitated histone H2A. To my knowledge, there is no mass spectrometric evidence of specific H2A methylation sites in yeast. However, multiple sites of lysine and arginine methylation have been found on mammalian H2A by mass spectrometry (Waldmann et al., 2011; Zhang et al., 2003). Furthermore, yeast incubated with ^{3}H-S-adenosyl methionine were found to have radioactive H2A, suggesting that yeast may have one or more H2A methylation sites (Miranda et al., 2006). There are 11 lysines and 10 arginines in yeast H2A, numbers too high to easily generate and test methylated peptides of each site for Ecm5-PHD interaction. However, *in vitro* binding assays with histones acid-extracted from yeast strains containing H2A point mutations at these sites as well as tail deletions may help isolate specific H2A modifications or regions that interact with the Ecm5 PHD finger.

The structural similarities between PHD fingers and RING-type ubiquitin ligases, as well as the sequence similarities between the Ecm5 PHD and a PHD finger shown to have ubiquitin ligase activity, prompted me to test all of the yeast PHD fingers for E3 ligase activity. While the Ecm5, Spp1, and second Rco1 PHD fingers were all ubiquitylated in our *in vitro* assay, we were disappointed to discover that the PHD fingers themselves were not the ligases responsible for this activity. Rather, a component (or components) of the wheat germ extract used to express these PHDs was the source of this activity.

It is curious that the Ecm5, Spp1, and second Rco1 PHD fingers are particularly good substrates for this activity. These PHD fingers do not contain more lysines than the other yeast PHD fingers, so it is unclear why they would make better substrates. While this could be solely an artifact of our experimental system, it is also possible that these PHD fingers are substrates for ubiquitylation *in vivo*. Owing to the vital nature of the ubiquitin pathway, many of the enzymes in this pathway are very highly conserved. Therefore, it is possible that the protein or proteins

in the wheat germ extract responsible for ubiquitin ligase activity have yeast homologs. Cellular Ecm5 protein levels are extremely low, suggesting the protein is expressed at very low levels and/or actively degraded. Experiments looking at Ecm5, Spp1, and Rco1 protein levels before and after yeast proteasome inhibition might reveal whether any of these proteins is ubiquitylated and degraded. Alternatively, stringent Ecm5, Spp1, and Rco1 pull-downs from proteasome-inhibited strains containing tagged ubiquitin, followed by western blotting with ubiquitin-tag specific antibodies might also reveal whether these proteins are ubiquitylated *in vivo*. It should be noted that in the Ecm5 pull-downs described in the next chapter of this work, we never detected ubiquitin by mass spectrometry. However, we did not inhibit the proteasome for our pull-downs, so if Ecm5 were targeted for degradation, we may not have precipitated enough of it to detect a ubiquitylated form. As an interesting connection to the work in the first part of this chapter, Jhd2 has been shown to be ubiquitylated by the RING finger ubiquitin ligase Not4 and degraded by the proteasome (Mersman et al., 2009).

Even though we were unable to find evidence for a yeast PHD finger possessing ubiquitin ligase activity in our *in vitro* assay, it remains possible that such a PHD might exist *in vivo*. If one of the yeast PHD fingers tested has activity but cannot fold properly as an isolated domain, requires another protein for activity, requires a separate substrate for activity, or cannot utilize wheat germ and human E1 and E2 homologs, our assay would have been unable to detect activity for that domain. Future *in vitro* ubiquitylation assays with PHD-containing protein complexes purified from yeast, may reveal as yet undescribed ubiquitin ligase functions for some of these domains. Further work may also shed light on our second and third hypotheses, possibly finding examples of PHD domain ubiquitin ligases that are regulated by histone methylation and/or catalyze histone ubiquitylation.

CHAPTER 3: EARLY ATTEMPTS TO DETERMINE ECM5 FUNCTION

Chapter Introduction

In parallel to exploring the chromatin interactions of the Jhd2 and Ecm5 PHD fingers, I sought to better understand the functions of these two proteins. Both Jhd2 and Ecm5 were found to have nuclear localization (Huh et al., 2003), and they each possess domains that are linked to chromatin function, suggesting they might act as chromatin regulators. In agreement with this, just after I started this work, Jhd2 was shown to be an H3K4 demethylase (Liang et al., 2007; Seward et al., 2007; Tu et al., 2007). However, the function of Jhd2-catalyzed demethylation remained unclear. The *ECM5* gene was discovered in a screen for mutants with cell wall defects, suggesting this protein might help regulate the cell wall (Lussier et al., 1997). Although Ecm5 also possesses a Jumonji C domain, the domain linked to histone demethylase activity, this protein was shown not to function as a demethylase, leaving the function of this protein unknown.

As part of a broader effort to determine the functions of Ecm5 and Jhd2, I immunoprecipitated these proteins and identified their interaction partners using mass spectrometry. These immunoprecipitation experiments, which were performed in collaboration with Beatrix (Trixi) Ueberheide in the laboratory of Brian Chait and are discussed in the first part of this chapter, culminated in the discovery of a new Rpd3 histone deacetylase complex containing Ecm5 and another PHD finger protein, Snt2. Based on the results of these experiments, and the PHD finger-histone pull-downs described in the previous chapter, I initially hypothesized that Ecm5 and Jhd2 might be involved in preventing transcription from cryptic

internal promoters within coding regions, similar to the function that has been reported for the Rpd3(S) complex (Carrozza et al., 2005b; Joshi and Struhl, 2005; Keogh et al., 2005). The second part of this chapter describes experiments undertaken to test this hypothesis. However, I was not able to find any evidence to support a role for Ecm5 and Jhd2 in preventing cryptic transcription, so I decided to focus my attention on the function of Ecm5 in the newly discovered Rpd3 complex. The third and final section of this chapter describes my attempts to screen for a function of Ecm5.

Ecm5 interacts with Snt2 and the Rpd3 histone deacetylase

In order to better understand the functions of Jhd2 and Ecm5, I set out to determine with which proteins they associated. Because individual domains within Jhd2 and Ecm5 are homologous to different parts of the mammalian JARID proteins, I hypothesized that Jhd2 and Ecm5 might interact with one another and function as a complex. In this model, yeast would use two separate but physically associated polypeptides function like a single JARID protein does in mammalian cells. Thus, in addition to looking for new Jhd2 and Ecm5 interaction partners, I wanted to test if these two proteins interacted with one another. To address these questions, I initiated a collaboration with Trixi Ueberheide in the Chait laboratory to take advantage of the lab's expertise in protein purification and mass spectrometry. *ECM5* and *JHD2* were tagged at their C-termini with a Protein A (PrA) tag and immunoprecipitated (IPed) from cryogenically-prepared Ecm5-PrA and Jhd2-PrA lysates, under relatively mild conditions to maintain protein associations.

The cryogenic lysis method was developed by Michael Rout's laboratory as a superior method for purifying intact protein complexes (Oeffinger et al., 2007). This method involves spinning down cells to be harvested, resuspending them in a cryoprotectant solution, and then pipetting small droplets of cells into liquid nitrogen to quickly freeze them. Once frozen, cells are milled in a liquid nitrogen-cooled metal chamber with ball bearings, lysing them at cryogenic temperatures. Cryogenic lysis was chosen because it offered a number of benefits over other methods of yeast lysis. Because cells are rapidly frozen and kept cool during the entire lysis, proteases have less time to degrade proteins of interest. Furthermore, proteins are less likely to separate from interaction partners. In addition, large amounts of starting lysate from multiple large batches of cultures can be generated before actually performing the IP, which was necessary for us to obtain enough material, because the Ecm5 and Jhd2 proteins are only present in low amounts *in vivo* (Ghaemmaghami et al., 2003).

We initially focused our attention on the purification of Jhd2-PrA and its interaction partners. However, other than contaminating background proteins known to associate with the PrA tag (Gavin et al., 2002; Shevchenko et al., 2008), we failed to identify any other proteins co-precipitating with Jhd2-PrA (data not shown). We tried various purification and wash conditions, but four separate attempts at the Jhd2-PrA purification failed to identify any credible Jhd2-interaction partners. Thus, we were unable to find support for the idea that Jhd2 and Ecm5 associate, and could not identify any other proteins stably associated with Jhd2.

We next purified PrA-tagged Ecm5, and resolved Ecm5-PrA co-purifying proteins by SDS-PAGE (Figure 3.1A). Bands detectable by Coomassie staining were excised and analyzed using MALDI mass spectrometry. We again identified some known contaminants of

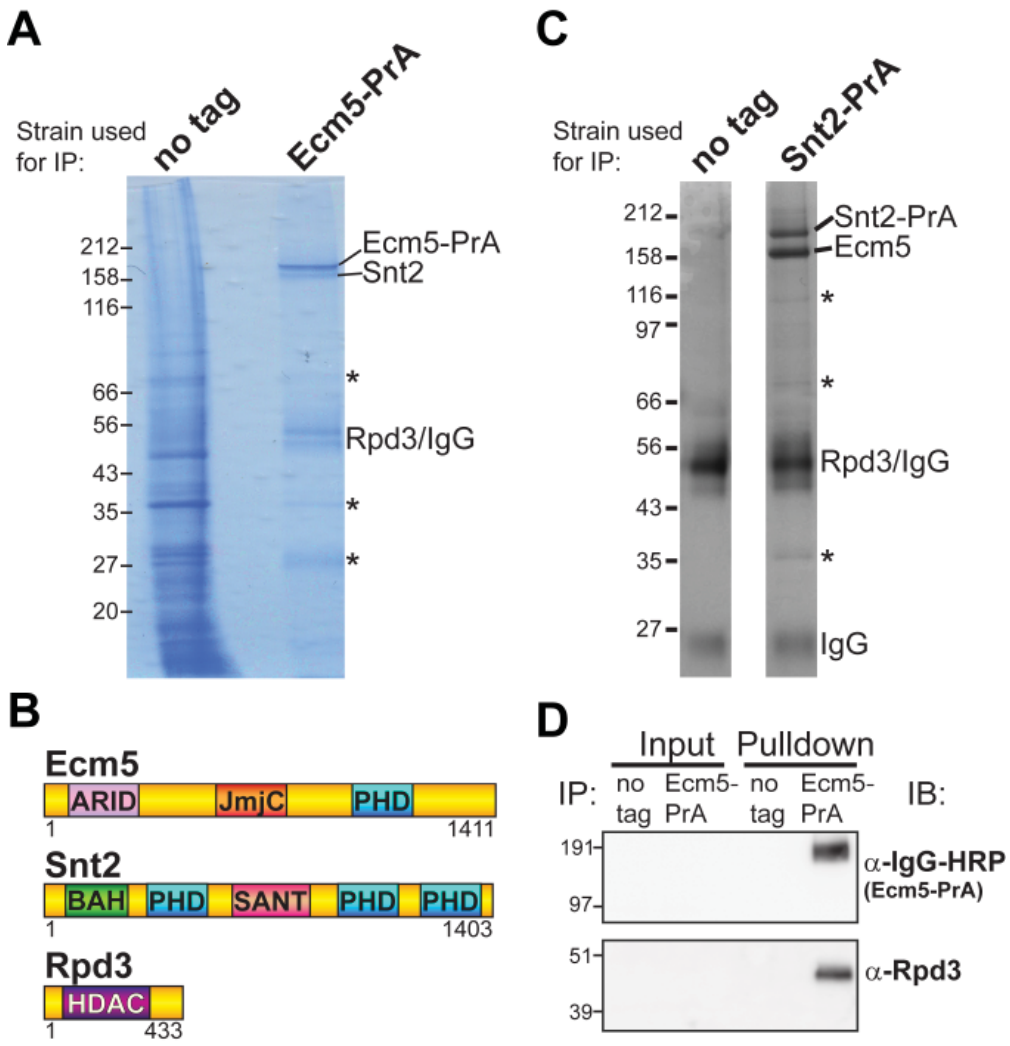

Figure 3.1 Ecm5 interacts with Snt2 and the Rpd3 histone deacetylase

A. PrA purifications from Ecm5-PrA or untagged yeast lysates were separated by SDS-PAGE, and stained with Gel Code Blue Protein Stain. Stained bands were identified using mass spectrometry, and identified Ecm5-PrA-interacting proteins are labeled to the right of the gel image. IgG, which elutes from the resin and runs at the same point on the gel as Rpd3, is also identified. Asterisks mark contaminants. **B.** Diagrams of the Ecm5, Snt2, and Rpd3 domain structures. ARID: AT Rich Interaction Domian; JmjC: Jumonji C domain; PHD: plant homeodomain finger; BAH: bromo-adjacent homology domain; SANT: Spt3-Ada3-N'CoR-TFIIS domain; HDAC: histone deacetylase domain. **C.** Silver-stained gel of eluate from control and Snt2-PrA purifications. Eluate proteins identified by mass spectrometric analysis are indicated next to their respective bands, and contaminants are marked with asterisks. **D.** Eluates from an Ecm5-PrA purification were immunoblotted with an HRP-conjugated-secondary antibody (to detect Ecm5-PrA) and an Rpd3 antibody.

PrA purifications, many of which were also present in the control IP from an untagged strain (bands marked with asterisk in Figure 3.1A). We did not detect any band the size of Jhd2 in the Ecm5-PrA purification. However, we did identify two proteins co-purifying with tagged Ecm5 that were not in our untagged control purification. The first, which migrated as a band of approximately 160 kDa just below Ecm5-PrA, was identified as the yeast Snt2 protein. A second band around 50 kDa in size, that ran with IgG on the gel, was identified as the histone deacetylase Rpd3.

Snt2 is named after its SANT (Swi3, Ada2, N-CoR, and TFIIB") domain (Figure 3.1B). These domains are found in many HAT and HDAC complexes, and individual SANTs have been shown to mediate histone interactions and modulate HAT and HDAC activity (Boyer et al., 2004). Snt2 also contains three PHD fingers of its own as well as a BAH (bromo-adjacent homology) domain, another known chromatin interaction module (Armache et al., 2011; Kuo et al., 2012). The wealth of domains known to mediate chromatin interaction in the Snt2 protein suggests this protein is highly likely to have a function on chromatin. Consistent with this idea, Snt2 was found to reside at the promoters of a small number of genes by chromatin immunoprecipitation (ChIP), suggesting this protein might function directly in gene regulation (Harbison et al., 2004).

Rpd3 is a histone deacetylase and a key subunit of two other yeast complexes: Rpd3(S) and Rpd3(L) (Figure 3.2). The Rpd3(L) complex is the larger of the two known Rpd3 complexes, with 12 reported subunits (Carrozza et al., 2005b; Keogh et al., 2005). This complex localizes to the promoters of numerous genes and regulates transcription (Carrozza et al., 2005a). Consistent with the known association between deacetylated histones and transcriptional

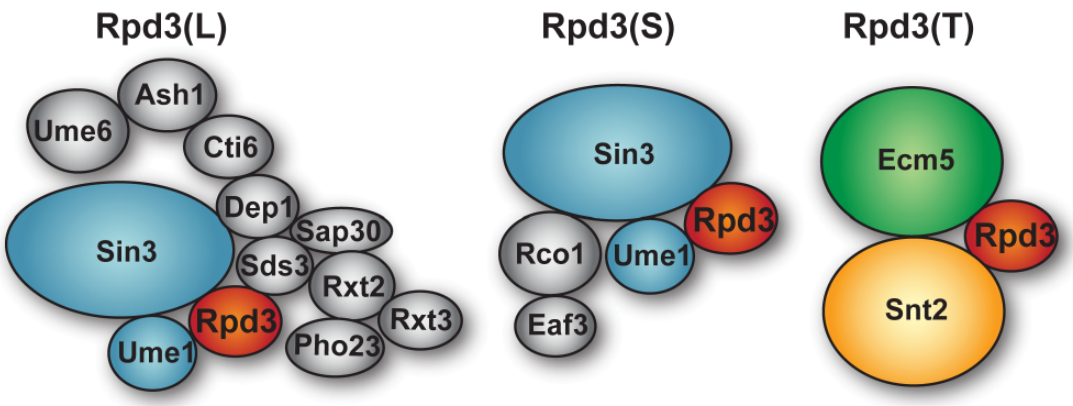

Figure 3.2 The Rpd3 deacetylase is a subunit of two other yeast complexes
Diagram showing subunits of the Rpd3(L) and Rpd3(S) complexes, as well is the Rpd3(T) complex described in this thesis. Rpd3 is in red, and other shared components between Rpd3(L) and (S) complexes are in blue.

repression, the Rpd3(L) complex generally functions as a transcriptional repressor (Allfrey et al., 1964; Kadosh and Struhl, 1998; Vidal and Gaber, 1991), but the complex also functions as an activator at a subset of genes (De Nadal et al., 2004; Ruiz-Roig et al., 2010; Sertil et al., 2007). The Rpd3(S) complex was first fully purified and analyzed by mass spectrometry in 2005, and found to consist of the subunits Sin3, Ume1, and Rpd3, which are shared with the Rpd3(L) complex, as well as the Rpd3(S)-unique subunits Eaf3 and Rco1 (Carrozza et al., 2005b; Keogh et al., 2005). Rpd3(S) localizes to both gene bodies and promoters where it helps suppress various types of noncoding or aberrant transcription (Carrozza et al., 2005b; Joshi and Struhl, 2005; Keogh et al., 2005). Members of the Rpd3(L) and (S) complexes were not detected in the Ecm5-PrA purification, suggesting that Ecm5, Snt2, and Rpd3 constitute a third Rpd3 complex.

In order to confirm the associations between Ecm5, Snt2, and Rpd3, we first repeated our Ecm5 purification. As expected, we again detected Snt2 and Rpd3 co-purifying with Ecm5 (data not shown). To further confirm these interactions, we PrA-tagged *SNT2*, and purified this protein along with its interaction partners. A portion of the Snt2-PrA purification was visualized by SDS-PAGE analysis followed by silver staining (Figure 3.1C). We subjected the remainder of the eluted proteins for liquid chromatographic-mass spectrometric (LC-MS) analysis, to identify any Snt2 co-purifying proteins. Only peptides from known contaminants were found in a control purification from an untagged strain. In contrast, peptides matching both Ecm5 and Rpd3, in addition to tagged Snt2 were detectable in the Snt2-PrA purification. Intriguingly, further MS-MS analysis on Snt2 peptides in the purification determined that serine 641 of Snt2 is phosphorylated, suggesting a possible method of regulation for this protein. Peptides matching subunits of the Rpd3(L) and (S) complexes were not detected in the Snt2-PrA purification.

To fully confirm these interactions, we purified Rpd3 and its interaction partners using an Rpd3-PrA strain. We were able to identify 10 out of 12 of the known Rpd3(L) subunits and 5 out of 5 Rpd3(S) subunits in the Rpd3-PrA purification, confirming that our purification conditions preserved Rpd3 complex associations (Table 3.1). In addition, peptides matching Ecm5 and Snt2 were also identified, although in much lower abundance. In order to be certain that Ecm5 and Snt2 co-purified with Rpd3, we separated some of the Rpd3-PrA eluate by SDS-PAGE, Coomassie stained the gel, and excised the bands corresponding in size to Ecm5 and Snt2. Mass spectrometric analysis clearly identified Ecm5 and Snt2 (>20 peptides each) in these bands (data not shown). As further confirmation of these associations, I performed a separate PrA purification with lysates from the Ecm5-PrA and untagged strains. Rpd3 was clearly detected in eluates from the Ecm5-PrA purification by immunoblot (Figure 3.1D). Taken together, these experiments show that Ecm5, Snt2, and the Rpd3 histone deacetylase form a third Rpd3 complex, which I have named the Rpd3(tiny), or Rpd3(T), complex.

Exploring whether Jhd2 and the Rpd3(T) complex repress cryptic transcription

Based on these interaction results, I hypothesized that Ecm5 might help recruit or stabilize this new histone deacetylase complex to specific genomic locations, where the complex might have a repressive function. I also suspected the Jhd2 H3K4 demethylase would repress transcription, because H3K4me is associated with gene activation (Briggs et al., 2001; Nishioka et al., 2002; Santos-Rosa et al., 2002; Wang et al., 2001). As discussed in the previous chapter, there was initial reason to believe that both the Jhd2 and Ecm5 PHD fingers might interact with H3K36me3, suggesting both proteins might be recruited to gene bodies. (My own peptide pull-

Table 3.1 Summary of proteins identified by LC-MS analysis of Rpd3-PrA IP [a]

Protein	log(e)	% protein coverage	unique peptides	total peptides	Known Rpd3(L) or (S) subunit	Also in Snt2-PrA IP
Sin3	-618.8	32	48	126	L and S	
Rco1	-301.0	38	24	58	S	
Ume1	-254.5	42	19	49	L and S	
Rpd3	-247.8	42	18	46	L and S	Yes
Dep1	-186.2	34	17	24	L	
Eaf3	-158.0	31	13	32	S	
Cct2	-120.0	25	10	12		
Cct4	-115.6	21	10	14		
Cct3	-105.6	21	11	14		
Sds3	-105.1	40	9	15	L	
Cct7	-100.7	23	10	15		
Rxt2	-100.0	18	7	18	L	
Rxt3	-89.1	27	7	16	L	
Cct6	-88.7	16	8	10		
Cct5	-86.7	16	8	8		
Tcp1	-77.3	13	8	9		
Pho23	-66.0	15	5	10	L	
Asc1[b]	-60.4	22	6	6		
Cti6	-57.6	15	5	7	L	
Ash1	-57.3	11	6	6	L	
Rpp2B[b]	-48.3	45	4	5		Yes
Rpp2A[b]	-38.0	44	4	6		Yes
Bmh1	-35.3	15	3	3		
Ilv1	-32.8	6	4	4		
Rps6B[b]	-27.0	13	2	3		Yes
Ecm5	-23.7	2.8	3	3		Yes
Rps12[b]	-23.3	21	3	3		
Rps16B[b]	-20.9	22	3	3		
Pfk1[b]	-20.6	3.4	2	2		
Rpl6B[b]	-18.6	13	2	2		
Snt2	-18.3	2	3	3		Yes
Acc1[b]	-18.1	1.4	3	3		

[a] Proteins also found in BY4741 IP or known to be contaminants of PrA IPs (Shevchenko *et al* ., 2008; Gavin *et al.* , 2002) are not shown.

[b] While not previously reported as PrA IP contaminants, these proteins are highly abundant in yeast cells and are likely to also be contaminants.

down experiments eventually failed to confirm associations of these PHDs with H3K36me3-pepetides, but this work was undertaken before I had completed these experiments.) The possibility of these potentially repressive proteins being recruited to gene bodies immediately reminded me of the Rpd3(S) complex, and its recruitment to gene bodies to repress transcription in aberrantly initiating from cryptic promoters within genes.

At least two classes of short aberrant transcripts have been described in yeast. One class was first described by Francoise Wyers and colleagues, who noticed that deletion of the nuclear exosome exonuclease Rrp6 resulted in accumulation of short transcripts, 250-600 nucleotides long, originating from intergenic regions (Wyers et al., 2005). Because wild-type cells rapidly degrade these transcripts, Wyers and colleagues named them "cryptic unstable transcripts" or CUTs . CUTs are capped at their 5' ends and polyadenylated by the TRAMP (Trf4, Air1/2, and Mtr4 polyadenylation) complex, promoting their rapid degradation by the nuclear exosome (Rrp6, Mtr4/Dob1, and Rrp47/Lrp1) in wild-type yeast. Deletion of TRAMP complex subunits, as well as subunits of the Nrd1-Nab3-Sen1 complex, which are required for the association of CUTs with the exosome, promotes accumulation of these transcripts (Arigo et al., 2006; Vasiljeva and Buratowski, 2006; Wyers et al., 2005).

Not to be confused with CUTs, a second class of aberrant transcripts was first described by Fred Winston's laboratory, who noticed that mutant yeast with reduced levels of the histone chaperone Spt6 accumulated short transcripts initiating from the middle of certain genes (Kaplan et al., 2003). This work went on to show that in cells lacking Spt6, chromatin inside of these genes was more sensitive to micrococcal nuclease, suggesting that Spt6 is required to restore proper chromatin structure in the wake of transcribing RNA Polymerase II (Pol II). Thus, Craig

Kaplan, Fred Winston, and colleagues proposed that without proper restoration of chromatin structure after transcription, inappropriate transcription could initiate from regions within genes that happened to resemble promoters. Like CUTs, these genic cryptic transcripts, which I refer to as simply "cryptic transcripts" for the rest of this work, are poly-adenylated and capped on their 5' ends, but in contrast to CUTs, cryptic transcripts are not actively produced and degraded at high levels in wild-type cells. Rather, cryptic transcripts appear to be a phenotypic readout for yeast mutants with problems maintaining proper chromatin structure at transcribed genes. For this reason, mutations in other proteins involved in chromatin regulation and transcriptional elongation also result in accumulation of cryptic transcripts. For instance deletion of the *BUR1* or *BUR2* genes, which encode subunits of a cyclin-dependent kinase important for transcriptional elongation, also results in this phenotype (Kaplan et al., 2003). In addition, a report from Kevin Struhl's laboratory found that a mutation in the *SPT16* gene, encoding a subunit of the FACT transcriptional elongation complex, results in increased Pol II density at the 3' ends of genes and initiation of cryptic transcripts (Mason and Struhl, 2003).

As mentioned earlier, the Rpd3(S) complex has also been linked to repression of cryptic transcripts. The chromodomain of the Eaf3 subunit and the PHD finger of the Rco1 subunit both interact with H3K36me2/3, and both K36me interactions have been shown to work together to recruit Rpd3(S) to gene bodies to deacetylate genic histones (Krogan et al., 2003; Li et al., 2007; Li et al., 2003; Xiao et al., 2003). Thus, deletion of Rpd3(S) subunits results in increased histone acetylation at the 3' ends of genes, and accumulation of cryptic transcripts (Carrozza et al., 2005b; Joshi and Struhl, 2005; Keogh et al., 2005). I hypothesized that, like Rpd3(S), Jhd2 and the Rpd3(T) complex might also be recruited to gene coding regions by interactions between

H3K36me3 and the Jhd2 and Ecm5 PHD fingers. Once recruited to gene bodies, Rpd3 and Jhd2 might deacetylate and demethylate histones, respectively, helping to maintain a chromatin state inside of gene bodies that is repressive to cryptic transcription (Figure 3.3).

Testing the 6-azaurcil sensitivity of *ecm5* and *snt2* mutants

In order to test my hypothesis, I first tested whether *ecm5* or *jhd2* knockouts had differential growth on 6-azauracil (6-AU). When cells are treated with this chemical, their intracellular GTP levels are depleted, slowing down transcriptional elongation (Exinger and Lacroute, 1992). While wild-type cells can grow on 6-AU, mutants with defects in transcriptional elongation display sensitivity to this chemical, presumably because the elongation defects caused by 6-AU and those caused by the mutation synergistically create a transcriptional burden severe enough to impede growth (Archambault et al., 1992). Conversely, yeast with mutations that stimulate transcriptional elongation and promote cryptic transcription have been shown be 6-AU resistant (Keogh et al., 2005). I therefore reasoned that if Ecm5 and Jhd2 are involved in repressing cryptic transcription, strains lacking these proteins might show 6-AU resistance.

Because 6-AU is most effective when combined with uracil-free media, I first transformed wild-type and knockout strains with the high-copy uracil plasmid pRS426 (Christianson et al., 1992), to allow them to grow without uracil. I used the *set2* knockout strain as a positive control for these assays, since this mutant has been shown to be 6-AU resistant (Keogh et al., 2005; Kizer et al., 2005). As expected, *set2* knockout cells consistently showed resistance to 6-AU (Figure 3.4). Intriguingly, *jhd2* mutant cells were also

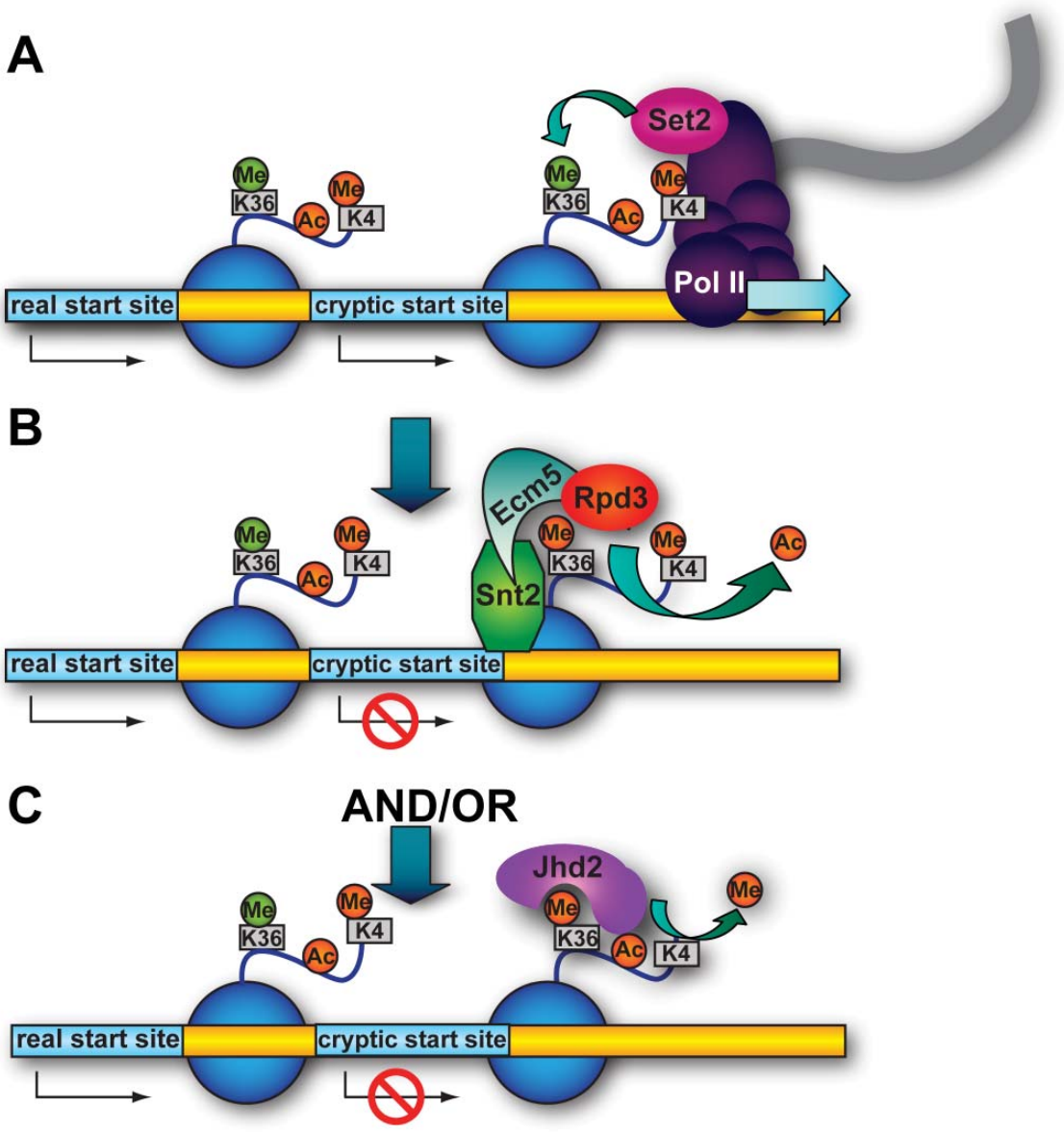

Figure 3.3 Model for how Jhd2 and/or the Rpd3(T) complex could suppress cryptic transcription

A. High levels of H3K36me are established within gene bodies by the Set2 methyltransferase, which interacts with elongating RNA polymerase II. **B.** The Rpd3(T) complex might then be recruited to open reading frames via interactions between H3K36me3 and the Ecm5 PHD domain, allowing Rpd3 to deacetylate histones inside of coding sequences, repressing cryptic transcription. **C.** Similarly, interactions between H3K36me and the Jhd2 PHD finger might recruit Jhd2 to open reading frames to demethylate H3K4 in these regions and repress transcription from cryptic internal promoters.

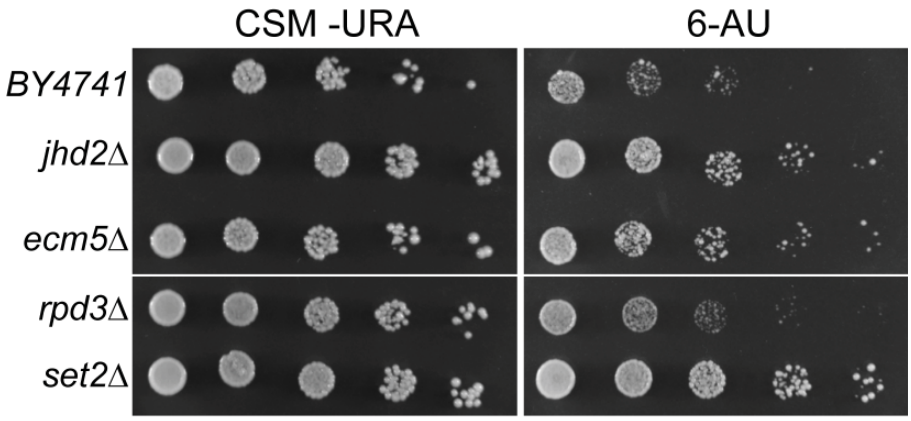

Figure 3.4 *ecm5* and *jhd2* mutants sometimes show enhanced growth on 6-AU
Five-fold serial dilutions wild-type (BY4741) or indicated mutant strains containing the uracil plasmid pRS426 were spotted on complete synthetic media lacking uracil (CSM-URA) or CSM-URA supplemented with 100 μg/mL 6-azauracil (6-AU). Plates were imaged after 3 days.

consistently 6-AU resistant, suggesting that in the absence of Jhd2, transcriptional elongation is enhanced. The *rpd3* knockout strain also showed modest 6-AU resistance. However, the *ecm5* knockout strain performed inconsistently in this assay, showing 6-AU resistance in some assays but not in others. Thus, while these assays suggested that Jhd2 might function to repress chromatin in coding regions, I could not conclude that Ecm5 did the same.

Looking for cryptic transcripts by qPCR

As another way of testing whether Jhd2 and Ecm5 are involved in preventing cryptic transcription, I checked for the accumulation of cryptic transcripts in *jhd2* and *ecm5* knockout strains, using quantitative RT-PCR (qPCR). I reasoned that if cryptic transcripts are accumulating in these strains, cDNA from *jhd2* and *ecm5* knockouts would show higher qPCR signal at the 3' end of cryptic transcript genes, compared to wild-type signal, without also showing higher signal at the 5' end of the genes (which would suggest complete gene up-regulation, rather than a specific accumulation of the shorter cryptic transcript). To test this idea, I purified RNA from wild-type yeast as well as *jhd2* and *ecm5* knockout strains and converted it to cDNA. The cDNA from *jhd2* and *ecm5* knockout strains completely lacked detectable signals from *JHD2*- and *ECM5*-specific primers, respectively, confirming that each gene was deleted from its knockout strain (data not shown). However, in *jhd2* and *ecm5* knockout cells, levels of the *STE11* gene, which is known to contain cryptic internal promoters, were similar to wild-type at all portions of the gene tested (Figure 3.5A). Similarly, levels of *SPB4*, another gene known to contain a cryptic promoter, were the same as or lower than wild-type levels, at both the 5' and 3' end of the gene (Figure 3.5B). Thus, the qPCR assay did not provide any evidence that Jhd2 and the Rpd3(T) complex repress cryptic transcription.

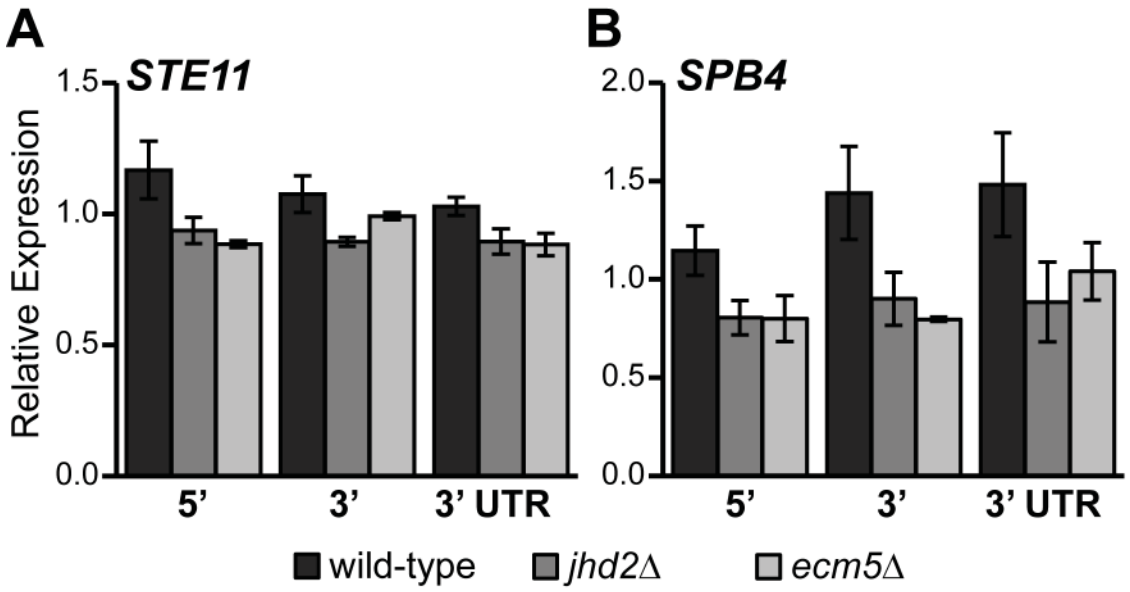

Figure 3.5 *ecm5* and *jhd2* mutants do not show increased expression of the 3' ends of known cryptic transcript genes by qPCR

Random hexamer-primed cDNA from wild-type (BY4741) or indicated knockout strains was used for qPCRs with primer pairs corresponding to the 5' end (5'), 3' end (3'), or 3' untranslated region (3' UTR) of the *STE11* [**A**] and *SPB4* [**B**] genes. qPCRs are normalized to signal from the *ACT1* gene, and graphs show means and SEMs for three biological replicates.

Northern blots to assay from cryptic transcripts

While these results suggest that Jhd2 and the Rpd3(T) complex do not suppress cryptic transcripts, it was possible that the qPCR-based technique was not sensitive enough to detect increases in cryptic transcripts that were in much lower abundance than the full-length transcripts. Therefore, I also assayed for the presence of cryptic transcripts in *ecm5* and *jhd2* mutants, using northern blotting, which unlike a qPCR assay, separates different transcripts from the same gene by size, allowing detection of shorter transcripts that are far less abundant than their full size counterparts. As a positive control for these assays, I used RNA from *set2* and *eaf3* knockout strains, which as described above, are known to accumulate cryptic transcripts. I used oligo-dT beads to enrich for polyadenylated (poly-A^+) RNA from total RNA taken from wild-type yeast and various knockout strains, and blotted this enriched RNA with probes to the 3' ends of *STE11* and *SPB4*. While this enrichment step did not entirely eliminate rRNA from my samples, as can be seen by the two cross-reacting bands in my northern blots (Figure 3.6, marked with x's), cryptic transcripts were clearly detected in cells lacking Set2 or Eaf3 (Figure 3.6, marked with green arrows). Cryptic *STE11* transcripts were also detected in the *rpd3*Δ strain, albeit at lower levels. However, cryptic *SPB4* transcripts were not detected in this strain, possibly as a result of Rpd3 having many cellular functions, resulting in pleiotropic effects when this gene is deleted. In contrast to the *set2* and *eaf3* knockout strains, knockouts for *ecm5*, *snt2*, and *jhd2*, did not show cryptic *STE11* or *SPB4* transcripts.

Intriguingly, *ecm5* and *snt2* mutants did show higher levels of a 6kb RNA species cross reacting with the 3' *STE11* and *SPB4* probes (Figure 3.6, marked with asterisks). For the *ecm5*Δ RNA, this may be partially explained by overloading of the gel, since more *ecm5*Δ

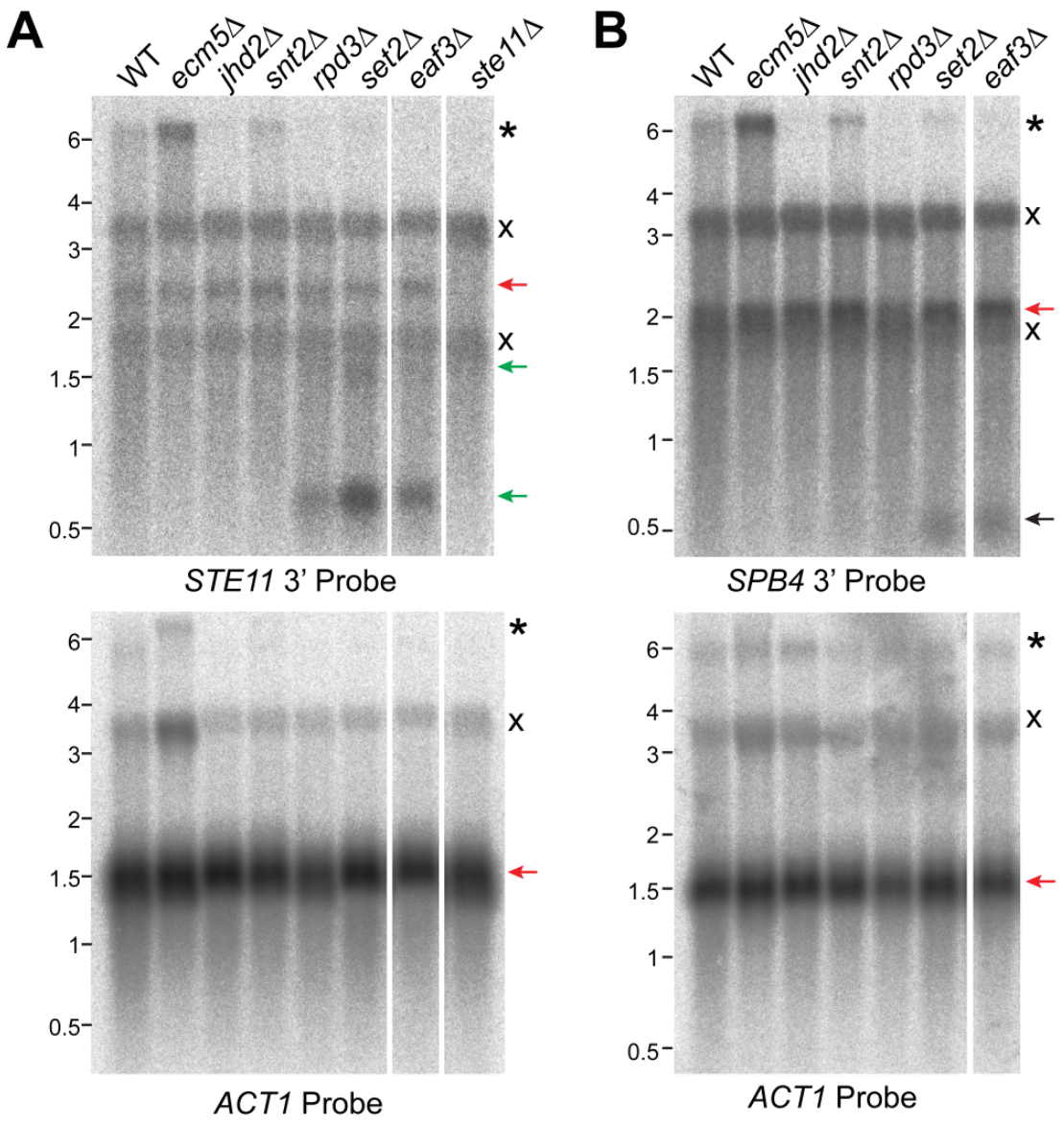

Figure 3.6 Northern blots to look for cryptic transcripts in *ecm5* or *jhd2* mutants
Poly-A$^+$-enriched RNA from the indicated wild-type (WT) or knockout strains was subjected to northern blotting with probes corresponding to the 3' end of the *STE11* or *SPB4* genes (top panels of **A** and **B**, respectively). A probe to *ACT1* was used as a loading control (bottom panels). The full-length transcript and the shorter, cryptic transcripts are marked by red and green arrows, respectively. Contaminating rRNA, which remained even after poly-A$^+$-enrichment, is marked with x's, and a longer RNA species enriched in *ecm5* and *snt2* knockouts, is marked with asterisks. The sizes from an RNA ladder (in kb) are shown to the left of each panel.

RNA is also detected with the *ACT1* loading control probe. However, the *snt2*Δ lane does not appear to be overloaded and also shows increased levels of the 6kb species. This species may be longer isoforms of *STE11* and *SPB4*, only present in *jhd2* and *ecm5* mutants. It could also be an unprocessed rRNA precursor present at higher levels in these mutants, that the poly-A^+ enrichment failed to fully eliminate and that cross-reacted with the probes. It remains unclear whether this is a true and interesting transcriptional difference between *ecm5* and *snt2* mutant or an artifact of these experiments. However, taken together, these experiments failed to find any evidence that either Jhd2 or the Rpd3(T) complex represses cryptic transcription.

Exploring other possible Ecm5 functions: the *ecm5* knockout does not have cell wall defects but does show increased expression of a gene encoding a cell wall protein

Unable to find any evidence that Ecm5 was involved in preventing cryptic transcription, I next attempted a number of experiments to get at what the function of this protein might be. Many of these experiments involved spotting serial dilutions of wild-type and *ecm5*Δ onto plates supplemented with chemicals that perturb various pathways, and looking differential growth under these conditions. These plate assays are summarized in Table 3.2. I first set out to confirm the cell wall defect phenotype that had been reported for the *ecm5* knockout strain, by seeing if *ecm5* knockouts displayed sensitivity to Calcofluor White, a chemical that binds to and interferes with the chitin in the yeast cell wall (Lussier et al., 1997; Ram et al., 1994). In addition to the wild-type strain, a *bar1* knockout, which contains the same G418-resistance gene as the other knockout strains was used as a negative control for these assays. This knockout lacks an excreted protease only used for mating, and was therefore not expected to have any

Table 3.2 Summary of plate spotting assays in which the *ecm5* knockout strain grew no differently than a wild-type strain

Additive or Treatment	Concentration or amount	Pathway or component assayed by treatment
37°C		General growth defect
23°C		General growth defect
6-azauracil (6AU)	50, 70, or 100 μg/mL	Transcription elongation
sodium dodecyl sulfate (SDS)	0.01 or 0.015 %	Cell wall
Calcofluor White	10, 50, or 100 μg/mL	Cell wall
methyl methane sulfonate (MMS)	0.03%	DNA damage response
UV radiation	4 mJ	DNA damage response
hydroxyurea (HU)	100 or 150 mM	DNA synthesis
camptothecin	10 μg/mL	DNA synthesis
benomyl	5 or 20 mM	Mitosis
YP Glycerol	3%	Cellular respiratory system
YP Galactose	2%	Cellular respiratory system
YP Raffinose	2%	Cellular respiratory system
hygromycin	30 μg/mL	Translation
NaCl	1 M	Osmolarity stress response
sorbitol	1.2 M	Osmolarity stress response
caffeine	10 mM	MAP kinase
bathocuproinedisulfonic acid (BCS) / bathophenanthroline disulfonate (BPS)	100 μM each	Sensitivity to low copper/ion levels

cell wall phenotypes. As additional controls for this assay, I used knockouts for *chs3* and *gas1*, which are known to be Calcofluor White resistant and sensitive, respectively (Ram et al., 1994; Roncero et al., 1988). As expected, the *chs3*Δ strain grew better than wild-type on YPD plates supplemented with Calcofluor White, while the *gas1*Δ strain showed little or no growth (Figure 3.7A). However, several independently derived *ecm5* knockout strains did not show Calcofluor White sensitivity. Similar results were found with *ecm5* knockout strains derived from the W303 yeast background strain (data not shown).

Growth on media containing sodium dodecyl sulfate (SDS) is another way to assay for cell wall defects (Shimizu et al., 1994). I therefore spotted the same set of strains on YPD plates supplemented with 0.015% SDS (Figure 3.7B). The *gas1* mutant again showed sensitivity to this cell wall-disrupting treatment. Again, however, *ecm5* knockout strains grew similarly to wild-type. While I was tempted to conclude from these experiments that Ecm5 protein function was completely unrelated to the yeast cell well, a microarray experiment I conducted to compare gene expression between wild-type and *ecm5* mutant cells did find a difference in the expression of *FIT1*, which encodes a cell wall mannoprotein (data not shown) (Protchenko et al., 2001). I was unable to validate most of the hits from this microarray screen, but I did confirm that cells lacking Ecm5 had higher levels of *FIT1* mRNA (Figure 3.7C). Taken together, these results suggest that while an *ecm5* knockout strain derived from the BY4741 or W303 background strain does not have impaired cell walls, Ecm5 may nevertheless have a role in cell wall function by ensuring proper expression of certain cell wall genes.

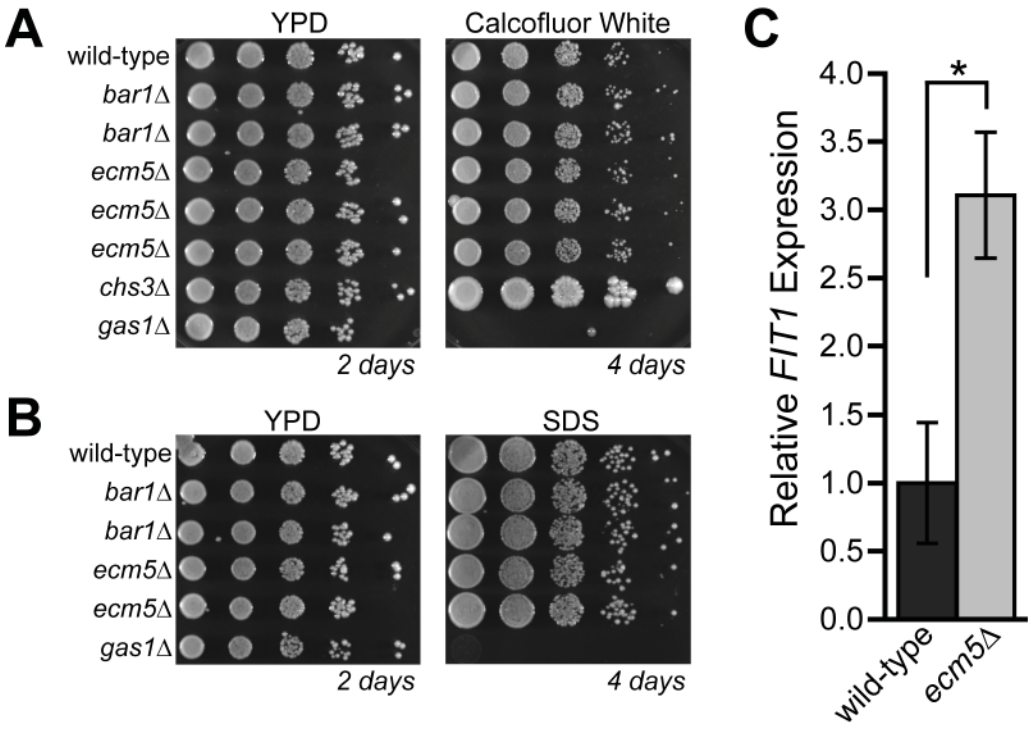

Figure 3.7 *ecm5* and *jhd2* knockouts are not sensitive to chemicals that disrupt the cell wall

Five-fold serial dilutions wild-type (BY4741) or indicated mutant strains were spotted on rich media (YPD) or YPD supplemented with 100 μg/mL Calcofluor White [**A**] or 0.015% sodium dodecyl sulfate (SDS) [**B**]. Plates were photographed after the number of days indicated under each image. **C.** qPCR analysis of *FIT1* expression in wild-type and *ecm5* knockout strains. Expression values were normalized to *ACT1* expression. Graph shows means and SEMs for 3 biological replicates.

Exploring whether Ecm5 is involved in the cellular morphogenesis checkpoint

Without any evidence that Ecm5 is required for intact cell wall, I next turned my attention to another phenotype originally reported for the *ecm5* knockout strain, elongated bud necks with drooping buds. Cell division in budding yeast is asymmetric: smaller daughter cells bud off of larger mother cells. Each daughter cell then grows into a mother and produces her own daughter cells. During cell division, the bud emerging from the mother cell forms the basis for the future daughter cell. The neck of the bud, the point of attachment between this structure the mother cell, is formed by a ring of septin proteins and acts as the conduit through which all components that the mother cell partitions to the daughter must pass (Merlini and Piatti, 2011). Thus, the proper formation of the bud neck and bud structures is vitally important to proper cell proliferation. In accordance with the importance of these structures, yeast have mechanisms in place to ensure that bud and bud neck are structured and properly. One such mechanism, the cell morphogenesis checkpoint, arrests the cell cycle in response to bud neck defect (Theesfeld et al., 2003).

The cell morphogenesis checkpoint is triggered by improper arrangement of the septin proteins that make up the bed neck. Normally, during late G1 and S phases, the Swe1 kinase (the budding yeast homolog of Wee1) accumulates in the nucleus. During S phase, a ring of septin proteins forms at the emerging bud, and a subpopulation of Swe1 leaves the nucleus and is recruited to the bud neck by the Hsl7 and Hsl1 proteins. Once at the bud neck, Swe1 is phosphorylated by the kinases Cdc5 and Cla4, promoting its degradation. As bud-neck localized Swe1 is degraded, more Swe1 is recruited from the nucleus, and in this manner, the cellular pool of Swe1 is diminished. If there is a defect in the septin organization at the bud neck or in the

actin-mediated transport of components to the emerging bud, Hsl7 is no longer recruited, and the Hsl1-Hsl7 complex no longer recruits Swe1 for destruction. The stabilized Swe1 is then free to phosphorylate the mitosis-promoting cyclin-dependent kinase Cdc28, thereby inactivating it, and triggering a G2 arrest.

Like the *ecm5* knockout strain, the *cla4* knockout also has an elongated bud neck phenotype (Cvrckova et al., 1995; Schmidt et al., 2003). Intriguingly, *cla4* mutants have similar doubling times to wild-type strains, suggesting that mutants that result in morphogenesis checkpoint activation can find ways to circumvent this checkpoint and keep dividing. In addition, *ECM5* gene expression is elevated in a strain lacking Cbk1, a kinase needed for apical bud growth, further linking Ecm5 with bud regulation (Bidlingmaier et al., 2001). Rpd3 has also been linked with bud regulation: combining the *rpd3* knockout with either *cla4* or *hsl7* mutants results in synthetic lethality (Ruault and Pillus, 2006; Ye et al., 2005).

To test whether *ECM5* deletion results in morphogenesis checkpoint activation, I immunoblotted whole cell extracts from wild-type and *ecm5*Δ cells with antibodies that recognize unmodified or phosphorylated Cdc28 (Figure 3.8). Consistent with the known function of Cla4 in this checkpoint, lysates from a *cla4*Δ strain had higher levels of Cdc28 phosphorylation. Cells lacking Hsl1, another protein needed to promote Swe1 degradation, also had higher levels of Cdc28 phosphorylation. However, cells lacking Ecm5, Snt2, or Rpd3 did not, suggesting deletion of Rpd3(T) complex members does not result in constitutive activation of the cellular morphogenesis checkpoint.

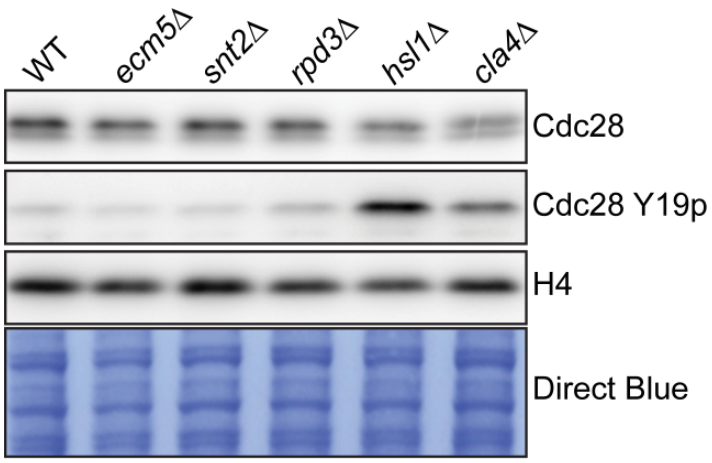

Figure 3.8 Cellular morphogenesis checkpoint signaling is not activated in *ecm5*, *snt2*, or *rpd3* knockouts

Whole cell extracts from a wild-type strain (WT) and the indicated knockout strains were blotted with antibodies against the Cdc28 cyclin, Cdc28 phosphorylated in tyrosine 19 (Cdc28 Y19p). A histone H4 blot and a Direct Blue 71 stain of the membrane are shown as loading controls. The *hsl1* and *cla4* knockout strains, which are known to have activated cell integrity checkpoints, are used as positive controls.

Exploring whether Ecm5 might be involved in the cell cycle or the DNA damage response

Hoping to get clues to the function of Ecm5 and the Rpd3(T) complex, I turned to publicly available high-throughput datasets. In particular, I focused on a study from Nevan Krogan's laboratory in which large numbers of yeast double knockout strains were screened for synthetic growth phenotypes (Collins et al., 2007). The *ecm5* knockout was one of the strains used in this screen, although the *snt2* knockout was not included. This study found a number of genes that showed synthetic genetic interactions with *ECM5* (Table 3.3).

I immediately noticed that the *TOP3* and *RMI1* genes, which encode two subunits of the DNA topoisomerase III complex, were both strongly synthetically sick in combination with *ECM5* deletion. This complex is involved in homologous recombination and DNA double strand break repair (Cejka et al., 2010; Hickson and Mankouri, 2011). Rpd3 has also been reported to antagonize the DNA damage response (Scott and Plon, 2003). I therefore wondered whether Ecm5 might be involved in DNA damage repair. In order to explore this, I spotted wild-type and *ecm5* knockout yeast strains onto plates treated with the DNA damaging agents (MMS and UV radiation) or chemicals that induce DNA replication stress (hydroxyurea or camptothecan). However, the *ecm5* knockout grew similarly to the wild-type strain under all these conditions (summarized in Table 3.2 and data not shown). After I completed these assays, I discovered that the *TOP3* and *RMI1* knockout strains were only pulled out of the Krogan laboratory screen because these mutants require a suppressor mutation in a gene near *ECM5* for vitality (Chang et al., 2005; Gangloff et al., 1994). *ECM5* is synthetically sick with these mutants because double mutants containing *ecm5*Δ no longer carry this suppressor mutation, and not due to the *ecm5* mutation, itself.

Table 3.3 *ECM5* Synthetic Genetic Interactions[a]

Mutants synthetically sick with *ecm5* knockout		
Gene	**Interaction Score**	**Function**
~~*TOP3*~~ [b]	~~-5.1~~	~~Subunit of DNA Topoisomerase III complex~~
~~*RMI1*~~ [b]	~~-4.3~~	~~Subunit of DNA Topoisomerase III complex~~
SAS2 [c]	-3.7	HAT that opposes transcriptional silencing
GCN1 [c]	-3.2	Amino acid starvation sensor
ASK10	-2.7	Oxidative stress sensor
SIC1	-2.5	CDK inhibitor that prevents premature S phase
Mutants synthetically healthier with *ecm5* knockout		
Gene	**Interaction Score**	**Function**
SIN3	2.4	Member of RPD3(L) and RPD3(S) complexes
OPI3	2.5	Enzyme involved in phospholipid anabolism

[a] From Collins et al., 2007 dataset. The more negative a score, the worse the double mutant combination grew compared to either single mutant. The more positive a score the better the double mutant combination grew. Scores above 2.5 or below -2.5 are considered significant.

[b] Both the *top3* and the *rmi1* knockout strains have a suppressor mutation in a gene on Chromosome XIII, near *ECM5*, allowing these mutants to survive. *ECM5* is synthetically sick with these mutants because double mutants containing *ecm5*Δ no longer carry this suppressor mutation, not due to the *ecm5* mutation itself.

[c] These mutants are also synthetically sick with an *rpd3* knockout

The *ecm5* knockout was also synthetically sick with cells lacking the CDK inhibitor Sic1, whose phosphorylation and destruction triggers the start of S phase (Verma et al., 1997). In addition, numerous studies have linked Rpd3 regulation of cell cycle genes (Bernstein et al., 2000; Robert et al., 2004; Takahata et al., 2009; Wu et al., 1999). I therefore wondered whether, as part of the Rpd3(T) complex, Ecm5 might play a role in the yeast cell cycle. I set out to characterize the cell cycle profiles of control and *ecm5* knockout strains using FACS cell cycle analysis. I arrested both strains using α-factor and monitored the arrest by looking for the presence of shmoos and the absence of buds in the microscope. I then released the synchronized cells into the cell cycle, and took aliquots every 20 minutes for cell cycle analysis, using flow cytometry. As can be seen in Figure 3.9, before release, wild-type cells had almost exclusively 1C DNA content, consistent with their arrest G1 phase. Within 40 minutes after release, many wild-type cells had 2C DNA content, indicating they had completed S phase. Between 60 and 80 minutes post-release, the number of cells with 1C DNA content increases again, consistent with cells that have completed mitosis. The profiles of the *ecm5* knockout strain were almost identical to wild-type profiles, showing that *ecm5* mutants have no obvious cell cycle defects. In addition, I tested growth on the microtubule inhibitor benomyl to see if the *ecm5* knockout had defects in mitosis, but again, the *ecm5* knockout strain grew similarly to wild-type in this assay (data summarized in Table 3.2). Consistent with these results, *ecm5* mutants had similar doubling times to wild-type cells in both rich (YPD) and less rich (synthetic defined with complete supplement mixture, or SD CSM) media (Table 3.4).

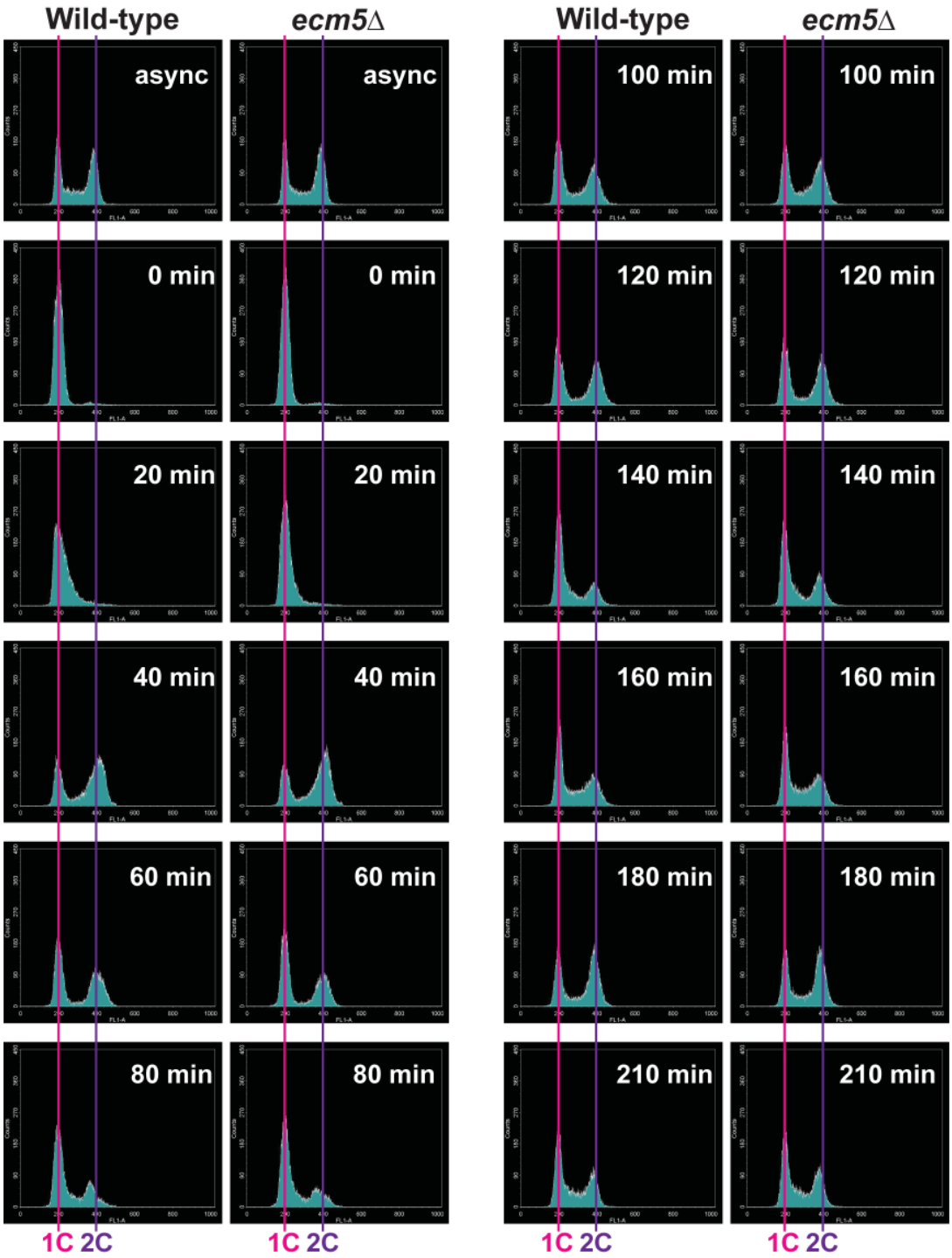

Figure 3.9 Cell cycle analysis of *ecm5* knockout cells

The *bar1* knockout strain ("Wild-type") and the *bar1*Δ *ecm5*Δ double knockout ("*ecm5*Δ") were synchronized using α-factor, and cells were taken at the indicated time points, stained with SYTOX green and analyzed by flow cytometry. Histograms of cell fluorescence at each timepoint are shown, with the positions of 1C and 2C DNA content indicated. Cells from asynchronously growing strains (async) were also analyzed.

Table 3.4 Growth rates in rich and moderate media[a]

Strain	YPD	SD CSM
wild-type	100 ± 6	125 ± 7
ecm5 Δ	97 ± 4	118 ± 5
snt2 Δ	98 ± 3	121 ± 3
rpd3 Δ	128 ± 2	138 ± 10

[a] doubling times in minutes, plus or minus standard deviation of 3 independent cultures

While Ecm5 is not required for cell cycle progression, it is possible that this protein is still involved in this process. Since the levels of many cell cycle proteins fluctuate over the course of the cell cycle, I checked whether Ecm5 protein levels changed at any point in the cycle. To that end, I synchronized a tagged Ecm5 strain, and immunoblotted cell lysates taken at various points after release to look for changes in Ecm5 protein levels (Figure 3.10). Levels of H3S10p, which are known to peak during mitosis (Wei et al., 1998), were clearly enriched starting between 40 and 60 minutes post-release, showing that these cells were well synchronized going into mitosis, although less so at later time-points. In contrast, levels of tagged Ecm5 protein remained constant throughout the cell cycle. Taken together, the results of these experiments do not provide any evidence that Ecm5 is involved in cell cycle progression, or DNA repair and replication.

Exploring whether Ecm5 is required for sporulation

Since Ecm5 protein levels are low in yeast grown under normal conditions, I wondered whether the primary function of this protein might be in a pathway not normally needed during vegetative growth, such as sporulation. Intriguingly, around this time, we received word that unpublished work from Marc Meneghini's laboratory had found that Jhd2 is required for proper sporulation. In addition, the Rpd3(L) complex is known to repress meiosis genes in vegetatively growing yeast, and *rpd3* mutants have sporulation defects (Bowdish and Mitchell, 1993; Dora et al., 1999; Lamb and Mitchell, 2001; Strich et al., 1989; Strich et al., 1994; Vidal and Gaber, 1991). I therefore tested whether an Ecm5 mutant has any defect in sporulation. Because the *BY4741* background strain that I have used for most of this work is known to be poor at

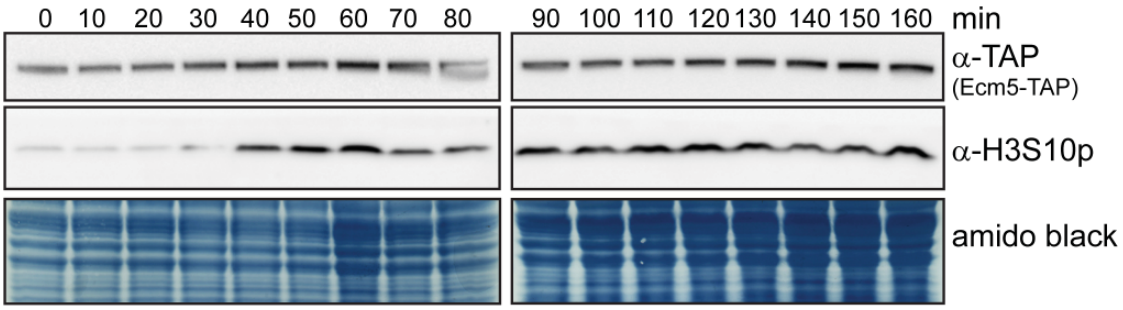

Figure 3.10 Ecm5-TAP protein levels over the course of the cell cycle

Whole cell extracts from an *ECM5-TAP bar1*Δ strain synchronized using α-factor were immunoblotted with antibodies against the TAP tag (to detect Ecm5-TAP levels) and H3S10 phosphorylation (H3S10p, a mitosis-specific mark). Numbers at the top show minutes after α-factor release. Bottom panels are amido black stains, used as a loading control.

sporulation, I created a homozygous diploid *ecm5* knockout strain on the highly-sporulating *SK1* genetic background, and grew wild-type and *ecm5*Δ SK1 strains in 1% potassium acetate solution to promote sporulation. However, the *ecm5* mutant showed no defects in tetrad formation (Figure 3.11A), and individual spores from sporulated *ecm5* mutant tetrads were fully viable (Figure 3.11B), showing Ecm5 is not required for sporulation.

Chapter 3 Discussion

The experiments described in this thesis chapter were all undertaken with the goal of better understanding the functions of Ecm5 and Jhd2. In order to achieve this goal, I first set out to determine Ecm5- and Jhd2-interacting proteins. Despite multiple attempts, Trixi and I were unable to identify any proteins interacting with Jhd2. While we tried a variety of purification conditions, it is possible that we failed to utilize the specific condition under which associations between Jhd2 and its interacting proteins were maintained. Alternatively, Jhd2 may function independently of other proteins in a stable complex. Trixi and I were able to show that Ecm5 interacts with Snt2 and the Rpd3 deacetylase. In good agreement with my results, shortly after I identified this complex, Anna Shevchenko and A. Francis Stewart reported identifying a complex consisting of Ecm5, Snt2, and Rpd3, which they called the Snt2 complex (Snt2C) (Shevchenko et al., 2008). Because Rpd3 is currently the only subunit in this complex known to have enzymatic activity, I favor the use of the name Rpd3(T) complex, which highlights the likely function of this complex as a deacetylase and promotes comparison to the other Rpd3 complexes.

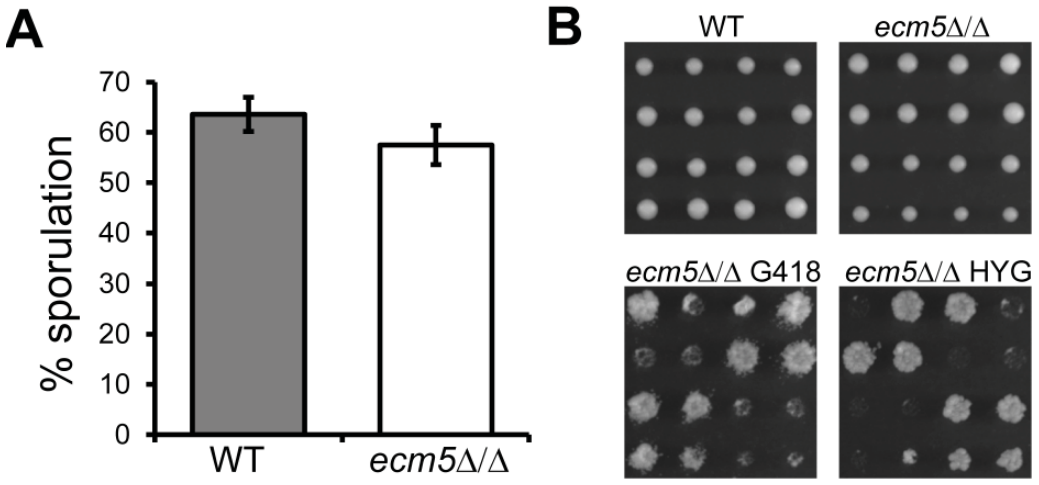

Figure 3.11 The *ecm5* knockout strain does not have sporulation defects
Wild-type (WT) SK1 and *ecm5Δ::G418/ecm5Δ::HYG* mutant yeast were transferred to 2% potassium acetate to induce sporulation. **A.** After 3 days, the number of tetrads was counted and divided by the total number of tetrads and unsporulated diploid cells in the sample to determine % sporulation. The graph shows the mean and standard deviation of 3 independently sporulated wild-type colonies and 4 independently sporulated *ecm5* knockout colonies. **B.** Representative tetrad dissections show that *ecm5Δ/Δ* spores are viable. Replica platings of the *ecm5Δ/Δ* tetrads onto plates containing G418 and hygromycin B (HYG, bottom panels), to select for each *ecm5* knockout allele, show the *ecm5* deletion segregates normally.

Based on the Ecm5 and Snt2 domain structures, and the known deacetylase activity of Rpd3, the Rpd3(T) complex is highly likely to function at chromatin. Regardless of whether we treated our extracts with DNAse, micrococcal nuclease, or nothing (in which case the DNA was partially sheared due to cryogenic lysis procedure), histones were never observed in our purifications. It is possible that this complex does not interact with chromatin. However, I believe it is more likely that our purification conditions promoted dissociation of the Rpd3(T) complex from nucleosomes. In support, experiments I described in Chapter 2 of this thesis found that the Ecm5 PHD finger could interact with histone H3. Additionally, in experiments I describe in the next Chapter of this work, I was able to clearly and repeatedly find Ecm5 and Snt2 localized to specific genomic regions by ChIP.

The existence of a third Rpd3 complex immediately prompts the question: how do the functions of these three complexes compare? Because of initial data suggesting the Ecm5 and Jhd2 PHD fingers could interact with H3K36me3, I immediately thought of the Rpd3(S) complex, which also contains subunits that interact with H3K36me2/3, and is required to prevent initiation from cryptic promoters within certain genes. I initially hypothesized that Jhd2 and the newly discovered Rpd3(T) complex might also prevent cryptic transcription. However, I was unable to find any evidence that levels of known cryptic transcripts were higher in strains lacking Ecm5 or Snt2, leaving no support for this hypothesis. It remains possible that Jhd2 or the Rpd3(T) complex does prevent cryptic transcription within coding sequences, but at different target genes than the two that I studied in these assays, or that higher levels of cryptic transcripts present in strains lacking these proteins are still too low to be detected in my assays. The cryptic transcripts in the *rpd3* knockout were just at the limit of detection in my northern blots, so levels

of cryptic transcripts lower than these would likely have been below the level of detection by this assay. It is also possible, that the Rpd3(T) complex acts redundantly with other factor(s) such that cryptic transcripts are only detectable *ecm5* or *snt2* knockouts also deleted for this other factor(s). To that end, it would be interesting to see whether deletion of *ecm5* enhanced the cryptic transcript phenotype of the *eaf3* and *rco1* knockout strains. However, it should be noted that in ChIP experiments that I will describe in the next chapter of this work, I did not see any Ecm5 or Snt2 enrichment at *STE11* or *SPB4* coding regions or promoters, making it unlikely that the Rpd3(T) complex has any direct function at these genes (data not shown).

In addition to preventing aberrant transcription from initiating within genes, a recent report shows that the Rpd3S complex plays a role in suppressing transcription of CUTs initiating from promoter regions (Churchman and Weissman, 2011). These authors report that *rco1* and *eaf3* knockouts have higher levels of antisense CUTs, initiating from the same start sites used by the coding transcripts. Since deletion of Set2 (but not Set1) also increases CUT transcription, the authors suggest that Rpd3(S) is recruited to the promoter regions where these CUTs are known to initiate through interactions with Set2-deposited H3K36me3 at the 3' ends of nearby genes. However, even the authors note that this model does not explain how the Rpd3(S) complex prevents CUT transcription at promoters that are not close to the 3' end of another gene. This new work affirms that aberrant transcription within coding regions is just the tip of the iceberg when it comes to noncoding transcription in yeast. Because my experiments only focused on a role for the Rpd3(T) complex in preventing aberrant transcripts within coding regions, I cannot say whether this complex is involved in other types of noncoding transcription, although the intriguing 6kb RNA species enriched in *ecm5* and *snt2* knockouts may point to some role

for Rpd3(T) in the pathways. Future experiments looking for altered levels of other kinds of noncoding transcripts in *ecm5* and *snt2* knockouts, either in combination with TRAMP and exosome mutants, or by directly sequencing RNA Pol II-associated transcripts, may uncover a role for the Rpd3(T) complex in regulating non-coding transcription. In addition, a northern blot with an rRNA proble, to look at whether *ecm5* and *snt2* knockout strains have altered rRNA processing, might be worthwhile.

While I was unable to confirm a role for the Rpd3(T) complex in suppressing cryptic transcription, I remained interested in gaining insight into the function(s) of this complex. Because of the cell wall phenotypes reported for the *ecm5* mutant, I thought that Ecm5 might be involved in regulating this structure, possibly by regulating expression of genes involved in cell wall maintenance. However, my own *ecm5* knockout strains showed no sensitivity to the cell wall disrupting agents calcofluor white and SDS. This discrepancy in findings may be due to the differences in genetic backgrounds used between this work and the previous Ecm5 study. My studies have all been conducted with mutants made in the S288C (BY4741) and W303 background strains, while the original isolation of the Ecm5 mutant was done using the AWM3CΔ630 background strain. There are at least a few reported examples of different mutants having different phenotypes in different genetic backgrounds (de Jesus Ferreira et al., 2001; Kucharczyk et al., 1999; Schoch et al., 1997; Trachtulcova et al., 2003). While I did not find any evidence that the cell walls of *ecm5* knockout cells were grossly defective, I did find up-regulation of a cell wall mannoprotein gene in the *ecm5* knockout strain, suggesting at least one link between Ecm5 and the yeast cell wall.

Cells lacking Ecm5 have also been reported to have elongated bud necks and drooping buds, suggesting Ecm5 might be required for proper formation of the bud or bud neck, and deletion of this gene might activate the cellular morphogenesis checkpoint. However, *ecm5* knockout cells did not have higher levels of Cdc28 phosphorylation, showing that this checkpoint is not constitutively active in *ecm5* knockouts. I have never noticed an elongated bud neck or drooping buds in my own microscopic examinations of *ecm5* mutants. However, the elongated bud neck phenotype is fairly subtle to detect using normal light microscopy, and I have trouble recognizing it even when pointed out in micrographs in published papers. Notably the elongated bud neck phenotype for *ecm5* mutants was reported by the same group who found the *ecm5* mutant had a cell wall defect, so it is also possible that this phenotype is only present in *ecm5* knockouts from the AWM3CΔ630 background.

As another means of getting at Ecm5 protein function I made use of a high-throughput screen for genes that synthetically interact with the *ecm5* knockout strain. There were many interesting genes pulled out from this screen. For instance deletion of *ECM5* relieved the growth defects associated with loss of Sin3, a subunit of both the other Rpd3 complexes, suggesting that Rpd3(T) may function in opposition to the Rpd3(S) and Rpd3(L) complexes. Because three of the genes in this screen had functions relating to DNA damage repair or cell cycle progression, I checked whether *ecm5* mutants had any defects in these pathways. However, I showed that the *ecm5* knockout strain is not sensitive to chemicals that disrupt DNA replication, trigger DNA damage, or interfere with mitotic microtubules and that *ecm5* knockout cells have normal cell cycle profiles, suggesting Ecm5 is not necessary for any of these processes. In addition, *ecm5* knockout cells have no discernible defects in sporulation. While it remains possible that Ecm5

plays a subtle and non-essential role in any of these processes, it seemed unwise to experiment further along these lines without a clear indication of involvement.

These early experiments into Ecm5 function were not very successful. However, there were other genes with *ECM5* synthetic phenotypes found in the Krogan laboratory's screen that I had yet to interrogate (Table 3.3). This screen found a genetic interaction between *ECM5* and the *SAS2* gene, which encodes a H4K16 acetyltransferase known to oppose transcriptional silencing. In contrast to the *SIN3* genetic interaction data discussed above, this genetic interaction suggests that the Rpd3(L) and (S) complexes might function similarly with regard to transcriptional silencing, since the Rpd3(L) complex has been shown to antagonize silencing (De Rubertis et al., 1996; Rundlett et al., 1996; Smith et al., 1999; Sun and Hampsey, 1999; Vannier et al., 1996). *ECM5* also had genetic interactions with *ASK10* and *GCN1*, genes which encode oxidative stress and amino acid starvation sensors, respectively, hinting that the Rpd3(T) complex might function in stress and metabolism signaling, an idea that forms the basis for the next chapter of this work.

CHAPTER 4: EXPLORING THE ROLE OF THE RPD3(T) COMPLEX IN THE OXIDATIVE STRESS RESPONSE AND METABOLIC REGULATION

Chapter Introduction

Despite obtaining some negative results in my early Ecm5 functional experiments, I remained eager to determine a function for the Rpd3(T) complex. Based on a genetic interaction reported by the Krogan laboratory, between *ECM5* and the *ASK10* oxidative stress sensor gene (Collins et al., 2007), I formed a new hypothesis that the Rpd3(T) complex might function in the yeast oxidative stress response. The first part of this chapter will focus on initial experiments I performed to look for evidence that Ecm5 and Snt2 are involved in this pathway, and the discovery that the *snt2* knockout strain is resistant to hydrogen peroxide (H_2O_2)-mediated oxidative stress. I will then discuss genome-wide chromatin immunoprecipitation (ChIP) experiments undertaken to map Ecm5 and Snt2 localization before and after oxidative stress. Because the results of this mapping found Ecm5 and Snt2 localized to gene promoter regions, I next wanted to determine whether there were any differences in gene expression in *ecm5* and *snt2* knockout strains before and after H_2O_2 stress. The third part of this chapter will describe RNA sequencing experiments undertaken to look for gene expression differences in these mutants, and to determine whether Ecm5 and Snt2 regulate the expression of their target genes.

While these ChIP and gene expression analyses isolated many genes involved directly in the oxidative stress response, they also identified genes involved in cellular metabolism functions such as protein translation, amino acid uptake and synthesis, and carbon usage. The association of the Rpd3(T) complex with metabolism genes suggests that rather than functioning solely in

detoxifying oxidative stress, this complex might function more broadly at the interface between cellular stress and nutrient metabolism. In order to see whether the Rpd3(T) complex also responds to metabolic stress, I conducted studies in the more nutrient-limited stationary phase of growth and with the TOR pathway inhibitor rapamycin, which is known to promote cellular changes that mimic amino acid starvation. The fourth part of this chapter will summarize these experiments, and show that the Rpd3(T) complex responds to nutrient stress.

Genetic links between the Rpd3(T) complex and oxidative stress

In the synthetic genetic screen performed by the Krogan laboratory, discussed in the previous chapter, one of the genes whose deletion showed synthetic sickness when combined with the *ecm5* knockout was *ASK10* (also known as *RGC2*). This gene was first discovered in a screen for mutants that result in transcriptional activation of *SKN7*, a transcription factor involved in the oxidative and heat stress responses (Page et al., 1996). A later report found that Ask10 associates with the RNA pol II holoenzyme and is phosphorylated in response to oxidative stress, suggesting that Ask10 may help regulate the yeast oxidative stress response (Cohen et al., 2003). More recently, Ask10 was shown to be involved in regulating the response to hyperosmotic stress, a condition that also triggers Ask10 phosphorylation (Beese et al., 2009).

Because of the genetic link between Ecm5 and Ask10, I hypothesized that the Rpd3(T) complex might help to mediate the oxidative stress response, or possibly a more general response to stress. In support of this, cells lacking Snt2 have higher levels of phosphorylated Slt2 (de Groot et al., 2001), a mitogen activated protein kinase (MAPK) homologous to the mammalian p42/p44 MAPK, that is activated in response to diverse extracellular stresses, including oxidative

and osmotic stress. In addition, many of the genes whose levels change in response to osmotic stress are genes whose promoters were found to contain Snt2 by ChIP-chip (Harbison et al., 2004; Miller et al., 2011). Thus, there were multiple lines of evidence to connect Ecm5 and Snt2 to cellular stress response.

Work from several groups has implicated Rpd3 and the Rpd3(L) complex in yeast stress response function. Cells lacking Rpd3 or Sin3 are sensitive to osmotic stress, and in response to high levels of NaCl, these proteins are recruited to the promoters of osmotic stress genes where they are required for gene activation (De Nadal et al., 2004). The Rpd3(L) complex is also recruited to stress response genes in response to heat shock, where it mediates both gene activation and repression (Kremer and Gross, 2009; Ruiz-Roig et al., 2010). In addition, Rpd3 is required for the activation of certain cell wall mannoproteins in response to hypoxia stress (Sertil et al., 2007). While Rpd3 is generally thought of as a transcriptional repressor, these reports suggest that in some cases, this protein can also activate transcription. Consistent with this idea, a microarray study found that Rpd3 is required for both activation and repression of the many genes whose expression change in response to heat shock, osmotic stress, or oxidative stress (Alejandro-Osorio et al., 2009).

Because of the genetic evidence linking Ecm5 to oxidative stress, and because of the connection between the Rpd3(L) complex and stress response pathways, I set out to determine whether the Rpd3(T) complex also functioned in the yeast oxidative stress response. I initially checked whether tagged Ecm5 and Snt2 protein levels change in response to treatment with 0.5 mM H_2O_2. While Ecm5 and Snt2-PrA levels did not change within the first couple of hours of H_2O_2 treatment, they each increased 4 hours after H_2O_2 treatment relative to the loading controls

(Figure 4.1A). No western blot signal was seen before or after treatment in whole cell extracts from an untagged strain, confirming that the Ecm5- and Snt2-PrA signal on these western blots was specific to the tagged proteins. In a second experiment, where a single Ecm5-PrA culture was grown and divided into two separate cultures, one receiving 0.4 mM H_2O_2, and the other receiving no treatment, Ecm5-PrA levels increased in response to H_2O_2 treatment but not in the no treatment control (Figure 4.1B). The increase in Ecm5 protein levels was not seen in every experiment I tried, but it was repeatable: 6 out of 8 experiments involving treatment with 0.4-0.5 mM H_2O_2 resulted in an increased in tagged Ecm5 protein levels. In contrast, the increase in Snt2-PrA after H_2O_2 treatment was only seen in 1 out of 4 experiments. The increased Ecm5 protein levels in response to oxidative stress could be explained by increased transcription, increased translation, or decreased degradation of Ecm5. However, qPCR experiments found that *ECM5* mRNA levels do not change significantly 30 minutes or 4 hours after H_2O_2 treatment (Figure 4.1C), suggesting the increases in Ecm5-PrA were the result of post-transcriptional mechanisms. *SNT2* mRNA levels did increase slightly 0.5 hours after H_2O_2 treatment but returned to baseline by 4 hours post-treatment (Figure 4.1D).

Because these results provided an early confirmation that Ecm5 and Snt2 might function in the oxidative stress response, I then tested whether *ecm5* and *snt2* knockouts showed differential growth on plates supplemented with H_2O_2. As a control for this assay, I used a strain lacking the Yap1 H_2O_2-response transcription factor, which is known to be H_2O_2-sensitive (Schnell et al., 1992). When plated on YPD containing moderate concentrations of H_2O_2 (concentrations in which the wild-type strain grew as well as on untreated plates, but the oxidative stress-sensitive *yap1* knockout could not grow), the *ecm5* and *snt2* knockout strains

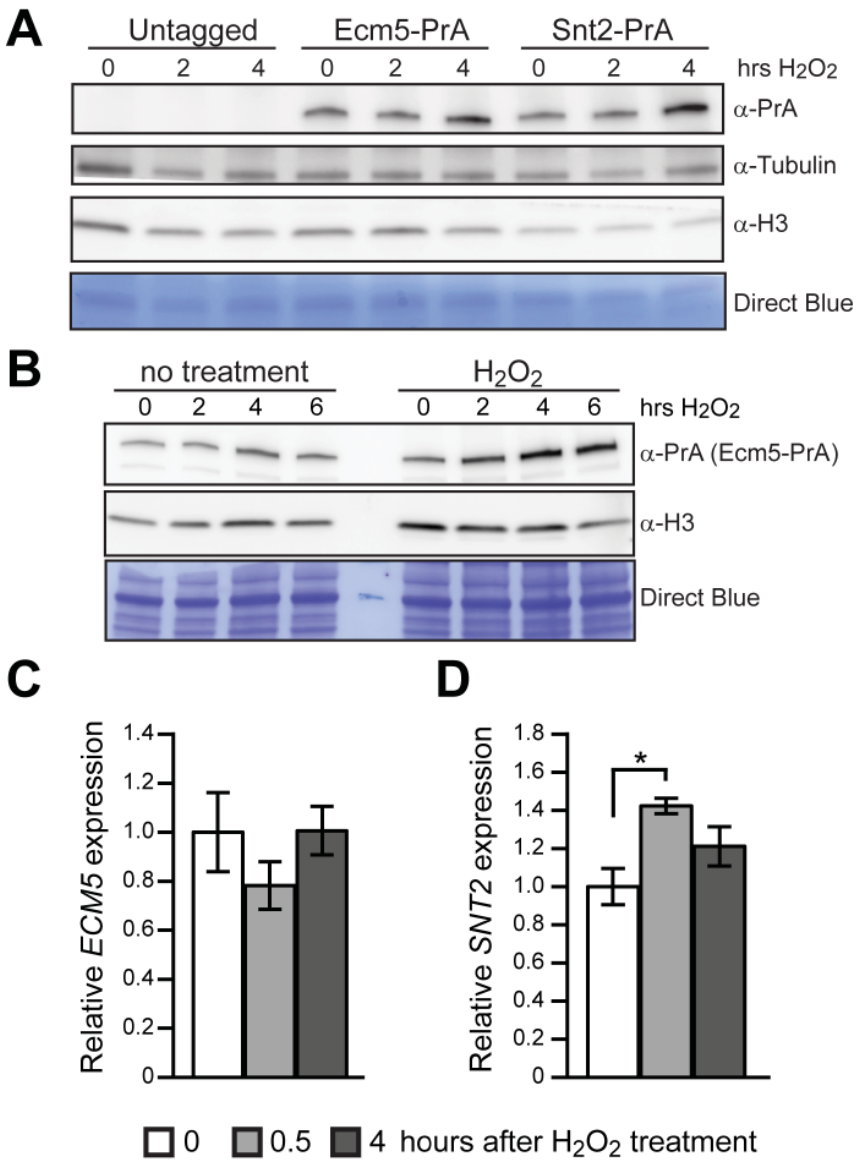

Figure 4.1 Ecm5 and Snt2 protein and mRNA levels before and after H_2O_2 stress

A. Protein A-tagged (and untagged control) strains were grown to mid-log phase in rich media, and treated with 0.5 mM H_2O_2. PrA western blots of whole cell extracts show Ecm5- and Snt2-PrA levels before and at indicated times (hrs: hours) after treatment. Blots for histone H3 and tubulin, as well as Direct Blue 71 membrane straining are shown as loading controls. **B.** PrA western blots on whole cell extracts as in A, except cells were treated with either 0.4 mM H_2O_2 or water alone (no treatment) as a control. **C and D.** qPCR expression analysis of *ECM5* (**C**) and *SNT2* (**D**) mRNA levels in wild-type cells and after 0.4 mM H_2O_2 treatment. Expression values were normalized to *ACT1* expression, and average expression in the wild-type untreated sample was set to 1. Graphs show averages and SEMs of qPCRs from 3 biological replicates. * $p<0.05$ by paired two-tailed t test.

grew very similarly to wild-type (Figure 4.2A, compare left and middle panels). Surprisingly however, on higher H_2O_2 concentrations, the *snt2* knockout strain was H_2O_2-resisitant, growing almost as well as on the untreated YPD control plate while the wild-type strain could barely grow (Figure 4.2A, right panel). A similar level of growth was seen with a strain lacking Gpr1, a G protein glucose sensor which was recently reported to be H_2O_2-resistant (Molin et al., 2011). Unlike the *snt2* knockout, the *ecm5* knockout strain had similar H_2O_2 sensitivity to the wild-type strain. The *rpd3* knockout strain has a known growth defect which can be seen by the smaller *rpd3*Δ colony size on the YPD control plate. While this strain also had smaller sized colonies on the 3.0 mM H_2O_2 plate, there were more *rpd3*Δ colonies than wild-type colonies on this plate, showing that like the *snt2* knockout, this mutant also was resistant to oxidative stress.

Having performed a great many plate spotting assays by this point in my graduate research without ever having seen a strong phenotype for the *ecm5* and *snt2* knockout strains, I was cautiously excited to finally see a phenotype for one of my mutants. However, I wanted to be sure this phenotype was truly due to deletion of *SNT2*, and not just an artifact of this particular strain. I therefore constructed new *ecm5*, *snt2*, and *rpd3* deletion strains on the *BY4742* background and subjected them to the same plate assay. The *snt2* knockout strain again showed resistance to high levels of H_2O_2 (Figure 4.2B). The *rpd3*Δ strain also showed moderate H_2O_2-resistance in this assay. To determine whether this result was specific to the oxidative stress response or was a more general stress resistance, I subjected these cells to osmotic stress by plating them on plates containing 1.2 M NaCl. Consistent with previous reports, the *rpd3* mutant showed a strong growth defect on high salt. However, the *snt2* mutant also grew better than wild-type and the *ecm5* knockout strain under these conditions, suggesting this knockout displays resistance to multiple kinds of stresses (Figure 4.2C).

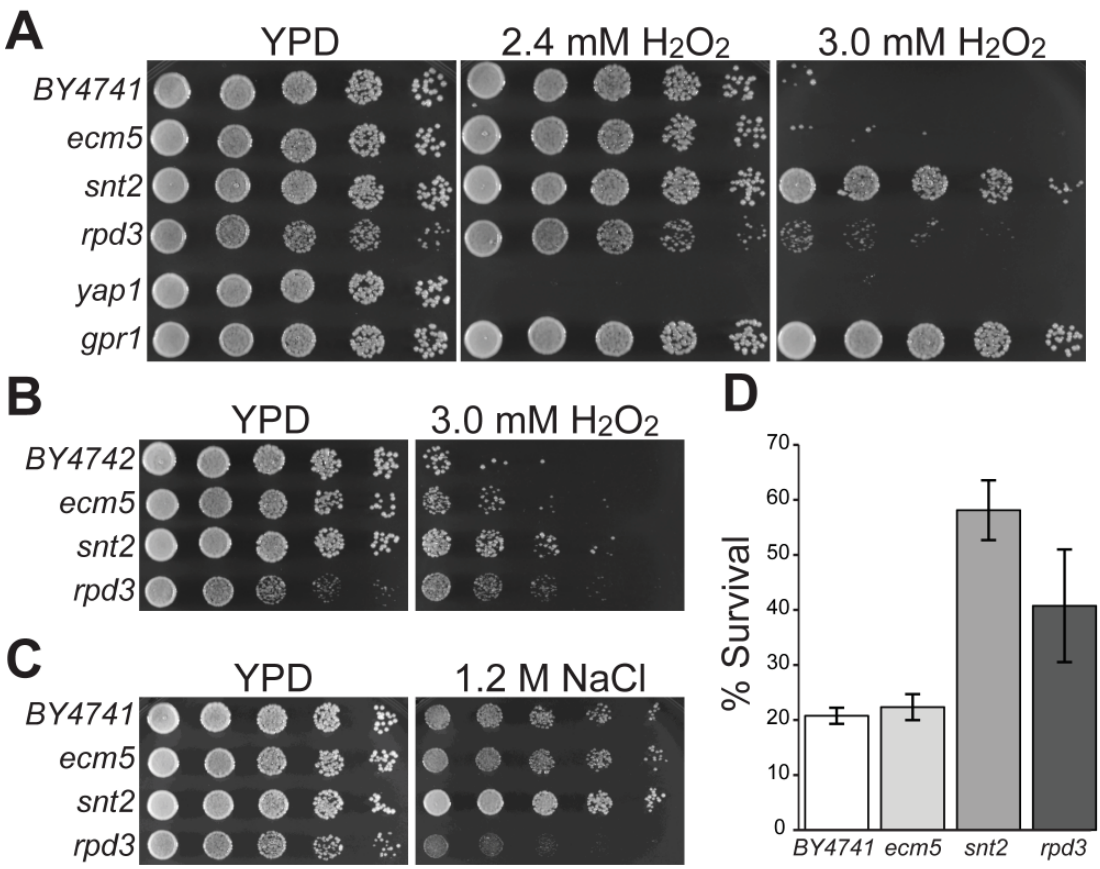

Figure 4.2 *snt2* mutants are resistant to oxidative and osmotic stress

A. Five-fold serial dilutions of mid-log phase cultures of wild-type (BY4741) or indicated knockout strains were spotted on rich media (YPD) or YPD supplemented with 2.4 or 3.0 mM hydrogen peroxide (H_2O_2). Plates were imaged after 2 days. **B.** Spotting assay as in A, with a separate set of knockout strains derived from the BY4742 background strain. **C.** Spotting assay as in A on YPD or YPD supplemented with 1.2 M NaCl. YPD control and NaCl plates were imaged after 2 and 3 days, respectively. **D.** The wild-type (BY4741) or knockout strains indicated were grown to mid-log phase, and cultures were treated with 0.4 mM H_2O_2 for 4 hours. Percent survival was determined by plating 1000 cells from each culture before and after treatment and counting viable colonies after two days' growth. Shown are means and SEMs from 3 biological replicates.

To further confirm that the *snt2* mutant was resistant to oxidative stress, I subjected the wild-type and *ecm5*, *snt2*, and *rpd3* knockout strains to a liquid survival assay. In this assay, each strain was grown to mid-log phase in YPD and treated with 0.4 mM H_2O_2 for 4 hours. Before and after treatment 1000 cells from each culture were plated onto YPD, and the number of colonies visible after 2 days' growth was counted to determine the number of viable cells at the time of plating. The percentage of cells alive after treatment, relative to the number of live cells before treatment was then determined. Under these conditions, the wild-type strain and the *ecm5* knockout strain each had about 20% survival (Figure 4.2D). Consistent with the plate assays, the *rpd3* and *snt2* knockouts showed enhanced survival in this assay, with 58% of *snt2*Δ cells and 41% of *rpd3*Δ cells surviving 4 mM H_2O_2 treatment. Taken together, these experiments show that both the *snt2* and *rpd3* knockout strains are resistant to H_2O_2-mediated oxidative stress, with the *snt2*Δ strain showing higher levels of resistance than the *rpd3*Δ strain.

Mapping the genomic localization of Ecm5 and Snt2 before and after oxidative stress

In order to get a better understanding of how the Rpd3(T) complex might function in the response to oxidative stress, I sought to map this complex's genomic localization using chromatin immunoprecipitation followed by deep-sequencing (ChIP-seq). Since Rpd3 is a constituent of at least two other chromatin-associated complexes, I set out to map the localization of the Rpd3(T)-unique Ecm5 and Snt2 subunits. A previous study had mapped genome-wide Snt2 associations using ChIP followed by microarray analysis, and found Snt2 at the promoters of a small number of genes (Harbison et al., 2004). Using this data, a separate group determined a binding motif for Snt2 and reported enrichment of this motif at the promoters of amine

transmembrane transporters (Ward and Bussemaker, 2008). While these studies offered some insight into the potential functions of Snt2 and the Rpd3(T) complex, the use of microarrays containing only a single probe for each promoter region limited the spatial resolution of this mapping. I therefore felt it necessary to map the localization of Snt2 myself using the newer ChIP-seq technology favored by the Allis laboratory, which provides better resolution, higher sensitivity, and more complete genome coverage than most microarrays. In addition, to my knowledge, no ChIP for Ecm5 had ever been performed, and I wanted to determine whether Ecm5 and Snt2 colocalized, as would be predicted if they are part of the same complex. Lastly, neither protein's localization has been mapped under conditions of oxidative stress, and given my genetic results, I was curious to see whether Ecm5 and Snt2 would respond H_2O_2 stress by localizing to new regions of the genome.

Ecm5 and Snt2 are highly colocalized by ChIP-seq

For these ChIP studies, I generated new strains in which *ECM5* or *SNT2* was tagged with 13 copies of the Myc epitope (hereafter referred to as the Myc tag). I grew both tagged strains along with an untagged control strain to mid-logarithmic (mid-log) phase in rich media, and harvested and fixed cells for ChIP. I then treated the remaining cultures with 0.4 mM H_2O_2, and harvested cells 30 minutes and 4 hours after treatment. I chose these two time-points because the former would allow me to look at the acute stress response, which has been shown to occur 5-30 minutes after H_2O_2 stress (Gasch et al., 2000) , while the latter coincided with the time when I found an increase in Ecm5 protein levels. Since H_2O_2 is a highly reactive chemical, the majority of H_2O_2-inflicted damage is likely to occur within minutes of addition of this chemical

to the media. However, cells given a mild dose of H_2O_2 are known to undergo adaptive changes that render them more resistant to larger doses of this stress in the future (Collinson and Dawes, 1992; Jamieson, 1992). Another reason I chose to map Ecm5 and Snt2 localization 4 hours after H_2O_2 treatment was to see whether there were any localization changes specific to this late time-point that might suggest Ecm5 and Snt2 involvement stress adaptation. While I never tested *ecm5* and *snt2* knockout strains for enhancement or loss of the adaptation, I was curious to see whether localization changes in these two proteins might reveal something about this process.

I then performed ChIP on these cells using an anti-Myc, and submitted both the input and the ChIP DNA from all samples for sequencing. Here, I was fortunate to work with Scott Dewell in Rockefeller University's Genomics Resource Center who performed the actual sequencing and analyzed and mapped the initial sequencing reads. The number of sequencing reads for each sample in this experiment are summarized Table A.1, in the Appendix of this work. In addition, Deyou Zheng, a computational biologist at Albert Einstein Medical College, provided assistance with data analysis.

Consistent with Ecm5 and Snt2 being members of the same complex, the ChIP-seq profiles of Ecm5 and Snt2 were almost identical. Before treatment, Ecm5 and Snt2 localized to a limited number of regions in the genome, in tight peaks, and regions containing high numbers of sequencing reads in the Ecm5 ChIP almost always had high read counts in the Snt2 ChIP (see Figure 4.3A for a representative chromosome). In almost all cases, regions of the genome containing high numbers reads in the Ecm5 and Snt2 ChIP tracks, had low read counts in the input and untagged control ChIP, confirming the specificity of these ChIP experiments. To quantitate the extent of Ecm5 and Snt2 colocalization, I used the MACS algorithm to

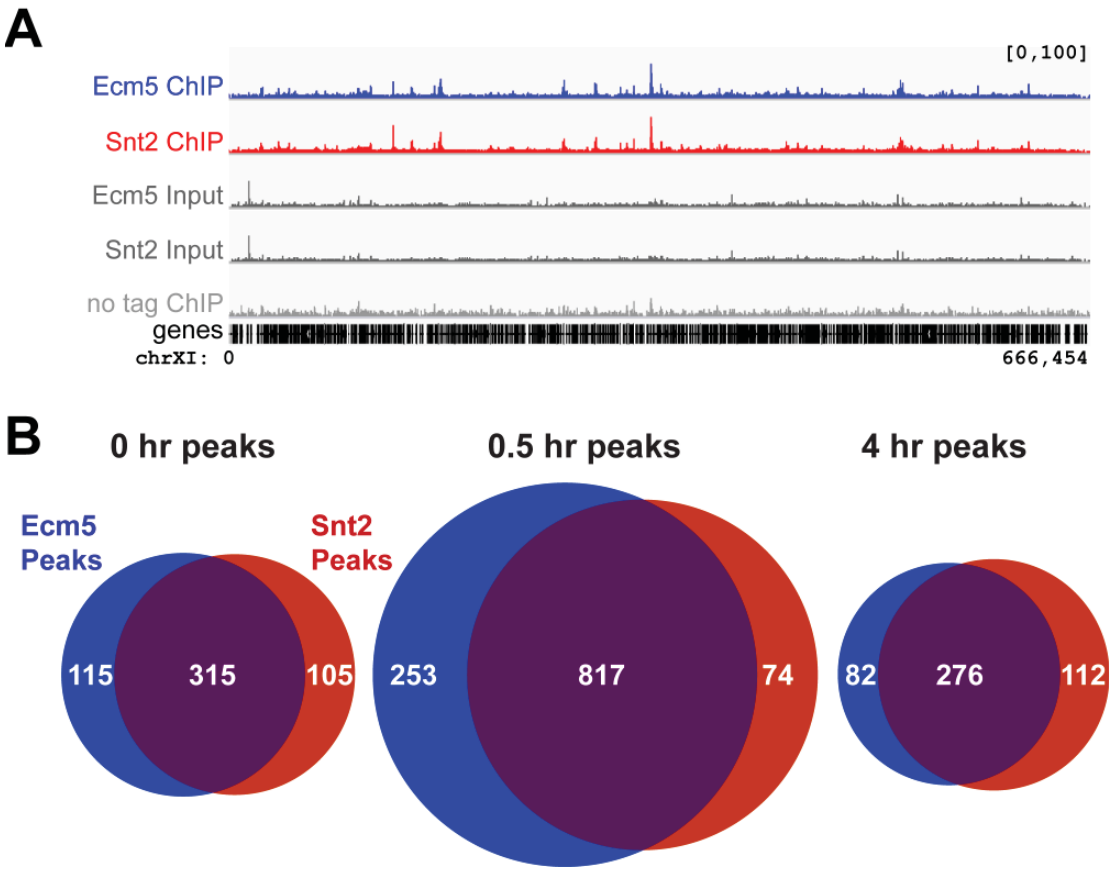

Figure 4.3 Ecm5 and Snt2 are highly colocalized

A. Ecm5- and Snt2-Myc ChIP profiles in untreated cells along a representative chromosome. The Y axis of each track represents the number of reads (in millions) spanning a genomic position normalized to the total number of reads for each sample. The numbers in square brackets above and to the right of the panel denote the scale [baseline, maximum] which is the same for all tracks. Input and no tag control tracks are shown under the ChIP tracks, and the location of yeast genes and genomic coordinates are shown at the bottom of the panel. **B.** Venn diagrams showing peaks of Ecm5 and Snt2 ChIP reads that overlapped by at least 200 bp.

computationally define peaks of ChIP enrichment – genomic loci with high numbers of Ecm5 and Snt2 sequencing reads compared to the untagged control ChIP (Zhang et al., 2008). This analysis found 430 and 420 peaks of Ecm5 and Snt2 reads, respectively, before treatment. I then determined the number Ecm5 and Snt2 peaks that overlapped by at least 200 bp. Remarkably, both before and after treatment, the majority of Ecm5 and Snt2 peaks overlapped, with 315 of the Ecm5 and Snt2 peaks overlapping in the untreated cells (Figure 4.3B). Taken together, the visual inspection of the ChIP-seq tracks and the computational peak calling both show that Ecm5 and Snt2 are highly colocalized, consistent with their functioning in the same complex.

Ecm5 and Snt2 localize to many new regions a half hour after H_2O_2 treatment

Surprisingly, 0.5 hours after H_2O_2 treatment, Ecm5 and Snt2 localized to many genomic loci. For example, in the representative region shown in Figure 4.4, arrows mark peaks of Ecm5 and Snt2 ChIP-seq reads that were either not present before treatment or strongly enriched after. The peaks are not present, or are much less enriched in the input and untagged control ChIP tracks, again showing the appearance of these peaks after treatment is specific to Ecm5 and Snt2. The computational peak calling confirmed that there were many more peaks of Ecm5 and Snt2 binding after treatment, finding 817 Ecm5/Snt2 shared peaks 0.5 hours after treatment, compared with 315 before (Figure 4.3B, and bottom tracks in Figure 4.4). This dramatic reassortment of Ecm5 and Snt2 was only transient, and by 4 hours after H_2O_2 treatment, Ecm5 and Snt2 profiles resembled those of untreated cells. Furthermore, 4 hours after treatment, the number of peaks called by the algorithm was reduced, with 276 only Ecm5/Snt2 shared peaks called, similar to the number of peaks found in untreated cells. Of those, about half, or 137 peaks overlapped

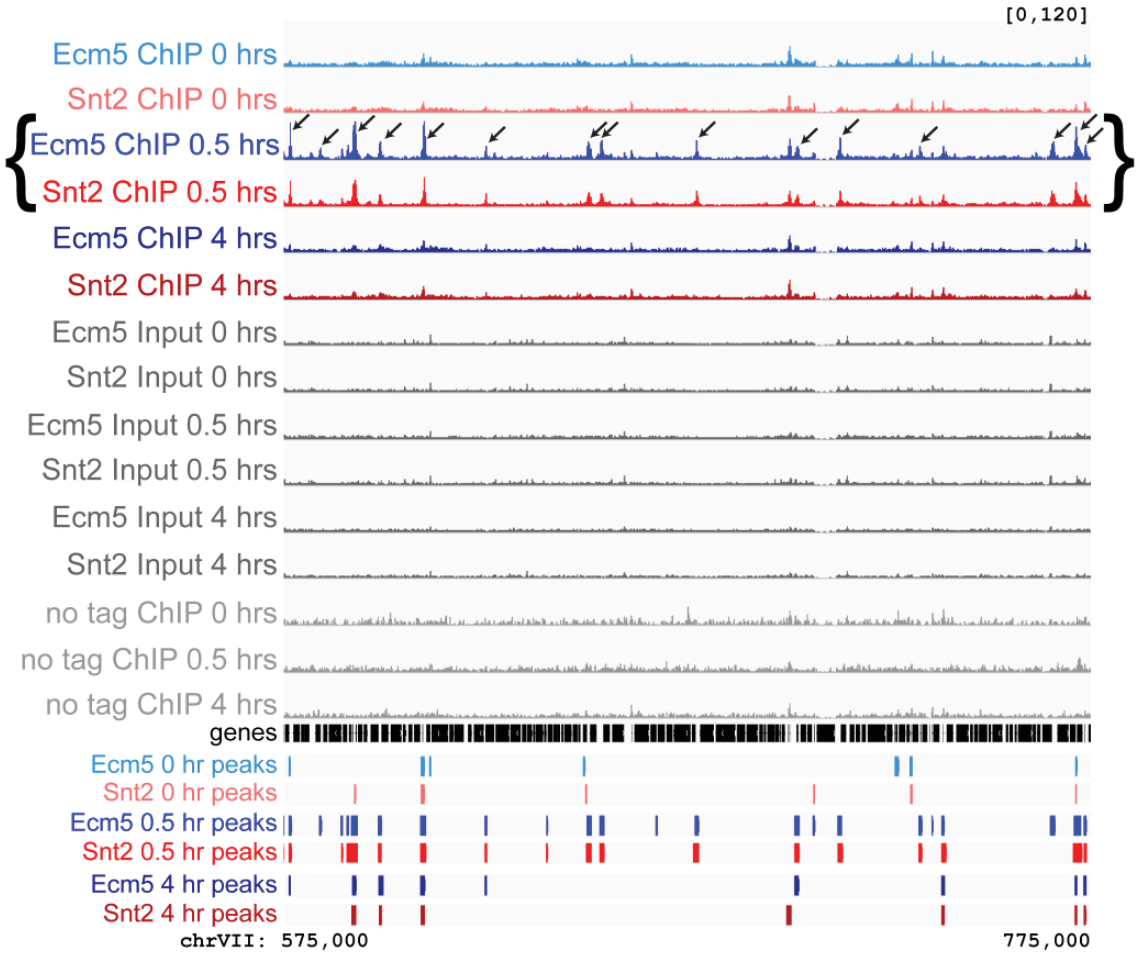

Figure 4.4 Ecm5 and Snt2 localize to many new regions after H_2O_2 treatment

Ecm5- and Snt2-Myc ChIP-seq tracks from both untreated and H_2O_2-treated yeast, depicted as in Figure 4.3, with arrows marking new or enhanced peaks in the 0.5 hour ChIPs (bracketed tracks). Peaks called by the MACS algorithm for each ChIP are shown under the tracks.

with peaks called before treatment. Peaks that were not shared between the two timepoints reflect mistakes in the peak calling (e.g. a weak peak that was called in one timepoint and not the other), and not differences in Ecm5 and Snt2 localization before and 4 hours after treatment. In summary, Ecm5 and Snt2 do not show localization changes 4 hours after treatment that would suggest they mediate adaptation to stress, but these proteins do localize to new regions of the genome as part of the acute response to H_2O_2 stress.

To confirm the ChIP-seq findings, I performed separate small-scale ChIP-qPCRs experiments, following the same H_2O_2 treatment protocol described above. I first focused on the promoter of the *ERG6* and *YAP1* genes, a region which shows a modest increase in Ecm5 and Snt2 localization 0.5 hours after H_2O_2 treatment by ChIP-seq (Figure 4.5A, left panel). *ERG6* encodes an enzyme that helps to synthesize ergosterol, a sterol that accumulates in yeast cell membranes after stress and promotes resistance (Lees et al., 1995; Swan and Watson, 1998). As described in the introduction to this work, *YAP1* encodes a transcription factor that is known to respond to oxidative stress (Rodrigues-Pousada et al., 2010). Since both *YAP1* and *ERG6* have been linked to stress, I was eager to confirm that Ecm5 and Snt2 were localized to these promoters after H_2O_2 treatment. In accordance with these results, in ChIP-qPCR experiments Ecm5- and Snt2-Myc were enriched (3- to 5-fold above an untagged control strain) at this promoter only after H_2O_2 treatment (Figure 4.5B, left panel).

I next focused on the *CYC3* and the *IPI3*/*YNL181W* shared promoters, which both had very high numbers of Ecm5 and Snt2 reads before and after treatment in the ChIP-seq experiment (Figure 4.5A middle and right panels). *CYC3* encodes an enzyme that helps generate active cytochrome C, one of the components of the mitochondrial ETC (Dumont et al., 1987).

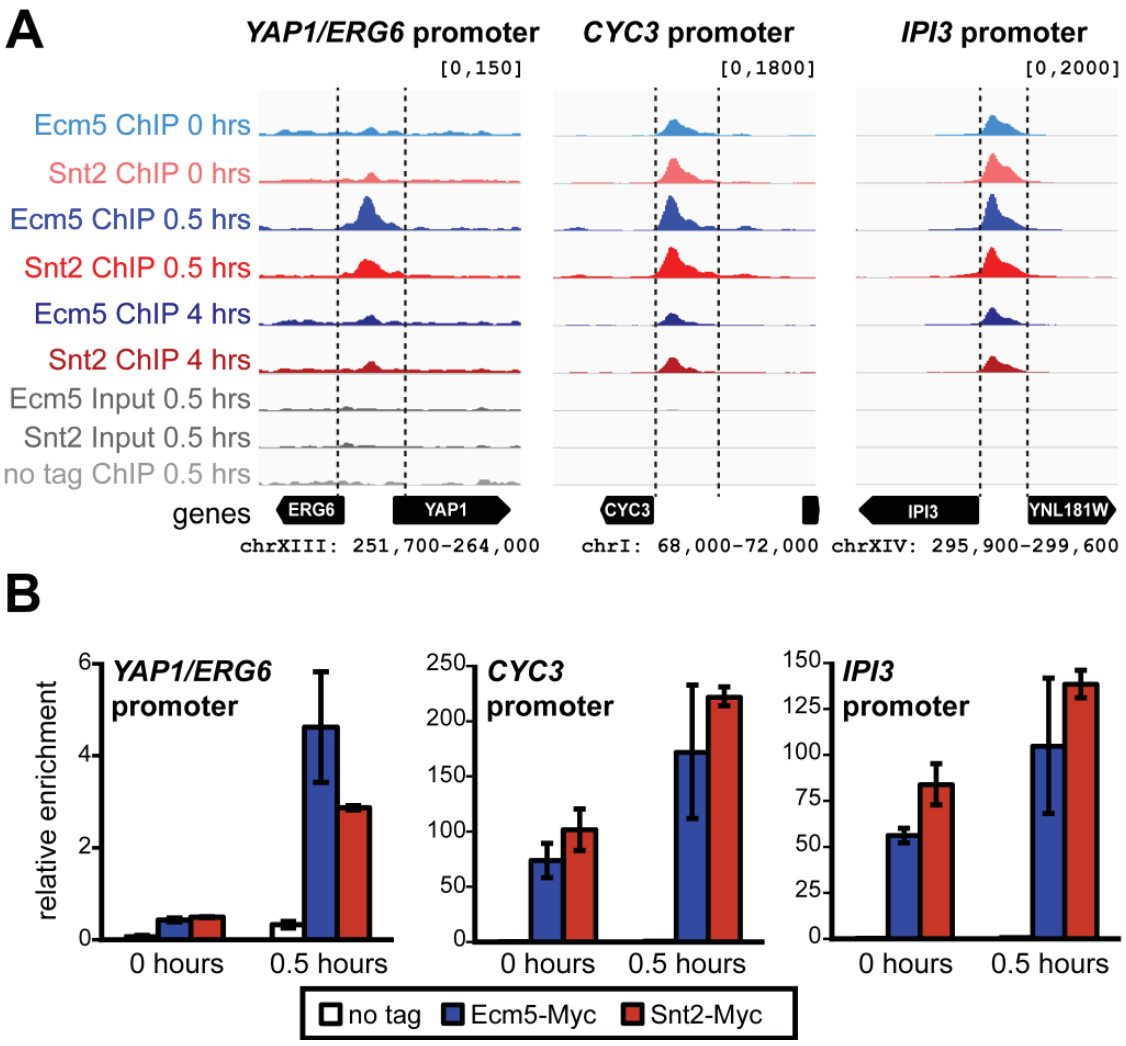

Figure 4.5 Small-scale confirmation of ChIP-seq

A. Ecm5 and Snt2 ChIP-seq enrichment before and after H_2O_2 treatment at the *ERG6/YAP1*, *CYC3*, and *IPI3/YNL181W* promoters, depicted as in Figure 4.3. **B.** Confirmation of the ChIP-seq results in [A] using using ChIP-qPCR. The relative ChIP enrichment was calculated by dividing the percent input for each replicate at the region of interest by the percent input in the middle of the *ACT1* gene, where Ecm5/Snt2 enrichment is low. Graphs show mean and SEM from 3 biological replicates.

IPI3 encodes a member of the Rix1 complex, responsible for processing rRNA (Krogan et al., 2004; Nissan et al., 2004), while *YNL181W* is believed to encode an oxidoreductase (Giaever et al., 2002). Thus, *CYC3*, *IPI3*, and *YNL181W* were all functionally linked to either cellular redox reactions or protein synthesis. Before and after treatment, at both promoters, the signal from the untagged control ChIP was almost undetectable (Figure 4.5B). In contrast, Ecm5 and Snt2 were clearly enriched at these promoters, and the enrichment was slightly higher 30 minutes after treatment. These findings confirm the reproducibility of the ChIP-seq findings, and also demonstrate the large dynamic range in the levels of Ecm5 and Snt2 enrichment found at different regions of the genome, which may reflect differences in the affinities of different sites for these proteins or differential Ecm5/Snt2 binding in different subsets of cells.

Ecm5 and Snt2 localize primarily to gene promoters and for a small number of highly expressed genes, to gene bodies

Both before and after treatment, Ecm5 and Snt2 were localized primarily to promoter regions of genes. As an example, Ecm5 and Snt2 localization to the *FUI1* and *PRE7* genes 0.5 hours after H_2O_2 treatment is clearly constrained to these genes' shared promoter (Figure 4.6A). In addition, as described above, Ecm5 and Snt2 are enriched in the promoter regions of the *ERG6/YAP1*, *CYC3* and *IPI3/YNL181W* genes (Figure 4.5A). To further analyze this trend, Scott Dewell aligned every yeast gene around its transcription start site (TSS), and then determined the average number of sequencing reads in 50 bp windows relative to the TSS's. This analysis found a very slight enrichment of Ecm5 and Snt2 reads approximately 250 bp upstream of the TSS before or 4 hours after H_2O_2 treatment (Figure 4.6C, left panels). The level

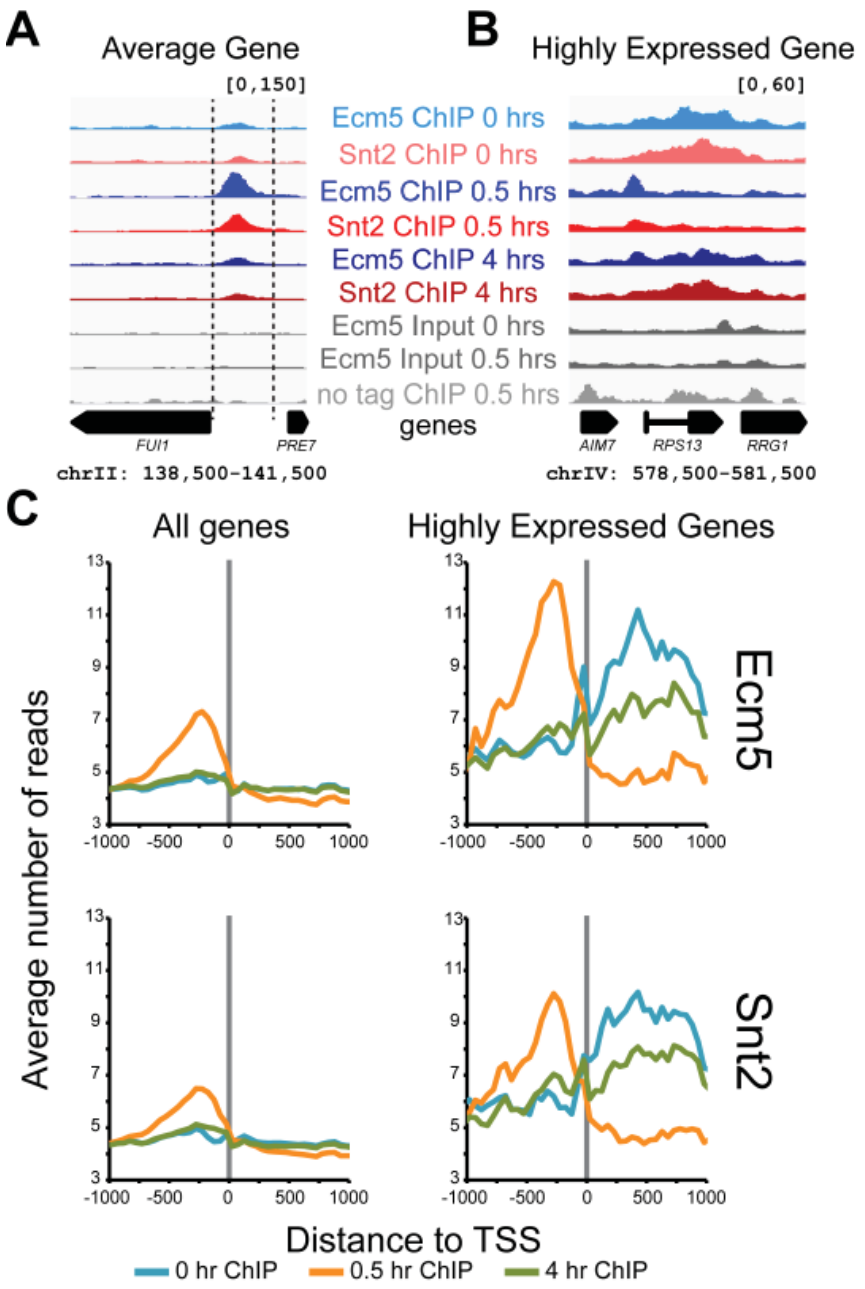

Figure 4.6 Alignment of H_2O_2 ChIP-seq reads around transcription start sites

A and B. Representative ChIP-seq tracks as in Figure 4.3, showing a typical (**A**) or a highly-expressed (**B**) Ecm5/Snt2 target gene. (**C**) All yeast genes (left panels) or the 100 most highly-expressed yeast genes (Miller et al., 2011; right panels) were aligned by their transcription start sites (TSSs) and the average number of Ecm5 (top panels) or Snt2 (bottom panels) ChIP-seq reads per 50 bp window relative to the TSSs for each ChIP experiment was calculated. Each average value was normalized to the total number of mapped reads for that experiment and divided by 1,000,000 to get normalized average numbers of reads at positions relative to the TSS.

of enrichment is small because at these time-points Ecm5 and Snt2 only localize to a small number of genes, and the signal from these genes is drowned out by the lack of enrichment at all the other yeast genes. However, 0.5 hours after H_2O_2 treatment, an enrichment of Ecm5 and Snt2 ChIP-seq reads is clearly visible 250 bp upstream of the TSS.

I also noticed a small number of genes enriched for Ecm5 and Snt2 in their coding regions in untreated cells. Intriguingly, in many of these examples, 0.5 hours after H_2O_2 treatment, Ecm5 and Snt2 were no longer enriched within the bodies of these genes, and were instead enriched at the 5' (and in some cases 3') ends. The *RPS13* gene is an example of one such gene (Figure 4.6B). I noticed that many of the genes displaying this trend were coded for either ribosomal proteins or metabolic enzymes, two categories of highly transcribed genes. At the same time that I observed this trend, Scott independently obtained a list of the 100 most highly expressed yeast genes, based on a recent yeast gene expression study (Miller et al., 2011), and repeated his TSS localization analysis using only these genes. Remarkably, his TSS profiles matched what I had been seeing: at highly expressed genes, there is significant enrichment of Ecm5 and Snt2 reads 250-1000 bp downstream of the TSS before H_2O_2 treatment, and 0.5 hours after treatment, this enrichment has shifted to approximately 300 bp upstream of the TSS (Figure 4.6C, right panels). Taken together, these data show there are two patterns of Ecm5/Snt2 binding: Ecm5 and Snt2 localize to discrete peaks within promoters of most target genes, but also localize to gene bodies in some highly expressed genes. In the latter case, Ecm5 and Snt2 redistribute away from gene bodies and to the 5' and 3' ends of genes in response to H_2O_2-stress.

Ecm5 and Snt2 target genes have functions in stress response and metabolism

I next determined what categories of genes Ecm5 and Snt2 were targeting. To sort out which genes were targeted by Ecm5 and Snt2 generally, and which were specific to the H_2O_2 response, I next compared the 315 shared Ecm5/Snt2 ChIP peaks before H_2O_2 treatment with the 817 shared peaks 0.5 hours after treatment and determined which peaks in these two sets overlapped by at least 200 bp (Figure 4.7A). This analysis generated three lists of peaks: the 151 peaks of Ecm5/Snt2 binding present before H_2O_2 treatment but not after, the 652 peaks present only after treatment, and the 164 peaks present both before and after treatment. The first two lists of peaks represent regions of Ecm5 and Snt2 binding that are either enhanced or diminished by H_2O_2 treatment. In contrast, the last set of peaks represents constitutive Ecm5/Snt2 ChIP targets.

To compile lists of Ecm5/Snt2 target genes, I defined each gene's promoter as the region from 500 bp upstream of the start codon to the start codon. I then determined which gene promoters overlapped Ecm5/Snt2 shared peaks by at least 200 bp before and after H_2O_2 treatment, and used these gene lists as input for the FuncAssociate program which determines functional categories of genes enriched among each set (Berriz et al., 2009). This analysis found that target genes that only contained promoter-bound Ecm5 and Snt2 before treatment were enriched for translation and ribosome genes. The translation and ribosome gene categories were also enriched among targets with Ecm5 and Snt2 present only before or both before and after H_2O_2 treatment (Figure 4.7B, yellow and orange bars). In addition, genes involved in sugar metabolism (hexose biosynthetic process, gluconeogenesis) and retrotransposon function (transposition) were enriched among the general Ecm5/Snt2 targets, but not among H_2O_2-

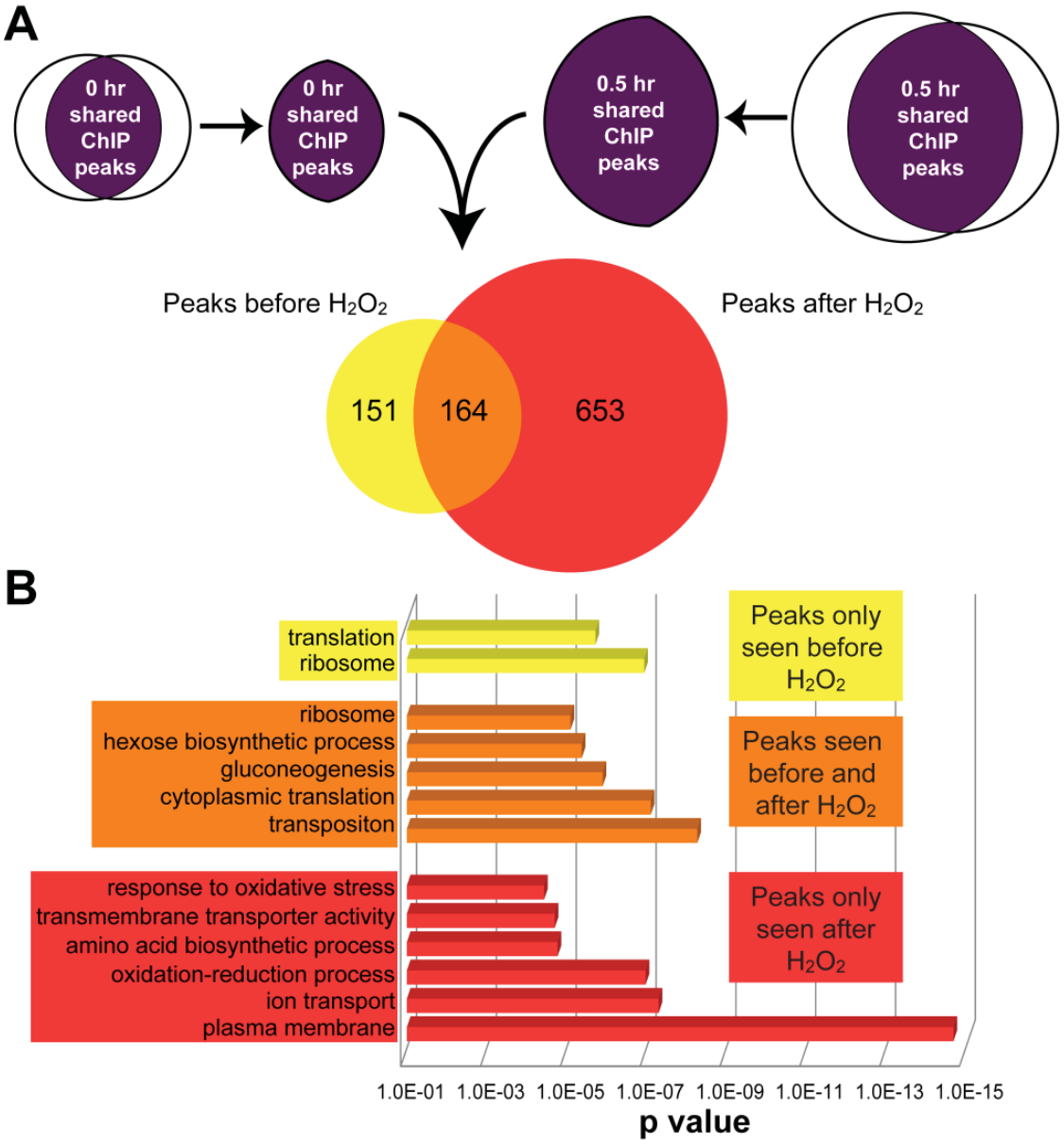

Figure 4.7 Gene ontology analysis of promoters containing peaks of Ecm5 and Snt2 ChIP-seq reads

A. Venn diagram showing the overlap between Ecm5 and Snt2 shared peaks before and 0.5 hours after H_2O_2 treatment. **B.** Categories of genes significantly over-represented among genes whose promoters contained Ecm5/Snt2 peaks before H_2O_2 treatment only (yellow), both before and after H_2O_2 treatment (orange), or after H_2O_2 treatment only (red).

specific targets, suggesting that regulation of carbohydrate metabolism and transposition genes may be general functions of the Rpd3(T) complex. The presence of retrotransposons among Ecm5 and Snt2 target genes is especially interesting, since recent studies have linked stress and nutrient starvation to retrotransposon activation (Morillon et al., 2000; Stamenova et al., 2008), a response that Ecm5 and Snt2 may help regulate.

Among the genes containing Ecm5 and Snt2 at their promoters only after H_2O_2 treatment, genes involved in the oxidative stress response, oxidation-reduction processes, plasma membrane functions, and amino acid transport and synthesis were enriched (Figure 4.7B, red bars). These are all categories of genes that would be expected to be up- or down-regulated to help cells recover from oxidative stress: in addition to the up-regulation of oxidative stress response genes to help yeast repair damage caused by the H_2O_2, genes involved in oxidative-reductive metabolism would be expected to be up- or down-regulated to help the cell maintain the proper redox state in response to H_2O_2-triggered oxidation. Furthermore amino acid transporters and genes involved in amino acid biosynthesis might be important in helping cells remake proteins damaged by H_2O_2. Lastly, while not significant among the H_2O_2-specific Ecm5 and Snt2 target genes, functional analysis of the complete list of Ecm5 and Snt2 target genes 0.5 hours after H_2O_2 treatment revealed that cell wall genes are enriched among this set ($p=4.5x10^{-7}$). Approximately half of these genes had peaks of Ecm5 and Snt2 binding both before and after treatment, while the other half only had binding after, explaining why this category was not found significant when these two lists were separated. The regulation of cell wall genes by Ecm5 and Snt2 might explain the cell wall phenotypes reported for some *ecm5* mutants (Lussier et al., 1997). In summary, Ecm5 and Snt2 generally localize to genes involved in translation and sugar

metabolism, and in response to H_2O_2, these proteins localize to additional genes, whose functions directly reflect the needs of a cell trying to respond to and repair oxidative stress-induced damage.

Gene expression analysis of the *ecm5* and *snt2* knockout strains before and after H_2O_2 stress

Because Ecm5 and Snt2 localize to many gene promoters, I hypothesized that they might function in gene regulation. More specifically, because these proteins are in a complex with the Rpd3 histone deacetylase, and histone deacetylation and Rpd3 have both been linked to gene repression (Allfrey et al., 1964; Kadosh and Struhl, 1998; Vidal and Gaber, 1991), I thought the Rpd3(T) complex might repress genes in response to H_2O_2 stress. I therefore used RNA-sequencing (RNA-seq) to look for expression differences in cells lacking Ecm5 or Snt2, before and 0.5 hours after H_2O_2 treatment. I chose to only focus on the 0.5 hour time-point, because all of the Ecm5 and Snt2 localization changes happened at within this window, and were returned to the pre-treatment state by 4 hours. With Scott's help, cDNA from three biological replicates of each strain before and after H_2O_2 treatment was sequenced and aligned using the TopHat software, and genes showing differential expression from wild-type were identified using the Cuffdiff software (Trapnell et al., 2009; Trapnell et al., 2010). The numbers of sequencing reads for each sample are summarized in Table A.2, in the Appendix. I first sought to confirm the RNA-seq results by performing qPCRs on cDNA made from the same RNA samples submitted for sequencing, and found both techniques were in good agreement (Table 4.1).

Table 4.1 Comparison of expression ratios 0.5 hours after H_2O_2 treatment determined by RNA-seq and qPCR [a]

Gene	ChIP target	*ecm5*Δ qPCR[b, c]	*ecm5*Δ seq	*snt2*Δ qPCR[b, c]	*snt2*Δ seq
SNT2	never	1.12 ± 0.07	1.02	ud	0.00
ECM5	never	ud	0.00	1.31 ± 0.18	1.24
CYC3	all timepts	1.09 ± 0.17	1.01	1.81 ± 0.19	1.75
SSA3	all timepts	0.91 ± 0.06	0.86	0.94 ± 0.12	0.78
POT1	all timepts	0.91 ± 0.25	1.02	2.11 ± 0.34	2.04
BNR1	all timepts	1.19 ± 0.04	1.65	1.23 ± 0.03	1.99
IPI3	all timepts	1.10 ± 0.22	1.07	1.55 ± 0.15	2.62
YNL181W	all timepts	1.23 ± 0.05	1.23	1.52 ± 0.05	1.55
MSN1	all timepts	1.57 ± 0.06	1.35	1.03 ± 0.04	0.90
TRX2	0.5 hrs only	1.14 ± 0.09	1.00	1.47 ± 0.13	1.10
HSP12	0.5 hrs only	1.29 ± 0.36	1.18	4.40 ± 0.72	3.43
MAE1	0.5 hrs only	1.19 ± 0.23	0.97	0.69 ± 0.09	1.22
GAL7	0.5 hrs only	1.24 ± 0.18	1.24	1.37 ± 0.21	1.23
GAL10	0.5 hrs only	1.14 ± 0.04	1.08	0.93 ± 0.11	0.93
YAP1	0.5 hrs only	1.02 ± 0.06	1.10	1.20 ± 0.08	0.94
ERG6	0.5 hrs only	1.11 ± 0.05	0.93	1.10 ± 0.06	1.32
EXG1	0.5 hrs only	1.02 ± 0.14	0.99	1.22 ± 0.11	1.13

[a] Ratio of expression in mutant strain 0.5 hours after treatment compared to expression in wild-type strain at that time

[b] qPCR values are shown +/- SEM for 3 biological replicates

[c] ud: undetectable by qPCR

In wild-type cells, 3127 genes had significant expression changes in response to H_2O_2 treatment (Table 4.2, statistical significance determined by Cuffdiff software). In comparison, a separate study reported 1294 genes up- or down-regulated at least two-fold after H_2O_2 treatment (Gasch et al., 2000). My study identified a larger number of genes in part because Cuffdiff uses a more lenient cut-off for significance: fold differences as low as 1.3 as can be considered significant if there are enough reads for the model to statistically call a difference. In addition, the slightly higher concentration of H_2O_2 I used (0.4 mM in my study compared to 0.32 mM in the Gasch study) may have accounted for larger number of genes changing in my experiment. Importantly, 1031 of the 1294 genes (80%) identified as responding to H_2O_2 in wild-type cells in the Gasch et al. study were also significantly up- or down-regulated in my study, confirming that my H_2O_2 treatment produced similar expression changes to what has been previously reported.

Because Ecm5 and Snt2 are part of the same complex, and localize to the same regions of the genome, I initially expected that knockouts for these two proteins would show similar gene expression changes. However, consistent with the lack of phenotype for the *ecm5* knockout strain I saw in my genetic assays, this strain had only a very limited effect on gene expression: before H_2O_2 treatment only 33 genes were significantly up- or down-regulated in the *ecm5* knockout strain *relative* to expression in the wild-type stain, and after treatment, only 7 genes had altered expression (Table 4.2). Both before and after treatment *ECM5* was the most significantly down-regulated gene in the *ecm5* knockout strain. Interestingly, 5 out of the 14 genes up-regulated in the *ecm5* knockout strain before treatment, were cell wall mannoproteins genes, including the *FIT1* gene, whose up-regulation in *ecm5*Δ cells I discussed in the previous chapter. The up-regulation of these cell wall proteins in the *ecm5* knockout strain may be responsible for the cell wall phenotypes reported in this mutant (Lussier et al., 1997).

Table 4.2 Summary of Gene Expression Differences [a]

Gene sets being compared			# genes down	# genes up	total # genes	overlap[b]
0 hr *ecm5* Δ	vs.	0 hr wild-type	19	14	33	11
0 hr *snt2* Δ	vs.	0 hr wild-type	38	134	172	
0.5 hr *ecm5* Δ	vs.	0.5 hr wild-type	6	1	7	1
0.5 hr *snt2* Δ	vs.	0.5 hr wild-type	262	475	737	
0.5 hr wild-type	vs.	0 hr wild-type	1412	1715	3127	

[a] numbers of genes significantly up- or down-regulated in each comparison, with significance determined by the Cuffdiff program

[b] total number of genes up- or down-regulated in both *ecm5* Δ and *snt2* Δ at this time-point

In contrast, the *snt2* knockout strain had a much larger number of genes differentially expressed, with 172 genes significantly up- or down-regulated compared to wild-type expression before treatment and 737 genes up- or down-regulated compared to wild-type after treatment (Table 4.2). *SNT2* was the most down-regulated gene in the *snt2* knockout strain before and after treatment. At both time-points, there was little to no overlap between the genes in the *ecm5*Δ strain and the genes in the *snt2*Δ strain that were misexpressed, suggesting that despite being associated with Snt2, Ecm5 does not function in the same manner as Snt2 with respect to gene regulation. Of the 737 genes with up- or down-regulated in the *snt2* knockout compared to wild-type expression 0.5 hours after H_2O_2 stress, 573 (78%, $p = 4.1x10^{-75}$) were also genes whose expression was up- or down-regulated in wild-type cells 0.5 hours after H_2O_2 treatment, compared to wild-type expression before treatment. The high degree of overlap between genes misregulated in the *snt2* knockout strain and genes whose expression change as a part of the wild-type response to H_2O_2 treatment further implicate Snt2 in the oxidative stress response.

Genes showing differential expression in the *snt2* knockout fall into the same functional categories as genes found to be Ecm5/Snt2 targets by ChIP

Using FuncAssociate, I identified categories of genes showing expression changes in the *snt2* knockout before and after H_2O_2 stress. Similar to the sets of genes identified as Ecm5/ Snt2 ChIP targets, many of these genes had roles in metabolism. For instance, many of the genes up- or down-regulated in the *snt2* mutant before H_2O_2 treatment were involved in energy homeostasis functions such as acetyl-CoA metabolism, NAD metabolism, oxidation-reduction processes, and the tricarboxylic acid (TCA) cycle (p values: $8.8x10^{-7}$, $5.5x10^{-5}$, $1.3x10^{-6}$, and

5.8 x10^{-8}, respectively). After treatment, many of the genes showing expression differences fell into categories related to protein synthesis, including ribosome, translation, rRNA processing, nucleolus, and amino acid biosynthesis (p values: 1.3x10^{-16}, 2.1x10^{-9}, 1.37x10^{-16}, 1.18x10^{-19} 4.4x10^{-8}, respectively). In addition, genes involved in the yeast cell wall (p value 1.2x10^{-5}) were also enriched in the set of genes showing expression differences after H_2O_2 treatment.

Direct comparison of ChIP and Expression Data

Surprisingly, many of the gene targets of Ecm5/Snt2 binding either before or after H_2O_2 treatment showed no expression differences in the *ecm5* or *snt2* knockout strains at either time-point. Of the 312 Ecm5/Snt2 target genes in untreated cells, only 25 were over- or under-expressed at least 1.5-fold in the *snt2*Δ strain at that time-point. After H_2O_2 treatment 98 of the 312 genes were 1.5-fold over- or under-expressed in the *snt2* knockout strain compared to wild-type expression after treatment, suggesting that Ecm5 and Snt2 may mark some gene targets before Snt2 is required for their regulation. There were 1205 genes with Ecm5/Snt2 peaks in their promoters after H_2O_2 treatment, and of those, 403 were over- or under-expressed at least 1.5-fold in the *snt2*Δ strain at that time. In summary, only some of the Ecm5/Snt2 target genes require Snt2 for proper expression, and almost none require Ecm5.

To look more carefully at target genes most likely to be directly regulated by Snt2, I focused my attention on the 1205 genes that were found to have Ecm5/Snt2 peaks at their promoters 0.5 hours after H_2O_2 treatment. Of those, 813 (66%) changed expression at least 1.5 fold in wild-type cells in response to H_2O_2 stress, and 403 (33%) were misexpressed in the *snt2*Δ strain after H_2O_2 treatment. There were 309 target genes that were on both lists, and I felt these

would be most interesting for future study (Figure 4.8A). Thus, I was able to identify 309 genes that contained Ecm5 and Snt2 at their promoters after H_2O_2 treatment, changed expression in wild-type cells in response to H_2O_2, and were also misexpressed in *snt2*Δ cells 0.5 hours after treatment.

As discussed above, I originally expected that direct targets of Snt2 would have higher expression levels in the *snt2* knockout strain than in wild-type. Surprisingly, however, the gene expression patterns proved much more complicated. To get a broad sense of gene expression patterns before and after treatment, Deyou generated heatmaps, showing the expression profiles of these genes clustered into 4 groups (Figure 4.8B, with clusters labeled above the heatmap). The first group is made up of genes whose expression levels were low before H_2O_2 treatment, were induced in wild-type cells after treatment, and were induced even more strongly in the *snt2* knockout. The second group of genes also had low basal expression that was induced in wild-type cells after treatment, and in *snt2* knockout cells, these genes were either not induced at all in response to treatment or were induced less in the wild-type strain. In contrast, the third and fourth groups were genes repressed upon H_2O_2 treatment that were either repressed more weakly or more strongly than wild-type levels, respectively in *snt2*Δ cells after treatment. Since direct targets of the Snt2 could be either activated or repressed in the *snt2* knockout strain, Snt2 seems likely to be capable of promoting both transcriptional activation and repression, depending on the context.

As another way to look at this data, I plotted the $\log_2$ expression ratios of each of the 309 genes on a two-dimensional plot (Figure 4.9, top left panel). In this plot, each dot represents one gene, and the x-axis represents the $\log_2$ ratio of expression in wild-type cells 0.5 hours after H_2O_2

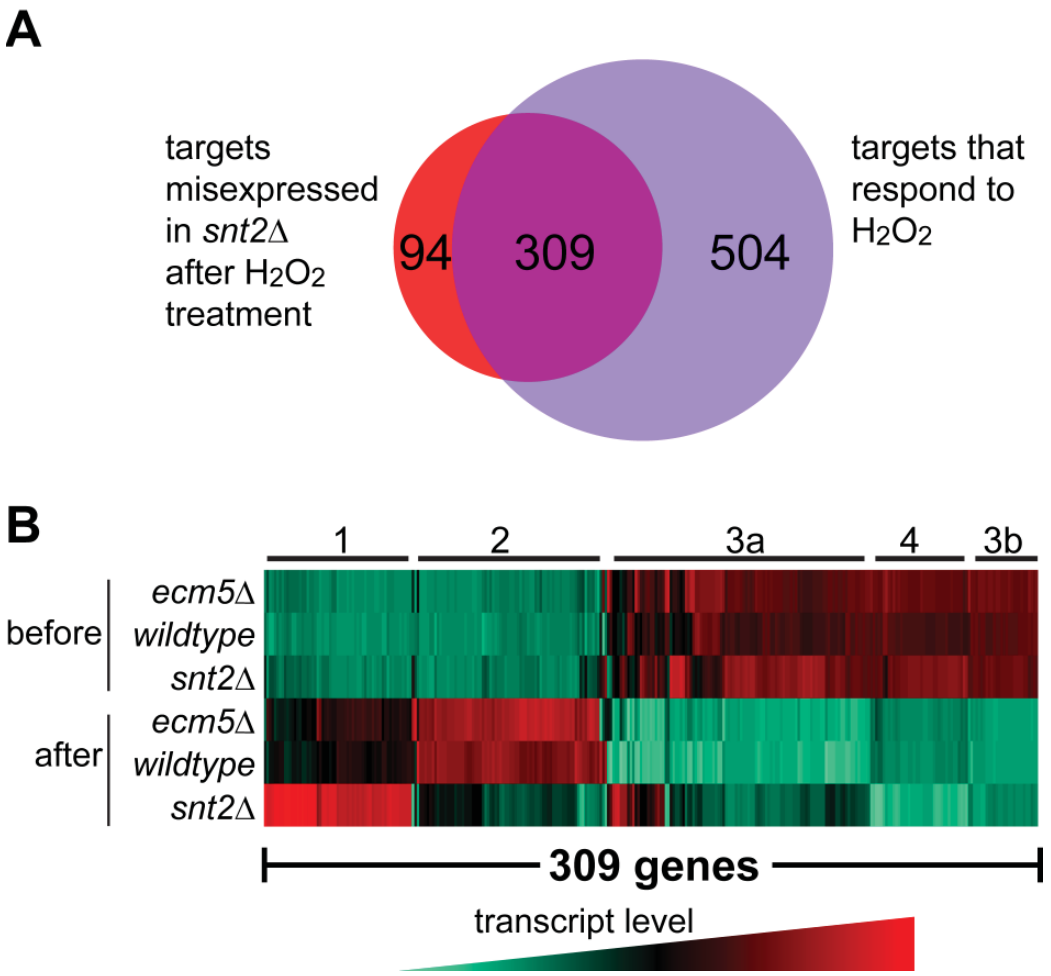

Figure 4.8 Ecm5 and Snt2 ChIP target genes that change expression in wild-type cells in response to H_2O_2 and are misexpressed in the *snt2*Δ strain after H_2O_2 treatment

A. Genes with shared peaks of Ecm5 and Snt2 ChIP-seq reads at their promoters 0.5 hours after H_2O_2 treatment were selected. Of those, genes whose expression was 1.5-fold higher or lower in the *snt2* knockout strain after H_2O_2 treatment compared to wild-type expression levels at that time (genes misexpressed in *snt2*Δ) were isolated (red circle), and genes whose expression was 1.5-fold higher or lower after H_2O_2 treatment in wild-type cells compared to wild-type expression before treatment (H_2O_2 response genes) were isolated (purple circle). The Venn diagram shows the overlap of these two gene sets (309 genes). **B.** Heatmap showing the RNA-seq expression levels of the 309 shared genes descrived in (A) in the indicated strains before and 0.5 hours after H_2O_2 treatment. The color key for the heatmap is shown below the panel. The heatmap can be roughly divided into 4 clusters, labeled above the panel, based on whether genes increase or decrease expression in wild-type cells after treatment, and whether expression in the *snt2* knockout strain after treatment is higher or lower than wild-type expression at that timepoint.

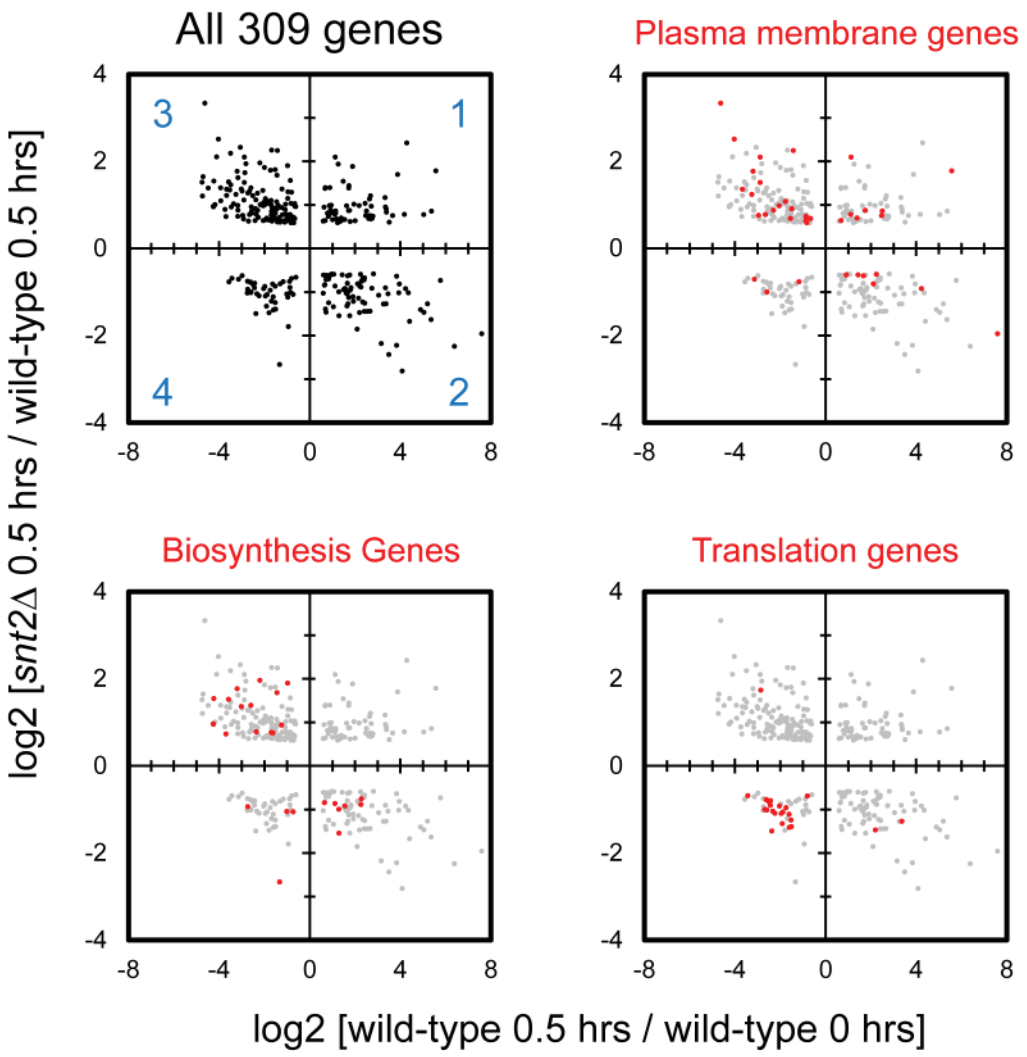

Figure 4.9 Different subsets of the 309 genes respond differently to the absence of Snt2
Dot plots showing the $\log_2$ expression ratios of the 309 genes identified in Figure 4.8. The xaxis for these plots is the $\log_2$ ratio of expression in wild-type cells 0.5 hours after H_2O_2 treatment compared to expression in wild-type cells before treatment. The y axis is the log2 ratio of expression in the *snt2* knockout strain 0.5 hours after treatment compared to expression in wild-type cells after treatment. The top left panel shows all 309 genes in black, with regions of the graph corresponding to the four clusters described in Figure 4.9 labeled in blue. The remaining panels have points representing genes that are part of the indicated functional categories highlighted in red.

treatment compared with wild-type expression before treatment. Similarly, the y-axis represents the $\log_2$ ratio of expression in the *snt2*Δ strain after H_2O_2 treatment compared with wild-type expression values after treatment. Thus, genes that fall in the top right quadrant of the plot, for example, represent genes that are induced in wild-type cells in response to H_2O_2 stress, and over-expressed in *snt2*Δ cells after stress. This quadrant roughly corresponds to group 1 in the heatmap in Figure 4.8B. Based on this plot, it is clear that while there are slightly more genes in the top-left quadrant of the plot (or group 3 the heatmap), overall, there is no strong pattern of expression.

I next looked for categories of genes whose members were enriched among these 309 genes, to see if distinct patterns of gene expression could be discerned for different types of genes. I identified genes involved in the plasma membrane, cellular biosynthesis, and translation as being over-represented among the 309 genes. Interestingly, these different categories of genes showed different expression patterns. The biosynthesis genes, were largely repressed in wild-type cells following H_2O_2 stress, consistent with the cell halting new biosynthesis until damaged molecules could be repaired. In *snt2* knockout cells, these genes were both up- and down-regulated relative to wild-type, showing no clear pattern of regulation (Figure 4.9, bottom left panel). In contrast, most plasma membrane genes were over-expressed in the *snt2* knockout strain after treatment, suggesting that overall, Snt2 functions to repress genes in this category after H_2O_2 stress (Figure 4.9, top right panel). The clearest expression pattern could be seen for translation genes, which were almost all down-regulated in wild-type cells in response to H_2O_2, and under-expressed (down-regulated too much) in *snt2*Δ cells, suggesting that Snt2 might be needed for activation of this set of genes (Figure 4.9, bottom right panel). Notably many of these

genes were the highly expressed genes enriched for Ecm5 and Snt2 in their gene bodies before treatment at their 5' and 3' ends after, suggesting that this localization pattern is correlated with Snt2 activation function. In summary, Snt2 can function to both activate and repress genes, with different functional categories associated with different Snt2 behavior.

Comparing nutrient stress and oxidative stress responses

Despite treating cells in the experiments described above with an agent to induce oxidative stress, every experiment identified genes with metabolic functions. This is perhaps unsurprising given that, as discussed in the introduction to this thesis, stress and metabolism are highly linked. In addition, there is genetic evidence linking the Rpd3(T) complex to metabolism. The synthetic genetic screen I described in the previous chapter found that the *ecm5* knockout is synthetically sick in combination with deletion of the amino acid starvation sensor Gcn1 (Table 3.3). Furthermore, a newer *ECM5* synthetic genetic screen (Zheng et al., 2010), the results of which are listed in Table 4.3, also uncovered multiple genes linked to oxidative stress and nutrient metabolism, including *GLN3* and *GAT2*, transcription factors that regulate genes involved in amino acid metabolism. I therefore wondered whether Rpd3(T) complex function could be directly linked to nutrient metabolism.

Ecm5 protein levels decrease in stationary phase

To investigate whether the Rpd3(T) complex has a role in nutrient metabolism, I first determined whether levels of these complex members change as cells enter stationary phase. In contrast to the logarithmic phase of yeast growth, in which yeast have abundant nutrients and

Table 4.3 Knockouts that have synthetic growth phenotypes in combination with *ecm5*Δ [a]

Gene	Score	Function
GLN3	-4.8	Activator of genes regulated by nitrogen catabolite repression
IXR1	-3.8	Transcription factor involved in oxygen regulation
GAT2	-3.7	Transcription factor similar to Gln3 & Dal80 repressed by leucine
CTI6	-3.1	Subunit of Rpd3(L) complex
BAS1	-2.5	Transcription factor involved in purine and histidine biosynthesis
SOD1	-2.4	Detoxifies reactive oxygen species
RPA34	-2.2	RNA polymerase I subunit
MDS3	2.2	Putative component of the TOR regulatory pathway
OPI1	2.2	Transcriptional regulator of phospholipid biosynthesis genes

[a] Data from Zheng *et al.,* 2010. Positive scores denote mutations that in combination with the *ecm5* knockout that grew better than either single mutant alone, and negative scores denote genes that were synthetically sick with *ecm5* Δ.

grow and divide at their maximal rate, stationary phase occurs when yeast cells have exhausted most of the nutrients in their media (generally within 12-24 hours of inoculation in rich media), and do not have enough nutrients left to synthesize the precursors needed for growth. Many cellular and metabolic changes occur as yeast shift to stationary phase, including the transition from anaerobic glycolysis to aerobic fermentation known as the diauxic shift (Galdieri et al., 2010). In addition stationary phase yeast have thicker cell walls, accumulate storage carbohydrates, and are more resistant to stress (Werner-Washburne et al., 1993). Despite not actively dividing, yeast can remain viable in stationary phase for significant periods of time, and will resume growth and division if supplemented with nutrients (Lillie and Pringle, 1980). Because yeast in stationary phase remain alive but are quiescent, stationary phase growth has been suggested to be a good model for aging in mammalian systems (Chen et al., 2005). To determine whether protein levels of the Rpd3(T) complex members change during stationary phase, I cultured PrA-tagged Ecm5, Snt2, and Rpd3 strains in YPD for 7 days, taking aliquots of cells each day for whole cell extracts. Snt2 and Rpd3 protein levels remained roughly constant at all time-points (Figure 4.10 A and B). In contrast, levels of tagged Ecm5 decreased starting around 24 hours after the initial culture inoculation (Figure 4.10C). This result was opposite to what happened to Ecm5 protein levels upon acute H_2O_2 treatment. It is possible that the same mechanisms that render stationary phase cells more resistant to oxidative stress underlie this difference in Ecm5 reaction to H_2O_2 (Galdieri et al., 2010).

Levels of H4K16 acetylation are known to increase as yeast cells reproductively age (have many daughters) (Dang et al., 2009). Because of the link between this histone modification and yeast aging, I thought it would be interesting to check whether H4K16ac levels increase as cells

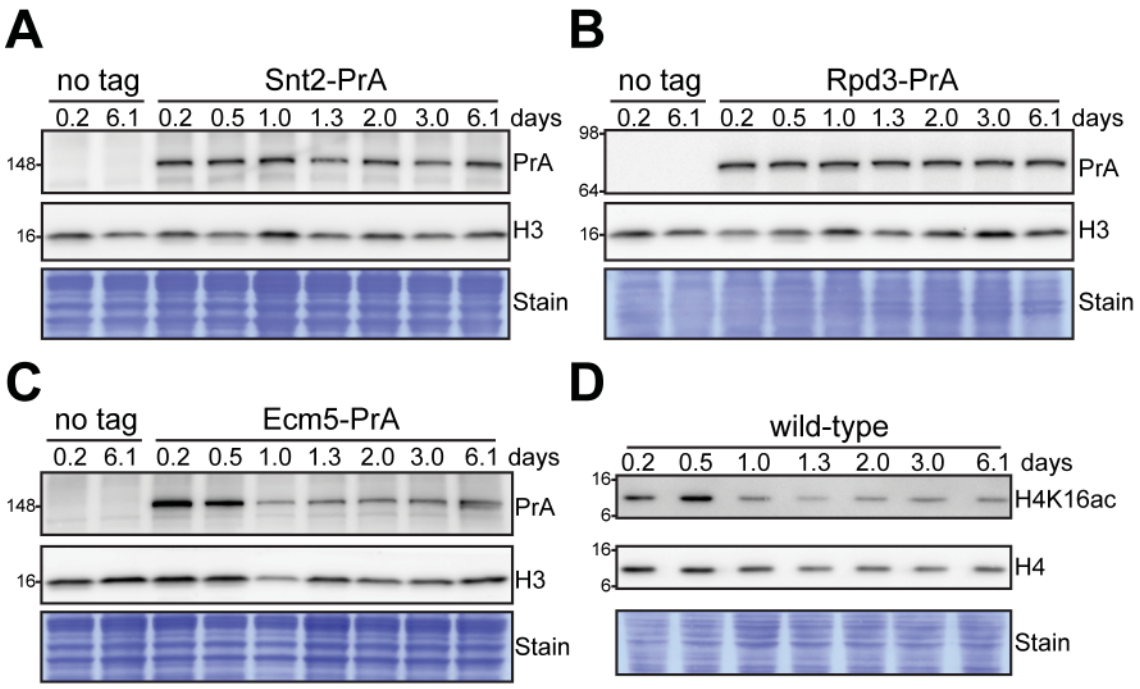

Figure 4.10 Comparison of H4K16ac and tagged Ecm5, Snt2, and Rpd3 protein levels before and during stationary phase

A-C. PrA-tagged Snt2, Rpd3, or Ecm5 strains as well as an untagged control strain were cultured for one week in rich media (YPD). Whole cell extracts taken at the indicated times after inoculation were analyzed by immunoblotting to measure tagged Snt2 (**A**) Rpd3 (**B**) and Ecm5 (**C**) protein levels. Direct Blue 71-stained membranes and immunoblots for histone H3 are shown as loading controls. (**D**) An immunoblot showing H4K16ac levels in a wild-type strain at the indicated times post-inoculation. An H4 immunoblot and Direct Blue stained membrane are shown as loading controls. Numbers to the left of blots denote molecular weights.

enter stationary phase, which is a model of chronological aging. Surprisingly, I saw a decrease in H4K16ac as cells entered stationary phase (Figure 4.10D). A recent publication also reported finding decreased H4K16ac levels by mass spectrometry, in stationary phase cells, consistent with my findings (Ngubo et al., 2011). Usually replicative lifespan and chronological lifespan models of aging in yeast are thought of as being similar, but these results suggest there are meaningful differences between these two aging models.

Mutants lacking Snt2 are resistant to the TOR pathway inhibitor rapamycin

The ChIP and gene expression studies described earlier in this chapter link Ecm5 and Snt2 to genes involved in many aspects of metabolism, including sugar utilization, amino acid transport, as well as the TCA cycle and redox reactions. However, the categories of genes that seemed to come up most often were translation and ribosome. I therefore chose to extend these studies to involve direct perturbation of protein metabolism using the chemical rapamycin. Rapamycin is an inhibitor of the yeast target of rapamycin complex 1, or TORC1, which is responsible for sensing and signaling the availability of extracellular nutrients such as amino acids (Wei and Zheng, 2011). When nutrients are abundant, TORC1 signaling is active, telling yeast cells to keep growing while there are enough raw materials to do so, and promoting translation initiation and ribosome biogenesis. In addition, active TORC1 represses cellular stress response and nitrogen-catabolite repression (NCR) genes. However, when nitrogen-rich nutrients become scarce, the TOR pathway is inhibited, leading to the repression of translation and ribosome genes and the activation of stress and NCR genes. By inhibiting this pathway, rapamycin treatment mimics this amino acid starvation response. As with the oxidative stress

response, several studies have already implicated Rpd3(L) complex function in the response to rapamycin (Humphrey et al., 2004; Rohde and Cardenas, 2003; Tsang et al., 2003).

I first wanted to see whether the *snt2* knockout strain showed any resistance to rapamycin. I spotted wild-type or *ecm5*, *snt2*, or *rpd3* knockout strains onto SD CSM (synthetic defined with complete supplement mixture) plates supplemented with either DMSO or 50 nM rapamycin. I chose to use the less nutrient rich SD CSM, instead of YPD, for these experiments because I was concerned that cells grown in rich media might have a chance to accumulate nutrient reserves that would allow them to be more resistant to nutrient stress in ways that would mask true stress-resistant phenotypes. All strains grew similarly to wild-type in SD CSM supplemented with DMSO alone, and the growth defect seen when the *rpd3* knockout strain was grown in YPD was almost completely gone on the SD CSM media (Figure 4.11). Consistent with what has been reported in the literature, the *rpd3* knockout strain was resistant to rapamycin treatment (Tsang et al., 2003). In addition, the *snt2*Δ strain also showed resistance, linking Snt2 protein function to metabolic as well as oxidative stress.

Mapping Ecm5 and Snt2 localization before and after rapamycin treatment

I next mapped Ecm5 and Snt2 localization before and after rapamycin treatment using ChIP-seq. This experiment was done similarly to the H_2O_2 ChIP-seq experiment, except that for reasons mentioned above, strains were grown in SD CSM media, and after harvesting the cells at the initial time-point, each culture was split into two and treated either with DMSO, as a control, or with rapamycin. The rapamycin treatment clearly had an effect on the cells, since cells receiving this treatment had slower growth (based on OD600 measurements) than cells treated

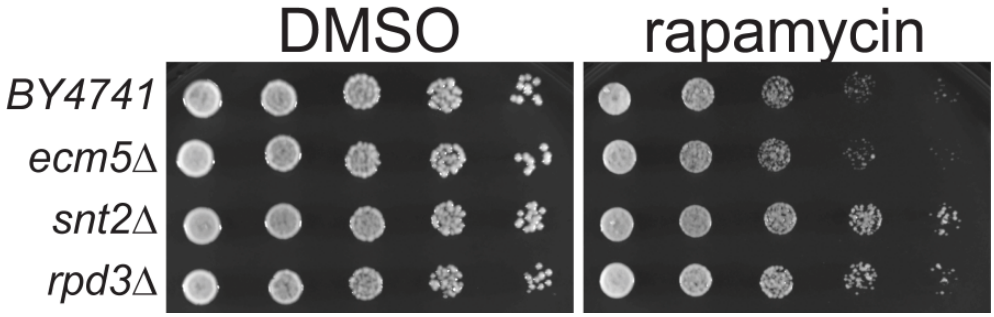

Figure 4.11 The *snt2* knockout strain is resistant to rapamycin
Five-fold serial dilutions of mid-log phase cultures of wild-type (BY4741) and *ecm5*Δ, *snt2*Δ, and *rpd3*Δ strains were spotted on the SD CSM plates supplemented with either DMSO or 50 nM rapamycin. Plates were photographed 3 days later.

with DMSO (data not shown). The ChIP-seq read counts for this experiment are summarized in Table A.3, in the Appendix.

Interestingly, cells grown in SD CSM media without any additional treatment did not show the same patterns of Ecm5/Snt2 enrichment found in cells grown in YPD. Rather, the ChIP profiles of untreated cells grown in SD CSM were actually more similar to the H_2O_2-treated cells grown in YPD (see Figure 4.12A for a representative region of the genome). Of the 278 Ecm5/Snt2 shared peaks in cells grown in SD CSM before rapamycin treatment, almost half overlapped with peaks only found in YPD-grown cells 0.5 hours after H_2O_2 treatment (Figure 4.12B). The similarities in Ecm5/Snt2 localization in cells grown in less rich media and H_2O_2-treated cells suggest that that H_2O_2 stress and the stress of not having as many nutrients trigger some of the same responses.

Just as H_2O_2 treatment triggered new sites of Ecm5/Snt2 ChIP enrichment, so too did rapamycin treatment, resulting in 558 shared peaks 0.5 hours after treatment, compared to 278 peaks before treatment. Most of these new sites of Ecm5/Snt2 enrichment were also enriched after H_2O_2 treatment, suggesting that both treatments lead to a similar response, with regard to Ecm5 and Snt2. I compared peaks of Ecm5/Snt2 binding 0.5 hours after rapamycin treatment with peaks found in DMSO-treated cells to generate three lists of peaks – those that were only seen in rapamycin-treated cells (rapamycin-specific targets), those that were seen in both DMSO- and rapamycin-treated cells (general targets), and those that were only seen in DMSO-treated cells (targets that Ecm5 and Snt2 leave in response to rapamycin treatment) (Figure 4.13A). Different types of genes were targeted by the peaks in each list (Figure 4.13A). General targets of Ecm5/Snt2, tended to be genes involved in sugar metabolism, amino acid transport, as well

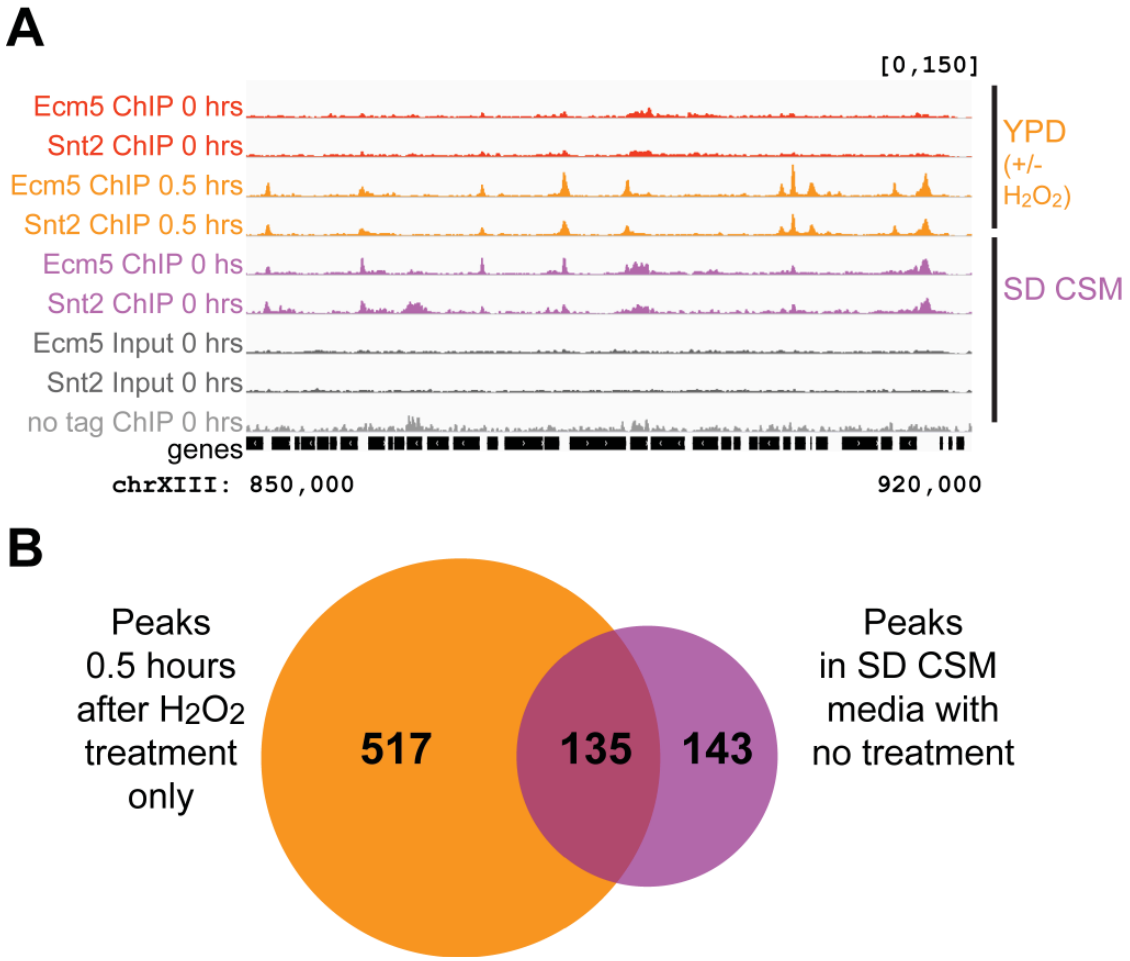

Figure 4.12 Ecm5 and Snt2 ChIP profiles in less rich media resemble profiles 0.5 hours after H_2O_2 treatment in rich media

A. Ecm5- and Snt2-Myc ChIP-seq tracks from both untreated and H_2O_2-treated yeast grown in YPD, and untreated yeast grown in SD CSM. **B.** Overlap between Ecm5/Snt2 ChIP peaks seen in YPD-grown cells only after H_2O_2 treatment and peaks in SD CSM-grown cells prior to rapamycin treatment.

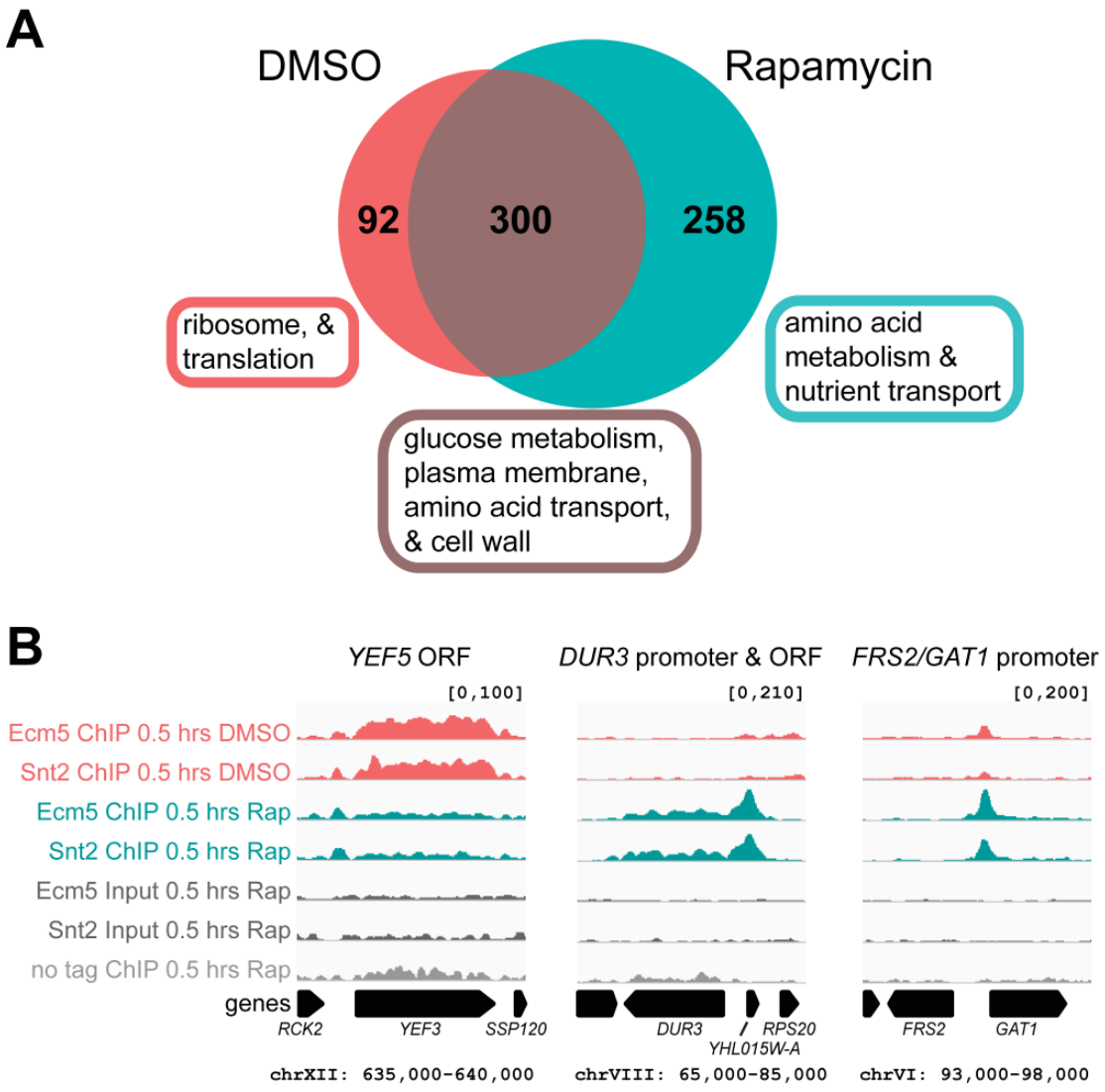

Figure 4.13 Rapamycin-specific peaks are involved in amino acid metabolism

A. Overlap between Ecm5/Snt2 ChIP peaks 0.5 hours after rapamycin treatment and peaks 0.5 hours after DMSO control treatment. Categories of genes enriched among the three sets of genes whose promoters contain each set of ChIP peaks are listed next to their corresponding section in the diagram. **B.** Specific examples of genes showing changes in Ecm5/Snt2 ChIP enrichment in response to rapamycin treatment at the promoter and/or ORF region.

as cell wall and membrane maintenance. Genes whose promoters were enriched for Ecm5/Snt2 before treatment and in DMSO-treated cells, but not in rapamycin treated cells were involved in the ribosome and translation. For instance, *YEF5*, a gene which encodes a translation elongation factor, is enriched for Ecm5 and Snt2 throughout its gene body before and 0.5 hours after DMSO-treatment, but this enrichment is gone in cells treated with rapamycin (Figure 4.13B, left panel). (While the majority of Ecm5/Snt2 enrichment at the gene is seen within the coding region of *YEF5*, enough of this peak overlapped with the promoter region that it was pulled out in this analysis). In contrast, genes involved in amino acid metabolism and nutrient transport were enriched among the rapamycin-specific targets. For instance, the gene body and promoter of the gene encoding the Dur3 nitrogen transporter, and the promoter of the gene encoding the Gat1 transcriptional activator of involved in nitrogen signaling, only show Ecm5 and Snt2 enrichment after rapamycin treatment (Figure 4.13B, middle and right panels). In summary, consistent with rapamycin treatment inhibiting protein synthesis and promoting nitrogen uptake and metabolism, this chemical caused Ecm5 and Snt2 to relocate away from genes involved in translation and to genes involved in amino acid metabolism and nutrient transport.

Unlike H_2O_2, which only induces transient changes in Ecm5 and Snt2 localization, rapamycin treatment led to changes in localization that were more long lasting: the ChIP-seq profiles of Ecm5- and Snt2-tagged strains 4 hours after treatment were very similar to those seen at the earlier, 0.5 hour time-point (data not shown). Curiously, there were approximately 40 genes that showed increased levels of Ecm5 and Snt2 localization in their gene bodies 4 hours after DMSO treatment. For instance, high numbers of Ecm5 and Snt2 reads were found in the gene bodies of the *MET6* and *MET3* genes 4 hours after DMSO treatment, but not after

rapamycin treatment (Figure 4.14A and B). I noticed that many of these genes were known to be involved in the biosynthesis of the sulfurous amino acids methionine or cysteine. Indeed, an analysis of genes known to be involved in the sulfur metabolism pathway revealed that all but 2 genes were enriched for Ecm5 and Snt2 4 hours after DMSO treatment (Figure 4.14C). Since the DMSO-control cells were able to grow and divide at a normal rate, they were quite dense when I harvested them. In contrast, cells that received rapamycin treatment slowed down their cycling and had not gotten as dense at this late time-point. Therefore, the localization of Ecm5 and Snt2 to these sites may be part of some kind of response to the cultures getting dense and beginning to undergo the diauxic shift. More likely, Ecm5 and Snt2 may be localizing to sulfur metabolism genes as a direct response to prolonged exposure DMSO, which itself is a sulfur-containing molecule, suggesting that caution should be used when using DMSO as a control.

Chapter 4 Discussion

The experiments described in this chapter present multiple lines of evidence that the Rpd3(T) complex functions in the yeast oxidative stress and metabolic stress response pathways. First, Ecm5 protein levels were found to respond to changes in stress and nutrient levels. Ecm5 levels increased in some experiments in response to H_2O_2 treatment. In contrast, Ecm5 protein levels decreased as cells entered stationary phase of growth, a state where nutrients are limiting. Given that stationary phase is generally thought to be a state in which cells are exposed to increased levels of oxidative stress, presumably because of the increased amount of respiration occurring during this phase (Galdieri et al., 2010), it is somewhat surprising that Ecm5 protein levels would respond differently to entry into stationary phase and H_2O_2 treatment. However,

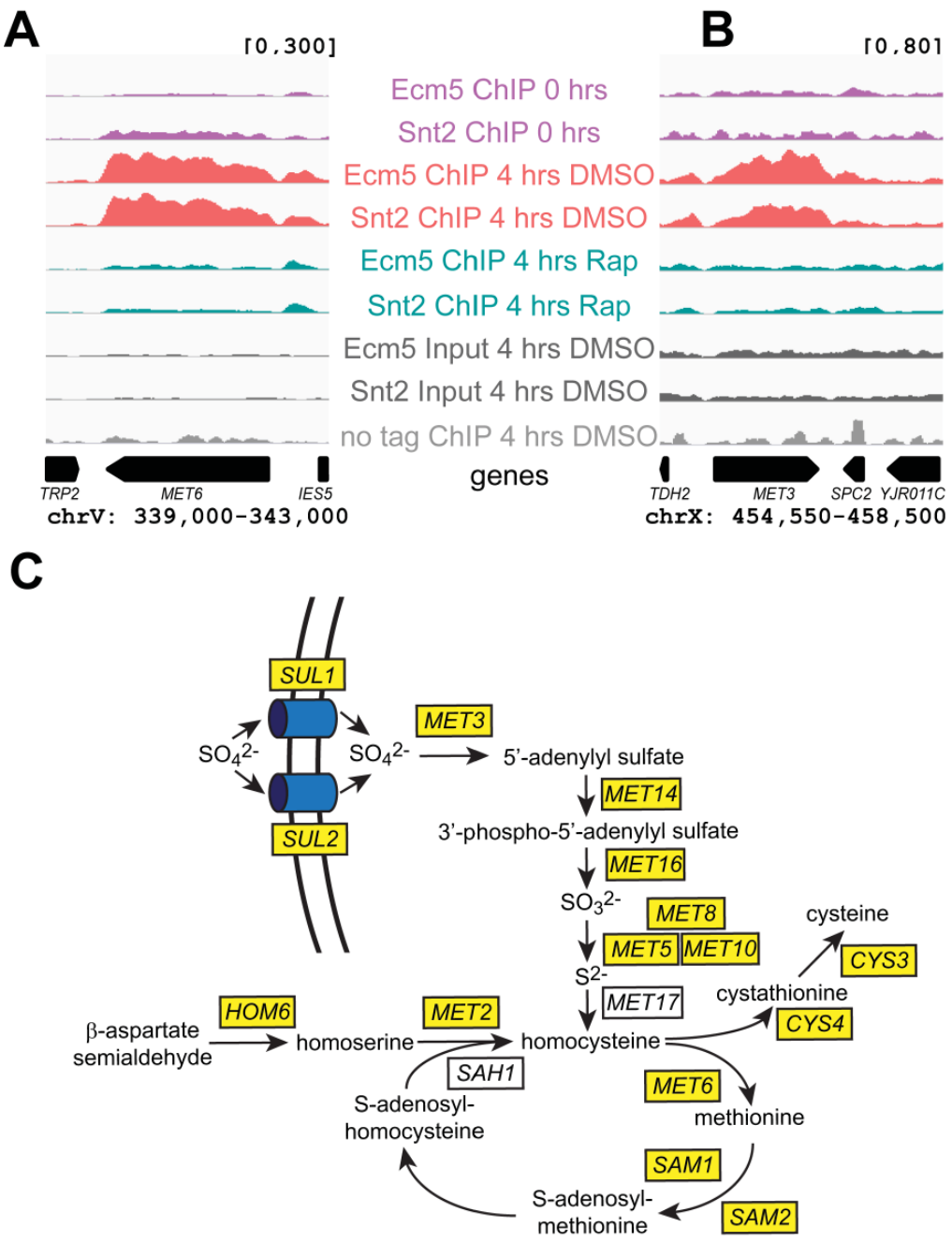

Figure 4.14 Ecm5/Snt2 localize to sulfur metabolism gene bodies in DMSO-treated cells
A. Examples of sulfur metabolism genes with increased numbers of Ecm5/Snt2 ChIP-seq reads 4 hours after DMSO treatment. ChIP-seq tracks are as in Figure 4.3. **B.** Diagram of sulfur metabolism with genes involved in boxes. Boxes around genes enriched for Ecm5/Snt2 ChIP reads 4 hours after DMSO treatment are colored yellow.

unlike cells growing exponentially and suddenly encountering an unexpected dose of H_2O_2, stationary phase cells are known to be resistant to stress (Galdieri et al., 2010). This difference between stationary phase growth and acute H_2O_2 stress may underlie the differential Ecm5 protein response to these two states. Furthermore, some studies have called into question the idea that cells undergoing respiration have increased levels of oxidative stress. One study found that cells undergoing respiration as a response to calorie restriction actually had lower levels of H_2O_2 released per O_2 consumed (Barros et al., 2004). The authors of this study suggest that active respiration may promote efficient electron flow through the mitochondrial electron transport chain and prevent electron leakage that leads to ROS formation.

Second, I have shown that the *snt2* knockout strain is resistant to H_2O_2-mediated oxidative stress, both on solid media and in liquid culture. The increased growth of the *snt2* knockout on H_2O_2-containing plates could be because *snt2*Δ cells divided more rapidly than wild-type cells once plated or because more *snt2*Δ cells survived the initial plating. The results of the liquid survival assay, which measures survival independent of growth rate, support the latter possibility. These findings suggest that the Rpd3(T) complex might actively promote cell death in response to H_2O_2 treatment. While yeast are not normally associated with programmed cell death, prior research from former Allis laboratory graduate student Sung Hee Ahn Upton showed that H_2O_2 can trigger an apoptosis-like cell death process in yeast, and that a knockout for the *rpd3* histone deacetylase has increased survival in H_2O_2 (Ahn et al., 2006; Ahn et al., 2005). My experiments confirmed this finding and found that the *snt2* knockout had even better survival, suggesting that in response to H_2O_2 the Rpd3(T) complex has a role in promoting apoptosis.

The higher level of stress resistance seen with the *snt2* knockout strain compared to that of the *rpd3* knockout was surprising given that they are members of the same complex. It is possible that Snt2 has a function in the oxidative stress response that is independent from Rpd3's role. Alternatively, since Rpd3 is known to have many cellular roles, and functions in two complexes separate from the Rpd3(T) complex, the less severe stress resistance seen with the *rpd3* knockout may reflect pleiotropic effects simultaneously promote and impede resistance to oxidative stress.

As a third piece of evidence that the Rpd3(T) complex functions nutrient metabolism, I have shown that in unstressed cells, the genes whose promoters are enriched for Ecm5 and Snt2 have translation and carbohydrate metabolism functions. Furthermore, Ecm5 and Snt2 ChIP profiles were shown to be radically different 0.5 hours after H_2O_2 treatment. In response to H_2O_2, Ecm5 and Snt2 were found to localize to many new gene promoters and to redistribute away from the gene bodies and into 5' and 3'regions of certain highly expressed genes. Moreover, the types of genes that Ecm5 and Snt2 localize to in untreated cells were functionally distinct from the H_2O_2-specific targets. In contrast with the genes involved in translation and carbohydrate metabolism that were general Ecm5 and Snt2 targets, after H_2O_2 stress Ecm5 and Snt2 localized to genes involved in amino acid metabolism, transmembrane transport, oxidation-reduction reactions, cell wall and plasma membrane function, and response to oxidative stress. H_2O_2 treatment is known to inhibit protein translation, which allows cells time to clear proteins and metabolites damaged by H_2O_2 before resuming biosynthesis (Shenton et al., 2006). This inhibition of protein synthesis requires Gcn1, one of the proteins whose deletion that was found to result in synthetic sickness in combination with an *ecm5* knockout (Collins et al., 2007). The

presence of Ecm5 and Snt2 at amino acid metabolism genes and the redistribution of Ecm5 and Snt2 from gene bodies to promoter regions of ribosomal protein genes after H_2O_2 treatment may reflect a potential role for Ecm5 and Snt2 in regulating this translational inhibition and the subsequent cellular need to generate new amino acids for when translation resumes.

As further evidence that the Rpd3(T) complex functions in the oxidative and nutrient stress pathways, *rpd3* and *snt2* mutants were also resistant to the TOR inhibitor rapamycin, which promotes an amino acid starvation response in yeast. Furthermore, just as H_2O_2 treatment stimulated many new Ecm5/Snt2 genomic associations, so too did rapamycin treatment. While the H_2O_2-specific Ecm5 and Snt2 targets were involved in myriad stress and metabolism functions, the smaller number of rapamycin-specific targets tended to be genes involved in amino acid metabolism. Even before rapamycin treatment, the mere growth of cells in the less rich SD CSM media already prompted Ecm5 and Snt2 association with more targets than the number of genes targeted when cells are grown in YPD, and many of these targets were genes that Ecm5 and Snt2 localize to in response to H_2O_2 treatment. These results suggest that whatever cellular state is triggered by H_2O_2 treatment resembles the state of cells without an abundance of nutrients around. In support of this idea, one study found that cells starved for an essential amino acid had increased levels of reactive oxygen species, suggesting that lack of nutrients can directly promote oxidative stress (Eisler et al., 2004). More recently, starving yeast were shown to up-regulate oxidative stress response genes (Petti et al., 2011). One open question from this work is whether the relocalization of Ecm5 and Snt2 upon H_2O_2 treatment is a direct consequence of oxidative stress signaling or a secondary consequence of the high degree of crosstalk known to exist between the stress and nutrient signaling pathways.

A final piece of evidence linking the Rpd3(T) complex to oxidative and nutrient stress is that the genes over- or under-expressed in the *snt2* knockout strain are also involved in these pathways. Moreover, there is a high degree of overlap between genes misexpressed in the *snt2*Δ strain after H_2O_2 treatment and genes whose expression levels change in wild-type cells in response to H_2O_2. In contrast to the gene expression changes seen in the *snt2*Δ strain, the *ecm5*Δ strain had very few genes misexpressed, consistent with the genetic data showing that deletion of Ecm5 did not promote H_2O_2 or rapamycin resistance. More discussion of the potential reasons why deletion of *ECM5* does not show the same striking phenotypes as *SNT2* deletion will be presented in the final discussion chapter to this thesis.

Of course, the key question is whether the Rpd3(T) complex localizes to target genes to regulate gene expression. The majority of Ecm5 and Snt2 target genes both before and after H_2O_2 treatment show no expression differences in the *snt2*Δ strain. While surprising, this result is consistent with two other reports about the Rpd3(L) complex, which showed this complex is localized at the promoters of ribosomal protein genes whose expression do not change when Rpd3 is deleted (Kurdistani et al., 2002; Rohde and Cardenas, 2003). These studies and my own findings suggest that in many cases the Rpd3(T) complex may be poised at target genes, waiting for a signal or additional factor needed for the complex to affect gene expression.

I did isolate a subset of 309 genes that contained Ecm5 and Snt2 at their promoters, changed expression in wild-type cells, and were also differentially expressed in the *snt2* knockout strain after H_2O_2 treatment. While I initially thought Rpd3(T) would be a repressive complex, I found that while some of these genes were over-expressed in the *snt2*Δ strain, others were repressed, suggesting that the link between Rpd3(T) function and gene expression is

complicated. Again, previous studies of the Rpd3(L) complex have paved the way for these findings, showing that this complex is needed for both activation and repression of target genes in response to stress (Alejandro-Osorio et al., 2009; De Nadal et al., 2004). Genes falling within the same functional category were more likely to be regulated by Snt2 in similar ways. While not definitive, this result is consistent with a model in which different factors associate with the Rpd3(T) complex at different gene targets and modulate its activity, an idea I will discuss further in the next chapter.

Surprisingly, Ecm5 and Snt2 showed two distinct modes of binding. While in most cases, these proteins were localized in gene promoters, there were a number of genes that contained Ecm5 and Snt2 within their gene bodies in untreated cells. This pattern of binding was often correlated with highly expressed genes, so it would be interesting to see if H3K36me3 levels, which are known to correlate with transcription level (Pokholok et al., 2005), are higher at these genes, which would be consistent with the Rpd3(T) complex being recruited to these genes through the reported weak interaction between the Ecm5 PHD finger and this mark (Shi et al., 2007). After H_2O_2 treatment, Ecm5 and Snt2 were no longer enriched in the coding regions of these genes, but rather appeared to relocalize to the 5' and 3' ends. Intriguingly, genes that had this pattern of localization were generally repressed upon H_2O_2 treatment, and in many cases were even more repressed after treatment in the *snt2*Δ strain, suggesting that this pattern of localization is correlated with Rpd3(T) acting as a transcriptional activator. In summary, Ecm5 and Snt2 localize to promoters and some coding regions of genes involved in stress and metabolism, and Snt2 is required for the proper expression levels of a subset of the Ecm5 and Snt2 target genes, suggesting that the Rpd3(T) complex may function to regulate gene expression in response to metabolic and oxidative stress signals.

CHAPTER 5: GENERAL DISCUSSION

The study of yeast PHD fingers led to the discovery of a new chromatin regulatory complex

The research described in this thesis was undertaken with the goal of learning more about the functions of the PHD finger-containing proteins Jhd2 and Ecm5. Because of the domain structures of Ecm5 and Jhd2, and because both proteins are localized to the nucleus, I hypothesized that they would function to regulate chromatin. Early support for this hypothesis came from my own pull-down experiments showing that the PHD fingers of both proteins interact with histone H3. In addition, studies from other laboratories have successfully mapped Jhd2 on chromatin using the ChIP technique (Ingvarsdottir et al., 2007; Radman-Livaja et al., 2010), and shown that this protein can act as an H3K4 demethylase (Liang et al., 2007; Seward et al., 2007; Tu et al., 2007). My own ChIP experiments have successfully mapped the genomic localization of Ecm5, as well as its interaction partner, Snt2. In addition, I have characterized an Ecm5-containing complex that also contains Snt2 and the Rpd3 deacetylase. I have chosen to call this complex the Rpd3(T) complex, to highlight its catalytic deacetylase subunit. This allows the reservation of the term Snt2C to refer to a possible subcomplex containing Ecm5 and Snt2 only, which I will discuss more below. Thus, both Ecm5 and Jhd2 bind to chromatin and contain or are associated with histone-directed enzymatic activity.

I have shown that members of the Rpd3(T) complex are not required to prevent cryptic transcription, a known function for another Rpd3-containing complex, Rpd3(S). In addition, I have demonstrated that *ecm5* knockout cells do not have obvious defects in the cell wall, DNA damage repair, the cell cycle, the cellular morphogenesis checkpoint, meiosis, or sporulation.

Rather, a genetic interaction between *ECM5* and a gene required for the yeast oxidative stress response led me to uncover a role for Rpd3(T) in regulating the yeast oxidative stress and nutrient metabolism pathways.

The many domains in Ecm5 and Snt2 are likely to work in combination to recruit or stabilize the Rpd3(T) complex on chromatin

Many of the domains in Ecm5 and Snt2 are part of families with known functions in chromatin interaction, including the PHD finger, a domain that has been a focus of this research. It is likely that these domains help promote or stabilize Rpd3(T) complex binding on chromatin. I have shown that the Ecm5 PHD finger interacts with histone H3 and have found a moderate enrichment for H3K36me3 in the H3 pulled-down. The Gozani lab has also reported that the Ecm5 PHD interacts with H3K36me3, albeit weakly (Shi et al., 2007). While I was unable to confirm a direct association between the Ecm5 PHD and H3K36me3, possibly because of the weakness of this reported interaction, I did find that Ecm5 and Snt2 localize to the gene bodies of highly transcribed genes, which are known to have the highest levels of H3K36me3 (Pokholok et al., 2005). At these genes, the high levels of this mark may compensate for a weak Ecm5-PHD interaction in helping this complex bind to or remain at these chromatin regions.

In an interesting twist for a project that was initiated because of PHD fingers, Snt2 has three PHDs of its own. Gozani and colleagues reported that the second Snt2 PHD could interact very weakly with H3K36me as well as with an H3 peptide centered around K79, irrespective of methylation status (Shi et al., 2007). They were unable to find associations between the other two Snt2 PHDs and the chromatin marks they tested. These domains may interact with some

of the more recently described sites of yeast lysine methylation mentioned in the introductory chapter, with arginine methylation, or with non-histone proteins. In addition to PHD fingers, Ecm5 contains an ARID domain, and Snt2 contains BAH and SANT domains. In other proteins, these domains have been shown to mediate DNA or histone interactions (Armache et al., 2011; Boyer et al., 2004; Kuo et al., 2012), and it is likely that multiple weak DNA or histone interactions mediated through these individual domains work in combination to recruit Ecm5 and Snt2 to specific chromatin locations, or to stabilize these proteins on chromatin once recruited. The kinetic and thermodynamic cases for how multiple weak interactions allow chromatin regulators to bind tightly but reversibly to their substrates has been well described in a review on the topic of "multivalency" in chromatin associations from Dr. Alex Ruthenburg and colleagues, and the references therein (Ruthenburg et al., 2007). In the future, it would be interesting to produce the Snt2 BAH, SANT, and three PHD domains recombinantly, singly and in combination, and to test them all for histone binding in pull-down assays. Future ChIP experiments with tagged Ecm5 or Snt2 strains containing point mutations in these various domains may also reveal interesting functions for these domains in mediating interactions between Rpd3(T) and chromatin.

Potential models for the role of Rpd3(T) in regulating stress and metabolism

In the previous chapter, I presented multiple lines of evidence that the Rpd3(T) complex regulates yeast metabolism and the oxidative stress response. A key question that is unresolved in this work is what is the exact mechanism for this regulation. The exact nature of the signal that promotes Ecm5 and Snt2 localization to new promoter regions in less rich media and after

oxidative stress remains unclear, as does the mechanism by which Ecm5 and Snt2 promote changes in gene expression at a subset of their targets. The simplest model for the latter question would be if Rpd3(T) were recruited to gene promoters (and sometimes coding regions) so that Rpd3 could deacetylate these regions and repress the gene targets. However, there is no clear pattern of expression differences of these genes in the *snt2* knockout: some genes are up-regulated in the absence of Snt2, while others are down-regulated. Furthermore, I identified a large number of Ecm5 and Snt2 target genes whose expression was no different than wild-type expression levels either before or after stress. These findings demonstrate that the link between Rpd3(T) complex function and gene regulation is more complicated than the simple model that Rpd3(T) represses target genes.

Precedence for more complicated types of gene regulation exists in the literature. For example, a single factor in yeast can be associated with both activating and repressing activity, depending on the context. A study from Fred Winston's laboratory has shown that the yeast Hap1 protein, which is known to activate genes during aerobic growth, also directly represses ergosterol biosynthesis genes during hypoxia (Hickman and Winston, 2007). Hap1 localizes to the promoters of the ergosterol genes both during hypoxia, when it is needed for repression, and during aerobic growth, when it is needed for activation of these genes, and cellular concentrations of heme dictate whether Hap1 acts as an activator or a repressor. In this example, whether Hap1 activates or represses genes depends on the state of the entire cell, whereas my data suggest Snt2 function might be capable of activating or repressing genes in the same cell, although it is possible that genes that were over- or under-expressed in the *snt2* knockout strain came two a different subpopulations of cells within the culture (e.g. cells that experienced high levels of H_2O_2 vs. cells that received lower doses).

There are other possible models for how Snt2 could promote both gene activation and repression (Figure 5.1). Snt2 may exist as part of two distinct complexes, one whose sole other member is Ecm5, and one that also contains Rpd3 – Rpd3(T). The mass spectrometric results I discussed in the third chapter show that Rpd3 can associate with Ecm5 and Snt2, but they do not rule out a possible subcomplex consisting of Ecm5 and Snt2 only. The Rpd3(T) complex may localize to the promoters that require Snt2 for repression, while and Ecm5 Snt2 subcomplex localizes to other promoters and gene bodies to promote activation (possibly by recruiting additional transcription factors) (Figure 5.1A). An Rpd3-indendent function for Snt2 might explain why the *snt2* knockout strain has markedly better survival in response to H_2O_2 stress than the *rpd3* knockout, although it is also possible that pleiotropic effects of *RPD3* deletion are responsible for this result. In theory, Ecm5 and Snt2 could also have functions independent from one another. However, within the genome, I do not see regions where one is bound without the other, suggesting Ecm5 and Snt2 function as a unit on chromatin. One of the most important next experiments for this work will be to use ChIP to map Rpd3 localization before and after oxidative stress, and see whether some targets of Ecm5 and Snt2 binding are not Rpd3 targets.

Another possibility is that the Rpd3 localizes to all the same genes that Ecm5 and Snt2 localize to, and depending on which other factors are present, can promote gene activation or repression. As mentioned earlier, other studies have found examples of genes containing Rpd3 at their promoters that require Rpd3 for activation (De Nadal et al., 2004; Ruiz-Roig et al., 2010; Sertil et al., 2007; Sharma et al., 2007). This could be the result of the Rpd3(T) complex recruiting different factors that either promote or repress transcription (Figure 5.1B). It is possible that in some cases, deacetylation of specific histone lysines might promote

Figure 5.1 Models for possible ways that Snt2 might directly regulate both gene activation and repression

A. Ecm5 and Snt2 might be recruited without Rpd3 to promoters that require Snt2 for activation, subsequently recruiting transcription factors, while other promoters might recruit the entire Rpd3(T) complex for HDAC-mediated repression. **B.** The Rpd3(T) complex might be recruited to promoters that require Snt2 for activation, where the complex functions primarily to recruit other transcription factors (Txn factor), while at promoters that require Snt2 for repression, Rpd3(T) might recruit transcriptional repressors (Rep). **C.** Different regulatory factors (Factor) interacting with Rpd3(T) may change the preferred histone lysine substrates of Rpd3, with deacetylation of specific histone lysines potentially promoting transcription and deacetylation of other histone lysines repressing it. **D.** Different regulatory factors (Factor) interacting with Rpd3(T) may change the preferred substrate of Rpd3 to a non-histone protein, with deacetylation of the non-histone substrate potentially promoting transcription and deacetylation of a histone substrate repressing it.

Figure 5.1 Models for possible ways that Snt2 might directly regulate both gene activation and repression

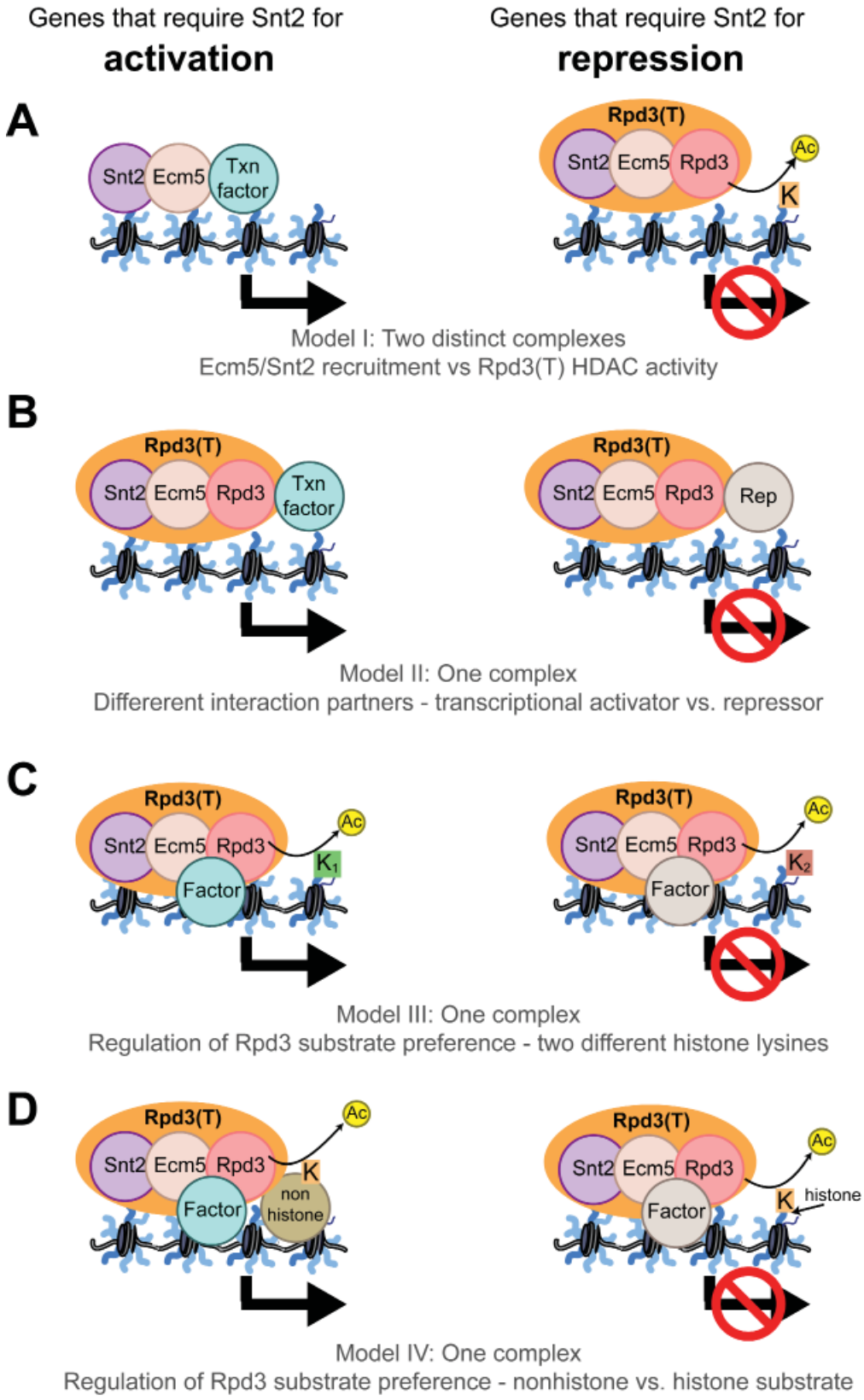

transcriptional activity (Figure 5.1C). It also remains possible that despite being bound to chromatin, Rpd3(T) does not affect histone acetylation at the genes it activates, but rather deacetylates non-histone factors that are recruited in the vicinity of this complex, which then promote transcription (Figure 5.1D). These models are not exclusive, and combinations of two or more of them, could be happening *in vivo*.

Another Rpd3-containing complex, Rpd3(L), has also been shown to regulate stress and metabolism genes (De Nadal et al., 2004; Humphrey et al., 2004; Kremer and Gross, 2009; Rohde and Cardenas, 2003; Ruiz-Roig et al., 2010; Tsang et al., 2003). Like the *snt2* knockout strain, knockouts for Rpd3(L) subunits have been shown to be rapamycin resistant (Rohde and Cardenas, 2003). In addition, a recent study has found that in response to TOR pathway activation, the Rpd3(L) complex localizes to and represses ribosomal biogenesis and ribosomal protein gene promoters (Huber et al., 2011). In this research, I have also found Ecm5 and Snt2 localized at promoters and in some cases, gene bodies, of these types of genes. Therefore, the Rpd3(T) complex could possibly be a subcomplex of Rpd3(L) that only associates under conditions of oxidative or nutrient stress. This could explain why Ecm5 and Snt2 were never detected in IPs for Rpd3(L) subunits, and why Rpd3(L) subunits were not detected in my own Ecm5 and Snt2 IPs, all of which were performed in lysates from unstressed cells. It would be interesting to repeat these IPs in cells treated with H_2O_2 or rapamycin to look for new associations.

Could plant homeodomain fingers act as redox sensors?

Reactive oxygen species (ROS) are damaging to cells in part because they can directly oxidate cysteine side chains of proteins. While this oxidation generally renders proteins nonfunctional, and is therefore deleterious, cysteine oxidation can have a positive role in regulating cellular response to redox status. In yeast, the Yap1 transcription factor is one of the better examples of this type of regulation. As discussed in the introductory chapter, Yap1 is normally exported from the nucleus, but when intracellular levels of H_2O_2 are high, two cysteines in Yap1 are oxidized, forming an intramolecular bond. This results in a conformation change that masks Yap1's nuclear export sequence, allowing it to accumulate in the nucleus and activate oxidative stress response genes.

The PHD finger is a domain defined by the presence of multiple cysteine residues, which are required for the proper folding of this module. Oxidation of PHD cysteines, which would be expected to perturb these folds, would likely alter or prevent the chromatin associations of these modules. Not all cysteines are equally good substrates for oxidation (Le Moan et al., 2006). Nevertheless, I speculate that if PHD domains can become oxidized in response to higher levels of cellular ROS, the proteins or complexes containing these domains might then rely more on their other chromatin-interacting motifs for chromatin localization, and might therefore localize to different regions of the genome. Cells might use PHDs as redox sensors as a mechanism to alter the genomic associations of PHD finger proteins, resulting in differential gene regulation in response to oxidative stress.

If such a mechanism does exist in yeast cells, the Rpd3(T) complex would be a good candidate complex for redox sensing. While Ecm5 appears to be dispensable for complex

function, the three Snt2 PHD domains may not be. I have already demonstrated that Ecm5 and Snt2 localize to new loci in response to H_2O_2 treatment. This might be an indirect effect of H_2O_2 treatment, but it is possible that H_2O_2 treatment directly oxidizes one or more Snt2 PHD fingers, resulting in a conformational change that allows Ecm5 and Snt2 to bind to new regions in the genome. Future experiments that map complex localization before and after oxidative stress in cells with mutations in the Snt2 PHD cysteines might provide evidence for this mechanism. Because of the concern that cysteine mutation might just destabilize or unfold Snt2, it would be important to establish that the localization of Snt2 containing PHD point mutations was normal in the absence of oxidative stress. In addition, it would be interesting to perform western blots for tagged Snt2 on whole cell extracts from untreated and H_2O_2-treated cells, using non-reducing conditions, to look directly for evidence of disulfide bond formation.

What does Ecm5 do, and why does the mutant lack a phenotype in these assays?

The ultimate goal that drove this research was to gain insights into the function(s) of Ecm5, and it was a genetic interaction with *ECM5* that led me to test whether the Rpd3(T) complex was involved in the oxidative stress response. I was therefore surprised to find that the *snt2* knockout strain had such dramatic phenotypes while the *ecm5* knockout strain did not. The high degree of genomic colocalization these two proteins have made this result all the more surprising. Thus, in spite of great strides in identifying interaction partners for Ecm5 and finding roles for them in oxidative stress and cellular metabolism pathways, at the end of this project, I am left facing the same question I had when I began: just what exactly does Ecm5 do?

It is possible that Ecm5 physically associates with Snt2 and Rpd3, but is not needed for their genomic localization or association with one another. If this is the case, Snt2-mediated gene regulation would not be expected to be perturbed in cells lacking Ecm5, which would explain how so few genes' expression levels differ from wild-type in *ecm5* knockout cells. Future ChIP experiments in strains where one member of the Rpd3(T) complex is tagged and one member is deleted could help to unravel the mechanism for this complex biology.

While very preliminary, in H_2O_2 plate assays, the *ecm5*Δ *snt2*Δ double mutants have phenotypes more similar to *ecm5*Δ cells, or somewhere in between *ecm5* knockouts and *snt2* knockouts, suggesting that the functions of Ecm5 and Snt2 might be opposed (Figure 5.2A). It is possible that in wild-type cells, Ecm5 functions to inhibit Rpd3 activity and that Snt2 prevents Ecm5 from doing this, allowing Rpd3 to remain active at Rpd3(T) target genes, and enact gene expression changes that cause cells to be sensitive to H_2O_2 (Figure 5.2B). Under this model, in *ecm5*Δ cells, Rpd3 would be active, and would sensitize cells to H_2O_2. In *snt2*Δ cells, there would be nothing protecting Rpd3 from Ecm5-mediated repression, causing Rpd3 to be inactivated. Without Rpd3-mediated changes in gene expression, cells would remain resistant to H_2O_2. In *rpd3*Δ cells, the gene expression changes that promote H_2O_2-mediated cell death would not occur, resulting in H_2O_2-resistant cells. However, other effects from the loss of Rpd3(L) and Rpd3(S) complex function may blunt the H_2O_2 resistance, explaining why *rpd3*Δ cells are less resistant than *snt2*Δ cells. In *ecm5*Δ *snt2*Δ double mutants, Rpd3 would be active, promoting cell death in response to H_2O_2 stress, explaining why this double mutant phenotypically is more similar to wild-type and *ecm5*Δ yeast strains and not the *snt2* knockout strain. This model would also suggest that in certain cell states, Ecm5 could be freed from Snt2-mediated repression, and could actively inhibit Rpd3.

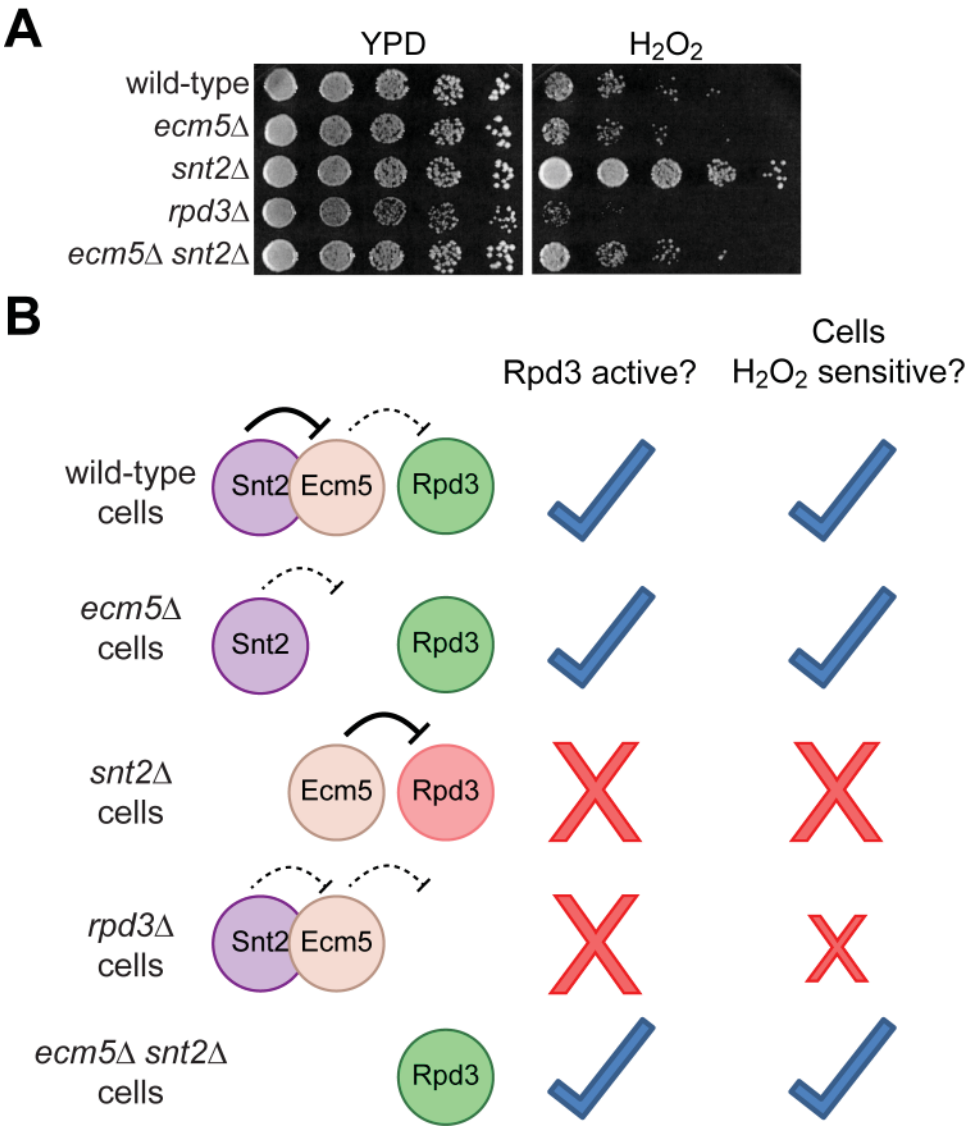

Figure 5.2 Preliminary evidence that Ecm5 and Snt2 might oppose one another and a model for how this might work

A. Dilutions of saturated overnight cultures of the indicated mutant strains were spotted onto YPD alone or YPD supplemented with 4 mM H_2O_2. Plates were imaged after 2 days. **B.** The phenotypic resemblance of the *ecm5 snt2* double knockout strain to the *ecm5* single knockout strain could be explained by a model where Ecm5 represses Rpd3 function and Snt2 represses Ecm5. In wild-type cells, these activities would result in active Rpd3, which could promote changes that sensitize cells to H_2O_2. The corresponding states for each mutant are diagramed below the wild-type case.

At the moment, this model is speculative, and will require further testing to confirm. To that end, it will be important to determine what happens to Rpd3(T) complex composition when one member of the complex is deleted. In addition, *in vitro* histone deacetylation assays with Rpd3(T) complex purified from cells lacking either Ecm5 or Snt2 could test whether Ecm5 represses Rpd3 activity, and whether Snt2 inhibits this repression. Because of the difficulties of purifying large quantities of Rpd3(T) complex, *in vitro* deacetylase assays with fully recombinant Rpd3 alone, or in complex with recombinant Ecm5 and/or Snt2, may be a more feasible way to see whether Ecm5 and Snt2 affect Rpd3 activity. In support of this model, Yi Zhang's laboratory has shown that the presence of the non-Rpd3 subunits of the *Drosophila* homolog of the Rpd3(T) complex inhibits Rpd3 activity (Lee et al., 2009).

As I mentioned in the introductory chapter, Ecm5 contains a JmjC domain that seemingly does not have demethylase activity. While this domain lacks the conserved residues predicted to interact with Fe(II), it retains some of the residues predicted to bind to α-ketoglutarate (Figure 5.3). The JmjC domain is part of a larger superfamily of domains with oxygenase activity (Loenarz and Schofield, 2008). Other functions for domains in this family include the post-translational modification of proteins by prolyl-hydroxylation and arginine demethylation. While the Fe(II)-binding triad of histidine, aspartate or glutamate, and histidine is conserved in most members of this family, this triad is not universal. Therefore, an intriguing possibility is that the Ecm5 JmjC possesses a catalytic activity distinct from lysine demethylation. Future *in vitro* reactions with Ecm5 purified from yeast, may reveal such an activity.

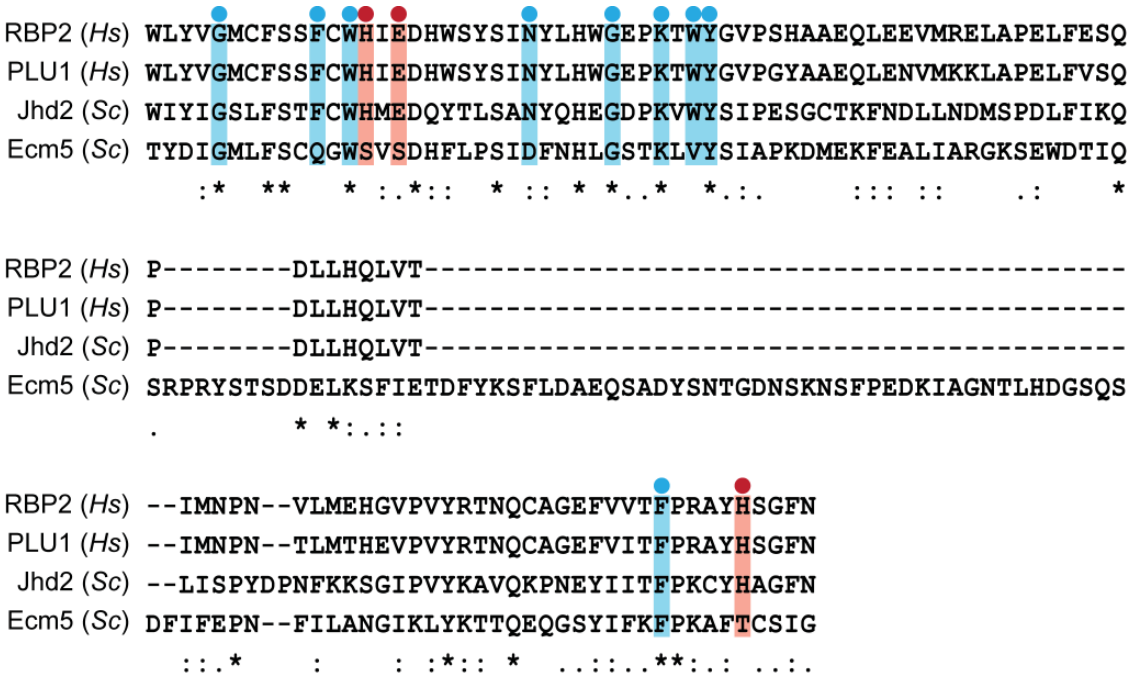

Figure 5.3 The Ecm5 JmjC domain possesses many of the residues predicted to bind α-ketoglutarate

JmjC domain alignments consisting of amino acids 470-575, 486-591, 414-521, and 509-667 of the full-length RBP2 (*Homo sapiens*, NCBI accession # NP_00103068), PLU1 (*Homo sapiens* # NP_006609), Jhd2 (*S. cerevisiae*, # NP_012653.1), and Ecm5 (*S. cerevisiae*, # NP_013901.1), respectively, with askterisks, colons , and periods under fully, strongly, and weakly conserved residues, respectively. Predicted Fe(II) binding residues are highlighted in light red, and predicted α-ketoglutarate-binding residues are in light blue. Predicted residues come from Klose et al., 2007; Yamane et al., 2007; and Li et al. 2008.

Evolutionary reasons for the *snt2* mutant phenotype and competitive fitness of this strain

I have shown that increased numbers of cells survive H_2O_2-mediated stress when *SNT2* or *RPD3* is deleted, compared to survival in a wild-type strain, suggesting that part of the function of the Snt2 and Rpd3 is to inhibit cell division and promote cell death in response to high levels of oxidative stress. Unlike H_2O_2 treatment, rapamycin treatment, which mimics nutrient stress, does not promote cell death, but rather just slows cell division (data not shown), and strains lacking Snt2 or Rpd3 are resistant to rapamycin. These results suggest that in response to oxidative stress Rpd3 and Snt2 act to promote cell death, while in response to nutrient stress Rpd3 and Snt2 act to inhibit cell division.

It might at first, seem counterintuitive that yeast would evolve a protein complex that would slow down their growth or promote cell death. In multicellular organisms, the case can be made that the quiescence or death of one cell may be important for the survival and reproductive success of the whole organism, and so makes good evolutionary sense. Yeast, on the other hand, are only single cells, and should therefore have evolved mechanisms that promote the fastest growth and reproduction. Nonetheless, the existence of a cell death pathway in yeast has now been well-documented, and scientists have speculated that death of chronogically aged or stressed yeast cells may allow for the release of nutrients into the media which promote the growth and survival of healthier yeast cells within the population as a whole (Herker et al., 2004; Madeo et al., 2004). While this strategy is disadvantageous for the dying cell, it benefits the rest of the population, and given that yeast cells within a population are genetically similar, a population benefit also helps the cell that has died to pass on its genes. A similar mechanism is known to occur in the bacterium *Bacillus subtilis*. When *Bacillus* cells are starved for nutrients,

a fraction of the cells undergo a switch that allows them to secrete extracellular factors that kill the cells around them (Claverys and Havarstein, 2007). The secreting cells can then feed on the remains of their dead siblings. This behavior has been delightfully named "cannibalism," and is also proposed to help this species survive extreme stress.

In keeping with these ideas, I hypothesize that Rpd3 and Snt2 inhibit cell growth in response to nutrient stress because in the long run, continuing to divide under such stress would be deleterious to the yeast population. Inhibiting growth in response to low levels of stress allows cells time to repair damage, conserve energy, and regenerate key molecules. In cells too damaged to successfully keep reproducing, cell death allows that other cells to at least gain a nutritional benefit, which may provide them with the energy needed to activate their own stress defense pathways. Based on these hypotheses, I expect that *snt2*Δ cells would have a fitness defect compared to wild-type cells. To test this idea, I have performed a preliminary competition experiment, in which equal numbers of wild-type and *snt2*Δ cells were inoculated into SD CSM and cultured over several days. Cultures were diluted with fresh media each day, to avoid looking for differences in chronological age. Surprisingly, under these conditions, *snt2*Δ cells out-competed wild-type cells, as measured by the proportion of total cells in the culture that possessed the G418 resistance marker and therefore were deleted for *SNT2* (Figure 5.4). In hindsight, this may be because the conditions of this experiment were conducive to growth. Perhaps only under extreme stress conditions, where it is vital that cells not divide until damage is repaired, and that damaged cells clear the way for intact ones, would a fitness defect emerge for the *snt2* knockout strain. Future competition experiments that test various stress conditions, such as repeated exposure to H_2O_2, rapamycin treatment, starvation media, or chronological aging, may reveal such a defect.

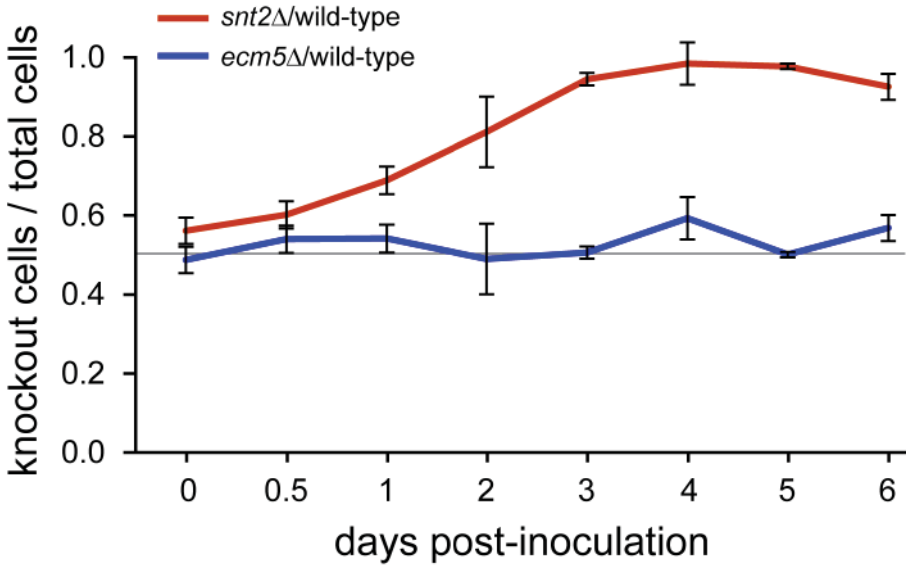

Figure 5.4 The *snt2* knockout strain out-competes the wild-type strain

Equal numbers of wild-type and either *ecm5* or *snt2* knockout cells were co-inoculated into the same SD CSM cultures. Immediately and 12 hours after inoculation, samples were taken, diluted, and plated to determine the numbers of wild-type and knockout cells in each culture. After 24 hours in culture, and each subsequent day, cultures were diluted to $2x10^5$ cells/mL in fresh media, and samples were taken, diluted, and plated for counting. Dilutions of cultures were plated on both knockout-selective and non-selective media, and viable colonies were counted two days post-plating. The number of viable knockout cells in a sample was then divided by the total number of cells in that same sample. Graphs show the means and SEMs of these ratios for 3 replicates each for competitions between *snt2*Δ and wild-type and between *ecm5*Δ and wild-type strains.

The implications of this research: live long, stay healthy, and drink up!

I initially embarked on this project with the hope that anything I learned about Jhd2 or Ecm5 might be applicable to their human homologs, the JARID proteins. Excitingly, there is evidence for human complex similar to Rpd3(T). The human RBP2/JARID1A protein has been shown to be a member of a large complex that includes a PHD finger-containing protein called Pf1 and the Rpd3 homolog HDAC2 (Hayakawa et al., 2007). It would be interesting to use ChIP-seq to map the localization of subunits of this complex in human cell lines before and after exposure to ROS or nutrient starvation conditions to see if this complex associates with different genomic regions in response to these insults. It is now well established that increased exposure to oxidative stress and perturbed cellular metabolism contribute to numerous human disease states, including cancer, diabetes, and age-related neuropathies (Alic and Partridge, 2011; Dazert and Hall, 2011; Lin and Beal, 2006; Roberts and Sindhu, 2009). Therefore, if humans contain a pathway analogous to Rpd3(T) that is responsible for regulating metabolism and stress response, understanding this complex may have important implications for understanding the factors that contribute to these diseases.

This research may also have applications in combatting pathogenic fungi. There are numerous species of fungi that can infect the human body. *Candida albicans* is the most common human fungal pathogen, causing opportunistic infections in humans (Beck-Sague and Jarvis, 1993). *C. albicans* populates the gastrointestinal tract, and oral and vaginal mucosa of most people. For healthy individuals, and this does not generally pose a problem (Kim and Sudbery, 2011). However, in patients whose immune systems are compromised, as a result of diseases like AIDS, blood cancers, or the use of immunosuppressive therapies, *C. albicans*

infections can escape immune control, causing infection of the skin, infection of the mouth (thrush), infection of the throat (esophagitis), and infection of the bloodstream (candidimia). Even though anti-fungal treatments for *Candida* are available, once this pathogen has infected the bloodstream, it is fatal in more than 50% of cases (Andes et al., 2012). In healthy individuals, macrophages fight infections of this fungus by generating ingesting *C. albicans* cells and generating superoxide (Vazquez-Torres and Balish, 1997), so the oxidative stress response pathways of this fungus act as key virulence factors. A better understanding of how these pathways allow *Candida* to resist stress could be used to design new treatments for this pathogen.

While the human health implications for the research described in this thesis should not be belittled, these findings may also have relevance outside of the biomedical sphere. The production of beer, wine, and other alcoholic beverages depends on the efficient fermentation of sugars into alcohol by *S. cerevisiae*. In fact, the word "cerevisiae" comes from the Latin "of beer." Yeast are known to actively up-regulate oxidative stress response genes during beer fermentation (Higgins et al., 2003; James et al., 2003). Furthermore, the oxidation of compounds in the beer can have profound effects on the beer's flavor (Bamforth and Lentini, 2009; Vanderhaegen et al., 2006). Therefore, the beer industry actively researches the yeast oxidative stress response, seeking strains that have a strong oxidative stress response and that also secrete antioxidants that will prevent oxidation of compounds in the beer (Berner and Arneborg, 2012). The research described in this thesis regarding how yeast regulate their sugar metabolism and respond to oxidative stress may have important implications for helping to craft a better beer. While no beer made from genetically-modified yeast is currently sold commercially, this is likely

to change in the future, and genetic alterations that tinker with Rpd3(T) function may create a yeast strain that makes a better beer. Even without genetically engineering, screening wild yeast isolates for strains with altered levels of the proteins in this pathway, may lead to the discovery of exciting new beer strains. Lastly, understanding the environmental factors that contribute to Rpd3(T) mediated response may help brewers find small changes they can make to their beer-making procedures that can result in tastier outputs.

MATERIALS AND METHODS

Yeast strains and culture conditions

All *S. cerevisiae* strains used for this research are listed in Table M.1. With the exception of the strains used for sporulation assays, which were made on the SK1 background, all strains are isogenic to BY4741 or BY4742, which are derivatives of S288C. Transformation of yeast, culturing, media preparation, and general strain handling were all performed using the methods described in *Methods in Yeast Genetics* and the references therein (Amberg et al., 2005). The uracil plasmid pRS426 was transformed following a previously published protocol for yeast plasmid transformation (Elble, 1992). Where indicated in Table M.1, deletion strains come from the *S. cerevisiae* haploid nonessential genome deletion library (Winzeler et al., 1999), and all deletions were verified by PCR. Additional deletion strains were created by targeting the kanMX4 or hphMX4 antibiotic resistance cassettes to the genes of interest (Goldstein and McCusker, 1999; Wach et al., 1994). Yeast were cultured in either YPD (1% yeast extract, 2% peptone, 2% dextrose) or Synthetic Defined Media with Complete Supplement Mixture [SD CSM, 0.17% yeast nitrogen base without amino acids or ammonium sulfate, 0.5% ammonium sulfate, 0.079% complete supplement mixture (CSM, MP Biomedicals), 2% dextrose]. Cultures were grown at 30^{o}C with 200 rpm shaking.

Recombinant PHD Preparation

Yng1, Jhd2, and Ecm5 PHDs (amino acids 141-219, 221-300, and 1232-1295 of the full-length proteins, respectively) were cloned into pGEX-6P-1 (Amersham Pharmacia) which added an N-terminal gluthathione S-transferase (GST) tag. Constructs were transformed into BL21 *E.*

Table M.1 Yeast strains used in this research [a]

Strain	Genotype	Source
BY4741	MAT**a** *his3-1 leu2-0 met15-0 ura3-0*	Open Biosystems
BY4742	MATα *his3-1 leu2-0 lys2-0 ura3-0*	Open Biosystems
CDAY094	*MAT* **a** *his3-1 leu2-0 met15-0 ura3-0 set2 Δ::KanMX4*	Open Biosystems
CDAY120	*MAT* **a** *his3-1 leu2-0 met15-0 ura3-0 snt2 Δ::KanMX4*	Open Biosystems
CDAY121	*MAT* **a** *his3-1 leu2-0 met15-0 ura3-0 eaf3 Δ::KanMX4*	Open Biosystems
CDAY133	*MAT* **a** *his3-1 leu2-0 met15-0 ura3-0 ste11 Δ::KanMX4*	Open Biosystems
CDAY144	*MAT* **a** *his3-1 leu2-0 met15-0 ura3-0 cla4 Δ::KanMX4*	Open Biosystems
CDAY146	*MAT* **a** *his3-1 leu2-0 met15-0 ura3-0 hsl1 Δ::KanMX4*	Open Biosystems
CDAY150	*MAT* **a** *his3-1 leu2-0 met15-0 ura3-0 yap1 Δ::KanMX4*	Open Biosystems
CDAY183	*MAT* **a** *his3-1 leu2-0 met15-0 ura3-0 gpr1 Δ::KanMX4*	Open Biosystems
CDAY185[b]	*MAT* **a** *his3-1 leu2-0 met15-0 ura3-0 bar1 Δ::KanMX4*	This study
CDAY186[b]	*MAT* **a** *his3-1 leu2-0 met15-0 ura3-0 ecm5 Δ::KanMX4*	This study
CDAY187[b]	*MAT* **a** *his3-1 leu2-0 met15-0 ura3-0 ecm5 Δ::KanMX4*	This study
CDAY244	*MAT* **a** *his3-1 leu2-0 met15-0 ura3-0 jhd2 Δ::KanMX4*	Open Biosystems
CDAY246	*MAT* **a** *his3-1 leu2-0 met15-0 ura3-0 ecm5 Δ::KanMX4*	Open Biosystems
CDAY316	*MAT* **a** *his3-1 leu2-0 met15-0 ura3-0 bar1 Δ::KanMX4*	Open Biosystems
CDAY344	*MAT* **a** *his3-1 leu2-0 met15-0 ura3-0 SNT2-PrA::HIS3*	This study
CDAY345	*MAT* **a** *his3-1 leu2-0 met15-0 ura3-0 RPD3-PrA::HIS3*	This study
CDAY378	*MAT* **a** *his3-1 leu2-0 met15-0 ura3-0 rpd3 Δ::KanMX4*	This study
CDAY491	*MAT* **a** *his3-1 leu2-0 met15-0 ura3-0 chs3 Δ::KanMX4*	Open Biosystems
CDAY492	*MAT* **a** *his3-1 leu2-0 met15-0 ura3-0 gas1 Δ::KanMX4*	Open Biosystems
CDAY510	*MAT* **a** *his3-1 leu2-0 met15-0 ura3-0 ECM5-PrA::HIS3*	This study
CDAY507	MATα *his3-1 leu2-0 lys2-0 ura3-0 ecm5 Δ::HphMX4*	This study
CDAY508	MATα *his3-1 leu2-0 lys2-0 ura3-0 snt2 Δ::HphMX4*	This study
CDAY509	MATα *his3-1 leu2-0 lys2-0 ura3-0 rpd3 Δ::HphMX4*	This study
CDAY193	*MAT* **a** *his3-1 leu2-0 met15-0 ura3-0 bar1 Δ::KanMX4 ecm5 Δ::HphMX4*	This study
CDAY194	*MAT* **a** *his3-1 leu2-0 met15-0 ura3-0 bar1 Δ::KanMX4 ECM5-TAP::HIS3*	This study
CDAY512	*MAT* **a** *his3-1 leu2-0 met15-0 ura3-0 ECM5-13Myc::KanMX4*	This study
CDAY511	*MAT* **a** *his3-1 leu2-0 met15-0 ura3-0 SNT2-13Myc::KanMX4*	This study
SKY163	*MAT* **a** *ho::LYS2 lys2 ura3 leu2::hisG* (SK1 background)	Dr. Scott Keeney
SKY164	*MAT* α *ho::LYS2 lys2 ura3 leu2::hisG* (SK1 background)	Dr. Scott Keeney
SKY165	MAT**a**/MATα *ho::LYS2/ho::LYS2 lys2/lys2 ura3/ura3 leu2::hisG/leu2::hisG* (SK1 background)	Dr. Scott Keeney
CDAY513	*MAT* **a** *ho::LYS2 lys2 ura3 leu2::hisG ecm5 Δ::KanMX4* (SK1 background)	This study
CDAY514	*MATa ho::LYS2 lys2 ura3 leu2::hisG ecm5 Δ::HphMX4* (SK1 background)	This study
CDAY515	*MATa/MATα ho::LYS2/ho::LYS2 lys2/lys2 ura3/ura3 leu2::hisG/leu2::hisG ecm5 Δ::KanMX4/ecm5D::HphMX4* (SK1 background)	This study

[a] All strains are on the S288C background (isogenic to BY4741 or BY4742) except the indicated SK1 strains

[b] These additional *ecm5* and *bar1* knockout strains were used in Figure 3.7. With the exception of the sporulation experiments, all other experiments involving *ecm5* and *bar1* knockout strains were conducted with CDAY246 and CDAY316, respectively.

coli, and induced by adding isopropyl-β-D-thiogalactopyranoside (IPTG) (fc 0.2 mM) and incubating 15-20 hours. *E. coli* containing GST fusion proteins were lysed using sonication and lysates were purified using Glutathione Sepharose 4B (Amersham Pharmacia) following manufacturer's recommendations. The Yng1 W180E point mutation was created using QuikChange Site-Directed Mutagenesis Kit (Stratagene).

In vitro histone binding assays

To prepare histone acid extract, wild-type yeast were lysed by cryogenic lysis method (described below), and lysates were resuspended in 0.4 N H_2SO_4 and incubated for 30 minutes with rotation at 4°C. Acid-soluble histones were separated from insoluble pellet and precipitated with TCA. Binding assays were performed by mixing acid extracts from $5.5x10^8$ cell equivalents with 1 μg GST-tagged PHD finger or GST alone in binding buffer (150 mM NaCl, 20 mM HEPES pH7.9, 25% glycerol, 1.5 mM $MgCl_2$, 0.2 mM EDTA, 1 mM PMSF, 0.2% Triton X-100) for 1 hour at room temperature with nutation. Glutathione Sepharose 4B resin (Amersham Pharmacia – 25 μL) was then added and assays were nutated for 1 hour. Resin was washed 3 times with wash buffer (300 mM KCl, 20 mM HEPES pH 7.9, 0.2% Triton X-100) and one time in final wash buffer (4 mM HEPES pH 7.5, 10 mM NaCl). Reactions were separated on 12% SDS-PAGE gels, and transferred to PVDF membranes by dry transfer method. Antibodies used to probe membranes were: α-H3 (Abcam ab1791), α-H4 (Abcam ab10158), α-H2A (UBI ab07-146), α-H2B (UBI 07-371), α-H3K4me3 (Abcam ab8580), α-H3K4me2 (Abcam ab7766), α-H3K36me3 (Abcam ab9050), and α-GST (RPB1236, Amersham).

Peptide pull-down assay

High capacity streptavidin agarose (Thermo/Pierce) was washed 2x in PBS and mixed with excess amounts of the following peptides in PBS: H3(1-20), H3(1-20)K4me3, H3(27-46), and H3(27-46)me3. Peptides and resin were incubated 3 hours at room temperature, and washed 3x PBS with 1% Triton X-100, and 1x in PBS. For pull-downs, 20 μL 50% bead slurries were mixed with 10μg GST-tagged PHD or GST alone in peptide binding buffer [20 mM HEPES pH 7.9, 125 mM KCl, 0.1% Triton X-100, Complete Protease Inhibitor (Roche)] and incubated 2 hours at 4°C. Pull-downs were washed 3x in wash A [20 mM HEPES pH 7.9, 300 mM KCl, 0.1% Triton X-100], 1x in wash B [4 mM HEPES pH 7.9, 10 mM KCl], and eluted in boiling SDS-Loading Buffer. Elutions were separated on 4-20% Tris-Glycine Gels (Invitrogen) and stained with Coomassie.

***In vitro* translation and ubiquitylation assays**

PHD fingers from *S. cerevisiae* Ecm5 (amino acids 1210-1318 of the full-length protein), Snt2 (289-397 – PHD1, 1010-1125 – PHD2, and 1148-1279 – PHD3), Set3 (89-194), Yng1 (127-219), Jhd2 (227-313), Yng2 (200-282), Pho23 (252-330), Jhd1 (1-100), Set4 (132-238), Nto1 (235-341 – PHD1 and 345-469 – PHD2), Rco1 (232-337 – PHD1 and 386-500 – PHD2), Bye1 (44-162), Cti6 (44-151), Spp1 (1-100), and *S. pombe* Msc1 (1143-1248) were cloned into a pCS2^{+} vector with a 6-Myc tag and an SP6 promoter (Ben-Saadon et al., 2006). pCS2^{+}-Ring1B and pCS2^{+}Ring1B with the RING domain deletion were gifts from Ronen Sadeh. Cysteine point mutations were introduced using the QuikChange Site-Directed Mutagenesis Kit (Stratagene). *In vitro* translations were performed using the Promega Tnt SP6 High-Yield Wheat Germ

Protein Expression System per manufacturer's instructions with the following specifications: 250 ng plasmid were used, reactions were supplemented with ^{35}S methionine, and reactions were incubated at 30°C for 2 hours.

For ubiquitylation assays, translated PHDs or Ring1B were added to a reaction mix consisting of 40 mM Tris pH 7.5, 5 mM $MgCl_2$, 2 mM DTT, 2.5 μM ubiquitin aldehyde (Enzo Life Sciences), 5 μg recombinant ubiquitin (Sigma), 3 μM E2 enzyme, and 5 mM ATPγS (Roche), to a final volume of 10 μL and incubated at 30°C for 1 hour. Reactions and input translations were separated on 4-12% Bis-Tris gels (Invitrogen) which were dried and imaged using a phosphorimager. For experiments testing ubiquitin or E1 requirements, and E2 concentrations, reaction mixes were altered as indicated in the figures. Recombinant human UbcH13/Mms2 and hHR6A were purchased from Enzo Life Sciences, and recombinant human E1 was a gift from Jaehoon Kim from Robert Roeder's laboratory. For reactions with bacterial S30 system, PHDs (same amino acids listed above) were cloned into the pT7-7 vector (Tabor and Richardson, 1985), and translated using the S30 T7 High-Yield Protein Expression System (Promega) per manufacturer's instructions with the following modifications: 11 ng plasmid was used, and ^{35}S methionine was added to the translations which were incubated for 1 hour at 37°C.

Purification of Jhd2 interaction partners and Rpd3(T) complex

Yeast strains in were constructed containing a Protein A (PrA) tag (Aitchison et al., 1995) at the C terminus of Jhd2, Ecm5, Snt2, or Rpd3. Tagged strains as well as an untagged control strain, were grown in 10L batches to mid log phase. Cells were collected by centrifugation and

prepared for cryolysis as described previously (Oeffinger et al., 2007). Briefly, pellets were mixed with freezing solution [1.2% polyvinyvinylpyrrolidone (PVP), 20 mM HEPES pH 7.4, 10 mg/mL PMSF, 0.04 mg/mL pepstatin], in a ratio of 100 μL solution per mL of cell pellet. This mixture was frozen in small droplets in liquid nitrogen, and frozen cell droplets were stored at 80°C before lysis. For lysis, ~10g frozen cells at a time were milled in a Retsch PM100 Mill, using the 125 mL-sized chamber. Mill settings were 3 minute cycles at 400 rpm, switching directions at 1 minute intervals. Mill chamber and ball bearings were cooled in liquid nitrogen before milling, chamber was recooled in liquid nitrogen between 3 minute cycles. This was done for 8-12 total cycles, until very few intact cells were visible when samples of the lysate were viewed under the microscope.

Cryolysates from tagged strains or untagged control (20-30g each, depending in the IP, $34.5x10^{11}$ cell equivalents) were resuspended in IP Buffer [20 mM HEPES pH 7.4, 2 mM MgCl, 300 mM NaCl, 0.1% Triton X-100, 0.1% Tween-20, 110 mM potassium acetate, 0.1 mg/mL PMSF, 2 ug/mL pepstatin, 0.5% protease inhibitor cocktail for fungal and yeast cells (Sigma)] in a ratio of 25 mL of buffer to 5 g lysate. Recombinant DNase I was added (Roche, 30 units/g lysate), and lysates were rocked 10 minutes at room temperature. Lysates were then homogenized using a Polytron homogenizer on setting 4 for 10 seconds and centrifuged for 10 minutes at 2300 g to precipitate insoluble material. Buffer equilibrated, IgG-conjugated Dynabeads, made following the protocol of Cristea et al. (2005), were added to each clarified lysate (10 uL beads/g lysate), and IPs were incubated 1 hour at 4°C with nutation. IPs were washed 5 times in IP Buffer, and 2 times in IP Buffer lacking detergents. Samples were eluted by incubating twice in 0.5 N NH_4OH,

0.5 mM EDTA for 15 minutes at room temperature with agitation, and eluted samples were dried in a speedvac.

For the Ecm5-PrA IP, eluted proteins were reduced with dithiothreitol (DTT), alkylated with iodoacetamide, and separated on 1D SDS PAGE. Protein bands were stained with Gel Code Blue Stain Reagent (Thermo Scientific), and bands were excised for mass spectrometric identification. For the Snt2-PrA and Rpd3-PrA IPs, 5% of each elutate was analyzed by silver stain gel and 50% was reserved for mass spectrometry. The remaining Rpd3-PrA eluate was later separated on a gel and stained with Gel Code Blue. Stained bands on the gel were excised for additional mass spectrometric identification.

To confirm Rpd3 association with Ecm5, eluate from a separate, small-scale Ecm5-PrA IP was separated on a 4-20% Tris Glycine gel (Invitrogen), and transferred to PVDF membranes by wet transfer method. The membrane was cut in two and probed with the antibodies that recognize the PrA tag (rabbit-α-goat-IgG-HRP secondary antibody, Dako P0160) or Rpd3 (sc6654, Santa Cruz Biotechnology).

Mass spectrometric identification of immunoprecipitated proteins

For the Ecm5-PrA and untagged control IPs, excised bands were destained with 50% methanol in 100 mM ammonium bicarbonate. The gel bands were dehydrated and digested overnight at room temperature in 100 mM ammonium bicarbonate with 50 ng sequencing-grade modified trypsin (Promega). The digestion was stopped and the tryptic peptides extracted by adding

an aqueous solution of 5% formic acid, 0.2% trifluoroacetic acid (v/v) and reverse phase resin (POROS 20 R2, Perseptive Biosystems). After light shaking at 4°C for 4 hours the resin was washed with 0.5% acetic acid and the bound peptides were eluted with 40% acetonitrile followed by elution with 80% acetonitrile in 0.5% acetic acid. The eluents were combined and concentrated in a speedvac.

The concentrate was pressure-loaded onto a nano-HPLC column with integrated 15μm emitter (360 x 75 μm PicoTip emitter, New Objective) packed with 6 cm of 5μm C18 beads (YMC ODS AQ). The peptides were eluted with a linear gradient of 0-40%B in 50 min and 40-100%B in 70 min (A = 0.1M acetic acid, B = 70% acetonitrile in 0.1M acetic acid) using an Agilent 1100 binary HPLC and analyzed on a Finnigan LTQ-XL mass spectrometer (Thermo Fisher) equipped with a nano-HPLC microelectrospray ionization source. The mass spectrometer was operated in a data dependent mode were one full scan mass spectrum was followed by 10 collision activated dissociation (CAD) mass spectra of the 10 most abundant ions. The fragmented ions were set on an exclusion list for 40 s and the cycle repeated throughout the data acquisition. The resulting spectra were searched against the *Saccharomyces cervisiae* database using the search program X! tandem.

For Snt2-PrA, Rpd3-PrA, and control IPs, after elutions were dried by speedvac, samples were resuspended in 100 mM ammonium bicarbonate, reduced and alkylated (same procedure as for the gel) and digested with trypsin for 8 hours at 37°C digested overnight. The digestion was stopped by acidifying the solution with glacial acetic acid. The solution was pressure loaded

onto self-packed pre columns (360x75 um), rinsed with 0.5% acetic acid to remove salt and butt-connected to the nano-HPLC column. Peptides were separated, eluted and identified as described above. For further validation of the Rpd3-PrA IP results, the remaining 50% of this IP was treated as described for the Ecm5-PrA IP, with focus on excising the bands corresponding in molecular weight to Ecm5 and Snt2.

Plate spotting assays

YPD, SD CSM, or SD CSM-URA media containing 2% agar was autoclaved, media was allowed to cool to approximately 60^{o}C, and supplements were added to the final concentrations indicated in tables and figures. Saturated overnight cultures (for spotting assays in Chapters 3 and 5) or exponentially-growing mid-logarithmic (mid-log) phase cultures (for assays in Chapter 4) were diluted to 5x10^{6} cells/mL in YPD, and this was diluted 1:5 in YPD 4 more times, for a total of 5 serial dilutions. 4 μL of each dilution were spotted onto control or treated plates, which were incubated at 30^{o}C (unless otherwise indicated) for 2-5 days, and imaged once spots or colonies were clearly visible.

Rapamycin, 6AU (6-azauracil), calcofluor white (fluorescence brightener 28), caffeine, MMS (methyl methanesulfonate), benomyl (methyl 1-(butylcarbamoyl)-2-benzimidazolecarbamate), BCS (bathocuproinedisulfonic acid), and BPS (bathophenanthroline disulfonate) were purchased from Sigma-Aldrich. HU (hydroxyurea) was purchased from Acros. Camptothecan was purchased from Calbiochem/EMD chemicals. Hygromycin B was purchased from Invitrogen, and H_2O_2 was purchased from Fisher.

Yeast RNA Preparation

For RNA preparations, wild-type and knockout strains were grown to mid-log phase in YPD, and harvested by centrifugation followed by flash freezing in liquid nitrogen. Cells were stored at 80^{o}C before RNA was prepared. RNA was extracted using hot acid phenol, as previously described (Collart and Oliviero, 2001). RNA quality was assessed using the Nanodrop spectrophotometer (Thermo Scientific), by measuring the 260 nM wavelength absorption, by checking for a clean peak of absorption, and by ensuring that the 260nm/280 nM ratio was >1.8. RNA was also assessed by separation on formaldehyde agarose gels followed by ethidium bromide staining to examine rRNA bands for degradation. For qPCR, total RNA was treated with DNase I (Ambion). For northern blots, Poly-A^{+} RNA was enriched from total RNA using an Oligotex mRNA kit (Qiagen).

For RNA-sequencing experiments, wild-type, *ecm5*Δ, and *snt2*Δ yeast strains were grown in YPD to mid-log phase (~1x10^{7} cells/mL), at which point 40 mL of each strain were separated, centrifuged to isolate cells, and flash frozen. H_2O_2 was added to each culture to a final concentration of 0.4 mM, and cultures were harvested 0.5 and 4 hours later. Cells were stored at 80^{o}C before RNA was prepared as described above.

Reverse transcription and quantitative PCR-based expression analysis

DNase I treated RNA was converted to cDNA using the Superscript III First Strand Synthesis Kit (Invitrogen), following manufacturer's instructions. For quantitative PCR (qPCR) assays in Chapter 3, random hexamers were used to prime cDNA formation, while oligo dT was used to

prime the cDNA used for the qPCRs in Chapter 4. Reverse transcribed cDNA was then used in qPCR reactions with SYBR Green reagent (Applied Biosystems), and incorporated fluorescence was measured either on a Strategene Mx3000p Instrument (for qPCR assays in Chapter 3) or on an Applied Biosystems StepOnePlus Real Time PCR System(for qPCR assays in Chapter 4). Primers for all qPCR reactions are listed in Table M.2. Dilutions of pooled cDNAs were used to generate standard curves for each primer set, and qPCR reactions were quantitated based on comparison to the standard curve, and normalized to the relative expression of *ACT1*. All expression experiments were done with three biological replicates.

Northern blots

1 μg of poly-A^+-enriched RNA from each strain was separated on a formaldehyde agarose gel and transferred to Hybond membrane (GE Healthcare) using capillary transfer, after denaturing gel in 0.05 N NaOH for 30 minutes and neutralizing in 0.1 M Tris-HCl pH7.5 for 30 minutes. After UV-crosslinking RNA to the membrane, the membrane was incubated on top of boiling water for 1 minute, and incubated in prehybridization solution (50% formamide, 10% dextran sulfate, 1M NaCl, 0.05M Tris HCl pH 7.5, 0.1% SDS, 0.1% sodium pyrophosphate, 0.26% polyvinylpyrolidone, 0.26% BSA, 0.26% Ficoll, 0.33 mM EDTA, and 500 μg/mL boiled ssDNA) for 42°C for 6 hours. Membrane was then incubated in hybridization solution (50% formamide, 10% dextran sulfate, 1M NaCl, 0.05M Tris HCl pH 7.5, 0.1% SDS, 0.1% sodium pyrophosphate, 0.2% polyvinylpyrolidone, 0.2% BSA, 0.2% Ficoll, 0.25 mM EDTA, and 500 μg/mL boiled ssDNA) containing boiled radiolabeled probe, at 42°C for 20-24 hours. The membrane was washed 2x in 2X SSC for 15 minutes at room temperature, 2x in 2X SSC, 0.5% SDS at 65°C for 30 minutes, and 2x in 0.1X SSC for 30 minutes, and was then imaged using a phosphorimager.

Table M.2 Primers used for expression qPCRs, ChIP qPCRs, and northern blotting

Primer target	Forward sequence (5'-3')	Reverse sequence (5'-3')	Use
STE11 ORF 5' end	AGGGCACTGACTTACTAATTGGTGACGA	GCACTGAATAAAGCTATCCAGGTATTGAGTG	Expression qPCR
STE11 ORF 3' end	TGGTCTACAGGATGTGTTGTCATTGAAATG	TGTGCCTATTTTGAAGATCGCTTGC	Expression qPCR
STE11 3' UTR	CCTAGTGCCCTTGAATTGCTGCA	GGCCAGAGCACTTTAGTGCCATAAAA	Expression qPCR
SPB4 ORF 5' end	AGGACAGGACTCGATGTTATGGGTTTT	ATCAACTACTACATCCTTGTTGCCAGCA	Expression qPCR
SPB4 ORF 3' end	AGCGTGGTCAGATAAAACATTGACGAA	CGAGCTCTTCTGCTTTCAATTCTTCCTCTAT	Expression qPCR
SPB4 3' UTR	AAAGCTATCCAAGGCAATTTTGACGAC	CACTATGATGCTACAAGATCATCCATTGGT	Expression qPCR
FIT1 ORF	GGCGAAAGTATTACTACTACGATAACTGCTA	CCTTCTCCTGCCCAGACAAAAGT	Expression qPCR
ECM5 ORF	GCGGAGTGCTGTAATTCCTACTTCA	GTTTCAGGTGCAAACGGTGCTG	Expression qPCR
SNT2 ORF	CCTGCTGGCGAGCCTTATTATGTT	TTAGCAGGGAAGACCGATGTTGTC	Expression qPCR
CYC3 ORF	GGCCCTCCGTAGAAATCCAAGACGTATC	CAAGAACTACCATTCGACAGGCACGACT	Expression qPCR
SSA3 ORF	CCTAATCGTTCTATCAACCCGGATGAGG	TAGGGACAATGGCGCAACATCCAATAAT	Expression qPCR
POT1 ORF	AAAGGATCAAGACGAGTTCGCTGCG	CCCTTCGTCCGACTGGCAAATTGAG	Expression qPCR
BNR1 ORF	GAGATGTTTTGTAAATTCTTATAAGCAGCCCCC	TAATCCGAAGTGCATGCCTCAGGAC	Expression qPCR
IPI3 ORF	CCCGTGACAGATTTCCAAGTTTCTTCTAGTC	GCCTTCTGCTTCTTTTTGCTGCCTATTAAAC	Expression qPCR
YNL181W ORF	ACCCCATGGTTCCATATCACCGGAC	TGTGATTTGAGCAATTTGTGGGAGATTCGT	Expression qPCR
MSN1 ORF	AGCAGCAACTCTTCTCAATCACGGCAGTCTCCT	ACTGTTCCTCCTCAAATGTCGGCACGCTCTC	Expression qPCR
TRX2 ORF	TGACGCTGCTTTTTACAAGTTGGATGT	GACTCTGGTAACCTCCTTACCGCCC	Expression qPCR
HSP12 ORF	GTGTCCACGACTCTGCCGAAAAAGG	CGACGGCATCGTTCAACTTGGACTT	Expression qPCR
MAE1 ORF	CCCAGGTATCGGTTTAGGTGCCGTA	AGGTCTCGAGTCGCCCTCTCTTAGT	Expression qPCR
GAL7 ORF	CCAAATGGTGAAGGAGGACCTCGCCTCG	TCACCAGTCGCATTCAAAGGAGCCTGATGGA	Expression qPCR
GAL10 ORF	GGCCAAACGCGAACTGAAATGGCAGACCG	GCGGAAAATCTGGCCTCGACACCCCT	Expression qPCR
YAP1 ORF	GCGATGATGTACTCCCATTCATATCCGAGTCAC	AGGCTGGGATTGGTGTTAGAGGCAGCA	Expression qPCR
ERG6 ORF	ACCGGGTGGTACCTTTGCTGTTTACGAATGG	ACGTCGACATGGAACATCTTTGGGATACCATCA	Expression qPCR
EXG1 ORF	TGGACGATGATCCTTATGTTAGCGGCCTACA	AACCCGTTCTGCGAACCAGCGGCAC	Expression qPCR
ACT1 ORF	GTGCTGTCTTCCCATCTATCGTCG	TTGAGCTTCATCACCAACGTAGGAG	Control for all qPCRs
YAP1/ERG6 promoter	GTCTGCTCCTCACTTACTCTCGCTTCTCG	CCCGATCTTCGTATATGGTACCTCGTTCCCG	ChIP qPCR
CYC3 promoter	CCCACGCCGCGCAAGAGATA	ACACTGCGACAAAAGTGTGACCGA	ChIP qPCR
IPI3 promoter	AGAGTGATGATTTGATAGCGCCATTCTACA	TGGGCATCGATTTAAAATTTTCATTTAGTGGGA	ChIP qPCR
STE11 ORF 3' end	ATGGAACAGACACAAACAGC	GCGTGGCAAATAGTGACTAATTC	Northern probe
SPB4 ORF 3' end	GTGGTCAGATAAAACATTGACGAAAGAACG	GTCAAAATTGCCTTGGATAGCTTTGCTG	Northern probe
ACT1 ORF	CGGTTCTGGTATGTGTAAAGCCG	CCTTGATGTCACGGACAATTTCTC	Northern control probe

Double-stranded northern probes designed to hybridize to the 3′ ends of *STE11* and *SPB4* (bases 1641-2153 and 1604-1812, respectively, relative to the ATG start codon) were amplified by PCR from genomic DNA. A probe for *ACT1* (bases 36-640) was used as a loading control. Probes were radiolabeled using the RadPrime DNA Labeling System (Invitrogen), by incubating PCR fragments with Klenow, random hexamers, dATP, dGTP, dTTP, and 32P-dCTP overnight at room temperature.

Yeast whole cell extract preparation and immunoblotting

The indicated strains were grown to mid-log phase in YPD at 30^{o}C, and either harvested or treated as indicated in the text and then harvested by centrifugation. Whole cell extracts were prepared by resuspending cells in 20% TCA, adding glass beads (425-600 μM, Sigma), and bead beating in a Mini Bead Beater (Biospec Products). Extracts from 1x10^{7} cell equivalents were separated on 4-20% Tris Glycine gels (Invitrogen), and transferred to PVDF membranes by wet transfer method (300 mAmp, 90 minutes). Antibodies used to probe membranes were: α-Cdc2 (sc-53, Santa Cruz Biotechnology), α-Cdc2 Y19 phos (#9111S, Cell Signalling), α-H4 (ab10158, Abcam), α-H3S10p (12261), α-TAP (CAB10001, Open Biosystems), α-H4K16ac (#39167, Active Motif), α-H3 (ab1791, Abcam), α-β-Tubulin (T5201, Sigma). Membranes washed, incubated with secondary antibodies (swine-α-rabbit-IgG-HRP, Dako P0399 sheep-α-mouse-IgG-HRP, GE Healthcare NA931; and rabbit-α-goat-IgG-HRP, Dako P0160), incubated with Immobilon Western Chemiluminescent HRP Substrate (Millipore), and imaged with a Fujifilm LAS3000 Camera.

For immunoblot analysis of tagged protein levels before and after H_2O_2 treatment, Ecm5-PrA or Snt2-PrA yeast strains were inoculated into YPD and grown 5 hours until they were in mid-log phase, at which point samples were taken for the 0 hour timepoint. H_2O_2 was then added to a final concentration of 0.4 or 0.5 mM (as indicated in figures), and cells were harvested 2 hours, 4 hours, and 6 hours later. In one experiment an untagged strain was used as a control, while in another, the Ecm5-PrA strain was grown but treated with water as a control. For immunoblot analysis of stationary phase yeast, untagged, Ecm5-PrA, Snt2-PrA, and Rpd3-PrA strains were inoculated into YPD. Cultures were allowed to grow for 7 days, and cells were harvested at the times indicated in Figure 4.10. Whole cell lysates were obtained and immunoblots performed as described above.

Yeast cell cycle analysis

Cultures of *bar1*Δ, *ecm5*Δ *bar1*Δ, and *ECM5-TAP bar1*Δ strains were grown to mid-log phase in YPD, and synchronized using α-factor, which was purchased from GenScript, using a previously published protocol (Amberg et al., 2005). Synchronies were monitored in the microscope, to look for very few or no budded cells and shmoo formation. Synchronized cells were collected by centrifugation, washed in pre-warmed media, and resuspended in fresh media to release cells from arrest. Samples were taken every 20 minutes for fluorescence activated cell sorting (FACS) analysis, or every 10 minutes for immunoblot analysis. For the latter, whole cell extracts were obtained and immunoblots performed as described above. Cells taken for FACS analysis were fixed in 67% ethanol overnight and prepared for FACS using the SYTOX Green (Molecular

Probes) DNA-binding dye as following a previously published protocol (Haase, 2004). FACS was performed in the Rockefeller University Flow Cytometry Resource Center. A FACSCalibur instrument (BD Biosciences) was used to collect the data, using the 488 nM laser for excitation and the FL2 detector.

Sporulation assays and spore analysis

For sporulation analysis, the *ECM5* gene was deleted from wild-type haploid MAT***a*** and MATα SK1 background strains (strains SKY163 and SKY164, respectively – gifts from Scott Keeney), generating MAT***a*** *ecm5*Δ*::kanMX4* and MATα *ecm5*Δ*::hphMX4*. These two strains were mated to make an ecm5Δ/Δ diploid strain. The wild-type diploid SK1 strain (165) and the *ecm5*Δ/Δ diploid strain were struck on YPG (YP Glycerol) just prior to sporulating to ensure their respiratory competence. Cells were then patched onto YPD plates and incubated overnight at 30°C. Cells were transferred to sterile 1% potassium acetate solution, and incubated at 30°C for 3 days. The number of tetrads was divided by the total number of tetrads and diploid cells (based on hemocytometer counting) to determine the percent sporulation for each strain. More than 500 cells or tetrads were counted per strain, for 3 independent wild-type replicates and 4 independent *ecm5*Δ/Δ replicates.

For tetrad dissections, tetrads were collected by centrifugation, resuspended in 0.05 mg/mL zymolyase 10T (US Biological) in 1M sorbitol, and incubated at 30°C for 20 minutes with nutating to digest the ascospore. Digested tetrads were diluted 1:25 and placed on ice. 10 μL of digested tetrads were dripped down the middle of a YPD plate, and an Axioscope 40 microscope

fitted with an Axioscope Tetrad Manipulation System (Zeiss) was used to dissect individual tetrads onto clean sections of the plate. Plates were incubated at 30°C and imaged after 2 days. Plates were then replica-plated onto YPD-G418 and YPD-Hygromycin plates to select for individual *ecm5* knockout alleles. Selection plates were grown overnight at 30°C and imaged the next day.

Determination of doubling times

YPD or SD CSM cultures were inoculated with each strain, and allowed to grow at least 5 hours to mid-log phase. Samples of each culture were taken each hour for at least 8 hours and analyzed using the Beckman Coulter DU800 Spectrophotometer to determine optical densities at 600 nm (OD600s). For each culture, optical densities were plotted as a function of time in Excel, and an exponential trendline ($y=ae^{bx}$) was fitted to the curve, where y is OD600 and x is time. The doubling time was then determined by taking ln(2)/b, based on the following derivation:

The formula for exponential growth is $C_2 = C_1 * 2^{(x/D)}$, where C_1 is the initial concentration of cells, C_2, is the final concentration of cells, x is the time in culture, and D is the doubling time. If $e^{\ln 2}$ is substituted for 2, the equation becomes: $C_2 = C_1 * e^{(x*\ln 2/D)}$, which is in the same form as the exponential trendline. From this, b=ln 2/D, and therefore, D=ln 2/b.

Doubling times were determined for 3 independent cultures and then averaged.

H_2O_2 survival assays

Wild-type, *ecm5*Δ, *snt2*Δ, or *rpd3*Δ yeast strains were inoculated into YPD and grown to mid-log phase. An aliquot of each culture was taken, and the cell concentrations were determined by taking OD600 spectrophotometer readings and comparing to a previously determined standard curve relating OD600 readings and cells/mL measured on a hemocytometer. Aliquots were diluted in YPD to 1667 cells/mL, and 6 x 100 μL of each aliquot were plated on YPD (167 cells per plate, 1000 cells total). H_2O_2 was then added to each culture to a final concentration of 0.4 mM, and cultures were put back in the 30°C shaking incubator. 4 hours after H_2O_2 addition, another aliquot was taken, diluted, and plated as described above. After 2 days, the number of viable colonies on each plate was counted, and for each culture, the number of viable cells at the 4 hour timepoint was divided by the number of viable cells before H_2O_2 addition, to determine percent survival. Three independent replicates were performed for each strain, and the percent survival values were averaged across replicates.

Chromatin immunoprecipitation

For the H_2O_2 ChIP-sequencing experiments, cells for sequencing, Ecm5-Myc, Snt2-Myc, and an untagged control strain (BY4741) were inoculated into 1.5L YPD cultures, and grown to mid-log phase (~$2x10^7$ cells/mL). From each culture, 400 mL were separated and fixed by adding formaldehyde to a final concentration of 1%, shaking at room temperature for 20 minutes, and adding glycine to a final concentration of 125 mM to quench. Cells were then centrifuged, washed 4 times in cold PBS, and flash frozen in liquid nitrogen. H_2O_2 was added to the remaining culture to a final concentration of 0.4 mM, and 0.5 and 4 hours after H_2O_2 addition, cells were fixed and harvested as described above.

ChIP was performed essentially as described (Aparicio et al., 2005)B, with the following modifications. Cells were resuspended in lysis buffer (50 mM HEPES pH 7.5, 1 mM EDTA, 140 mM NaCl, 1% Triton X-100, 0.1% sodium deoxycholate, 1 mM PMSF, 5.8 μM pepstatin, and 0.5 μg/mL leupeptin) to a final concentration of $4x10^9$ cells/mL and lysed by bead beating with zirconia-silica beads (Biospec Products), alternating between 3 minutes in the bead beater and 1 minute on ice, for 10 cycles. Lysates were then sonicated in 1 mL aliquots using a Bioruptor Sonicator, set on high, cycling between 30 seconds on and 30 seconds off for 100 minutes total time. After sonication, DNA was purified from an aliquot of each sample and run on an agarose gel to ensure DNA was sheared to between 150 and 400 bp.

Chromatin from identical samples was pooled, and 16 μg monoclonal Myc 9E10 antibody (#05-419, Millipore) were added to each sample. Samples were incubated 16 hours at 4°C with rotation. The next day, 160 μL of Magna ChIP Protein G magnetic beads (Millipore) were used to IP each sample. After washing, crosslinks were reversed, and input and IP DNA were purified over Qiagen PCR purification columns and eluted in 25 μL Tris pH 8.0. Purified DNA was incubated with 30 μg RNase A for 3 hours at 37°C (Fisher Scientific), purified over a second Qiagen column with 25 μL elution, and 5 μL of the elution was saved for qPCR analysis. The remaining 20 μL of each sample were used to build sequencing libraries. Small-scale ChIPs were performed similarly except that $1x10^9$ cells, 2 μg anti-Myc antibody, and 20 μL Protein G beads were used per ChIP.

For ChIP-seq of rapamycin treated samples, Ecm5-Myc, Snt2-Myc, and an untagged control strain (BY4741) were inoculated into 2L SD CSM cultures, and grown to mid-log phase (~$2x10^7$ cells/mL). For the 0 hour timepoint, 450 mL of each culture were taken and fixed as described. Cultures were split into two flasks, one that received DMSO, and one that received rapamycin (final concentration 100 nM). After 0.5 hours, 450 mL of each culture were taken and fixed, and 4 hours after rapamycin addition, 250 mL of each culture were taken and fixed. ChIPs were performed as described above.

Preparation of samples for sequencing and sequencing

ChIP sequencing libraries were prepared using a TruSeq DNA sample prep (Illumina), following manufacturer's instructions, except that lower concentrations of TruSeq adapters were used: 8% of the recommended adapter concentration was used with the H_2O_2 ChIP samples, because the amount of DNA in these samples was expected to be much lower than the recommended started amount, since the kit is designed for making libraries out of genomic DNA. For the rapamycin ChIP samples, 3.2% of the recommended adapter concentration was used, because the 8% used for the H2O2 library preparations still created dimers that were detectable after the amplification step. For the final amplification step, 20 cycles of PCR were used for the H_2O_2 -treated samples and 21 cycles for the rapamycin-treated samples. Samples of each library were analyzed by agarose gel to assess library size distribution and quality.

RNA sequencing libraries were prepared from 4 μg total RNA using a TruSeq RNA sample prep (Illumina) per manufacturer's instructions. For the final amplification step, 15 cycles of PCR were used.

All libraries were validated using the nanodrop spectrophotometer, to check concentration and for a clean peak, and using an Agilent Bioanalyzer to more accurately determine size and quantity of DNA in libraries. As a final verification, qPCR was purified on an aliquot from the final libraries, using primers to the *CYC3* promoter, which is a previously reported Snt2 ChIP target (Harbison et al., 2004), to ensure that DNA from this region is enriched in ChIP libraries relative to input libraries. Libraries were sequenced on an Illumina HiSeq 2000 at the Rockefeller University Genomics Resource Center.

Alignment and analysis of sequencing data

Reads from ChIP-seq experiments were aligned to the *S. cerevisiae* genome (SacCer2) using the Bowtie alignment software (Langmead et al., 2009). Unique reads that mapped to a single location with no more than two mismatches were kept and used to generate genome-wide distributions of Ecm5 or Snt2 binding and for peak identification.

The Galaxy server (https://main.g2.bx.psu.edu/) was used for a much of the sequencing data analysis. The software MACS, which was run off the Galaxy server, was used to identify peaks in the Ecm5 and Snt2 ChIP and input datasets using the time-matched ChIP from the untagged strain as a control (Zhang et al., 2008). Peaks identified in the ChIP samples that were also identified in the inputs were discarded. Peaks that were shared between Ecm5 and Snt2 were determined by asking the Intersect program on the Galaxy server to return genomic intervals where the intervals defining Ecm5 and Snt2 peaks overlapped by at least 200 bp. In cases where the number of peaks differed depending on whether Ecm5 or Snt2 was the first dataset (e.g.

places where 1 Ecm5 peak encompasses a region of the genome that contains two Snt2 peaks), the intersected list with the lower number of peaks was used. A list of yeast genes was obtained from the UCSC Genome Browser (http://genome.ucsc.edu/). Yeast promoter regions were defined by asking the Get Flanks program on Galaxy to return the 500 bp upstream of the start codon of each yeast gene. The Intersect program was then asked to return the names of genes whose promoter regions overlapped with shared Ecm5/Snt2 peaks by at least 200 bp. These genes were then used for functional gene ontology analysis using the FuncAssociate program (Berriz et al., 2009). For the transcription start site (TSS) analysis, the TSS's of all genes were taken from the UCSC Genome Browser. TSS profiles were generated using a custom script that divides each gene into 50 bp windows surrounding the TSS, and counts the average number of reads at all genes within those windows per million mapped reads. This analysis was repeated with the top 100 most highly expressed yeast genes, taken from a separate study (Miller et al., 2011).

Reads from RNA-seq experiments were aligned to the *S. cerevisiae* genome using the software TopHat (Trapnell et al., 2009). The Cufflinks and Cuffdiff software were then used to generate expression values for each gene in each sample and ratios of expression for genes between samples (Trapnell et al., 2010). These programs were all executed from the Galaxy server. The heatmap was generated using a custom clustering script.

Competitive Fitness Assays

Wild-type, *ecm5*Δ, and *snt2*Δ strains were patched onto YPD and grown overnight at 30°C. These cells were then used to inoculate precultures in SD CSM media, which were grown overnight at 30°C. The next morning, OD600 spectrophotometer readings of dilutions of the precultures were used to determine cell concentrations. Equal numbers of wild-type and *ecm5*Δ or *snt2*Δ cells were inoculated into SD CSM media, such that each culture started out with $2x10^5$ cells/mL total. After inoculating, aliquots of each culture were taken, diluted and plated on YPD or YPD G418, aiming for approximately 120 cells per plate with 6 YPD plates and 6 YPD G418 plates per culture. After 12 hours, aliquots of each culture were taken, diluted, and plated as described above. After 24 hours in culture and each subsequent day, OD600 readings were used to determine the cell concentration in each culture, cultures were diluted to $2x10^5$ cells/mL in fresh SD CSM media, and aliquots were taken, diluted, and plated as described above. The dilution of cultures with fresh media each day ensured that the experiment tested competitive fitness and not just which strain had longer chronological lifespan. For each set of plates, 2 days after plating, colonies were counted, and for each culture, the number of colonies on the YPD G418 plates (which was proportional to the number of knockout cells in culture) was divided by the number of colonies on the YPD plates (which was proportional to the total number of cells in culture). Three wild-type vs. *ecm5*Δ competitions and three wild-type vs *snt2*Δ competitions were performed, and results from replicates were averaged.

APPENDIX: SUMMARY OF SEQUENCING DATA

Table A.1 Summary of H_2O_2 ChIP Sequencing Experiment

Tagged Protein	Hours in H2O2	Sample Type	Total reads	Mapped reads	Unique mapped reads
Ecm5	0	Input	28,295,702	15,273,967	5,643,276
Ecm5	0.5	Input	22,909,380	13,151,691	5,561,167
Ecm5	4	Input	39,727,733	20,848,784	6,740,075
Snt2	0	Input	27,365,600	15,357,724	5,739,398
Snt2	0.5	Input	42,683,503	24,516,988	7,063,753
Snt2	4	Input	34,116,437	17,555,329	5,347,058
no tag	0	Input	31,822,746	17,370,972	5,008,902
no tag	0.5	Input	34,006,523	21,111,301	6,208,824
no tag	4	Input	28,407,276	14,296,990	4,472,443
Ecm5	0	ChIP	21,760,477	5,212,692	2,402,615
Ecm5	0.5	ChIP	6,867,046	2,375,846	1,633,360
Ecm5	4	ChIP	15,077,789	4,506,079	2,691,366
Snt2	0	ChIP	16,155,488	4,304,928	2,378,090
Snt2	0.5	ChIP	15,547,676	5,260,090	2,909,979
Snt2	4	ChIP	11,013,555	3,749,991	2,500,991
no tag	0	ChIP	7,347,106	371,969	206,204
no tag	0.5	ChIP	6,097,041	457,695	308,474
no tag	4	ChIP	6,552,081	701,401	386,352

Table A.2 Summary of H_2O_2 RNA Sequencing Experiment

Strain	Hours in H2O2	Replicate	Total reads[a]
wild-type	0	1	20,656,926
wild-type	0	2	17,782,762
wild-type	0	3	19,447,488
ecm5 Δ	0	1	21,309,201
ecm5 Δ	0	2	15,599,524
ecm5 Δ	0	3	27,143,791
snt2 Δ	0	1	17,136,385
snt2 Δ	0	2	10,737,589
snt2 Δ	0	3	11,835,765
wild-type	0.5	1	20,072,162
wild-type	0.5	2	17,891,568
wild-type	0.5	3	17,272,990
ecm5 Δ	0.5	1	22,524,310
ecm5 Δ	0.5	2	18,952,106
ecm5 Δ	0.5	3	18,422,551
snt2 Δ	0.5	1	12,780,970
snt2 Δ	0.5	2	13,573,158
snt2 Δ	0.5	3	18,808,481

[a] Unlike the ChIP-seq reads, the RNA-seq reads were allowed to map to more than one location in the genome. Therefore, the number of mapped reads for each sample was larger than the number of reads, and was not included in this table

Table A.3 Summary of Rapamycin ChIP Sequencing Data

Tagged Protein	treatment	Hours in treatment	Sample type	Total reads	Mapped reads	Unique mapped reads
Ecm5		0	Input	15,156,256	11,242,797	2,781,458
Ecm5	DMSO	0.5	Input	6,650,029	5,582,798	1,880,298
Ecm5	Rap	0.5	Input	7,709,035	6,115,675	1,925,375
Ecm5	DMSO	4	Input	10,009,578	8,058,697	1,822,179
Ecm5	Rap	4	Input	18,399,901	13,750,794	2,297,172
Snt2	before	0	Input	10,978,718	7,929,728	2,292,978
Snt2	DMSO	0.5	Input	5,554,268	3,949,078	766,241
Snt2	Rap	0.5	Input	7,219,758	5,585,895	723,114
Snt2	DMSO	4	Input	10,250,674	7,932,152	2,261,611
Snt2	Rap	4	Input	23,088,457	18,351,090	2,389,241
no tag	before	0	Input	15,829,166	12,463,596	4,221,696
no tag	DMSO	0.5	Input	21,238,322	17,644,124	3,458,614
no tag	Rap	0.5	Input	11,486,058	8,743,609	2,771,713
no tag	DMSO	4	Input	16,429,834	13,334,911	4,537,281
no tag	Rap	4	Input	23,362,487	19,146,996	4,387,226
Ecm5	before	0	ChIP	11,539,682	8,242,984	1,867,189
Ecm5	DMSO	0.5	ChIP	9,216,471	6,832,224	2,481,197
Ecm5	Rap	0.5	ChIP	9,637,442	6,788,133	2,295,274
Ecm5	DMSO	4	ChIP	18,335,359	11,867,038	2,863,849
Ecm5	Rap	4	ChIP	15,827,557	11,728,158	1,829,553
Snt2	before	0	ChIP	8,676,488	6,624,246	754,857
Snt2	DMSO	0.5	ChIP	6,725,151	5,317,231	1,150,591
Snt2	Rap	0.5	ChIP	10,861,435	8,651,576	1,117,058
Snt2	DMSO	4	ChIP	18,408,953	14,177,116	3,673,604
Snt2	Rap	4	ChIP	19,785,498	15,328,696	3,757,861
no tag	before	0	ChIP	6,352,112	3,101,839	244,293
no tag	DMSO	0.5	ChIP	11,586,362	6,514,316	411,755
no tag	Rap	0.5	ChIP	5,778,491	2,595,547	396,846
no tag	DMSO	4	ChIP	7,176,745	2,839,710	263,942
no tag	Rap	4	ChIP	6,722,864	795,893	79,603

REFERENCES

Abate, G., Bastonini, E., Braun, K.A., Verdone, L., Young, E.T., and Caserta, M. (2012). Snf1/AMPK regulates Gcn5 occupancy, H3 acetylation and chromatin remodelling at S. cerevisiae ADY2 promoter. Biochim Biophys Acta *1819*, 419-427.

Adegbola, A., Gao, H., Sommer, S., and Browning, M. (2008). A novel mutation in JARID1C/SMCX in a patient with autism spectrum disorder (ASD). Am J Med Genet A *146A*, 505-511.

Ahn, S.H., Diaz, R.L., Grunstein, M., and Allis, C.D. (2006). Histone H2B deacetylation at lysine 11 is required for yeast apoptosis induced by phosphorylation of H2B at serine 10. Mol Cell *24*, 211-220.

Ahn, S.H., Henderson, K.A., Keeney, S., and Allis, C.D. (2005). H2B (Ser10) phosphorylation is induced during apoptosis and meiosis in S. cerevisiae. Cell Cycle *4*, 780-783.

Ai, X., and Parthun, M.R. (2004). The nuclear Hat1p/Hat2p complex: a molecular link between type B histone acetyltransferases and chromatin assembly. Mol Cell *14*, 195-205.

Aitchison, J.D., Rout, M.P., Marelli, M., Blobel, G., and Wozniak, R.W. (1995). Two novel related yeast nucleoporins Nup170p and Nup157p: complementation with the vertebrate homologue Nup155p and functional interactions with the yeast nuclear pore-membrane protein Pom152p. J Cell Biol *131*, 1133-1148.

Alejandro-Osorio, A.L., Huebert, D.J., Porcaro, D.T., Sonntag, M.E., Nillasithanukroh, S., Will, J.L., and Gasch, A.P. (2009). The histone deacetylase Rpd3p is required for transient changes in genomic expression in response to stress. Genome Biol *10*, R57.

Alepuz, P.M., Jovanovic, A., Reiser, V., and Ammerer, G. (2001). Stress-induced map kinase Hog1 is part of transcription activation complexes. Mol Cell *7*, 767-777.

Alic, N., Higgins, V.J., Pichova, A., Breitenbach, M., and Dawes, I.W. (2003). Lipid hydroperoxides activate the mitogen-activated protein kinase Mpk1p in Saccharomyces cerevisiae. J Biol Chem *278*, 41849-41855.

Alic, N., and Partridge, L. (2011). Death and dessert: nutrient signalling pathways and ageing. Curr Opin Cell Biol *23*, 738-743.

Allegra, P., Sterner, R., Clayton, D.F., and Allfrey, V.G. (1987). Affinity chromatographic purification of nucleosomes containing transcriptionally active DNA sequences. J Mol Biol *196*, 379-388.

Allfrey, V.G., Faulkner, R., and Mirsky, A.E. (1964). Acetylation and Methylation of Histones and Their Possible Role in the Regulation of Rna Synthesis. Proc Natl Acad Sci U S A *51*, 786-794.

Allis, C.D., Bowen, J.K., Abraham, G.N., Glover, C.V., and Gorovsky, M.A. (1980). Proteolytic processing of histone H3 in chromatin: a physiologically regulated event in Tetrahymena micronuclei. Cell *20*, 55-64.

Amberg, D.C., Burke, D.J., and Strathern, J.N., eds. (2005). Methods in Yeast Genetics, 2005 edn (Cold Spring Harbor, NY, Cold Spring Harbor Laboratory Press).

Andes, D.R., Safdar, N., Baddley, J.W., Playford, G., Reboli, A.C., Rex, J.H., Sobel, J.D., Pappas, P.G., and Kullberg, B.J. (2012). Impact of Treatment Strategy on Outcomes in Patients with Candidemia and Other Forms of Invasive Candidiasis: A Patient-Level Quantitative Review of Randomized Trials. Clin Infect Dis *54*, 1110-1122.

Annunziato, A.T., and Seale, R.L. (1983). Histone deacetylation is required for the maturation of newly replicated chromatin. J Biol Chem *258*, 12675-12684.

Aparicio, O., Geisberg, J.V., Sekinger, E., Yang, A., Moqtaderi, Z., and Struhl, K. (2005). Chromatin immunoprecipitation for determining the association of proteins with specific genomic sequences in vivo. Curr Protoc Mol Biol *Chapter 21*, Unit 21 23.

Aravind, L., Iyer, L.M., and Koonin, E.V. (2003). Scores of RINGS but no PHDs in ubiquitin signaling. Cell Cycle *2*, 123-126.

Archambault, J., Lacroute, F., Ruet, A., and Friesen, J.D. (1992). Genetic interaction between transcription elongation factor TFIIS and RNA polymerase II. Mol Cell Biol *12*, 4142-4152.

Argentaro, A., Yang, J.C., Chapman, L., Kowalczyk, M.S., Gibbons, R.J., Higgs, D.R., Neuhaus, D., and Rhodes, D. (2007). Structural consequences of disease-causing mutations in the ATRX-DNMT3-DNMT3L (ADD) domain of the chromatin-associated protein ATRX. Proc Natl Acad Sci U S A *104*, 11939-11944.

Arigo, J.T., Eyler, D.E., Carroll, K.L., and Corden, J.L. (2006). Termination of cryptic unstable transcripts is directed by yeast RNA-binding proteins Nrd1 and Nab3. Mol Cell *23*, 841-851.

Armache, K.J., Garlick, J.D., Canzio, D., Narlikar, G.J., and Kingston, R.E. (2011). Structural basis of silencing: Sir3 BAH domain in complex with a nucleosome at 3.0 A resolution. Science *334*, 977-982.

Avery, O.T., Macleod, C.M., and McCarty, M. (1944). Studies on the Chemical Nature of the Substance Inducing Transformation of Pneumococcal Types : Induction of Transformation by a Desoxyribonucleic Acid Fraction Isolated from Pneumococcus Type III. J Exp Med *79*, 137-158.

Ayton, P.M., and Cleary, M.L. (2001). Molecular mechanisms of leukemogenesis mediated by MLL fusion proteins. Oncogene *20*, 5695-5707.

Baker, L.A., Allis, C.D., and Wang, G.G. (2008). PHD fingers in human diseases: disorders arising from misinterpreting epigenetic marks. Mutat Res *647*, 3-12.

Bamforth, C.W., and Lentini, A. (2009). The flavor instability of beer. *Beer: A Quality Perspective*, 85-109.

Bandhakavi, S., Xie, H., O'Callaghan, B., Sakurai, H., Kim, D.H., and Griffin, T.J. (2008). Hsf1 activation inhibits rapamycin resistance and TOR signaling in yeast revealed by combined proteomic and genetic analysis. PLoS One *3*, e1598.

Banerjee, T., and Chakravarti, D. (2011). A peek into the complex realm of histone phosphorylation. Mol Cell Biol *31*, 4858-4873.

Bannister, A.J., and Kouzarides, T. (1996). The CBP co-activator is a histone acetyltransferase. Nature *384*, 641-643.

Bannister, A.J., and Kouzarides, T. (2011). Regulation of chromatin by histone modifications. Cell Res *21*, 381-395.

Bannister, A.J., Zegerman, P., Partridge, J.F., Miska, E.A., Thomas, J.O., Allshire, R.C., and Kouzarides, T. (2001). Selective recognition of methylated lysine 9 on histone H3 by the HP1 chromo domain. Nature *410*, 120-124.

Barker, M.G., Brimage, L.J., and Smart, K.A. (1999). Effect of Cu,Zn superoxide dismutase disruption mutation on replicative senescence in Saccharomyces cerevisiae. FEMS Microbiol Lett *177*, 199-204.

Barrett, A., Madsen, B., Copier, J., Lu, P.J., Cooper, L., Scibetta, A.G., Burchell, J., and Taylor-Papadimitriou, J. (2002). PLU-1 nuclear protein, which is upregulated in breast cancer, shows restricted expression in normal human adult tissues: a new cancer/testis antigen? Int J Cancer *101*, 581-588.

Barros, M.H., Bandy, B., Tahara, E.B., and Kowaltowski, A.J. (2004). Higher respiratory activity decreases mitochondrial reactive oxygen release and increases life span in Saccharomyces cerevisiae. J Biol Chem *279*, 49883-49888.

Basu, A., Rose, K.L., Zhang, J., Beavis, R.C., Ueberheide, B., Garcia, B.A., Chait, B., Zhao, Y., Hunt, D.F., Segal, E., *et al.* (2009). Proteome-wide prediction of acetylation substrates. Proc Natl Acad Sci U S A *106*, 13785-13790.

Beck-Sague, C., and Jarvis, W.R. (1993). Secular trends in the epidemiology of nosocomial fungal infections in the United States, 1980-1990. National Nosocomial Infections Surveillance System. J Infect Dis *167*, 1247-1251.

Beck, T., and Hall, M.N. (1999). The TOR signalling pathway controls nuclear localization of nutrient-regulated transcription factors. Nature *402*, 689-692.

Beese, S.E., Negishi, T., and Levin, D.E. (2009). Identification of positive regulators of the yeast fps1 glycerol channel. PLoS Genet *5*, e1000738.

Ben-Saadon, R., Zaaroor, D., Ziv, T., and Ciechanover, A. (2006). The polycomb protein Ring1B generates self atypical mixed ubiquitin chains required for its in vitro histone H2A ligase activity. Mol Cell *24*, 701-711.

Benaroudj, N., Lee, D.H., and Goldberg, A.L. (2001). Trehalose accumulation during cellular stress protects cells and cellular proteins from damage by oxygen radicals. J Biol Chem *276*, 24261-24267.

Berner, T.S., and Arneborg, N. (2012). The role of lager beer yeast in oxidative stability of model beer. Lett Appl Microbiol *54*, 225-232.

Bernstein, B.E., Tong, J.K., and Schreiber, S.L. (2000). Genomewide studies of histone deacetylase function in yeast. Proc Natl Acad Sci U S A *97*, 13708-13713.

Berriz, G.F., Beaver, J.E., Cenik, C., Tasan, M., and Roth, F.P. (2009). Next generation software for functional trend analysis. Bioinformatics *25*, 3043-3044.

Bian, C., Xu, C., Ruan, J., Lee, K.K., Burke, T.L., Tempel, W., Barsyte, D., Li, J., Wu, M., Zhou, B.O.*, et al.* (2011). Sgf29 binds histone H3K4me2/3 and is required for SAGA complex recruitment and histone H3 acetylation. EMBO J *30*, 2829-2842.

Bidlingmaier, S., Weiss, E.L., Seidel, C., Drubin, D.G., and Snyder, M. (2001). The Cbk1p pathway is important for polarized cell growth and cell separation in Saccharomyces cerevisiae. Mol Cell Biol *21*, 2449-2462.

Bienz, M. (2006). The PHD finger, a nuclear protein-interaction domain. Trends Biochem Sci *31*, 35-40.

Billing, R.J., and Bonner, J. (1972). The structure of chromatin as revealed by deoxyribonuclease digestion studies. Biochim Biophys Acta *281*, 453-462.

Bilsland, E., Molin, C., Swaminathan, S., Ramne, A., and Sunnerhagen, P. (2004). Rck1 and Rck2 MAPKAP kinases and the HOG pathway are required for oxidative stress resistance. Mol Microbiol *53*, 1743-1756.

Bjorses, P., Halonen, M., Palvimo, J.J., Kolmer, M., Aaltonen, J., Ellonen, P., Perheentupa, J., Ulmanen, I., and Peltonen, L. (2000). Mutations in the AIRE gene: effects on subcellular location and transactivation function of the autoimmune polyendocrinopathy-candidiasis-ectodermal dystrophy protein. Am J Hum Genet *66*, 378-392.

Bowdish, K.S., and Mitchell, A.P. (1993). Bipartite structure of an early meiotic upstream activation sequence from Saccharomyces cerevisiae. Mol Cell Biol *13*, 2172-2181.

Boyer, L.A., Latek, R.R., and Peterson, C.L. (2004). The SANT domain: a unique histone-tail-binding module? Nat Rev Mol Cell Biol *5*, 158-163.

Briggs, S.D., Bryk, M., Strahl, B.D., Cheung, W.L., Davie, J.K., Dent, S.Y., Winston, F., and Allis, C.D. (2001). Histone H3 lysine 4 methylation is mediated by Set1 and required for cell growth and rDNA silencing in Saccharomyces cerevisiae. Genes Dev *15*, 3286-3295.

Brownell, J.E., and Allis, C.D. (1995). An activity gel assay detects a single, catalytically active histone acetyltransferase subunit in Tetrahymena macronuclei. Proc Natl Acad Sci U S A *92*, 6364-6368.

Brownell, J.E., Zhou, J., Ranalli, T., Kobayashi, R., Edmondson, D.G., Roth, S.Y., and Allis, C.D. (1996). Tetrahymena histone acetyltransferase A: a homolog to yeast Gcn5p linking histone acetylation to gene activation. Cell *84*, 843-851.

Bryk, M., Banerjee, M., Murphy, M., Knudsen, K.E., Garfinkel, D.J., and Curcio, M.J. (1997). Transcriptional silencing of Ty1 elements in the RDN1 locus of yeast. Genes Dev *11*, 255-269.

Bumgarner, S.L., Dowell, R.D., Grisafi, P., Gifford, D.K., and Fink, G.R. (2009). Toggle involving cis-interfering noncoding RNAs controls variegated gene expression in yeast. Proc Natl Acad Sci U S A 106, 18321-18326.

Cai, L., Sutter, B.M., Li, B., and Tu, B.P. (2011). Acetyl-CoA induces cell growth and proliferation by promoting the acetylation of histones at growth genes. Mol Cell *42*, 426-437.

Campos, E.I., Martinka, M., Mitchell, D.L., Dai, D.L., and Li, G. (2004). Mutations of the ING1 tumor suppressor gene detected in human melanoma abrogate nucleotide excision repair. Int J Oncol *25*, 73-80.

Candau, R., Moore, P.A., Wang, L., Barlev, N., Ying, C.Y., Rosen, C.A., and Berger, S.L. (1996). Identification of human proteins functionally conserved with the yeast putative adaptors ADA2 and GCN5. Mol Cell Biol *16*, 593-602.

Cao, R., Wang, L., Wang, H., Xia, L., Erdjument-Bromage, H., Tempst, P., Jones, R.S., and Zhang, Y. (2002). Role of histone H3 lysine 27 methylation in Polycomb-group silencing. Science *298*, 1039-1043.

Capili, A.D., Schultz, D.C., Rauscher, I.F., and Borden, K.L. (2001). Solution structure of the PHD domain from the KAP-1 corepressor: structural determinants for PHD, RING and LIM zinc-binding domains. EMBO J *20*, 165-177.

Carrozza, M.J., Florens, L., Swanson, S.K., Shia, W.J., Anderson, S., Yates, J., Washburn, M.P., and Workman, J.L. (2005a). Stable incorporation of sequence specific repressors Ash1 and Ume6 into the Rpd3L complex. Biochim Biophys Acta *1731*, 77-87; discussion 75-76.

Carrozza, M.J., Li, B., Florens, L., Suganuma, T., Swanson, S.K., Lee, K.K., Shia, W.J., Anderson, S., Yates, J., Washburn, M.P., *et al.* (2005b). Histone H3 methylation by Set2 directs deacetylation of coding regions by Rpd3S to suppress spurious intragenic transcription. Cell *123*, 581-592.

Carrozza, M.J., Utley, R.T., Workman, J.L., and Cote, J. (2003). The diverse functions of histone acetyltransferase complexes. Trends Genet *19*, 321-329.

Cejka, P., Cannavo, E., Polaczek, P., Masuda-Sasa, T., Pokharel, S., Campbell, J.L., and Kowalczykowski, S.C. (2010). DNA end resection by Dna2-Sgs1-RPA and its stimulation by Top3-Rmi1 and Mre11-Rad50-Xrs2. Nature *467*, 112-116.

Chandrasekharan, M.B., Huang, F., and Sun, Z.W. (2010). Histone H2B ubiquitination and beyond: Regulation of nucleosome stability, chromatin dynamics and the trans-histone H3 methylation. Epigenetics *5*, 460-468.

Chang, M., Bellaoui, M., Zhang, C., Desai, R., Morozov, P., Delgado-Cruzata, L., Rothstein, R., Freyer, G.A., Boone, C., and Brown, G.W. (2005). RMI1/NCE4, a suppressor of genome instability, encodes a member of the RecQ helicase/Topo III complex. EMBO J *24*, 2024-2033.

Chau, V., Tobias, J.W., Bachmair, A., Marriott, D., Ecker, D.J., Gonda, D.K., and Varshavsky, A. (1989). A multiubiquitin chain is confined to specific lysine in a targeted short-lived protein. Science *243*, 1576-1583.

Chen, B., Campos, E.I., Crawford, R., Martinka, M., and Li, G. (2003). Analyses of the tumour suppressor ING1 expression and gene mutation in human basal cell carcinoma. Int J Oncol *22*, 927-931.

Chen, H., Lin, R.J., Schiltz, R.L., Chakravarti, D., Nash, A., Nagy, L., Privalsky, M.L., Nakatani, Y., and Evans, R.M. (1997). Nuclear receptor coactivator ACTR is a novel histone acetyltransferase and forms a multimeric activation complex with P/CAF and CBP/p300. Cell *90*, 569-580.

Chen, H.Y., Sun, J.M., Zhang, Y., Davie, J.R., and Meistrich, M.L. (1998). Ubiquitination of histone H3 in elongating spermatids of rat testes. J Biol Chem *273*, 13165-13169.

Chen, L., Matsubara, N., Yoshino, T., Nagasaka, T., Hoshizima, N., Shirakawa, Y., Naomoto, Y., Isozaki, H., Riabowol, K., and Tanaka, N. (2001). Genetic alterations of candidate tumor suppressor ING1 in human esophageal squamous cell cancer. Cancer Res *61*, 4345-4349.

Chen, Q., Ding, Q., and Keller, J.N. (2005). The stationary phase model of aging in yeast for the study of oxidative stress and age-related neurodegeneration. Biogerontology *6*, 1-13.

Chicoine, L.G., Schulman, I.G., Richman, R., Cook, R.G., and Allis, C.D. (1986). Nonrandom utilization of acetylation sites in histones isolated from Tetrahymena. Evidence for functionally distinct H4 acetylation sites. J Biol Chem *261*, 1071-1076.

Choudhary, C., Kumar, C., Gnad, F., Nielsen, M.L., Rehman, M., Walther, T.C., Olsen, J.V., and Mann, M. (2009). Lysine acetylation targets protein complexes and co-regulates major cellular functions. Science *325*, 834-840.

Choy, J.S., Mishra, P.K., Au, W.C., and Basrai, M.A. (2012). Insights into assembly and regulation of centromeric chromatin in Saccharomyces cerevisiae. Biochim Biophys Acta. In press, available online February 2012.

Christensen, J., Agger, K., Cloos, P.A., Pasini, D., Rose, S., Sennels, L., Rappsilber, J., Hansen, K.H., Salcini, A.E., and Helin, K. (2007). RBP2 belongs to a family of demethylases, specific for tri-and dimethylated lysine 4 on histone 3. Cell *128*, 1063-1076.

Christianson, T.W., Sikorski, R.S., Dante, M., Shero, J.H., and Hieter, P. (1992). Multifunctional yeast high-copy-number shuttle vectors. Gene *110*, 119-122.

Chruscicki, A., Macdonald, V.E., Young, B.P., Loewen, C.J., and Howe, L.J. (2010). Critical determinants for chromatin binding by Saccharomyces cerevisiae Yng1 exist outside of the plant homeodomain finger. Genetics *185*, 469-477.

Churchman, L.S., and Weissman, J.S. (2011). Nascent transcript sequencing visualizes transcription at nucleotide resolution. Nature *469*, 368-373.

Clague, M.J., and Urbe, S. (2010). Ubiquitin: same molecule, different degradation pathways. Cell *143*, 682-685.

Claverys, J.P., and Havarstein, L.S. (2007). Cannibalism and fratricide: mechanisms and raisons d'etre. Nat Rev Microbiol *5*, 219-229.

Cohen, T.J., Lee, K., Rutkowski, L.H., and Strich, R. (2003). Ask10p mediates the oxidative stress-induced destruction of the Saccharomyces cerevisiae C-type cyclin Ume3p/Srb11p. Eukaryot Cell *2*, 962-970.

Collart, M.A., and Oliviero, S. (2001). Preparation of yeast RNA. Curr Protoc Mol Biol *Chapter 13*, Unit13 12.

Collins, S.R., Miller, K.M., Maas, N.L., Roguev, A., Fillingham, J., Chu, C.S., Schuldiner, M., Gebbia, M., Recht, J., Shales, M., *et al.* (2007). Functional dissection of protein complexes involved in yeast chromosome biology using a genetic interaction map. Nature *446*, 806-810.

Collinson, L.P., and Dawes, I.W. (1992). Inducibility of the response of yeast cells to peroxide stress. J Gen Microbiol *138*, 329-335.

Coscoy, L., Sanchez, D.J., and Ganem, D. (2001). A novel class of herpesvirus-encoded membrane-bound E3 ubiquitin ligases regulates endocytosis of proteins involved in immune recognition. J Cell Biol *155*, 1265-1273.

Cristea, I.M., Williams, R., Chait, B.T., and Rout, M.P. (2005). Fluorescent proteins as proteomic probes. Mol Cell Proteomics *4*, 1933-1941.

Crowe, J.H., Crowe, L.M., and Chapman, D. (1984). Preservation of membranes in anhydrobiotic organisms: the role of trehalose. Science *223*, 701-703.

Cvrckova, F., De Virgilio, C., Manser, E., Pringle, J.R., and Nasmyth, K. (1995). Ste20-like protein kinases are required for normal localization of cell growth and for cytokinesis in budding yeast. Genes Dev *9*, 1817-1830.

D'Autreaux, B., and Toledano, M.B. (2007). ROS as signalling molecules: mechanisms that generate specificity in ROS homeostasis. Nat Rev Mol Cell Biol *8*, 813-824.

Dai, C., and Gu, W. (2010). p53 post-translational modification: deregulated in tumorigenesis. Trends Mol Med *16*, 528-536.

Daly, M.M., and Mirsky, A.E. (1955). Histones with high lysine content. J Gen Physiol *38*, 405-413.

Dang, W., Steffen, K.K., Perry, R., Dorsey, J.A., Johnson, F.B., Shilatifard, A., Kaeberlein, M., Kennedy, B.K., and Berger, S.L. (2009). Histone H4 lysine 16 acetylation regulates cellular lifespan. Nature *459*, 802-807.

Dazert, E., and Hall, M.N. (2011). mTOR signaling in disease. Curr Opin Cell Biol *23*, 744-755.

de Groot, P.W., Ruiz, C., Vazquez de Aldana, C.R., Duenas, E., Cid, V.J., Del Rey, F., Rodriquez-Pena, J.M., Perez, P., Andel, A., Caubin, J., et al. (2001). A genomic approach for the identification and classification of genes involved in cell wall formation and its regulation in Saccharomyces cerevisiae. Comp Funct Genomics 2, 124-142.

de Jesus Ferreira, M.C., Bao, X., Laize, V., and Hohmann, S. (2001). Transposon mutagenesis reveals novel loci affecting tolerance to salt stress and growth at low temperature. Curr Genet *40*, 27-39.

de Nadal, E., and Posas, F. (2010). Multilayered control of gene expression by stress-activated protein kinases. EMBO J *29*, 4-13.

De Nadal, E., Zapater, M., Alepuz, P.M., Sumoy, L., Mas, G., and Posas, F. (2004). The MAPK Hog1 recruits Rpd3 histone deacetylase to activate osmoresponsive genes. Nature *427*, 370-374.

De Rubertis, F., Kadosh, D., Henchoz, S., Pauli, D., Reuter, G., Struhl, K., and Spierer, P. (1996). The histone deacetylase RPD3 counteracts genomic silencing in Drosophila and yeast. Nature *384*, 589-591.

De Virgilio, C., and Loewith, R. (2006). Cell growth control: little eukaryotes make big contributions. Oncogene *25*, 6392-6415.

Dechant, R., and Peter, M. (2008). Nutrient signals driving cell growth. Curr Opin Cell Biol *20*, 678-687.

Dirmeier, R., O'Brien, K.M., Engle, M., Dodd, A., Spears, E., and Poyton, R.O. (2002). Exposure of yeast cells to anoxia induces transient oxidative stress. Implications for the induction of hypoxic genes. J Biol Chem *277*, 34773-34784.

Dora, E.G., Rudin, N., Martell, J.R., Esposito, M.S., and Ramirez, R.M. (1999). RPD3 (REC3) mutations affect mitotic recombination in Saccharomyces cerevisiae. Curr Genet *35*, 68-76.

Douglas, J., Hanks, S., Temple, I.K., Davies, S., Murray, A., Upadhyaya, M., Tomkins, S., Hughes, H.E., Cole, T.R., and Rahman, N. (2003). NSD1 mutations are the major cause of Sotos syndrome and occur in some cases of Weaver syndrome but are rare in other overgrowth phenotypes. Am J Hum Genet *72*, 132-143.

Dul, B.E., and Walworth, N.C. (2007). The plant homeodomain fingers of fission yeast Msc1 exhibit E3 ubiquitin ligase activity. J Biol Chem *282*, 18397-18406.

Dumont, M.E., Ernst, J.F., Hampsey, D.M., and Sherman, F. (1987). Identification and sequence of the gene encoding cytochrome c heme lyase in the yeast Saccharomyces cerevisiae. EMBO J *6*, 235-241.

Duncan, E.M., Muratore-Schroeder, T.L., Cook, R.G., Garcia, B.A., Shabanowitz, J., Hunt, D.F., and Allis, C.D. (2008). Cathepsin L proteolytically processes histone H3 during mouse embryonic stem cell differentiation. Cell *135*, 284-294.

Durrin, L.K., Mann, R.K., Kayne, P.S., and Grunstein, M. (1991). Yeast histone H4 N-terminal sequence is required for promoter activation in vivo. Cell *65*, 1023-1031.

Eberharter, A., Ferrari, S., Langst, G., Straub, T., Imhof, A., Varga-Weisz, P., Wilm, M., and Becker, P.B. (2001). Acf1, the largest subunit of CHRAC, regulates ISWI-induced nucleosome remodelling. EMBO J *20*, 3781-3788.

Eberharter, A., John, S., Grant, P.A., Utley, R.T., and Workman, J.L. (1998). Identification and analysis of yeast nucleosomal histone acetyltransferase complexes. Methods *15*, 315-321.

Eickbush, T.H., Watson, D.K., and Moudrianakis, E.N. (1976). A chromatin-bound proteolytic activity with unique specificity for histone H2A. Cell *9*, 785-792.

Eisler, H., Frohlich, K.U., and Heidenreich, E. (2004). Starvation for an essential amino acid induces apoptosis and oxidative stress in yeast. Exp Cell Res *300*, 345-353.

Elble, R. (1992). A simple and efficient procedure for transformation of yeasts. Biotechniques *13*, 18-20.

Evans, P., and Halliwell, B. (2001). Micronutrients: oxidant/antioxidant status. Br J Nutr *85 Suppl 2*, S67-74.

Exinger, F., and Lacroute, F. (1992). 6-Azauracil inhibition of GTP biosynthesis in Saccharomyces cerevisiae. Curr Genet *22*, 9-11.

Fang, S., and Weissman, A.M. (2004). A field guide to ubiquitylation. Cell Mol Life Sci *61*, 1546-1561.

Fattaey, A.R., Helin, K., Dembski, M.S., Dyson, N., Harlow, E., Vuocolo, G.A., Hanobik, M.G., Haskell, K.M., Oliff, A., Defeo-Jones, D.*, et al.* (1993). Characterization of the retinoblastoma binding proteins RBP1 and RBP2. Oncogene *8*, 3149-3156.

Fiedler, M., Sanchez-Barrena, M.J., Nekrasov, M., Mieszczanek, J., Rybin, V., Muller, J., Evans, P., and Bienz, M. (2008). Decoding of methylated histone H3 tail by the Pygo-BCL9 Wnt signaling complex. Mol Cell *30*, 507-518.

Fierz, B., Chatterjee, C., McGinty, R.K., Bar-Dagan, M., Raleigh, D.P., and Muir, T.W. (2011). Histone H2B ubiquitylation disrupts local and higher-order chromatin compaction. Nat Chem Biol *7*, 113-119.

Finley, D., Sadis, S., Monia, B.P., Boucher, P., Ecker, D.J., Crooke, S.T., and Chau, V. (1994). Inhibition of proteolysis and cell cycle progression in a multiubiquitination-deficient yeast mutant. Mol Cell Biol *14*, 5501-5509.

Fisher-Adams, G., and Grunstein, M. (1995). Yeast histone H4 and H3 N-termini have different effects on the chromatin structure of the GAL1 promoter. EMBO J *14*, 1468-1477.

Flaus, A., and Owen-Hughes, T. (2011). Mechanisms for ATP-dependent chromatin remodelling: the means to the end. FEBS J *278*, 3579-3595.

Flemming, W. (1882). Zellsubstanz, Kern und Zelltheilung.

Frank, D., Doenecke, D., and Albig, W. (2003). Differential expression of human replacement and cell cycle dependent H3 histone genes. Gene *312*, 135-143.

Freinbichler, W., Colivicchi, M.A., Stefanini, C., Bianchi, L., Ballini, C., Misini, B., Weinberger, P., Linert, W., Vareslija, D., Tipton, K.F.*, et al.* (2011). Highly reactive oxygen species: detection, formation, and possible functions. Cell Mol Life Sci *68*, 2067-2079.

Fridovich, I. (1995). Superoxide radical and superoxide dismutases. Annu Rev Biochem *64*, 97-112.

Galdieri, L., Mehrotra, S., Yu, S., and Vancura, A. (2010). Transcriptional regulation in yeast during diauxic shift and stationary phase. OMICS *14*, 629-638.

Gangloff, S., McDonald, J.P., Bendixen, C., Arthur, L., and Rothstein, R. (1994). The yeast type I topoisomerase Top3 interacts with Sgs1, a DNA helicase homolog: a potential eukaryotic reverse gyrase. Mol Cell Biol *14*, 8391-8398.

Garcia, B.A., Hake, S.B., Diaz, R.L., Kauer, M., Morris, S.A., Recht, J., Shabanowitz, J., Mishra, N., Strahl, B.D., Allis, C.D.*, et al.* (2007). Organismal differences in post-translational modifications in histones H3 and H4. J Biol Chem *282*, 7641-7655.

Gardner, K.E., Zhou, L., Parra, M.A., Chen, X., and Strahl, B.D. (2011). Identification of lysine 37 of histone H2B as a novel site of methylation. PLoS One *6*, e16244.

Gasch, A.P., Spellman, P.T., Kao, C.M., Carmel-Harel, O., Eisen, M.B., Storz, G., Botstein, D., and Brown, P.O. (2000). Genomic expression programs in the response of yeast cells to environmental changes. Mol Biol Cell *11*, 4241-4257.

Gavin, A.C., Bosche, M., Krause, R., Grandi, P., Marzioch, M., Bauer, A., Schultz, J., Rick, J.M., Michon, A.M., Cruciat, C.M., *et al.* (2002). Functional organization of the yeast proteome by systematic analysis of protein complexes. Nature *415*, 141-147.

Ghaemmaghami, S., Huh, W.K., Bower, K., Howson, R.W., Belle, A., Dephoure, N., O'Shea, E.K., and Weissman, J.S. (2003). Global analysis of protein expression in yeast. Nature *425*, 737-741.

Giaever, G., Chu, A.M., Ni, L., Connelly, C., Riles, L., Veronneau, S., Dow, S., Lucau-Danila, A., Anderson, K., Andre, B., *et al.* (2002). Functional profiling of the Saccharomyces cerevisiae genome. Nature *418*, 387-391.

Goldknopf, I.L., Taylor, C.W., Baum, R.M., Yeoman, L.C., Olson, M.O., Prestayko, A.W., and Busch, H. (1975). Isolation and characterization of protein A24, a "histone-like" non-histone chromosomal protein. J Biol Chem *250*, 7182-7187.

Goldstein, A.L., and McCusker, J.H. (1999). Three new dominant drug resistance cassettes for gene disruption in Saccharomyces cerevisiae. Yeast *15*, 1541-1553.

Goll, M.G., and Bestor, T.H. (2002). Histone modification and replacement in chromatin activation. Genes Dev *16*, 1739-1742.

Gottschling, D.E., Aparicio, O.M., Billington, B.L., and Zakian, V.A. (1990). Position effect at S. cerevisiae telomeres: reversible repression of Pol II transcription. Cell *63*, 751-762.

Green, E.M., Mas, G., Young, N.L., Garcia, B.A., and Gozani, O. (2012). Methylation of H4 lysines 5, 8 and 12 by yeast Set5 calibrates chromatin stress responses. Nat Struct Mol Biol *19*, 361-363.

Gu, W., and Roeder, R.G. (1997). Activation of p53 sequence-specific DNA binding by acetylation of the p53 C-terminal domain. Cell *90*, 595-606.

Guermah, M., Palhan, V.B., Tackett, A.J., Chait, B.T., and Roeder, R.G. (2006). Synergistic functions of SII and p300 in productive activator-dependent transcription of chromatin templates. Cell *125*, 275-286.

Haase, S.B. (2004). Cell cycle analysis of budding yeast using SYTOX Green. Curr Protoc Cytom *Chapter 7*, Unit 7 23.

Haghnazari, E., and Heyer, W.D. (2004). The Hog1 MAP kinase pathway and the Mec1 DNA damage checkpoint pathway independently control the cellular responses to hydrogen peroxide. DNA Repair (Amst) *3*, 769-776.

Hall, D.A., Zhu, H., Zhu, X., Royce, T., Gerstein, M., and Snyder, M. (2004). Regulation of gene expression by a metabolic enzyme. Science *306*, 482-484.

Han, J., Zhou, H., Li, Z., Xu, R.M., and Zhang, Z. (2007). The Rtt109-Vps75 histone acetyltransferase complex acetylates non-nucleosomal histone H3. J Biol Chem *282*, 14158-14164.

Hanover, J.A. (2010). Epigenetics gets sweeter: O-GlcNAc joins the "histone code". Chem Biol *17*, 1272-1274.

Happel, N., and Doenecke, D. (2009). Histone H1 and its isoforms: contribution to chromatin structure and function. Gene *431*, 1-12.

Harbison, C.T., Gordon, D.B., Lee, T.I., Rinaldi, N.J., Macisaac, K.D., Danford, T.W., Hannett, N.M., Tagne, J.B., Reynolds, D.B., Yoo, J.*, et al.* (2004). Transcriptional regulatory code of a eukaryotic genome. Nature *431*, 99-104.

Hayakawa, T., Ohtani, Y., Hayakawa, N., Shinmyozu, K., Saito, M., Ishikawa, F., and Nakayama, J. (2007). RBP2 is an MRG15 complex component and down-regulates intragenic histone H3 lysine 4 methylation. Genes Cells *12*, 811-826.

Hebbes, T.R., Thorne, A.W., and Crane-Robinson, C. (1988). A direct link between core histone acetylation and transcriptionally active chromatin. EMBO J *7*, 1395-1402.

Hedbacker, K., and Carlson, M. (2008). SNF1/AMPK pathways in yeast. Front Biosci *13*, 2408-2420.

Heintzman, N.D., Stuart, R.K., Hon, G., Fu, Y., Ching, C.W., Hawkins, R.D., Barrera, L.O., Van Calcar, S., Qu, C., Ching, K.A.*, et al.* (2007). Distinct and predictive chromatin signatures of transcriptional promoters and enhancers in the human genome. Nat Genet *39*, 311-318.

Heitz, E. (1928). Das Heterochromatin der Moose. I. Jahrb Wiss Bot *69*, 762-818.

Hepworth, S.R., Friesen, H., and Segall, J. (1998). NDT80 and the meiotic recombination checkpoint regulate expression of middle sporulation-specific genes in Saccharomyces cerevisiae. Mol Cell Biol *18*, 5750-5761.

Hereford, L., Fahrner, K., Woolford, J., Jr., Rosbash, M., and Kaback, D.B. (1979). Isolation of yeast histone genes H2A and H2B. Cell *18*, 1261-1271.

Herker, E., Jungwirth, H., Lehmann, K.A., Maldener, C., Frohlich, K.U., Wissing, S., Buttner, S., Fehr, M., Sigrist, S., and Madeo, F. (2004). Chronological aging leads to apoptosis in yeast. J Cell Biol *164*, 501-507.

Herrero, E., Ros, J., Belli, G., and Cabiscol, E. (2008). Redox control and oxidative stress in yeast cells. Biochim Biophys Acta *1780*, 1217-1235.

Hewish, D.R., and Burgoyne, L.A. (1973). Chromatin sub-structure. The digestion of chromatin DNA at regularly spaced sites by a nuclear deoxyribonuclease. Biochem Biophys Res Commun *52*, 504-510.

Hewitt, E.W., Duncan, L., Mufti, D., Baker, J., Stevenson, P.G., and Lehner, P.J. (2002). Ubiquitylation of MHC class I by the K3 viral protein signals internalization and TSG101-dependent degradation. EMBO J *21*, 2418-2429.

Hicke, L. (2001). Protein regulation by monoubiquitin. Nat Rev Mol Cell Biol *2*, 195-201.

Hickman, M.J., Spatt, D., and Winston, F. (2011). The Hog1 mitogen-activated protein kinase mediates a hypoxic response in Saccharomyces cerevisiae. Genetics *188*, 325-338.

Hickman, M.J., and Winston, F. (2007). Heme levels switch the function of Hap1 of Saccharomyces cerevisiae between transcriptional activator and transcriptional repressor. Mol Cell Biol *27*, 7414-7424.

Hickson, I.D., and Mankouri, H.W. (2011). Processing of homologous recombination repair intermediates by the Sgs1-Top3-Rmi1 and Mus81-Mms4 complexes. Cell Cycle *10*, 3078-3085.

Higgins, V.J., Beckhouse, A.G., Oliver, A.D., Rogers, P.J., and Dawes, I.W. (2003). Yeast genome-wide expression analysis identifies a strong ergosterol and oxidative stress response during the initial stages of an industrial lager fermentation. Appl Environ Microbiol *69*, 4777-4787.

Hong, S.P., and Carlson, M. (2007). Regulation of snf1 protein kinase in response to environmental stress. J Biol Chem *282*, 16838-16845.

Howe, L., Kusch, T., Muster, N., Chaterji, R., Yates, J.R., 3rd, and Workman, J.L. (2002). Yng1p modulates the activity of Sas3p as a component of the yeast NuA3 Hhistone acetyltransferase complex. Mol Cell Biol *22*, 5047-5053.

Huang, F., Chandrasekharan, M.B., Chen, Y.C., Bhaskara, S., Hiebert, S.W., and Sun, Z.W. (2010). The JmjN domain of Jhd2 is important for its protein stability, and the plant homeodomain (PHD) finger mediates its chromatin association independent of H3K4 methylation. J Biol Chem *285*, 24548-24561.

Huang, J., and Berger, S.L. (2008). The emerging field of dynamic lysine methylation of non-histone proteins. Curr Opin Genet Dev *18*, 152-158.

Huber, A., French, S.L., Tekotte, H., Yerlikaya, S., Stahl, M., Perepelkina, M.P., Tyers, M., Rougemont, J., Beyer, A.L., and Loewith, R. (2011). Sch9 regulates ribosome biogenesis via Stb3, Dot6 and Tod6 and the histone deacetylase complex RPD3L. EMBO J *30*, 3052-3064.

Huh, W.K., Falvo, J.V., Gerke, L.C., Carroll, A.S., Howson, R.W., Weissman, J.S., and O'Shea, E.K. (2003). Global analysis of protein localization in budding yeast. Nature *425*, 686-691.

Huisinga, K.L., and Pugh, B.F. (2004). A genome-wide housekeeping role for TFIID and a highly regulated stress-related role for SAGA in Saccharomyces cerevisiae. Mol Cell 13, 573-585.

Humphrey, E.L., Shamji, A.F., Bernstein, B.E., and Schreiber, S.L. (2004). Rpd3p relocation mediates a transcriptional response to rapamycin in yeast. Chem Biol *11*, 295-299.

Hunt, L.T., and Dayhoff, M.O. (1977). Amino-terminal sequence identity of ubiquitin and the nonhistone component of nuclear protein A24. Biochem Biophys Res Commun *74*, 650-655.

Hyland, E.M., Molina, H., Poorey, K., Jie, C., Xie, Z., Dai, J., Qian, J., Bekiranov, S., Auble, D.T., Pandey, A., *et al.* (2011). An evolutionarily 'young' lysine residue in histone H3 attenuates transcriptional output in Saccharomyces cerevisiae. Genes Dev *25*, 1306-1319.

Ikeda, K., Steger, D.J., Eberharter, A., and Workman, J.L. (1999). Activation domain-specific and general transcription stimulation by native histone acetyltransferase complexes. Mol Cell Biol *19*, 855-863.

Imai, S., Armstrong, C.M., Kaeberlein, M., and Guarente, L. (2000). Transcriptional silencing and longevity protein Sir2 is an NAD-dependent histone deacetylase. Nature *403*, 795-800.

Ingvarsdottir, K., Edwards, C., Lee, M.G., Lee, J.S., Schultz, D.C., Shilatifard, A., Shiekhattar, R., and Berger, S.L. (2007). Histone H3 K4 demethylation during activation and attenuation of GAL1 transcription in Saccharomyces cerevisiae. Mol Cell Biol *27*, 7856-7864.

Ivanov, A.V., Peng, H., Yurchenko, V., Yap, K.L., Negorev, D.G., Schultz, D.C., Psulkowski, E., Fredericks, W.J., White, D.E., Maul, G.G., *et al.* (2007). PHD domain-mediated E3 ligase activity directs intramolecular sumoylation of an adjacent bromodomain required for gene silencing. Mol Cell *28*, 823-837.

Iwase, S., Lan, F., Bayliss, P., de la Torre-Ubieta, L., Huarte, M., Qi, H.H., Whetstine, J.R., Bonni, A., Roberts, T.M., and Shi, Y. (2007). The X-linked mental retardation gene SMCX/JARID1C defines a family of histone H3 lysine 4 demethylases. Cell *128*, 1077-1088.

Jackson, P.K., Eldridge, A.G., Freed, E., Furstenthal, L., Hsu, J.Y., Kaiser, B.K., and Reimann, J.D. (2000). The lore of the RINGs: substrate recognition and catalysis by ubiquitin ligases. Trends Cell Biol *10*, 429-439.

Jackson, V., Shires, A., Tanphaichitr, N., and Chalkley, R. (1976). Modifications to histones immediately after synthesis. J Mol Biol *104*, 471-483.

Jacobs, S.A., Taverna, S.D., Zhang, Y., Briggs, S.D., Li, J., Eissenberg, J.C., Allis, C.D., and Khorasanizadeh, S. (2001). Specificity of the HP1 chromo domain for the methylated N-terminus of histone H3. EMBO J *20*, 5232-5241.

James, T.C., Campbell, S., Donnelly, D., and Bond, U. (2003). Transcription profile of brewery yeast under fermentation conditions. J Appl Microbiol *94*, 432-448.

Jamieson, D.J. (1992). Saccharomyces cerevisiae has distinct adaptive responses to both hydrogen peroxide and menadione. J Bacteriol *174*, 6678-6681.

Jiang, T., Zhou, X., Taghizadeh, K., Dong, M., and Dedon, P.C. (2007). N-formylation of lysine in histone proteins as a secondary modification arising from oxidative DNA damage. Proc Natl Acad Sci U S A *104*, 60-65.

John, S., Howe, L., Tafrov, S.T., Grant, P.A., Sternglanz, R., and Workman, J.L. (2000). The something about silencing protein, Sas3, is the catalytic subunit of NuA3, a yTAF(II)30-containing HAT complex that interacts with the Spt16 subunit of the yeast CP (Cdc68/Pob3)-FACT complex. Genes Dev *14*, 1196-1208.

Johnson, E.M., Sterner, R., and Allfrey, V.G. (1987). Altered nucleosomes of active nucleolar chromatin contain accessible histone H3 in its hyperacetylated forms. J Biol Chem *262*, 6943-6946.

Johnson, L.M., Kayne, P.S., Kahn, E.S., and Grunstein, M. (1990). Genetic evidence for an interaction between SIR3 and histone H4 in the repression of the silent mating loci in Saccharomyces cerevisiae. Proc Natl Acad Sci U S A *87*, 6286-6290.

Johnston, M., and Kim, J.H. (2005). Glucose as a hormone: receptor-mediated glucose sensing in the yeast Saccharomyces cerevisiae. Biochem Soc Trans *33*, 247-252.

Jorgensen, P., Rupes, I., Sharom, J.R., Schneper, L., Broach, J.R., and Tyers, M. (2004). A dynamic transcriptional network communicates growth potential to ribosome synthesis and critical cell size. Genes Dev *18*, 2491-2505.

Joshi, A.A., and Struhl, K. (2005). Eaf3 chromodomain interaction with methylated H3-K36 links histone deacetylation to Pol II elongation. Mol Cell *20*, 971-978.

Kadosh, D., and Struhl, K. (1997). Repression by Ume6 involves recruitment of a complex containing Sin3 corepressor and Rpd3 histone deacetylase to target promoters. Cell *89*, 365-371.

Kadosh, D., and Struhl, K. (1998). Histone deacetylase activity of Rpd3 is important for transcriptional repression in vivo. Genes Dev *12*, 797-805.

Kalkhoven, E., Roelfsema, J.H., Teunissen, H., den Boer, A., Ariyurek, Y., Zantema, A., Breuning, M.H., Hennekam, R.C., and Peters, D.J. (2003). Loss of CBP acetyltransferase activity by PHD finger mutations in Rubinstein-Taybi syndrome. Hum Mol Genet *12*, 441-450.

Kaplan, C.D., Laprade, L., and Winston, F. (2003). Transcription elongation factors repress transcription initiation from cryptic sites. Science *301*, 1096-1099.

Kayne, P.S., Kim, U.J., Han, M., Mullen, J.R., Yoshizaki, F., and Grunstein, M. (1988). Extremely conserved histone H4 N terminus is dispensable for growth but essential for repressing the silent mating loci in yeast. Cell *55*, 27-39.

Keogh, M.C., Kurdistani, S.K., Morris, S.A., Ahn, S.H., Podolny, V., Collins, S.R., Schuldiner, M., Chin, K., Punna, T., Thompson, N.J., *et al.* (2005). Cotranscriptional set2 methylation of histone H3 lysine 36 recruits a repressive Rpd3 complex. Cell *123*, 593-605.

Kim, J., and Sudbery, P. (2011). Candida albicans, a major human fungal pathogen. J Microbiol *49*, 171-177.

Kim, S., Benguria, A., Lai, C.Y., and Jazwinski, S.M. (1999). Modulation of life-span by histone deacetylase genes in Saccharomyces cerevisiae. Mol Biol Cell *10*, 3125-3136.

Kim, T., and Buratowski, S. (2007). Two Saccharomyces cerevisiae JmjC domain proteins demethylate histone H3 Lys36 in transcribed regions to promote elongation. J Biol Chem *282*, 20827-20835.

Kimura, A., Matsubara, K., and Horikoshi, M. (2005). A decade of histone acetylation: marking eukaryotic chromosomes with specific codes. J Biochem *138*, 647-662.

Kimura, A., Umehara, T., and Horikoshi, M. (2002). Chromosomal gradient of histone acetylation established by Sas2p and Sir2p functions as a shield against gene silencing. Nat Genet *32*, 370-377.

Kizer, K.O., Phatnani, H.P., Shibata, Y., Hall, H., Greenleaf, A.L., and Strahl, B.D. (2005). A novel domain in Set2 mediates RNA polymerase II interaction and couples histone H3 K36 methylation with transcript elongation. Mol Cell Biol *25*, 3305-3316.

Kleff, S., Andrulis, E.D., Anderson, C.W., and Sternglanz, R. (1995). Identification of a gene encoding a yeast histone H4 acetyltransferase. J Biol Chem *270*, 24674-24677.

Klopf, E., Paskova, L., Sole, C., Mas, G., Petryshyn, A., Posas, F., Wintersberger, U., Ammerer, G., and Schuller, C. (2009). Cooperation between the INO80 complex and histone chaperones determines adaptation of stress gene transcription in the yeast Saccharomyces cerevisiae. Mol Cell Biol *29*, 4994-5007.

Klose, R.J., Gardner, K.E., Liang, G., Erdjument-Bromage, H., Tempst, P., and Zhang, Y. (2007a). Demethylation of histone H3K36 and H3K9 by Rph1: a vestige of an H3K9 methylation system in Saccharomyces cerevisiae? Mol Cell Biol *27*, 3951-3961.

Klose, R.J., Yan, Q., Tothova, Z., Yamane, K., Erdjument-Bromage, H., Tempst, P., Gilliland, D.G., Zhang, Y., and Kaelin, W.G., Jr. (2007b). The retinoblastoma binding protein RBP2 is an H3K4 demethylase. Cell *128*, 889-900.

Kornberg, R.D. (1974). Chromatin structure: a repeating unit of histones and DNA. Science *184*, 868-871.

Kornberg, R.D., and Thomas, J.O. (1974). Chromatin structure; oligomers of the histones. Science *184*, 865-868.

Kossel, A. (1884). Ueber einen peptonartigen Bestandtheil des Zellkerns. Zeitschrift für Physiologische Chemie *8*, 511.

Kowaltowski, A.J., de Souza-Pinto, N.C., Castilho, R.F., and Vercesi, A.E. (2009). Mitochondria and reactive oxygen species. Free Radic Biol Med *47*, 333-343.

Kremer, S.B., and Gross, D.S. (2009). SAGA and Rpd3 chromatin modification complexes dynamically regulate heat shock gene structure and expression. J Biol Chem *284*, 32914-32931.

Krogan, N.J., Kim, M., Tong, A., Golshani, A., Cagney, G., Canadien, V., Richards, D.P., Beattie, B.K., Emili, A., Boone, C., *et al.* (2003). Methylation of histone H3 by Set2 in Saccharomyces cerevisiae is linked to transcriptional elongation by RNA polymerase II. Mol Cell Biol *23*, 4207-4218.

Krogan, N.J., Peng, W.T., Cagney, G., Robinson, M.D., Haw, R., Zhong, G., Guo, X., Zhang, X., Canadien, V., Richards, D.P., *et al.* (2004). High-definition macromolecular composition of yeast RNA-processing complexes. Mol Cell *13*, 225-239.

Kucharczyk, R., Gromadka, R., Migdalski, A., Slonimski, P.P., and Rytka, J. (1999). Disruption of six novel yeast genes located on chromosome II reveals one gene essential for vegetative growth and two required for sporulation and conferring hypersensitivity to various chemicals. Yeast *15*, 987-1000.

Kundu, T.K., Palhan, V.B., Wang, Z., An, W., Cole, P.A., and Roeder, R.G. (2000). Activator-dependent transcription from chromatin in vitro involving targeted histone acetylation by p300. Mol Cell *6*, 551-561.

Kuo, A.J., Song, J., Cheung, P., Ishibe-Murakami, S., Yamazoe, S., Chen, J.K., Patel, D.J., and Gozani, O. (2012). The BAH domain of ORC1 links H4K20me2 to DNA replication licensing and Meier-Gorlin syndrome. Nature 484, 115-119.

Kuo, M.H., Zhou, J., Jambeck, P., Churchill, M.E., and Allis, C.D. (1998). Histone acetyltransferase activity of yeast Gcn5p is required for the activation of target genes in vivo. Genes Dev *12*, 627-639.

Kurdistani, S.K., and Grunstein, M. (2003). Histone acetylation and deacetylation in yeast. Nat Rev Mol Cell Biol *4*, 276-284.

Kurdistani, S.K., Robyr, D., Tavazoie, S., and Grunstein, M. (2002). Genome-wide binding map of the histone deacetylase Rpd3 in yeast. Nat Genet *31*, 248-254.

Lachner, M., O'Carroll, D., Rea, S., Mechtler, K., and Jenuwein, T. (2001). Methylation of histone H3 lysine 9 creates a binding site for HP1 proteins. Nature *410*, 116-120.

Lachner, M., O'Sullivan, R.J., and Jenuwein, T. (2003). An epigenetic road map for histone lysine methylation. J Cell Sci *116*, 2117-2124.

Lamb, T.M., and Mitchell, A.P. (2001). Coupling of Saccharomyces cerevisiae early meiotic gene expression to DNA replication depends upon RPD3 and SIN3. Genetics *157*, 545-556.

Lambert, A.J., and Brand, M.D. (2009). Reactive oxygen species production by mitochondria. Methods Mol Biol *554*, 165-181.

Langmead, B., Trapnell, C., Pop, M., and Salzberg, S.L. (2009). Ultrafast and memory-efficient alignment of short DNA sequences to the human genome. Genome Biol 10, R25.

Le Moan, N., Clement, G., Le Maout, S., Tacnet, F., and Toledano, M.B. (2006). The Saccharomyces cerevisiae proteome of oxidized protein thiols: contrasted functions for the thioredoxin and glutathione pathways. J Biol Chem *281*, 10420-10430.

Lee, K.K., and Workman, J.L. (2007). Histone acetyltransferase complexes: one size doesn't fit all. Nat Rev Mol Cell Biol *8*, 284-295.

Lee, M.G., Norman, J., Shilatifard, A., and Shiekhattar, R. (2007). Physical and functional association of a trimethyl H3K4 demethylase and Ring6a/MBLR, a polycomb-like protein. Cell *128*, 877-887.

Lee, N., Erdjument-Bromage, H., Tempst, P., Jones, R.S., and Zhang, Y. (2009). The H3K4 demethylase lid associates with and inhibits histone deacetylase Rpd3. Mol Cell Biol *29*, 1401-1410.

Lee, T.I., Causton, H.C., Holstege, F.C., Shen, W.C., Hannett, N., Jennings, E.G., Winston, F., Green, M.R., and Young, R.A. (2000). Redundant roles for the TFIID and SAGA complexes in global transcription. Nature *405*, 701-704.

Lees, N.D., Skaggs, B., Kirsch, D.R., and Bard, M. (1995). Cloning of the Late Genes in the Ergosterol Biosynthetic-Pathway of Saccharomyces-Cerevisiae - a Review. Lipids *30*, 221-226.

Levin, D.E. (2005). Cell wall integrity signaling in Saccharomyces cerevisiae. Microbiol Mol Biol Rev *69*, 262-291.

Li, B., Gogol, M., Carey, M., Lee, D., Seidel, C., and Workman, J.L. (2007). Combined action of PHD and chromo domains directs the Rpd3S HDAC to transcribed chromatin. Science *316*, 1050-1054.

Li, B., Howe, L., Anderson, S., Yates, J.R., 3rd, and Workman, J.L. (2003). The Set2 histone methyltransferase functions through the phosphorylated carboxyl-terminal domain of RNA polymerase II. J Biol Chem *278*, 8897-8903.

Li, F., Huarte, M., Zaratiegui, M., Vaughn, M.W., Shi, Y., Martienssen, R., and Cande, W.Z. (2008). Lid2 is required for coordinating H3K4 and H3K9 methylation of heterochromatin and euchromatin. Cell *135*, 272-283.

Li, H., Ilin, S., Wang, W., Duncan, E.M., Wysocka, J., Allis, C.D., and Patel, D.J. (2006). Molecular basis for site-specific read-out of histone H3K4me3 by the BPTF PHD finger of NURF. Nature *442*, 91-95.

Li, Y., and Li, H. (2012). Many keys to push: diversifying the 'readership' of plant homeodomain fingers. Acta Biochim Biophys Sin (Shanghai) *44*, 28-39.

Liang, G., Klose, R.J., Gardner, K.E., and Zhang, Y. (2007). Yeast Jhd2p is a histone H3 Lys4 trimethyl demethylase. Nat Struct Mol Biol *14*, 243-245.

Lillie, S.H., and Pringle, J.R. (1980). Reserve carbohydrate metabolism in Saccharomyces cerevisiae: responses to nutrient limitation. J Bacteriol *143*, 1384-1394.

Lin, M.T., and Beal, M.F. (2006). Mitochondrial dysfunction and oxidative stress in neurodegenerative diseases. Nature *443*, 787-795.

Lin, R., Leone, J.W., Cook, R.G., and Allis, C.D. (1989). Antibodies specific to acetylated histones document the existence of deposition- and transcription-related histone acetylation in Tetrahymena. J Cell Biol *108*, 1577-1588.

Lin, S.J., Kaeberlein, M., Andalis, A.A., Sturtz, L.A., Defossez, P.A., Culotta, V.C., Fink, G.R., and Guarente, L. (2002). Calorie restriction extends Saccharomyces cerevisiae lifespan by increasing respiration. Nature *418*, 344-348.

Liou, G.G., Tanny, J.C., Kruger, R.G., Walz, T., and Moazed, D. (2005). Assembly of the SIR complex and its regulation by O-acetyl-ADP-ribose, a product of NAD-dependent histone deacetylation. Cell *121*, 515-527.

Liu, C.L., Kaplan, T., Kim, M., Buratowski, S., Schreiber, S.L., Friedman, N., and Rando, O.J. (2005). Single-nucleosome mapping of histone modifications in S. cerevisiae. PLoS Biol *3*, e328.

Lochner, K., Siegler, G., Fuhrer, M., Greil, J., Beck, J.D., Fey, G.H., and Marschalek, R. (1996). A specific deletion in the breakpoint cluster region of the ALL-1 gene is associated with acute lymphoblastic T-cell leukemias. Cancer Res *56*, 2171-2177.

Loenarz, C., and Schofield, C.J. (2008). Expanding chemical biology of 2-oxoglutarate oxygenases. Nat Chem Biol *4*, 152-156.

Loewith, R., Jacinto, E., Wullschleger, S., Lorberg, A., Crespo, J.L., Bonenfant, D., Oppliger, W., Jenoe, P., and Hall, M.N. (2002). Two TOR complexes, only one of which is rapamycin sensitive, have distinct roles in cell growth control. Mol Cell *10*, 457-468.

Lower, K.M., Turner, G., Kerr, B.A., Mathews, K.D., Shaw, M.A., Gedeon, A.K., Schelley, S., Hoyme, H.E., White, S.M., Delatycki, M.B., *et al.* (2002). Mutations in PHF6 are associated with Borjeson-Forssman-Lehmann syndrome. Nat Genet *32*, 661-665.

Lu, P.J., Sundquist, K., Baeckstrom, D., Poulsom, R., Hanby, A., Meier-Ewert, S., Jones, T., Mitchell, M., Pitha-Rowe, P., Freemont, P., *et al.* (1999). A novel gene (PLU-1) containing highly conserved putative DNA/chromatin binding motifs is specifically up-regulated in breast cancer. J Biol Chem *274*, 15633-15645.

Lu, Z., Xu, S., Joazeiro, C., Cobb, M.H., and Hunter, T. (2002). The PHD domain of MEKK1 acts as an E3 ubiquitin ligase and mediates ubiquitination and degradation of ERK1/2. Mol Cell *9*, 945-956.

Luger, K., Mader, A.W., Richmond, R.K., Sargent, D.F., and Richmond, T.J. (1997). Crystal structure of the nucleosome core particle at 2.8 A resolution. Nature *389*, 251-260.

Luger, K. (2003). Structure and dynamic behavior of nucleosomes. Curr Opin Genet Dev 13, 127-135.

Lussier, M., White, A.M., Sheraton, J., di Paolo, T., Treadwell, J., Southard, S.B., Horenstein, C.I., Chen-Weiner, J., Ram, A.F., Kapteyn, J.C., *et al.* (1997). Large scale identification of genes involved in cell surface biosynthesis and architecture in Saccharomyces cerevisiae. Genetics *147*, 435-450.

Ma, X.J., Wu, J., Altheim, B.A., Schultz, M.C., and Grunstein, M. (1998). Deposition-related sites K5/K12 in histone H4 are not required for nucleosome deposition in yeast. Proc Natl Acad Sci U S A *95*, 6693-6698.

Madeo, F., Herker, E., Wissing, S., Jungwirth, H., Eisenberg, T., and Frohlich, K.U. (2004). Apoptosis in yeast. Curr Opin Microbiol *7*, 655-660.

Maeda, T., Takekawa, M., and Saito, H. (1995). Activation of yeast PBS2 MAPKK by MAPKKKs or by binding of an SH3-containing osmosensor. Science *269*, 554-558.

Martin, C., and Zhang, Y. (2005). The diverse functions of histone lysine methylation. Nat Rev Mol Cell Biol *6*, 838-849.

Martin, D.G., Baetz, K., Shi, X., Walter, K.L., MacDonald, V.E., Wlodarski, M.J., Gozani, O., Hieter, P., and Howe, L. (2006). The Yng1p plant homeodomain finger is a methyl-histone binding module that recognizes lysine 4-methylated histone H3. Mol Cell Biol *26*, 7871-7879.

Mas, G., de Nadal, E., Dechant, R., Rodriguez de la Concepcion, M.L., Logie, C., Jimeno-Gonzalez, S., Chavez, S., Ammerer, G., and Posas, F. (2009). Recruitment of a chromatin remodelling complex by the Hog1 MAP kinase to stress genes. EMBO J *28*, 326-336.

Mason, P.B., and Struhl, K. (2003). The FACT complex travels with elongating RNA polymerase II and is important for the fidelity of transcriptional initiation in vivo. Mol Cell Biol *23*, 8323-8333.

Matthews, A.G., Kuo, A.J., Ramon-Maiques, S., Han, S., Champagne, K.S., Ivanov, D., Gallardo, M., Carney, D., Cheung, P., Ciccone, D.N., *et al.* (2007). RAG2 PHD finger couples histone H3 lysine 4 trimethylation with V(D)J recombination. Nature *450*, 1106-1110.

McKenzie, E.A., Kent, N.A., Dowell, S.J., Moreno, F., Bird, L.E., and Mellor, J. (1993). The centromere and promoter factor, 1, CPF1, of Saccharomyces cerevisiae modulates gene activity through a family of factors including SPT21, RPD1 (SIN3), RPD3 and CCR4. Mol Gen Genet *240*, 374-386.

Merlini, L., and Piatti, S. (2011). The mother-bud neck as a signaling platform for the coordination between spindle position and cytokinesis in budding yeast. Biol Chem *392*, 805-812.

Mersman, D.P., Du, H.N., Fingerman, I.M., South, P.F., and Briggs, S.D. (2009). Polyubiquitination of the demethylase Jhd2 controls histone methylation and gene expression. Genes Dev *23*, 951-962.

Messner, S., and Hottiger, M.O. (2011). Histone ADP-ribosylation in DNA repair, replication and transcription. Trends Cell Biol *21*, 534-542.

Miller, C., Schwalb, B., Maier, K., Schulz, D., Dumcke, S., Zacher, B., Mayer, A., Sydow, J., Marcinowski, L., Dolken, L.*, et al.* (2011). Dynamic transcriptome analysis measures rates of mRNA synthesis and decay in yeast. Mol Syst Biol *7*, 458.

Miller, T.C., Rutherford, T.J., Johnson, C.M., Fiedler, M., and Bienz, M. (2010). Allosteric remodelling of the histone H3 binding pocket in the Pygo2 PHD finger triggered by its binding to the B9L/BCL9 co-factor. J Mol Biol *401*, 969-984.

Min, J., Zhang, Y., and Xu, R.M. (2003). Structural basis for specific binding of Polycomb chromodomain to histone H3 methylated at Lys 27. Genes Dev *17*, 1823-1828.

Miranda, T.B., Sayegh, J., Frankel, A., Katz, J.E., Miranda, M., and Clarke, S. (2006). Yeast Hsl7 (histone synthetic lethal 7) catalyses the in vitro formation of omega-N(G)-monomethylarginine in calf thymus histone H2A. Biochem J *395*, 563-570.

Mirsky, A.E. (1971). The structure of chromatin. Proc Natl Acad Sci U S A *68*, 2945-2948.

Mirsky, A.E., and Pollister, A.W. (1946). Chromosin, a Desoxyribose Nucleoprotein Complex of the Cell Nucleus. J Gen Physiol *30*, 117-148.

Mizzen, C.A., Yang, X.J., Kokubo, T., Brownell, J.E., Bannister, A.J., Owen-Hughes, T., Workman, J., Wang, L., Berger, S.L., Kouzarides, T.*, et al.* (1996). The TAF(II)250 subunit of TFIID has histone acetyltransferase activity. Cell *87*, 1261-1270.

Molin, M., Yang, J., Hanzen, S., Toledano, M.B., Labarre, J., and Nystrom, T. (2011). Life span extension and H(2)O(2) resistance elicited by caloric restriction require the peroxiredoxin Tsa1 in Saccharomyces cerevisiae. Mol Cell *43*, 823-833.

Morillon, A., Springer, M., and Lesage, P. (2000). Activation of the Kss1 invasive-filamentous growth pathway induces Ty1 transcription and retrotransposition in Saccharomyces cerevisiae. Mol Cell Biol *20*, 5766-5776.

Moriya, H., Shimizu-Yoshida, Y., Omori, A., Iwashita, S., Katoh, M., and Sakai, A. (2001). Yak1p, a DYRK family kinase, translocates to the nucleus and phosphorylates yeast Pop2p in response to a glucose signal. Genes Dev *15*, 1217-1228.

Muller, J., Hart, C.M., Francis, N.J., Vargas, M.L., Sengupta, A., Wild, B., Miller, E.L., O'Connor, M.B., Kingston, R.E., and Simon, J.A. (2002). Histone methyltransferase activity of a Drosophila Polycomb group repressor complex. Cell *111*, 197-208.

Murray, K. (1964). The Occurrence of Epsilon-N-Methyl Lysine in Histones. Biochemistry *3*, 10-15.

Nakayama, J., Rice, J.C., Strahl, B.D., Allis, C.D., and Grewal, S.I. (2001). Role of histone H3 lysine 9 methylation in epigenetic control of heterochromatin assembly. Science *292*, 110-113.

Ng, H.H., Feng, Q., Wang, H., Erdjument-Bromage, H., Tempst, P., Zhang, Y., and Struhl, K. (2002). Lysine methylation within the globular domain of histone H3 by Dot1 is important for telomeric silencing and Sir protein association. Genes Dev *16*, 1518-1527.

Ng, H.H., Robert, F., Young, R.A., and Struhl, K. (2003). Targeted recruitment of Set1 histone methylase by elongating Pol II provides a localized mark and memory of recent transcriptional activity. Mol Cell *11*, 709-719.

Ngubo, M., Kemp, G., and Patterton, H.G. (2011). Nano-electrospray tandem mass spectrometric analysis of the acetylation state of histones H3 and H4 in stationary phase in Saccharomyces cerevisiae. BMC Biochem *12*, 34.

Nishioka, K., Chuikov, S., Sarma, K., Erdjument-Bromage, H., Allis, C.D., Tempst, P., and Reinberg, D. (2002). Set9, a novel histone H3 methyltransferase that facilitates transcription by precluding histone tail modifications required for heterochromatin formation. Genes Dev *16*, 479-489.

Nissan, T.A., Galani, K., Maco, B., Tollervey, D., Aebi, U., and Hurt, E. (2004). A pre-ribosome with a tadpole-like structure functions in ATP-dependent maturation of 60S subunits. Mol Cell *15*, 295-301.

Oeffinger, M., Wei, K.E., Rogers, R., DeGrasse, J.A., Chait, B.T., Aitchison, J.D., and Rout, M.P. (2007). Comprehensive analysis of diverse ribonucleoprotein complexes. Nat Methods *4*, 951-956.

Ogryzko, V.V., Schiltz, R.L., Russanova, V., Howard, B.H., and Nakatani, Y. (1996). The transcriptional coactivators p300 and CBP are histone acetyltransferases. Cell *87*, 953-959.

Olins, A.L., and Olins, D.E. (1974). Spheroid chromatin units (v bodies). Science *183*, 330-332.

Org, T., Chignola, F., Hetenyi, C., Gaetani, M., Rebane, A., Liiv, I., Maran, U., Mollica, L., Bottomley, M.J., Musco, G., *et al.* (2008). The autoimmune regulator PHD finger binds to non-methylated histone H3K4 to activate gene expression. EMBO Rep *9*, 370-376.

Oudet, P., Gross-Bellard, M., and Chambon, P. (1975). Electron microscopic and biochemical evidence that chromatin structure is a repeating unit. Cell *4*, 281-300.

Ounap, K., Puusepp-Benazzouz, H., Peters, M., Vaher, U., Rein, R., Proos, A., Field, M., and Reimand, T. (2012). A novel c.2T > C mutation of the KDM5C/JARID1C gene in one large family with X-linked intellectual disability. Eur J Med Genet 55, 178-184.

Owen, D.J., Ornaghi, P., Yang, J.C., Lowe, N., Evans, P.R., Ballario, P., Neuhaus, D., Filetici, P., and Travers, A.A. (2000). The structural basis for the recognition of acetylated histone H4 by the bromodomain of histone acetyltransferase gcn5p. EMBO J *19*, 6141-6149.

Page, N., Sheraton, J., Brown, J.L., Stewart, R.C., and Bussey, H. (1996). Identification of ASK10 as a multicopy activator of Skn7p-dependent transcription of a HIS3 reporter gene. Yeast *12*, 267-272.

Parthun, M.R., Widom, J., and Gottschling, D.E. (1996). The major cytoplasmic histone acetyltransferase in yeast: links to chromatin replication and histone metabolism. Cell 87, 85-94.

Pascual, J., Martinez-Yamout, M., Dyson, H.J., and Wright, P.E. (2000). Structure of the PHD zinc finger from human Williams-Beuren syndrome transcription factor. J Mol Biol *304*, 723-729.

Pena, P.V., Davrazou, F., Shi, X., Walter, K.L., Verkhusha, V.V., Gozani, O., Zhao, R., and Kutateladze, T.G. (2006). Molecular mechanism of histone H3K4me3 recognition by plant homeodomain of ING2. Nature *442*, 100-103.

Petti, A.A., Crutchfield, C.A., Rabinowitz, J.D., and Botstein, D. (2011). Survival of starving yeast is correlated with oxidative stress response and nonrespiratory mitochondrial function. Proc Natl Acad Sci U S A *108*, E1089-1098.

Pokholok, D.K., Harbison, C.T., Levine, S., Cole, M., Hannett, N.M., Lee, T.I., Bell, G.W., Walker, K., Rolfe, P.A., Herbolsheimer, E., *et al.* (2005). Genome-wide map of nucleosome acetylation and methylation in yeast. Cell *122*, 517-527.

Pokholok, D.K., Zeitlinger, J., Hannett, N.M., Reynolds, D.B., and Young, R.A. (2006). Activated signal transduction kinases frequently occupy target genes. Science *313*, 533-536.

Poveda, A., Pamblanco, M., Tafrov, S., Tordera, V., Sternglanz, R., and Sendra, R. (2004). Hif1 is a component of yeast histone acetyltransferase B, a complex mainly localized in the nucleus. J Biol Chem *279*, 16033-16043.

Protchenko, O., Ferea, T., Rashford, J., Tiedeman, J., Brown, P.O., Botstein, D., and Philpott, C.C. (2001). Three cell wall mannoproteins facilitate the uptake of iron in Saccharomyces cerevisiae. J Biol Chem *276*, 49244-49250.

Radman-Livaja, M., Liu, C.L., Friedman, N., Schreiber, S.L., and Rando, O.J. (2010). Replication and active demethylation represent partially overlapping mechanisms for erasure of H3K4me3 in budding yeast. PLoS Genet *6*, e1000837.

Radomski, N., Kaufmann, C., and Dreyer, C. (1999). Nuclear accumulation of S-adenosylhomocysteine hydrolase in transcriptionally active cells during development of Xenopus laevis. Mol Biol Cell *10*, 4283-4298.

Ragvin, A., Valvatne, H., Erdal, S., Arskog, V., Tufteland, K.R., Breen, K., AM, O.Y., Eberharter, A., Gibson, T.J., Becker, P.B.*, et al.* (2004). Nucleosome binding by the bromodomain and PHD finger of the transcriptional cofactor p300. J Mol Biol *337*, 773-788.

Raisner, R.M., and Madhani, H.D. (2006). Patterning chromatin: form and function for H2A.Z variant nucleosomes. Curr Opin Genet Dev *16*, 119-124.

Ram, A.F., Wolters, A., Ten Hoopen, R., and Klis, F.M. (1994). A new approach for isolating cell wall mutants in Saccharomyces cerevisiae by screening for hypersensitivity to calcofluor white. Yeast *10*, 1019-1030.

Ramon-Maiques, S., Kuo, A.J., Carney, D., Matthews, A.G., Oettinger, M.A., Gozani, O., and Yang, W. (2007). The plant homeodomain finger of RAG2 recognizes histone H3 methylated at both lysine-4 and arginine-2. Proc Natl Acad Sci U S A *104*, 18993-18998.

Rando, O.J., and Winston, F. (2012). Chromatin and transcription in yeast. Genetics *190*, 351-387.

Rea, S., Eisenhaber, F., O'Carroll, D., Strahl, B.D., Sun, Z.W., Schmid, M., Opravil, S., Mechtler, K., Ponting, C.P., Allis, C.D.*, et al.* (2000). Regulation of chromatin structure by site-specific histone H3 methyltransferases. Nature *406*, 593-599.

Reader, J.C., Meekins, J.S., Gojo, I., and Ning, Y. (2007). A novel NUP98-PHF23 fusion resulting from a cryptic translocation t(11;17)(p15;p13) in acute myeloid leukemia. Leukemia *21*, 842-844.

Reytor, E., Perez-Miguelsanz, J., Alvarez, L., Perez-Sala, D., and Pajares, M.A. (2009). Conformational signals in the C-terminal domain of methionine adenosyltransferase I/III determine its nucleocytoplasmic distribution. FASEB J *23*, 3347-3360.

Ridsdale, J.A., and Davie, J.R. (1987). Chicken erythrocyte polynucleosomes which are soluble at physiological ionic strength and contain linker histones are highly enriched in beta-globin gene sequences. Nucleic Acids Res *15*, 1081-1096.

Rine, J., and Herskowitz, I. (1987). Four genes responsible for a position effect on expression from HML and HMR in Saccharomyces cerevisiae. Genetics *116*, 9-22.

Robert, F., Pokholok, D.K., Hannett, N.M., Rinaldi, N.J., Chandy, M., Rolfe, A., Workman, J.L., Gifford, D.K., and Young, R.A. (2004). Global position and recruitment of HATs and HDACs in the yeast genome. Mol Cell *16*, 199-209.

Roberts, C.K., and Sindhu, K.K. (2009). Oxidative stress and metabolic syndrome. Life Sci *84*, 705-712.

Robinson, P.J., An, W., Routh, A., Martino, F., Chapman, L., Roeder, R.G., and Rhodes, D. (2008). 30 nm chromatin fibre decompaction requires both H4-K16 acetylation and linker histone eviction. J Mol Biol *381*, 816-825.

Robzyk, K., Recht, J., and Osley, M.A. (2000). Rad6-dependent ubiquitination of histone H2B in yeast. Science *287*, 501-504.

Rodrigues-Pousada, C., Menezes, R.A., and Pimentel, C. (2010). The Yap family and its role in stress response. Yeast *27*, 245-258.

Rohde, J.R., and Cardenas, M.E. (2003). The tor pathway regulates gene expression by linking nutrient sensing to histone acetylation. Mol Cell Biol *23*, 629-635.

Roncero, C., Valdivieso, M.H., Ribas, J.C., and Duran, A. (1988). Isolation and characterization of Saccharomyces cerevisiae mutants resistant to Calcofluor white. J Bacteriol *170*, 1950-1954.

Ruault, M., and Pillus, L. (2006). Chromatin-modifiying enzymes are essential when the Saccharomyces cerevisiae morphogenesis checkpoint is constitutively activated. Genetics *174*, 1135-1149.

Ruiz-Carrillo, A., Wangh, L.J., and Allfrey, V.G. (1975). Processing of newly synthesized histone molecules. Science *190*, 117-128.

Ruiz-Roig, C., Vieitez, C., Posas, F., and de Nadal, E. (2010). The Rpd3L HDAC complex is essential for the heat stress response in yeast. Mol Microbiol *76*, 1049-1062.

Rundlett, S.E., Carmen, A.A., Kobayashi, R., Bavykin, S., Turner, B.M., and Grunstein, M. (1996). HDA1 and RPD3 are members of distinct yeast histone deacetylase complexes that regulate silencing and transcription. Proc Natl Acad Sci U S A *93*, 14503-14508.

Ruthenburg, A.J., Li, H., Patel, D.J., and Allis, C.D. (2007). Multivalent engagement of chromatin modifications by linked binding modules. Nat Rev Mol Cell Biol *8*, 983-994.

Sakabe, K., Wang, Z., and Hart, G.W. (2010). Beta-N-acetylglucosamine (O-GlcNAc) is part of the histone code. Proc Natl Acad Sci U S A *107*, 19915-19920.

Santos-Reboucas, C.B., Fintelman-Rodrigues, N., Jensen, L.R., Kuss, A.W., Ribeiro, M.G., Campos, M., Jr., Santos, J.M., and Pimentel, M.M. (2011). A novel nonsense mutation in KDM5C/JARID1C gene causing intellectual disability, short stature and speech delay. Neurosci Lett *498*, 67-71.

Santos-Rosa, H., Kirmizis, A., Nelson, C., Bartke, T., Saksouk, N., Cote, J., and Kouzarides, T. (2009). Histone H3 tail clipping regulates gene expression. Nat Struct Mol Biol *16*, 17-22.

Santos-Rosa, H., Schneider, R., Bannister, A.J., Sherriff, J., Bernstein, B.E., Emre, N.C., Schreiber, S.L., Mellor, J., and Kouzarides, T. (2002). Active genes are tri-methylated at K4 of histone H3. Nature *419*, 407-411.

Saugier-Veber, P., Drouot, N., Wolf, L.M., Kuhn, J.M., Frebourg, T., and Lefebvre, H. (2001). Identification of a novel mutation in the autoimmune regulator (AIRE-1) gene in a French family with autoimmune polyendocrinopathy-candidiasis-ectodermal dystrophy. Eur J Endocrinol *144*, 347-351.

Scheel, H., and Hofmann, K. (2003). No evidence for PHD fingers as ubiquitin ligases. Trends Cell Biol *13*, 285-287; author reply 287-288.

Schmidt, M., Varma, A., Drgon, T., Bowers, B., and Cabib, E. (2003). Septins, under Cla4p regulation, and the chitin ring are required for neck integrity in budding yeast. Mol Biol Cell *14*, 2128-2141.

Schnell, N., Krems, B., and Entian, K.D. (1992). The PAR1 (YAP1/SNQ3) gene of Saccharomyces cerevisiae, a c-jun homologue, is involved in oxygen metabolism. Curr Genet *21*, 269-273.

Schoch, C.L., Br-uning, A.R., Entian, K.D., Pretorius, G.H., and Prior, B.A. (1997). A Saccharomyces cerevisiae mutant defective in the kinesin-like protein Kar3 is sensitive to NaCl-stress. Curr Genet *32*, 315-322.

Schotta, G., Lachner, M., Sarma, K., Ebert, A., Sengupta, R., Reuter, G., Reinberg, D., and Jenuwein, T. (2004). A silencing pathway to induce H3-K9 and H4-K20 trimethylation at constitutive heterochromatin. Genes Dev *18*, 1251-1262.

Schultz, J. (1941). The Evidence of the Nucleoprotein Nature of the Gene. Cold Spring Harbor Symposia on Quantitative Biology *9*, 55-65.

Schulze, J.M., Wang, A.Y., and Kobor, M.S. (2010). Reading chromatin: insights from yeast into YEATS domain structure and function. Epigenetics *5*, 573-577.

Schwarz, K., Gauss, G.H., Ludwig, L., Pannicke, U., Li, Z., Lindner, D., Friedrich, W., Seger, R.A., Hansen-Hagge, T.E., Desiderio, S., *et al.* (1996). RAG mutations in human B cell-negative SCID. Science *274*, 97-99.

Scott, K.L., and Plon, S.E. (2003). Loss of Sin3/Rpd3 histone deacetylase restores the DNA damage response in checkpoint-deficient strains of Saccharomyces cerevisiae. Mol Cell Biol *23*, 4522-4531.

Sertil, O., Vemula, A., Salmon, S.L., Morse, R.H., and Lowry, C.V. (2007). Direct role for the Rpd3 complex in transcriptional induction of the anaerobic DAN/TIR genes in yeast. Mol Cell Biol *27*, 2037-2047.

Seward, D.J., Cubberley, G., Kim, S., Schonewald, M., Zhang, L., Tripet, B., and Bentley, D.L. (2007). Demethylation of trimethylated histone H3 Lys4 in vivo by JARID1 JmjC proteins. Nat Struct Mol Biol *14*, 240-242.

Sharma, V.M., Tomar, R.S., Dempsey, A.E., and Reese, J.C. (2007). Histone deacetylases RPD3 and HOS2 regulate the transcriptional activation of DNA damage-inducible genes. Mol Cell Biol *27*, 3199-3210.

Shenton, D., and Grant, C.M. (2003). Protein S-thiolation targets glycolysis and protein synthesis in response to oxidative stress in the yeast Saccharomyces cerevisiae. Biochem J *374*, 513-519.

Shenton, D., Smirnova, J.B., Selley, J.N., Carroll, K., Hubbard, S.J., Pavitt, G.D., Ashe, M.P., and Grant, C.M. (2006). Global translational responses to oxidative stress impact upon multiple levels of protein synthesis. J Biol Chem *281*, 29011-29021.

Shevchenko, A., Roguev, A., Schaft, D., Buchanan, L., Habermann, B., Sakalar, C., Thomas, H., Krogan, N.J., and Stewart, A.F. (2008). Chromatin Central: towards the comparative proteome by accurate mapping of the yeast proteomic environment. Genome Biol *9*, R167.

Shi, X., Hong, T., Walter, K.L., Ewalt, M., Michishita, E., Hung, T., Carney, D., Pena, P., Lan, F., Kaadige, M.R.*, et al.* (2006). ING2 PHD domain links histone H3 lysine 4 methylation to active gene repression. Nature *442*, 96-99.

Shi, X., Kachirskaia, I., Walter, K.L., Kuo, J.H., Lake, A., Davrazou, F., Chan, S.M., Martin, D.G., Fingerman, I.M., Briggs, S.D.*, et al.* (2007). Proteome-wide analysis in Saccharomyces cerevisiae identifies several PHD fingers as novel direct and selective binding modules of histone H3 methylated at either lysine 4 or lysine 36. J Biol Chem *282*, 2450-2455.

Shi, Y., Lan, F., Matson, C., Mulligan, P., Whetstine, J.R., Cole, P.A., and Casero, R.A. (2004). Histone demethylation mediated by the nuclear amine oxidase homolog LSD1. Cell *119*, 941-953.

Shimizu, J., Yoda, K., and Yamasaki, M. (1994). The hypo-osmolarity-sensitive phenotype of the Saccharomyces cerevisiae hpo2 mutant is due to a mutation in PKC1, which regulates expression of beta-glucanase. Mol Gen Genet *242*, 641-648.

Shogren-Knaak, M., Ishii, H., Sun, J.M., Pazin, M.J., Davie, J.R., and Peterson, C.L. (2006). Histone H4-K16 acetylation controls chromatin structure and protein interactions. Science *311*, 844-847.

Sims, R.J., 3rd, Nishioka, K., and Reinberg, D. (2003). Histone lysine methylation: a signature for chromatin function. Trends Genet *19*, 629-639.

Singer, M.A., and Lindquist, S. (1998). Multiple effects of trehalose on protein folding in vitro and in vivo. Mol Cell *1*, 639-648.

Singh, K.K. (2000). The Saccharomyces cerevisiae Sln1p-Ssk1p two-component system mediates response to oxidative stress and in an oxidant-specific fashion. Free Radic Biol Med *29*, 1043-1050.

Slavov, N., Macinskas, J., Caudy, A., and Botstein, D. (2011). Metabolic cycling without cell division cycling in respiring yeast. Proc Natl Acad Sci U S A *108*, 19090-19095.

Smith, J.S., and Boeke, J.D. (1997). An unusual form of transcriptional silencing in yeast ribosomal DNA. Genes Dev *11*, 241-254.

Smith, J.S., Caputo, E., and Boeke, J.D. (1999). A genetic screen for ribosomal DNA silencing defects identifies multiple DNA replication and chromatin-modulating factors. Mol Cell Biol *19*, 3184-3197.

Smith, M.M., and Andresson, O.S. (1983). DNA sequences of yeast H3 and H4 histone genes from two non-allelic gene sets encode identical H3 and H4 proteins. J Mol Biol *169*, 663-690.

Smith, S., and Stillman, B. (1991). Stepwise assembly of chromatin during DNA replication in vitro. EMBO J *10*, 971-980.

Sobacchi, C., Marrella, V., Rucci, F., Vezzoni, P., and Villa, A. (2006). RAG-dependent primary immunodeficiencies. Hum Mutat *27*, 1174-1184.

Sobel, R.E., Cook, R.G., Perry, C.A., Annunziato, A.T., and Allis, C.D. (1995). Conservation of deposition-related acetylation sites in newly synthesized histones H3 and H4. Proc Natl Acad Sci U S A *92*, 1237-1241.

Spange, S., Wagner, T., Heinzel, T., and Kramer, O.H. (2009). Acetylation of non-histone proteins modulates cellular signalling at multiple levels. Int J Biochem Cell Biol *41*, 185-198.

Spencer, T.E., Jenster, G., Burcin, M.M., Allis, C.D., Zhou, J., Mizzen, C.A., McKenna, N.J., Onate, S.A., Tsai, S.Y., Tsai, M.J.*, et al.* (1997). Steroid receptor coactivator-1 is a histone acetyltransferase. Nature *389*, 194-198.

Spicer, S.S., Hardin, J.H., and Greene, W.B. (1968). Nuclear precipitates in pyroantimonate-osmium tetroxide-fixed tissues. J Cell Biol 39, 216-221.

Stamenova, R., Dimitrov, M., Stoycheva, T., Pesheva, M., Venkov, P., and Tsvetkov, T.S. (2008). Transposition of Saccharomyces cerevisiae Ty1 retrotransposon is activated by improper cryopreservation. Cryobiology *56*, 241-247.

Stedman, E., and Stedman, E. (1951). The Basic Proteins of Cell Nuclei. Philos T Roy Soc B *235*, 565-&.

Stillman, D.J., Dorland, S., and Yu, Y. (1994). Epistasis analysis of suppressor mutations that allow HO expression in the absence of the yeast SW15 transcriptional activator. Genetics *136*, 781-788.

Strahl, B.D., and Allis, C.D. (2000). The language of covalent histone modifications. Nature *403*, 41-45.

Strahl, B.D., Grant, P.A., Briggs, S.D., Sun, Z.W., Bone, J.R., Caldwell, J.A., Mollah, S., Cook, R.G., Shabanowitz, J., Hunt, D.F.*, et al.* (2002). Set2 is a nucleosomal histone H3-selective methyltransferase that mediates transcriptional repression. Mol Cell Biol *22*, 1298-1306.

Strich, R., Slater, M.R., and Esposito, R.E. (1989). Identification of negative regulatory genes that govern the expression of early meiotic genes in yeast. Proc Natl Acad Sci U S A *86*, 10018-10022.

Strich, R., Surosky, R.T., Steber, C., Dubois, E., Messenguy, F., and Esposito, R.E. (1994). UME6 is a key regulator of nitrogen repression and meiotic development. Genes Dev *8*, 796-810.

Suka, N., Luo, K., and Grunstein, M. (2002). Sir2p and Sas2p opposingly regulate acetylation of yeast histone H4 lysine16 and spreading of heterochromatin. Nat Genet *32*, 378-383.

Sun, L., and Chen, Z.J. (2004). The novel functions of ubiquitination in signaling. Curr Opin Cell Biol *16*, 119-126.

Sun, Z.W., and Hampsey, M. (1999). A general requirement for the Sin3-Rpd3 histone deacetylase complex in regulating silencing in Saccharomyces cerevisiae. Genetics *152*, 921-932.

Swan, T.M., and Watson, K. (1998). Stress tolerance in a yeast sterol auxotroph: role of ergosterol, heat shock proteins and trehalose. Fems Microbiology Letters *169*, 191-197.

Tabor, S., and Richardson, C.C. (1985). A bacteriophage T7 RNA polymerase/promoter system for controlled exclusive expression of specific genes. Proc Natl Acad Sci U S A *82*, 1074-1078.

Takahashi, H., McCaffery, J.M., Irizarry, R.A., and Boeke, J.D. (2006). Nucleocytosolic acetyl-coenzyme a synthetase is required for histone acetylation and global transcription. Mol Cell *23*, 207-217.

Takahata, S., Yu, Y., and Stillman, D.J. (2009). The E2F functional analogue SBF recruits the Rpd3(L) HDAC, via Whi5 and Stb1, and the FACT chromatin reorganizer, to yeast G1 cyclin promoters. EMBO J *28*, 3378-3389.

Talbert, P.B., and Henikoff, S. (2010). Histone variants--ancient wrap artists of the epigenome. Nat Rev Mol Cell Biol *11*, 264-275.

Tan, M., Luo, H., Lee, S., Jin, F., Yang, J.S., Montellier, E., Buchou, T., Cheng, Z., Rousseaux, S., Rajagopal, N., *et al.* (2011). Identification of 67 histone marks and histone lysine crotonylation as a new type of histone modification. Cell *146*, 1016-1028.

Taunton, J., Hassig, C.A., and Schreiber, S.L. (1996). A mammalian histone deacetylase related to the yeast transcriptional regulator Rpd3p. Science *272*, 408-411.

Taverna, S.D., Ilin, S., Rogers, R.S., Tanny, J.C., Lavender, H., Li, H., Baker, L., Boyle, J., Blair, L.P., Chait, B.T., *et al.* (2006). Yng1 PHD finger binding to H3 trimethylated at K4 promotes NuA3 HAT activity at K14 of H3 and transcription at a subset of targeted ORFs. Mol Cell *24*, 785-796.

Taverna, S.D., Li, H., Ruthenburg, A.J., Allis, C.D., and Patel, D.J. (2007). How chromatin-binding modules interpret histone modifications: lessons from professional pocket pickers. Nat Struct Mol Biol *14*, 1025-1040.

Teperino, R., Schoonjans, K., and Auwerx, J. (2010). Histone methyl transferases and demethylases; can they link metabolism and transcription? Cell Metab *12*, 321-327.

Theesfeld, C.L., Zyla, T.R., Bardes, E.G., and Lew, D.J. (2003). A monitor for bud emergence in the yeast morphogenesis checkpoint. Mol Biol Cell *14*, 3280-3291.

Trachtulcova, P., Frydlova, I., Janatova, I., Dorosh, A., and Hasek, J. (2003). The W303 genetic background affects the isw2 delta mutant phenotype in Saccharomyces cerevisiae. Folia Microbiol (Praha) *48*, 745-753.

Trapnell, C., Pachter, L., and Salzberg, S.L. (2009). TopHat: discovering splice junctions with RNA-Seq. Bioinformatics *25*, 1105-1111.

Trapnell, C., Williams, B.A., Pertea, G., Mortazavi, A., Kwan, G., van Baren, M.J., Salzberg, S.L., Wold, B.J., and Pachter, L. (2010). Transcript assembly and quantification by RNA-Seq reveals unannotated transcripts and isoform switching during cell differentiation. Nat Biotechnol *28*, 511-515.

Tsang, C.K., Bertram, P.G., Ai, W., Drenan, R., and Zheng, X.F. (2003). Chromatin-mediated regulation of nucleolar structure and RNA Pol I localization by TOR. EMBO J *22*, 6045-6056.

Tse, C., Sera, T., Wolffe, A.P., and Hansen, J.C. (1998). Disruption of higher-order folding by core histone acetylation dramatically enhances transcription of nucleosomal arrays by RNA polymerase III. Mol Cell Biol *18*, 4629-4638.

Tsukada, Y., Fang, J., Erdjument-Bromage, H., Warren, M.E., Borchers, C.H., Tempst, P., and Zhang, Y. (2006). Histone demethylation by a family of JmjC domain-containing proteins. Nature *439*, 811-816.

Tu, B.P., Kudlicki, A., Rowicka, M., and McKnight, S.L. (2005). Logic of the yeast metabolic cycle: temporal compartmentalization of cellular processes. Science *310*, 1152-1158.

Tu, S., Bulloch, E.M., Yang, L., Ren, C., Huang, W.C., Hsu, P.H., Chen, C.H., Liao, C.L., Yu, H.M., Lo, W.S.*, et al.* (2007). Identification of histone demethylases in Saccharomyces cerevisiae. J Biol Chem *282*, 14262-14271.

Turner, B.M. (1991). Histone acetylation and control of gene expression. J Cell Sci *99 (Pt 1)*, 13-20.

Tzschach, A., Lenzner, S., Moser, B., Reinhardt, R., Chelly, J., Fryns, J.P., Kleefstra, T., Raynaud, M., Turner, G., Ropers, H.H.*, et al.* (2006). Novel JARID1C/SMCX mutations in patients with X-linked mental retardation. Hum Mutat *27*, 389.

Urban, J., Soulard, A., Huber, A., Lippman, S., Mukhopadhyay, D., Deloche, O., Wanke, V., Anrather, D., Ammerer, G., Riezman, H., *et al.* (2007). Sch9 is a major target of TORC1 in Saccharomyces cerevisiae. Mol Cell *26*, 663-674.

van Leeuwen, F., Gafken, P.R., and Gottschling, D.E. (2002). Dot1p modulates silencing in yeast by methylation of the nucleosome core. Cell *109*, 745-756.

van Zutven, L.J., Onen, E., Velthuizen, S.C., van Drunen, E., von Bergh, A.R., van den Heuvel-Eibrink, M.M., Veronese, A., Mecucci, C., Negrini, M., de Greef, G.E., *et al.* (2006). Identification of NUP98 abnormalities in acute leukemia: JARID1A (12p13) as a new partner gene. Genes Chromosomes Cancer *45*, 437-446.

Vanderhaegen, B., Neven, H., Verachtert, H., and Derdelinckx, G. (2006). The chemistry of beer aging - a critical review. Food Chem *95*, 357-381.

Vannier, D., Balderes, D., and Shore, D. (1996). Evidence that the transcriptional regulators SIN3 and RPD3, and a novel gene (SDS3) with similar functions, are involved in transcriptional silencing in S. cerevisiae. Genetics *144*, 1343-1353.

Vannier, D., Damay, P., and Shore, D. (2001). A role for Sds3p, a component of the Rpd3p/Sin3p deacetylase complex, in maintaining cellular integrity in Saccharomyces cerevisiae. Mol Genet Genomics *265*, 560-568.

Vasiljeva, L., and Buratowski, S. (2006). Nrd1 interacts with the nuclear exosome for 3' processing of RNA polymerase II transcripts. Mol Cell *21*, 239-248.

Vazquez-Torres, A., and Balish, E. (1997). Macrophages in resistance to candidiasis. Microbiol Mol Biol Rev *61*, 170-192.

Venters, B.J., Wachi, S., Mavrich, T.N., Andersen, B.E., Jena, P., Sinnamon, A.J., Jain, P., Rolleri, N.S., Jiang, C., Hemeryck-Walsh, C., *et al.* (2011). A comprehensive genomic binding map of gene and chromatin regulatory proteins in Saccharomyces. Mol Cell *41*, 480-492.

Verma, R., Annan, R.S., Huddleston, M.J., Carr, S.A., Reynard, G., and Deshaies, R.J. (1997). Phosphorylation of Sic1p by G1 Cdk required for its degradation and entry into S phase. Science *278*, 455-460.

Vidal, M., and Gaber, R.F. (1991). RPD3 encodes a second factor required to achieve maximum positive and negative transcriptional states in Saccharomyces cerevisiae. Mol Cell Biol *11*, 6317-6327.

Vilella, F., Herrero, E., Torres, J., and de la Torre-Ruiz, M.A. (2005). Pkc1 and the upstream elements of the cell integrity pathway in Saccharomyces cerevisiae, Rom2 and Mtl1, are required for cellular responses to oxidative stress. J Biol Chem *280*, 9149-9159.

Wach, A., Brachat, A., Pohlmann, R., and Philippsen, P. (1994). New heterologous modules for classical or PCR-based gene disruptions in Saccharomyces cerevisiae. Yeast *10*, 1793-1808.

Waldmann, T., Izzo, A., Kamieniarz, K., Richter, F., Vogler, C., Sarg, B., Lindner, H., Young, N.L., Mittler, G., Garcia, B.A., *et al.* (2011). Methylation of H2AR29 is a novel repressive PRMT6 target. Epigenetics Chromatin *4*, 11.

Wallace, D.C., and Fan, W. (2010). Energetics, epigenetics, mitochondrial genetics. Mitochondrion *10*, 12-31.

Wang, G.G., Song, J., Wang, Z., Dormann, H.L., Casadio, F., Li, H., Luo, J.L., Patel, D.J., and Allis, C.D. (2009). Haematopoietic malignancies caused by dysregulation of a chromatin-binding PHD finger. Nature *459*, 847-851.

Wang, H., Cao, R., Xia, L., Erdjument-Bromage, H., Borchers, C., Tempst, P., and Zhang, Y. (2001). Purification and functional characterization of a histone H3-lysine 4-specific methyltransferase. Mol Cell *8*, 1207-1217.

Wang, H., Zhai, L., Xu, J., Joo, H.Y., Jackson, S., Erdjument-Bromage, H., Tempst, P., Xiong, Y., and Zhang, Y. (2006). Histone H3 and H4 ubiquitylation by the CUL4-DDB-ROC1 ubiquitin ligase facilitates cellular response to DNA damage. Mol Cell *22*, 383-394.

Wang, Z., Song, J., Milne, T.A., Wang, G.G., Li, H., Allis, C.D., and Patel, D.J. (2010). Pro isomerization in MLL1 PHD3-bromo cassette connects H3K4me readout to CyP33 and HDAC-mediated repression. Cell *141*, 1183-1194.

Ward, L.D., and Bussemaker, H.J. (2008). Predicting functional transcription factor binding through alignment-free and affinity-based analysis of orthologous promoter sequences. Bioinformatics *24*, i165-171.

Wei, Y., Mizzen, C.A., Cook, R.G., Gorovsky, M.A., and Allis, C.D. (1998). Phosphorylation of histone H3 at serine 10 is correlated with chromosome condensation during mitosis and meiosis in Tetrahymena. Proc Natl Acad Sci U S A *95*, 7480-7484.

Wei, Y., and Zheng, X.F. (2011). Nutritional control of cell growth via TOR signaling in budding yeast. Methods Mol Biol *759*, 307-319.

Weissman, A.M. (2001). Themes and variations on ubiquitylation. Nat Rev Mol Cell Biol *2*, 169-178.

Wellen, K.E., and Thompson, C.B. (2010). Cellular metabolic stress: considering how cells respond to nutrient excess. Mol Cell *40*, 323-332.

Werner-Washburne, M., Braun, E., Johnston, G.C., and Singer, R.A. (1993). Stationary phase in the yeast Saccharomyces cerevisiae. Microbiol Rev *57*, 383-401.

West, M.H., and Bonner, W.M. (1980). Histone 2B can be modified by the attachment of ubiquitin. Nucleic Acids Res *8*, 4671-4680.

Winzeler, E.A., Shoemaker, D.D., Astromoff, A., Liang, H., Anderson, K., Andre, B., Bangham, R., Benito, R., Boeke, J.D., Bussey, H., *et al.* (1999). Functional characterization of the S. cerevisiae genome by gene deletion and parallel analysis. Science *285*, 901-906.

Woodcock, C.L., Safer, J.P., and Stanchfield, J.E. (1976). Structural repeating units in chromatin. I. Evidence for their general occurrence. Exp Cell Res *97*, 101-110.

Wu, M., Newcomb, L., and Heideman, W. (1999). Regulation of gene expression by glucose in Saccharomyces cerevisiae: a role for ADA2 and ADA3/NGG1. J Bacteriol *181*, 4755-4760.

Wyers, F., Rougemaille, M., Badis, G., Rousselle, J.C., Dufour, M.E., Boulay, J., Regnault, B., Devaux, F., Namane, A., Seraphin, B., *et al.* (2005). Cryptic pol II transcripts are degraded by a nuclear quality control pathway involving a new poly(A) polymerase. Cell *121*, 725-737.

Wysocka, J., Swigut, T., Xiao, H., Milne, T.A., Kwon, S.Y., Landry, J., Kauer, M., Tackett, A.J., Chait, B.T., Badenhorst, P., *et al.* (2006). A PHD finger of NURF couples histone H3 lysine 4 trimethylation with chromatin remodelling. Nature *442*, 86-90.

Xiao, H., Sandaltzopoulos, R., Wang, H.M., Hamiche, A., Ranallo, R., Lee, K.M., Fu, D., and Wu, C. (2001). Dual functions of largest NURF subunit NURF301 in nucleosome sliding and transcription factor interactions. Mol Cell *8*, 531-543.

Xiao, T., Hall, H., Kizer, K.O., Shibata, Y., Hall, M.C., Borchers, C.H., and Strahl, B.D. (2003). Phosphorylation of RNA polymerase II CTD regulates H3 methylation in yeast. Genes Dev *17*, 654-663.

Xin, X., Lan, C., Lee, H.C., and Zhang, L. (2007). Regulation of the HAP1 gene involves positive actions of histone deacetylases. Biochem Biophys Res Commun *362*, 120-125.

Xu, P., Duong, D.M., Seyfried, N.T., Cheng, D., Xie, Y., Robert, J., Rush, J., Hochstrasser, M., Finley, D., and Peng, J. (2009). Quantitative proteomics reveals the function of unconventional ubiquitin chains in proteasomal degradation. Cell *137*, 133-145.

Yamane, K., Tateishi, K., Klose, R.J., Fang, J., Fabrizio, L.A., Erdjument-Bromage, H., Taylor-Papadimitriou, J., Tempst, P., and Zhang, Y. (2007). PLU-1 is an H3K4 demethylase involved in transcriptional repression and breast cancer cell proliferation. Mol Cell *25*, 801-812.

Yang, X.J., Ogryzko, V.V., Nishikawa, J., Howard, B.H., and Nakatani, Y. (1996). A p300/CBP-associated factor that competes with the adenoviral oncoprotein E1A. Nature *382*, 319-324.

Ye, P., Peyser, B.D., Pan, X., Boeke, J.D., Spencer, F.A., and Bader, J.S. (2005). Gene function prediction from congruent synthetic lethal interactions in yeast. Mol Syst Biol *1*, 2005 0026.

Zaman, S., Lippman, S.I., Zhao, X., and Broach, J.R. (2008). How Saccharomyces responds to nutrients. Annu Rev Genet *42*, 27-81.

Zeng, J., Ge, Z., Wang, L., Li, Q., Wang, N., Bjorkholm, M., Jia, J., and Xu, D. (2010). The histone demethylase RBP2 Is overexpressed in gastric cancer and its inhibition triggers senescence of cancer cells. Gastroenterology *138*, 981-992.

Zhang, K., Chen, Y., Zhang, Z., and Zhao, Y. (2009). Identification and verification of lysine propionylation and butyrylation in yeast core histones using PTMap software. J Proteome Res *8*, 900-906.

Zhang, L., Eugeni, E.E., Parthun, M.R., and Freitas, M.A. (2003). Identification of novel histone post-translational modifications by peptide mass fingerprinting. Chromosoma *112*, 77-86.

Zhang, Y., Liu, T., Meyer, C.A., Eeckhoute, J., Johnson, D.S., Bernstein, B.E., Nusbaum, C., Myers, R.M., Brown, M., Li, W., *et al.* (2008). Model-based analysis of ChIP-Seq (MACS). Genome Biol *9*, R137.

Zheng, J., Benschop, J.J., Shales, M., Kemmeren, P., Greenblatt, J., Cagney, G., Holstege, F., Li, H., and Krogan, N.J. (2010). Epistatic relationships reveal the functional organization of yeast transcription factors. Mol Syst Biol *6*, 420.

Zhou, B.O., Wang, S.S., Zhang, Y., Fu, X.H., Dang, W., Lenzmeier, B.A., and Zhou, J.Q. (2011). Histone H4 lysine 12 acetylation regulates telomeric heterochromatin plasticity in Saccharomyces cerevisiae. PLoS Genet *7*, e1001272.

Zhou, J., Zhou, B.O., Lenzmeier, B.A., and Zhou, J.Q. (2009). Histone deacetylase Rpd3 antagonizes Sir2-dependent silent chromatin propagation. Nucleic Acids Res *37*, 3699-3713.